BIOBASED SEMI-AROMATIC POLYESTERS AND ADDITIVES: SYNTHESIS, CHARACTERIZATION, AND APPLICATION

by

RYAN K. MAYNARD

(Under the Direction of Jason Locklin)

ABSTRACT

As the global use of plastics continues to expand, the need to investigate alternate feedstocks for high-performance polymers is increasing. Lignin is a promising feedstock due to its widespread abundance and significant structural variety. In this work, a number of novel, lignin-derived monomers are synthesized, and resultant polymers are fully characterized for thermal, mechanical, and processing properties. First, a suite of nine polyester elastomers were synthesized. Iterative structural permutations provided a significant array of tensile properties, from brittle to exceptionally ductile thermoplastics. The effects of various structural features were investigated using melt rheology to correlate to properties. It was also demonstrated that these materials are easily chemically-recyclable in rapid timeframes. Building on this foundation, two novel, biobased crosslinkers were polymerized with a ductile thermoplastic elastomer at loadings between 0.25% and 5.0%. Significant improvement to tensile and cyclic tensile properties were achieved, and comprehensive rheological analysis was conducted to analyze the efficiency of crosslinking between the two additives. Two chemical-recycling experiments were conducted, and it was found that the crosslinked elastomers degraded extremely rapidly under basic conditions with excellent retention of monomer feed ratio. Finally, a novel, biobased

monomer was synthesized, and the polyester was fully characterized. Including two other previously reported ester-based monomers, three polyesters and six poly(ester amide)s were synthesized. The polymers were found to be remarkably thermally stable and exhibited a wide array of mechanical properties, including one example that exhibited excellent elastomeric recovery. This work ultimately describes the synthesis of many polyesters that encompass a very wide array of thermal, mechanical, and rheological properties and offers significant contributions toward characterization and applications of materials in this class.

INDEX WORDS: Semi-aromatic polyesters, lignin-derived polymers, structure-property relationships, thermoplastic elastomers, crosslinked polyesters, chemical recycling, polymer rheology, poly(ester amide)s, biobased polymers

BIOBASED SEMI-AROMATIC POLYESTERS AND ADDITIVES: SYNTHESIS, CHARACTERIZATION, AND APPLICATION

by

RYAN K. MAYNARD

B.S. Chem, The University of Georgia, 2019

A Dissertation Submitted to the Graduate Faculty of The University of Georgia in Partial

Fulfilment of the Requirements for the Degree

DOCTOR OF PHILOSOPHY

ATHENS, GEORGIA

2025

© 2025

Ryan K. Maynard

All Rights Reserved

BIOBASED SEMI-AROMATIC POLYESTERS AND ADDITIVES: SYNTHESIS, CHARACTERIZATION, AND APPLICATION

by

RYAN K. MAYNARD

Major Professor:

Committee:

Jason Locklin

Branson Ritchie

Vladimir Popik

Electronic Version Approved:

Ron Walcott Vice Provost for Graduate Education and Dean of the Graduate School The University of Georgia May 2025

DEDICATION

This work is dedicated to Rebekah –

an amazing scientist, the loveliest bride, and my very best friend.

ACKNOWLEDGEMENTS

There are so many people to acknowledge that helped me get to this point. More than any other person, I owe my success to my amazing wife, Rebekah. Going through PhDs together has been intense, and I honestly don't know if I could have done it without you. You are the greatest blessing of my life.

Next, I want to thank my family for their truly endless support. My mom and dad, who have been there every step of the way, and my siblings, Rachael and Justin. I have felt your support and love for my entire life, but it was especially appreciated these past five years. I am also so thankful for my four grandparents and the rest of my extended family.

I want to thank Jason for being a fantastic PI. We had a rough start with COVID and an even weirder finish with the lab burning down. I'll be forever grateful for your mentorship and for modeling what it means to be a truly dedicated and industrious scientist. I'm particularly glad we eventually figured out that we both enjoy doing redneck things in the woods. I'll be fond of those memories for my whole life.

I also have several past and present mentors to thank. Mike Davies, for teaching me chemistry in high school (which I hear you are still just as excited about as I am) and demonstrating that it's totally awesome to be excited about science. Dr. Andrew Thomas, for demonstrating that being a chemistry teacher can be fun. Dr. Richard Morrison, for taking me in as an undergraduate, and Dr. Kasey Leigh Yearty, for mentoring me. With their guidance, I knew for a fact I wanted to be a chemist for the rest of my life. I am also so grateful to Dr. Fritz Schaefer, with whom I have had numerous conversations about the intersection of Faith and

science. Dr. Evan White, for taking me on as a recently unemployed graduate, introducing me to the NMI, and teaching me some really handy Schlenk line secrets.

I would also like to thank my committee, Dr. Bran Richie and Dr. Vladimir Popik. I have learned valuable scientific lessons from you both over the past five years.

Without my undergraduate students, a lot of this work would have happened a good bit slower. I seriously lucked out when Imrie and Frida decided to come and work with me. You both learn incredibly fast and are very hard workers. Thanks for being awesome students to mentor.

I'd also like to thank the Locklin lab group members. I could write about all of you, past and present, but I can summarize it in the following: I can think of every Locklin Lab graduate student since 2020, and I am truly thankful to have worked with them all. Some of you are hilarious, all of you were kind, and I know some of you will be lifelong friends.

Speaking of friends, I have a lot of really good ones. A special thanks to my closest friends: Daniel, Ben, Chris, Matt, and Grant. Y'all have been there for me since way before graduate school.

A final, and most important thanks to my Lord and Savior, Jesus Christ, who has saved me and blessed me beyond my wildest dreams - far beyond what I deserve.

TABLE OF CONTENTS

Pa	ige
DEDICATION	iv
ACKNOWLEDGEMENTS	V
INTRODUCTION	1
Petroleum-Based Plastics	. 1
Biobased Aliphatic Polyesters	2
Biobased Semi-Aromatic Polymers: PBAT	3
Biobased Semi-Aromatic Polymers: PEF	5
Lignin as an Aromatic Feedstock	. 6
Objectives	7
References	9
SYNTHESIS AND STRUCTURE-PROPERTY RELATIONSHIPS OF LIGNIN- DERIVED SEMI-AROMATIC POLY(ETHER ESTER)S.	
Abstract	17
Introduction	17
Materials and Methods	20
Results and Discussion	24
Conclusions:	38
References:	40

IMPROVEMENT OF ELASTOMERIC RECOVERY IN LIGNIN-DERIVED THERMOPLASTIC POLYESTERS <i>VIA</i> THE INCORPORATION OF AABB-TYPE	
CROSSLINKERS4	١7
Abstract4	8
Introduction4	8
Materials and Methods	9
Results and Discussion	50
Conclusions	15
References	'6
SYNTHESIS AND CHARACTERIZATION OF LIGNIN-DERIVED POLY(ESTER	
AMIDE)S	
Abstract	8'
Introduction	18
Materials and Methods	30
Results and Discussion	36
Conclusions	0
References)2
CONCLUSIONS AND FUTURE DIRECTIONS)6
Conclusions 10)6
Future Directions)7
Literature Cited	19
APPENDICES	0
SUPPLEMENTAL INFORMATION FOR CHAPTER 2	1
SUPPLEMENTAL INFORMATION FOR CHAPTER 3	'3
SLIPPI EMENTAL INFORMATION FOR CHAPTER 4	7

CHAPTER 1

INTRODUCTION

Petroleum-Based Plastics

Plastics are used in virtually every area of modern society and are ubiquitous, both as valuable products and as undesirable environmental pollutants. ¹⁻⁴ As the scope of use of these materials increases, so does the necessity to synthesize more plastics and other polymers. Nearly all estimates suggest that the production and use of plastics will continually increase, roughly proportional to the increase of population over the next 50 years.⁵ A concerning factor is the feedstocks required for plastic production are nearly derived from petroleum sources. While petroleum is currently an abundant and inexpensive resource, its use as transportation fuel, chemical precursors, and other applications will eventually dwindle its supply. 6 As this occurs, the cost of petroleum, and its resultant products, will increase. In anticipation of this, significant work has been done to reduce the current reliance on petroleum as a feedstock for the most abundant commodities, especially polymers. In the last decade, numerous advances have been accomplished in the synthesis and development of polymers derived from sustainable resources such as fermentation, plant-derived biomass, carbon dioxide-derived polymers, and many other sources.⁷⁻⁹ These bioderived, or "biobased" polymers can offer competitive performance to petroleum-based polymers, while offering a long-term solution to the anticipated challenges of solely-petroleum based feedstocks. 10, 11

Biobased Aliphatic Polyesters

Figure 1.1: Common aliphatic polyesters including poly(4-hydroxybutyrate) (PHB), poly(lactic acid) (PLA) and poly(butylene succinate) (PBS).

In recent years, many commercially viable biobased polymers have been introduced that have properties suitable for use in a variety of industries. Polyhydroxyalkanoates (PHAs), a large class of copolymers derived from fermentation products of engineered bacteria, have been extensively investigated as alternatives to various petroleum-based polymers. ¹² Numerous applications have been demonstrated in the single-use packaging sphere, with some commercial success as well. ^{13, 14} PHAs also have the advantage of being biodegradable in many environments, including industrial composting, soil, and marine environments. However, the relatively poor thermal stability of PHAs poses significant challenges to production, which has been continually investigated by a multitude of groups and research efforts to overcome. ¹⁵⁻¹⁸

Poly (butylene dicarboxylate)s are available commercially with good thermal and mechanical properties. ¹⁹ However, although these products are completely biobased, they usually degrade very slowly outside of industrial composting settings. ^{20, 21} Considering that many plastics end up in the environment (soil, marine, and others), and that the United States has very little industrial composting infrastructure, this is considered a disadvantage of this class of materials that should be considered.

Likely the most abundant biobased polyester in the commercial market today is poly(lactic acid) (PLA). Derived from a variety of fermentation products, and especially from those of corn products, PLA is available in a number of grades from several commercial suppliers. PLA is available in a number of grades from several commercial suppliers. The various grades (based on the comonomer ratios of *D*-, *L*-, *or meso*-lactide) can tune crystallinity, mechanical properties, and thermal properties. A significant number of single-use commercial products have been produced from PLA including various food packaging items, cutlery, beverage containers, and more. However, as with poly (butylene dicarboxylate)s, a significant disadvantage exists with PLAs in that they are only compostable in industrial conditions. Despite their ubiquity (and often ambiguous descriptions of composability), PLAs require higher temperatures to initiate hydrolytic degradation. Only once a sufficiently low molecular weight is achieved can PLAs begin to degrade through microbial action. Because of this, most PLA items that are discarded into the environment will persist for many years.

Biobased Semi-Aromatic Polymers: PBAT

$$\mathsf{P}\left(\mathsf{O}\left(\mathsf{I}\left(\mathsf{O}\left(\mathsf{I}\left(\mathsf{O}\left(\mathsf{I}\right)\right)\right)\right)\right)$$

Figure 1.2: Structure of poly(butylene adipipate-*co*-terephthalate).

The above polyesters represent some of the most common and most relevant aliphatic polyesters available on the market today. However, it may be noted that there are relatively few examples of biobased and biodegradable polyesters on the commercial market that contain aromatic moieties. Likely the most commercially relevant example of a biobased aromatic

polyester is poly (butylene-adipate-*co*-terephthalate) (PBAT), which has a variety of trade names such as Ecoflex, Ecoworld, Eastar-Bio, and others. ²⁵ PBAT contains adipic acid and butylene glycol comonomers, which can be bioderived from fermentation and other processes. ^{26, 27} The polymer exhibits very good mechanical properties, excellent thermal stability for processing, and can be used in a variety of applications. ^{28, 29} Additionally, PBAT has the advantage of being compostable in many different environments, including industrial composting, home composting, and soil environments. ²⁵ However, despite the excellent performance of PBAT in both application and end-of-life, it is only considered partially biobased. Adipic acid is generally made through the oxidation of cyclohexanol, a petroleum byproduct. While some companies have developed biobased adipic acid (namely Toray Industries, Inc.), most adipic acid comes from petroleum sources as well. Most importantly, however, almost all TPA is currently made from petroleum sources.

Significant effort has been undertaken to develop bio-derived TPA, namely through the production of bio-based *p*-xylene (PX) which can undergo subsequent oxidation to yield bio-TPA. Recent efforts have included utilizing the Amoco process using isobutanol and 5-hydroxymethylfurfural to generate bio-PX, which can subsequently undergo oxidation to generate bio-TPA. Other efforts incorporate the Diels-Alder reaction of 2,5-dimethylfuran and ethylene, followed by subsequent dehydration to yield bio-PX. Although these processes show significant promise, there is still little adoption of bio-TPA, and therefore the production of fully biobased PBAT is extremely limited.

Biobased Semi-Aromatic Polymers: PEF

Figure 1.3: Structure of poly(ethylene furan-2,5-dicarboxylate) (PEF).

Other polymers of interest are poly-(alkyl)-2,5-furandicarboxylates such as poly(ethylene)2,5-furandicarboxylate (PEF). PEF is touted as a drop-in replacement for PET in terms of thermal and mechanical processing. Besides being completely biobased, PEF has excellent mechanical properties that lend it well to be used in beverage bottle and food packaging applications. Additionally, PEF has improved barrier properties in comparison to PET, attributed to the heteroatom oxygen in the aromatic furan moiety. However., the cost-competitive scale-up of PEF has proven to be a challenge. Primarily spearheaded by Avantium, PEF production has been an ongoing development for several years. Although large-scale production Avantium's FDCA was promised in 2024, production and application is still only accomplished in relatively small quantities.

Lignin as an Aromatic Feedstock

Figure 1.4: Generic structure of lignin

Because of the shortcomings in biobased aromatic polyesters available on the market today, it was of interest in our group to pursue novel feedstocks of polyesters that can contain aromatic moieties. When considering natural sources of aromatics, the first polymer that may be considered is lignin, as it is the second-most abundant biopolymer except cellulose.³⁴ Found in the cell walls of woody plants, most lignin is currently extracted as a waste product at paper pulping plants and subsequently burned for energy recovery. ³⁵⁻³⁷ With regards to polymeric structure, lignin is a large, three-dimensional polymer network that is heavily branched with significant irregularities present. ³⁸ The primary repeat units are phenylpropanoid units, with the most abundant segments being directly related to coumaryl alcohol, coniferyl alcohol, and sinapyl alcohols. Although much research has already been conducted using lignin directly in

polymers, the biological source of the lignin biomass directly impacts the ratio of comonomers, which can impact the properties of the resultant polymer blend. ^{35, 39-47}

Because of the inconsistencies in virgin lignin biomass, ⁴⁸ significant work has been done to "crack" lignin into its monomers (called "monolignols") *via* a number of depolymerization strategies. ⁴⁹⁻⁵¹ Potentially the most important of these strategies is hydrogenolysis, which uses a number of catalysts to cleave C-O and C-C bonds present in the lignin biomass. ^{46, 52} Another critical step is the oxidative depolymerization of lignin, which can be accomplished using a variety of techniques and abundant oxidizers, including oxygen. ^{42, 53} Alkaline hydrolysis techniques are also critical to cleave the phenolic backbones of lignin, lending it to further be depolymerized by other strategies such as those utilizing enzymes. ^{36, 54} With the increasing efforts toward more efficient depolymerization strategies of lignin, the use of monolignol-based polymers is an attractive route to biobased semi-aromatic polyesters.

Objectives

In previous work, several semi-aromatic polyesters have been synthesized from lignin-derived monomers. 49-51 This work seeks to expand upon this class of materials with various contributions and polymeric enhancements. First, the complete synthesis of a large class of biobased elastomers will be described. Complete characterization, including thermal, mechanical, and rheological properties will be conducted and reported. Novel polyesters will be compared for the structure-property relationships that can be attributed to iterative permutations of polymeric structure.

In the second section, the improvement of elastomeric behavior of the novel polyester $poly-\alpha$ -butylene-phloretate will be discussed using crosslinkers derived wholly from biobased

sources. Phloretic acid and erythritol dicarbonate will be utilized as completely bio-dervived starting materials to make an AABB crosslinker that can easily be incorporated into the polyester backbone. Likewise, a crosslinker based on 4,4' dihydroxy truxillic acid will be described, which is similarly derived entirely from molecules that can be sustainably sourced. Modifications to rheological and mechanical properties will be described, as well as a method for very small scale polycondensation reactions that can yield high molecular weight polyesters.

Finally, structure-property relationships of three lignin-derived polyesters, as well as their copolymers with ε-caprolactam and 11-amino undecanoic acid will be described.

Copolymerization of these esters with the biobased and potentially biobased aminoacids will yield novel, semi-aromatic poly(ester amide)s that are designed to exhibit high mechanical performance and exceptional thermal stability.

References

- (1) Wei, X.-F.; Yang, W.; Hedenqvist, M. S. Plastic pollution amplified by a warming climate. *Nature Communications* **2024**, *15* (1), 2052. DOI: 10.1038/s41467-024-46127-9.
- (2) Geyer, R.; Jambeck, J. R.; Law, K. L. Production, use, and fate of all plastics ever made. *Science Advances* **2017**, *3* (7), e1700782. DOI: doi:10.1126/sciadv.1700782.
- (3) Ostle, C.; Thompson, R. C.; Broughton, D.; Gregory, L.; Wootton, M.; Johns, D. G. The rise in ocean plastics evidenced from a 60-year time series. *Nature Communications* **2019**, *10* (1), 1622. DOI: 10.1038/s41467-019-09506-1.
- (4) MacLeod, M.; Arp, H. P. H.; Tekman, M. B.; Jahnke, A. The global threat from plastic pollution. *Science* **2021**, *373* (6550), 61-65. DOI: doi:10.1126/science.abg5433.
- (5) OECD. Global Plastics Outlook: Policy Scenarios to 2060. *OECD Publishing* **2022**. DOI: https://doi.org/10.1787/aa1edf33-en. .
- (6) Miller, R. G.; Sorrell, S. R. The future of oil supply. *Philos Trans A Math Phys Eng Sci* **2014**, *372* (2006), 20130179. DOI: 10.1098/rsta.2013.0179 From NLM.
- (7) Miller, S. A. Sustainable Polymers: Opportunities for the Next Decade. *ACS Macro Lett* **2013**, *2* (6), 550-554. DOI: 10.1021/mz400207g From NLM PubMed-not-MEDLINE.
- (8) Rosenboom, J.-G.; Langer, R.; Traverso, G. Bioplastics for a circular economy. *Nature Reviews Materials* **2022**, *7* (2), 117-137. DOI: 10.1038/s41578-021-00407-8.
- (9) The multifaceted challenges of bioplastics. *Nature Reviews Bioengineering* **2024**, *2* (4), 279-279. DOI: 10.1038/s44222-024-00181-6.

- (10) Cywar, R. M.; Rorrer, N. A.; Hoyt, C. B.; Beckham, G. T.; Chen, E. Y. X. Bio-based polymers with performance-advantaged properties. *Nature Reviews Materials* **2022**, *7* (2), 83-103. DOI: 10.1038/s41578-021-00363-3.
- (11) Xie, Y.; Gao, S.; Zhang, D.; Wang, C.; Chu, F. Bio-based polymeric materials synthesized from renewable resources: A mini-review. *Resources Chemicals and Materials* **2023**, *2* (3), 223-230. DOI: https://doi.org/10.1016/j.recm.2023.05.001.
- (12) Reddy, C.; Ghai, R.; Kalia, V. C. Polyhydroxyalkanoates: an overview. *Bioresource technology* **2003**, *87* (2), 137-146.
- (13) Ferri, M.; Papchenko, K.; Degli Esposti, M.; Tondi, G.; De Angelis, M. G.; Morselli, D.; Fabbri, P. Fully Biobased Polyhydroxyalkanoate/Tannin Films as Multifunctional Materials for Smart Food Packaging Applications. *ACS Applied Materials & Interfaces* **2023**, *15* (23), 28594-28605. DOI: 10.1021/acsami.3c04611.
- (14) Li, Z.; Yang, J.; Loh, X. J. Polyhydroxyalkanoates: opening doors for a sustainable future. *NPG Asia Materials* **2016**, *8* (4), e265-e265. DOI: 10.1038/am.2016.48.
- (15) Montano-Herrera, L.; Pratt, S.; Arcos-Hernandez, M. V.; Halley, P. J.; Lant, P. A.; Werker, A.; Laycock, B. In-line monitoring of thermal degradation of PHA during melt-processing by Near-Infrared spectroscopy. *New Biotechnology* **2014**, *31* (4), 357-363. DOI: https://doi.org/10.1016/j.nbt.2013.10.005.
- (16) Furutate, S.; Kamoi, J.; Nomura, C. T.; Taguchi, S.; Abe, H.; Tsuge, T. Superior thermal stability and fast crystallization behavior of a novel, biodegradable α-methylated bacterial polyester. *NPG Asia Materials* **2021**, *13* (1), 31. DOI: 10.1038/s41427-021-00296-x.

- (17) Carrasco, F.; Dionisi, D.; Martinelli, A.; Majone, M. Thermal stability of polyhydroxyalkanoates. *Journal of Applied Polymer Science* **2006**, *100* (3), 2111-2121. DOI: https://doi.org/10.1002/app.23586.
- (18) Larsson, M.; Markbo, O.; Jannasch, P. Melt processability and thermomechanical properties of blends based on polyhydroxyalkanoates and poly (butylene adipate-co-terephthalate). *RSC* advances **2016**, *6* (50), 44354-44363.
- (19) Aliotta, L.; Seggiani, M.; Lazzeri, A.; Gigante, V.; Cinelli, P. A Brief Review of Poly (Butylene Succinate) (PBS) and Its Main Copolymers: Synthesis, Blends, Composites, Biodegradability, and Applications. *Polymers (Basel)* **2022**, *14* (4). DOI: 10.3390/polym14040844 From NLM.
- (20) Kim, J.; Park, S.; Jung, S.; Yun, H.; Choi, K.; Heo, G.; Jin, H.-J.; Park, S.; Kwak, H. W. Biodegradation behavior of polybutylene succinate (PBS) fishing gear in marine sedimentary environments for ghost fishing prevention. *Polymer Degradation and Stability* **2023**, *216*, 110490. DOI: https://doi.org/10.1016/j.polymdegradstab.2023.110490.
- (21) Peñas, M. I.; Pérez-Camargo, R. A.; Hernández, R.; Müller, A. J. A Review on Current Strategies for the Modulation of Thermomechanical, Barrier, and Biodegradation Properties of Poly (Butylene Succinate) (PBS) and Its Random Copolymers. *Polymers* **2022**, *14* (5), 1025.
- (22) Sin, L. T.; Tueen, B. S. *Polylactic acid: a practical guide for the processing, manufacturing, and applications of PLA*; William Andrew, 2019.
- (23) Hussain, M.; Khan, S. M.; Shafiq, M.; Abbas, N. A review on PLA-based biodegradable materials for biomedical applications. *Giant* **2024**, *18*, 100261. DOI: https://doi.org/10.1016/j.giant.2024.100261.

- (24) Zaaba, N. F.; Jaafar, M. A review on degradation mechanisms of polylactic acid: Hydrolytic, photodegradative, microbial, and enzymatic degradation. *Polymer Engineering & Science* **2020**, *60* (9), 2061-2075. DOI: https://doi.org/10.1002/pen.25511.
- (25) Jian, J.; Xiangbin, Z.; Xianbo, H. An overview on synthesis, properties and applications of poly(butylene-adipate-co-terephthalate)–PBAT. *Advanced Industrial and Engineering Polymer Research* **2020**, *3* (1), 19-26. DOI: https://doi.org/10.1016/j.aiepr.2020.01.001.
- (26) Toray Invents 100% Bio-Based Adipic Acid from Sugars Derived from Inedible Biomass, Scaling Up for Application to Eco-Friendly Nylon 66. Toray Industries, 2022. (accessed 2024 November 4th).
- (27) Guo, H.; Liu, H.; Jin, Y.; Zhang, R.; Yu, Y.; Deng, L.; Wang, F. Advances in research on the bio-production of 1,4-butanediol by the engineered microbes. *Biochemical Engineering Journal* **2022**, *185*, 108478. DOI: https://doi.org/10.1016/j.bej.2022.108478.
- (28) Roy, S.; Ghosh, T.; Zhang, W.; Rhim, J.-W. Recent progress in PBAT-based films and food packaging applications: A mini-review. *Food Chemistry* **2024**, *437*, 137822. DOI: https://doi.org/10.1016/j.foodchem.2023.137822.
- (29) Elkholy, H. M.; Hamdani, S. S.; Alghaysh, M. O.; Wyman, I.; Duncan, E.; Wang, Y.; Li, K.; Rabnawaz, M. Design of Carboxylic Acid-Functionalized Poly(Butylene Adipate-co-Terephthalate) for Recyclable and Biodegradable Zero-Waste Paper Packaging. *Advanced Sustainable Systems* **2025**, *9* (1), 2400621. DOI: https://doi.org/10.1002/adsu.202400621. (30) Tomás, R. A. F.; Bordado, J. C. M.; Gomes, J. F. P. p-Xylene Oxidation to Terephthalic Acid: A Literature Review Oriented toward Process Optimization and Development. *Chemical Reviews* **2013**, *113* (10), 7421-7469. DOI: 10.1021/cr300298j.

- (31) Volanti, M.; Cespi, D.; Passarini, F.; Neri, E.; Cavani, F.; Mizsey, P.; Fozer, D. Terephthalic acid from renewable sources: early-stage sustainability analysis of a bio-PET precursor. *Green Chem* **2019**, *21* (4), 885-896.
- (32) Loos, K.; Zhang, R.; Pereira, I.; Agostinho, B.; Hu, H.; Maniar, D.; Sbirrazzuoli, N.; Silvestre, A. J.; Guigo, N.; Sousa, A. F. A perspective on PEF synthesis, properties, and end-life. *Frontiers in chemistry* **2020**, *8*, 585.
- (33) Wu, F.; Misra, M.; Mohanty, A. K. Challenges and new opportunities on barrier performance of biodegradable polymers for sustainable packaging. *Progress in Polymer Science* **2021**, *117*, 101395. DOI: https://doi.org/10.1016/j.progpolymsci.2021.101395.
- (34) Vermaas, J. V.; Crowley, M. F.; Beckham, G. T. Molecular Lignin Solubility and Structure in Organic Solvents. *ACS Sus. Chem. Eng.* **2020**, *8* (48), 17839-17850. DOI: 10.1021/acssuschemeng.0c07156.
- (35) Sun, Z.; Fridrich, B.; De Santi, A.; Elangovan, S.; Barta, K. Bright side of lignin depolymerization: toward new platform chemicals. *Chemical reviews* **2018**, *118* (2), 614-678.
- (36) Pollegioni, L.; Tonin, F.; Rosini, E. Lignin-degrading enzymes. *Febs j* **2015**, *282* (7), 1190-1213. DOI: 10.1111/febs.13224 From NLM.
- (37) Fang, Z.; Smith, J. R. L. *Production of Biofuels and Chemicals from Lignin*, 1st ed.; Springer Singapore: Imprint: Springer,, 2016. DOI: 10.1007/978-981-10-1965-4.
- (38) Zhong, R.; Cui, D.; Ye, Z.-H. Secondary cell wall biosynthesis. *New Phytologist* **2019**, *221* (4), 1703-1723. DOI: https://doi.org/10.1111/nph.15537.
- (39) Martínková, L.; Grulich, M.; Pátek, M.; Křístková, B.; Winkler, M. Bio-Based Valorization of Lignin-Derived Phenolic Compounds: A Review. *Biomolecules* **2023**, *13* (5), 717.

- (40) Qiang, H.; Wang, J.; Liu, H.; Zhu, Y. From vanillin to biobased aromatic polymers. *Polymer Chemistry* **2023**, *14* (37), 4255-4274.
- (41) Libretti, C.; Correa, L. S.; Meier, M. A. From waste to resource: advancements in sustainable lignin modification. *Green Chem* **2024**.
- (42) Andriani, F.; Lawoko, M. Oxidative Carboxylation of Lignin: Exploring Reactivity of Different Lignin Types. *Biomacromolecules* **2024**.
- (43) Subbotina, E.; Souza, L. R.; Zimmerman, J.; Anastas, P. Room temperature catalytic upgrading of unpurified lignin depolymerization oil into bisphenols and butene-2. *Nature Communications* **2024**, *15* (1), 5892. DOI: 10.1038/s41467-024-49812-x.
- (44) Hafezisefat, P.; Qi, L.; Brown, R. C. Lignin Depolymerization and Esterification with Carboxylic Acids to Produce Phenyl Esters. *ACS Sus. Chem. Eng.* **2023**, *11* (48), 17053-17060. DOI: 10.1021/acssuschemeng.3c05221.
- (45) Upton, B. M.; Kasko, A. M. Strategies for the Conversion of Lignin to High-Value Polymeric Materials: Review and Perspective. *Chemical Reviews* **2016**, *116* (4), 2275-2306. DOI: 10.1021/acs.chemrev.5b00345.
- (46) Tana, T.; Zhang, Z.; Beltramini, J.; Zhu, H.; Ostrikov, K. K.; Bartley, J.; Doherty, W. Valorization of native sugarcane bagasse lignin to bio-aromatic esters/monomers via a one pot oxidation–hydrogenation process. *Green Chem* **2019**, *21* (4), 861-873.
- (47) Kim, S.; Chung, H. Biodegradable Polymer: From Synthesis Methods to Applications of Lignin-graft-Polyester. *Green Chem* **2024**.
- (48) Ana, L.; Helena, P. Compositional Variability of Lignin in Biomass. In *Lignin*, Matheus, P. Ed.; IntechOpen, 2017; p Ch. 3.

- (49) Mialon, L.; Vanderhenst, R.; Pemba, A. G.; Miller, S. A. Polyalkylenehydroxybenzoates (PAHBs): Biorenewable aromatic/aliphatic polyesters from lignin. *Macromolecular Rapid Communications* **2011**, *32* (17), 1386-1392.
- (50) Winfield, D.; Ring, J.; Horn, J.; White, E. M.; Locklin, J. Semi-aromatic biobased polyesters derived from lignin and cyclic carbonates. *Green Chem* **2021**, *23* (23), 9658-9668. DOI: 10.1039/d1gc03135j.
- (51) Xanthopoulou, E.; Terzopoulou, Z.; Zamboulis, A.; Koltsakidis, S.; Tzetzis, D.; Peponaki, K.; Vlassopoulos, D.; Guigo, N.; Bikiaris, D. N.; Papageorgiou, G. Z. Poly(hexylene vanillate): Synthetic Pathway and Remarkable Properties of a Novel Alipharomatic Lignin-Based Polyester. *ACS Sus. Chem. Eng.* **2023**, *11* (4), 1569-1580. DOI: 10.1021/acssuschemeng.2c06507.
- (52) Shen, Z.; Shi, C.; Liu, F.; Wang, W.; Ai, M.; Huang, Z.; Zhang, X.; Pan, L.; Zou, J. J. Advances in heterogeneous catalysts for lignin hydrogenolysis. *Advanced Science* **2024**, *11* (1), 2306693.
- (53) Abdelaziz, O. Y.; Clemmensen, I.; Meier, S.; Costa, C. A.; Rodrigues, A. E.; Hulteberg, C. P.; Riisager, A. On the Oxidative Valorization of Lignin to High-Value Chemicals: A Critical Review of Opportunities and Challenges. *ChemSusChem* **2022**, *15* (20), e202201232.
- (54) Zhou, H.; Wang, H.; Perras, F. A.; Naik, P.; Pruski, M.; Sadow, A. D.; Slowing, I. I. Two-step conversion of Kraft lignin to nylon precursors under mild conditions. *Green Chem* **2020**, *22* (14), 4676-4682.

CHAPTER 2

SYNTHESIS AND STRUCTURE-PROPERTY RELATIONSHIPS OF LIGNIN-DERIVED SEMI-AROMATIC POLY(ETHER ESTER)S.

1

Abstract

Semi-aromatic polyesters derived from petroleum are an important class of polymers that encompass a wide variety of thermal and mechanical properties. Unfortunately, replacing the aromatic component with cost-competitive bioderived monomers is an ongoing challenge. This work describes the synthesis of nine different polyesters made from AB monomers that can be derived from lignin, starting with phloretic, coumaric, and ferulic acids and similar derivatives. The polyesters were synthesized at >50g scale and full characterization of the thermal, mechanical, and rheological properties is included. The polymers exhibit excellent thermal stability, a Tg range of 16°C-65°C, tensile moduli ranging from 4.6 MPa to 1200 MPa, and elongation at break ranging from 7.5% to greater than 3800%. To examine the effects of structural permutations among the polymer series, TTS master curves were constructed for seven polyesters using melt rheology. Properties such as packing length and characteristic ratio are described and compared amongst the series. Finally, it is demonstrated that these polyesters are easily chemically recycled to monomer in high yield.

Introduction

The global demand for plastics continues to increase, making the search for alternative feedstocks more critical than ever.²⁻⁴ Traditionally derived from petroleum, plastics have seen an increasing shift toward production using renewable resources like fermentation products, vegetable oils, sugars, terpenes, lignocellulosics, and various waste products.⁵⁻⁷ Although a number of biobased aliphatic polyesters such as poly(hydroxyalkanoates)⁸, poly(lactic acid)⁹ and poly(butylene dicarboxylate)s¹⁰ are commercially available, there are few commercially-available polyesters containing biobased aromatic moieties. Two polymers of industrial interest are

poly(butylene adipate-*co*-butylene terephthalate) (PBAT)¹¹ and poly(ethylene furanoate) (PEF).¹² In the case of PBAT, the adipic acid and butylene glycol portions can be derived from fermentation, albeit at a higher cost than the oil-derived monomer at current scales.¹³⁻¹⁵ However, the production of biobased terephthalic acid poses significant challenges and production is mainly limited to the laboratory or pilot scale.¹⁶⁻¹⁸ Currently, biobased terephthalic acid is not used to produce PBAT. Biobased 2,5-furandicarboxylic acid (FDCA) can be produced through fermentation and other processes, enabling the production of fully biobased PEF, which is touted as a drop-in replacement for poly(ethylene terephthalate).¹⁹ However, widespread adoption of PEF has not yet occurred.

Another feedstock of particular interest is lignin – the most abundant source of natural aromatics.²⁰ Currently, lignin is a byproduct of the paper industry that is burned for energy recovery, with only about 0.2% being used for other purposes.²¹⁻²³ Lignin is a macromolecule found in the secondary cell wall of woody biomass, with a high concentration of aromatics with varying substitutions of pendant methoxy groups.²⁴ The use of lignin in polymeric materials is appealing due to its high strength, thermal stability, and its ability to provide a source of aromatic feedstock with diverse chemical architectures.^{21, 25-33} Extensive research has already been conducted to incorporate lignin directly in polymer blends, functionalize lignin for compatibility with polymer matrices, and directly polymerize oligomers of lignin.³⁴⁻³⁶

However, the biological origin of lignin directly influences its molecular structure, which can lead to performance inconsistencies in composites and blends that use it as a direct component.³⁷ For this reason, significant efforts have been undertaken to efficiently crack lignin into various "monolignols" and other small molecule byproducts *via* a number of depolymerization strategies.³⁸⁻⁴⁰ These monolignols, once isolated, can be chemically modified through traditional

methods and then used as precursors for small molecule and polymer synthesis.⁴¹⁻⁴⁶ Previous work has demonstrated that polymers possessing a broad range of thermal and mechanical properties can be synthesized from lignin-derived monomers.³⁸⁻⁴⁰ Slight changes to the monomer structure have a dramatic influence on the overall properties of the resulting polymer.

This work focuses on modifications and variations of common monolignols: coumaric, phloretic, and ferulic acids. Alkylation of the phenolic moiety was accomplished *via* the ring-opening of cyclic carbonates, which can be synthesized from biobased sources with carbon dioxide or through transcarbonation reactions.^{39, 47} These reactions are carried out under neat conditions, offering an advantage over traditional etherification reactions that require haloalcohols and organic solvents. This synthetic strategy closely adheres to the principles of green chemistry by maximizing the atom economy of reactions and minimizing waste,⁴⁸ while simultaneously accessing fully biobased monomers at 50-100g scale.

In previous work, we demonstrated that amorphous phloretate- and ferulate-based polymers have a broad range of properties.³⁹ From this, structural analogues were envisioned that could provide direct comparisons in terms of their thermal, mechanical, and rheological properties. In this study, the synthesis and comprehensive characterization of nine polymers is presented, each exhibiting various structural permutations designed to elucidate the effects of tacticity, substituents, structural isomerism, and regioisomerism on their properties. Furthermore, it is demonstrated that these polymers can be chemically recycled *via* base hydrolysis in rapid timeframes.

Materials and Methods

Materials:

Phloretic acid, ferulic acid, (*E*)-*p*-coumaric acid, propylene carbonate, potassium carbonate, chloroform-*d*, and DMSO-*d6* were purchased from Oakwood Chemical. Propionic anhydride was purchased from ThermoFisher Scientific. Sodium propionate and ethylene carbonate were purchased from Fisher Scientific. α-Butylene carbonate was purchased from Ambeed, Inc. 10% palladium on carbon was purchased from Sigma Aldrich. All other reagents and solvents were purchased from commercial suppliers and used as received without further purification.

Synthesis of Monomers and Polymers:

Starting hydroxycarboxylic acids were either purchased from commercial suppliers or synthesized. Subsequent protection *via* Fisher esterification and alkylation yielded nine monomers of suitable purity that were polymerized in good to excellent yields by polycondensation. Detailed synthetic procedures and characterization for each compound is included in the Supporting Information.

Polyester synthesis was conducted in a 3-neck flask, with the volume being either 100 mL or 200 mL depending on the amount of monomer used. Sb₂O₃ was added to the flask, at 1 mol % relative to monomer, and 1000 ppm of 4-methoxyphenol to reduce undesired oxidation and darkening of the polymer. After the addition of the monomer, catalyst, and antioxidant, the flask was fitted with an internal thermocouple, a mechanical stirrer with an SP Bel-Art ® Safe-Lab bearing, and a short-path distillation head. The entire contents were then evacuated to <100 mTorr

and backfilled three times with dry nitrogen. Under a nitrogen atmosphere, the flask was heated from 160 °C to 220 °C at a rate of 10 °C/h with a heating mantle while stirring at 250 rpm. Once the final temperature was reached, vacuum was slowly applied to the flask over 15 minutes until the pressure reached <200 mTorr. The stirring was reduced to 150 rpm and the vacuum was held constant until the flask contents were too viscous to have efficient mixing. After this, the polymers were removed from the flask under nitrogen onto silicone release paper and collected in quantitative yields.

Molecular Weight and Structural Characterization:

¹H NMR spectra were recorded at room temperature with a Bruker Avance Neo 600 MHz instrument (USA) at a concentration of 10 mg/mL. Peak shifts in parts per million (ppm) were reported relative to the signal of chloroform-*d* at 7.26 ppm or DMSO-*d*6 at 2.50 ppm. ¹³C NMR spectra were recorded at room temperature with a Bruker Avance II 400 MHz instrument (USA) at a concentration of 10 mg/mL. Peak shifts in parts per million (ppm) were reported relative to the signal of chloroform-*d* at 77.16 ppm or DMSO-*d*6 at 39.52 ppm.

Molecular weight and dispersity (*Đ*) analyses were conducted on a Malvern OMNISEC RESOLVE gel permeation chromatography system (USA) with a refractometer detector. Samples were dissolved in HPLC-grade chloroform at a concentration of 1 mg/mL and filtered through a 0.2 μm PTFE filter before injection. Viscotek® T-Series Columns (T3000, T4000, and T6000) columns were regulated at 35 °C and were eluted with HPLC-grade chloroform at a rate of 1 mL/min. The resulting molecular weight data is reported relative to polystyrene standards.

Thermal Characterization:

Differential scanning calorimetry (DSC) analysis was conducted on a Discovery DSC 250 (TA Instruments, USA) differential scanning calorimeter equipped with an RCS 90 cooling system (TA Instruments, USA) under a 50 mL/min nitrogen purge. The samples (4–7 mg) were enclosed in aluminum T-zero pans. Samples were first heated from –20 °C to 200 °C at 10 °C/min to erase thermal history. Samples were subsequently cooled to –20 °C at 10 °C/min, followed by a second heating step to 200 °C at 10 °C/min. DSC data was reported from the second heating curve unless otherwise noted.

Thermal stability was quantified using thermogravimetric analysis (TGA) on a Discovery TGA (TA Instruments, USA). Approximately 7-12 mg of sample was heated from room temperature to 600 °C at 10 °C/min under a nitrogen atmosphere.

Injection Molding and Mechanical Characterization:

Melt extrusion was conducted using a Thermo-Fischer Haake Minilab II (USA) twin screw extruder and samples were injection molded using a Thermo-Fischer Haake Minijet Pro (USA) injection molding system. The polyesters were extruded at $T_g + 100$ °C and injection molded following optimized conditions (Table S1) into ASTM D638 Type V tensile specimens with magnesium stearate as a mold release agent.

Tensile performance of polyesters was evaluated using a Shimadzu AGS-X Universal Testing Machine (USA). Samples were tested at 25.3 ± 0.3 °C with a rate of 20 mm/min and data reported is the statistical average of 3 specimens. Poly(α -butylene phloretate) specimens were tested at 100 mm/min due to the high % elongation at break. All other polymers were tested at 20 mm/min using ASTM D638.⁴⁹ Note that not all samples broke within the required 5 min period.

Gel Content Characterization:

The gel content of the polyesters was determined using Soxhlet extraction. Thimbles were stored in a room with 50% humidity before being weighed. Polymer was added to the thimble, and the final mass was recorded before subjecting to continuous extraction over 24 hours in chloroform. The thimble was then dried for 24 hours at 60 °C under vacuum. The thimble was allowed to equilibrate for 24 hours in the same room with a relative humidity of 50 % before the final mass was analyzed. The insoluble catalyst was assumed to be uniformly distributed throughout the polymer, and the theoretical catalyst mass was subtracted from the final calculation.

Rheological Characterization:

Rheological experiments were conducted on a TA Instruments Discovery Hybrid Rheometer (USA) using a 25 mm parallel plate geometry with a 2100 μ m trim gap and a 2000 μ m running gap. A series of frequency sweeps at 1% oscillatory strain were conducted at temperature ranges from 120 °C – 25 °C with oscillation frequencies from 600 – 0.1 rads/s to construct corresponding time-temperature superposition (TTS) master curves. These master curves were used to investigate the entanglement molecular weight (M_e), packing length (p), and characteristic ratio (C_∞) each polyester. PEMC and PiPC were excluded from analysis due to the absence of a crossover point.

Melt densities of the polymers were measured using a Tinius Olsen MP1200, with a load weight of 2.16 kg, a travel distance of 6.35 cm, and a total of 3 captures for each polymer. The analysis temperature was optimized according to the polymer viscosity in the melt. The melt densities of PiPP, (*R*)-PiPP, and PiPHF were measured at 90 °C; *o*-PiPP and PEMP were measured at 80 °C; PiPMP and PαBP were measured at 60 °C.

Chemical Recycling to Monomer Study:

The polymer recyclability was demonstrated using (R)-PiPP. 75.0 g of (R)-PiPP ($M_w = 29.0 \text{ kDa}$, D: 1.4) was added to 750 mL of 2 M KOH in a solution of 2:1 water:ethanol in a 2 L steel pressure vessel (Series 4350; Parr Instrument Company, USA). The mixture was heated to 150 °C for 60 minutes with stirring before being cooled to room temperature. The resulting solution was filtered, cooled to 5 °C, and then acidified with 6 M HCl to pH = 2 resulting in a white precipitate of (R)-isopropyl phloretate ((R)-iPP). The precipitate was filtered and dried in a vacuum oven at 60 °C for 24 h to yield 70.1 g of a tan powder (80%). After this, 55 g of the recycled (R)-iPP was added to a 100 mL 3-neck flask and the previously described synthesis was followed to yield the polymer ($M_w = 42.2 \text{ kDa}$, D: 1.5).

Results and Discussion

Monomer Synthesis

Each of the starting hydroxycarboxylic acids in this study were derived wholly from lignin derived compounds or synthesized from precursors that can be extracted from lignin. In the case of phloretic acid and (*E*)-*p*-coumaric acid, the starting materials were available from commercial suppliers. The remaining four hydroxycarboxylic acids were accessed through high-yielding, scalable transformations, such as the Perkins condensation, Fisher esterification, or palladium-catalyzed hydrogenations, and were conducted at greater than 100 g scale. A summary of the commercially available and synthesized starting carboxylic acids is shown in Figure 2.1.

Figure 2.1: Commercially available (green) and synthesized (blue) hydroxycarboxylic acids used in this study.

Hydroxycarboxylic acids were protected via Fisher esterification in excellent to quantitative yields before being alkylated through the ring opening of cyclic carbonates (Scheme 2.1). Selected cyclic carbonates include biobased ethylene and propylene carbonates, alongside α -butylene carbonate, which is currently petroleum-derived. This synthetic strategy closely adheres to the principles of green chemistry, being highly atom-efficient while simultaneously avoiding the use of hazardous solvents and alkyl halides that are commonly used in phenolic alkylations.

1.
$$R_{1} = H, OMe$$

$$R_{2} = H, CH_{3}$$

$$R_{3} = H, CH_{3}, CH_{2}CH_{3}$$
1.1 eq. O

$$R_{3}$$

$$R_{4} = H, OMe$$

$$R_{2} = H, CH_{3}$$

$$R_{3} = H, CH_{3}, CH_{2}CH_{3}$$

Scheme 2.1: Synthesis of lignin-derived monomers using cyclic carbonates.

Polymer Synthesis:

Polymerization was conducted using melt-polycondensation with antimony trioxide (Sb₂O₃) as a catalyst. Sb₂O₃ is resistant to poisoning from water evolved over the course of the reaction and has sufficient catalytic activity to produce polyesters with molecular weights high enough to perform mechanical and rheological analysis.⁵⁰ High temperatures and prolonged reaction times can cause darkening of all polymers; therefore, 1000 ppm of MEHQ was added to each reaction as an antioxidant.

Significant variations in reaction times were observed in the polymerization of different monomers. It is well known that steric hinderance of substrates at or near the point of esterification will reduce the rate at which the reaction occurs. Consequently, the reaction durations required to produce high-viscosity polymer melts were extended up to 15 hours of *in vacuo* polycondensation. This was specifically observed for poly(isopropyl methylphloretate) (PiPMC), which has sterically bulky groups on both the alcohol and α -position of the carboxylic acid (Scheme 2.2).

Scheme 2.2: General synthesis of the polyesters by antimony-catalyzed melt polycondensation.

Table 2.1: Summary of thermal and mechanical data obtained for the polyesters in this study, including glass transition temperature (T_g), onset of degradation ($T_{d95\%}$), Young's Modulus (E), elongation at break (ε_b), and yield stress (σ_y).

Polymer	T _g (°C)	T _{d95%} (°C)	E (MPa)	ε _b (%)	σ _y (MPa)
PiPP	25	360	436 ±32	843 ± 71	1.11 ± 0.07
o-PiPP	27	360	864 ± 302	400 ± 45	7.18 ± 0.78
(R)-PiPP	25	328	644 ± 230	355 ± 36	1.80 ± 0.63

PEMP	21	415	4.6 ± 0.9	357 ± 37	n.d.
PiPMP	26	371	672 ± 80	886 ± 140	0.63 ± 0.17
ΡαΒΡ	16	378	7.3 ± 0.3	> 3800*	0.18 ± 0.12
PiPHF	29	372	1056 ± 114	188 ± 3.1	6.49 ± 0.06
PEMC	55	374	1200 ± 98	7.5 ± 2.5	10.6 ± 3.6
PiPC	65	363	n.d.	n.d.	n.d.

^{&#}x27;*' – indicates no sample rupture was observed; 'n.d.' – indicates that properties could not be determined.

Thermal Analysis:

Differential scanning calorimetry (DSC) was used to investigate thermal transitions of all polyesters (Table 2.1), which were found to be completely amorphous. Even in the case of isotactic (R)-PiPP, polymer melting transitions were never observed via DSC even after multiple attempts of annealing at different temperatures and inducing strain in the sample. The amorphous nature is likely due to the sterically-bulky isopropyl, α -butyl, and/or α -methylated groups of the polyesters, which appears to agree with the studies of other lignin-derived polymers. ^{39, 40} The glass transition temperatures (T_g) ranged from 16 °C – 29 °C among the polyesters that had saturated α - β -esters. The incorporation of unsaturated α - β -esters increased the T_g to 55 °C (PEMC) and 65 °C (PiPC) due to the rotational restrictions in the polymeric backbone.

The thermal stability of the polymers was investigated using thermogravimetric analysis (TGA). The polymers exhibited good thermal stability, with the lowest onset of degradation (5 % mass loss) being 328 °C ((R)-PiPP) and the highest being 415 °C (PEMP). Overall, the TGA data

indicated that the thermal stability of these materials was sufficient to be processed across a broad range of temperatures through melt extrusion and injection molding.

Mechanical Characterization

The mechanical performance of polyesters was evaluated through tensile testing of injected molded ASTM-D638 Type V dog bones. The polyesters exhibit significant variation in mechanical properties, ranging from brittle to extremely ductile. Due to the T_g of several polyesters being close to room temperature, the environmental conditions were carefully controlled to 25.3 ± 0.3 °C to avoid significant variation in properties. Figure 2 displays the wide array of mechanical properties observed in this study. The highest T_g polymer, PiPC, was too brittle to test and shattered immediately when attempts were made to secure the sample specimen to the testing machine.

The mechanical performance correlated with the T_g of the polyesters. PEMC, with a T_g of 55 °C, was a stiff polymer with a Young's modulus (E) of 1200 MPa and 7.5 % elongation at break (ϵ_b). As the T_g of the polyesters decreases, the ductility generally improves. PiPHF, with a T_g of 29 °C, exhibits an E of 1056 MPa and ϵ_b of 188 %, making it the highest-modulus polymer among those with α,β -unsaturated carboxylate groups. This is likely due to the increased rigidity imparted by the methoxy substituent. This trend continues with the decreasing T_g , with a decrease in E and increase in % ϵ for (R)-PiPP, o-PiPP, PEMP, PiPP, PiPMP, and P α BP (Table 2.1 and Figure 2.2). Remarkably, P α BP exhibited a relatively low modulus of 7.3 MPa but had an ϵ_b over 3800 %, reaching the travel limit of the tensile tester without sample fracture.

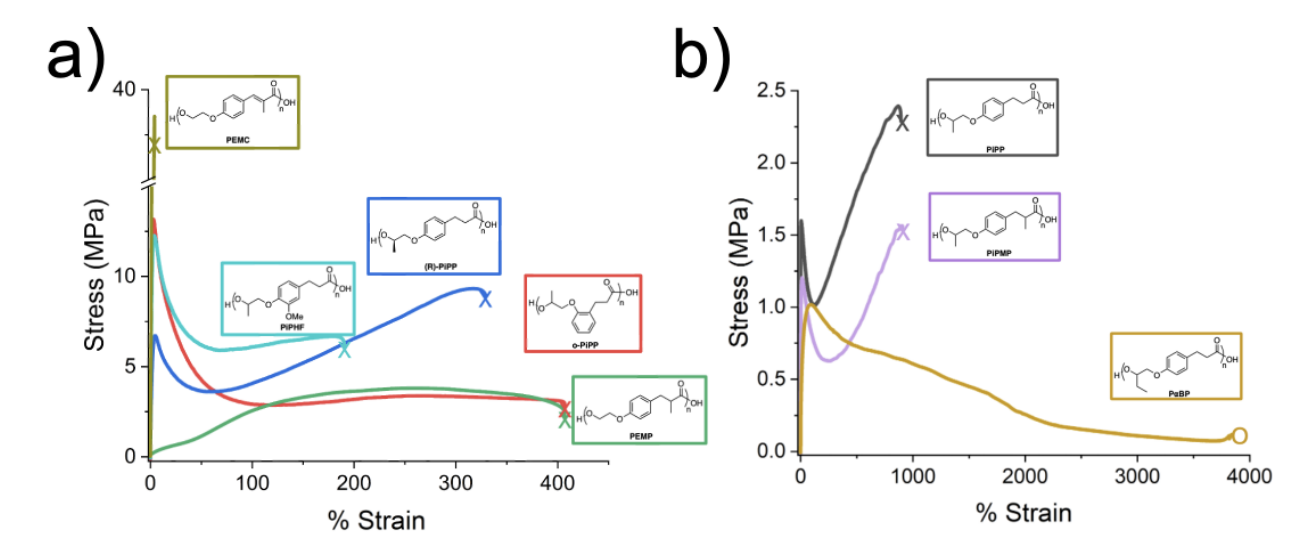


Figure 2.2: Mechanical properties of polyesters in this study. (a): Polymers with less than 500 % εb, (b): polyesters with greater than 500 % εb.

Gel Content and Rheological Characterization:

Melt rheology studies were conducted to explore how monomer structure influences the inherent properties of the polyesters. Time-temperature superposition (TTS) master curves were constructed for each polyester and comparing properties related to chain bulkiness and stiffness, such as packing length and characteristic ratio. Prior to rheological characterization, the gel content of each polyester was determined via Soxhlet extraction. Among the synthesized polyesters, only PEMC and PiPC had a gel content of \sim 6 % and \sim 36 %, respectively. This was likely the result of crosslinking between α , β -unsaturated carboxylic acids which is reported in derivatives of coumaric acid and cinnamic acid (Figure 2.3).⁵¹

Figure 2.3: Proposed thermal crosslinking reaction in PEMC and PiPC.

Due to the crosslinked nature of the polymers, the master curves for PEMC and PiPC were challenging to construct and were excluded from further rheological analysis. In contrast, the remaining seven polyesters exhibit crossover points in the TTS master curves (Error! Reference source not found and S2.3-S2.8). From the crossover modulus, the plateau modulus (G^0_N), entanglement molecular weight (M_e), packing length (p), and characteristic ratio (C_∞) can be estimated using established relationships. The plateau modulus can be estimated by finding the frequency of the loss modulus minimum and the "plateau" that occurs at this point. The storage modulus at the same frequency as the loss modulus minimum is described as the plateau modulus ($G^0_N = G'(\omega)_{G'' \to min}$). However, the polymers in this study exhibited little to no minimum in the loss modulus (Figure 2.4 and S2.3-S2.8), likely due to their relatively low molecular weights.

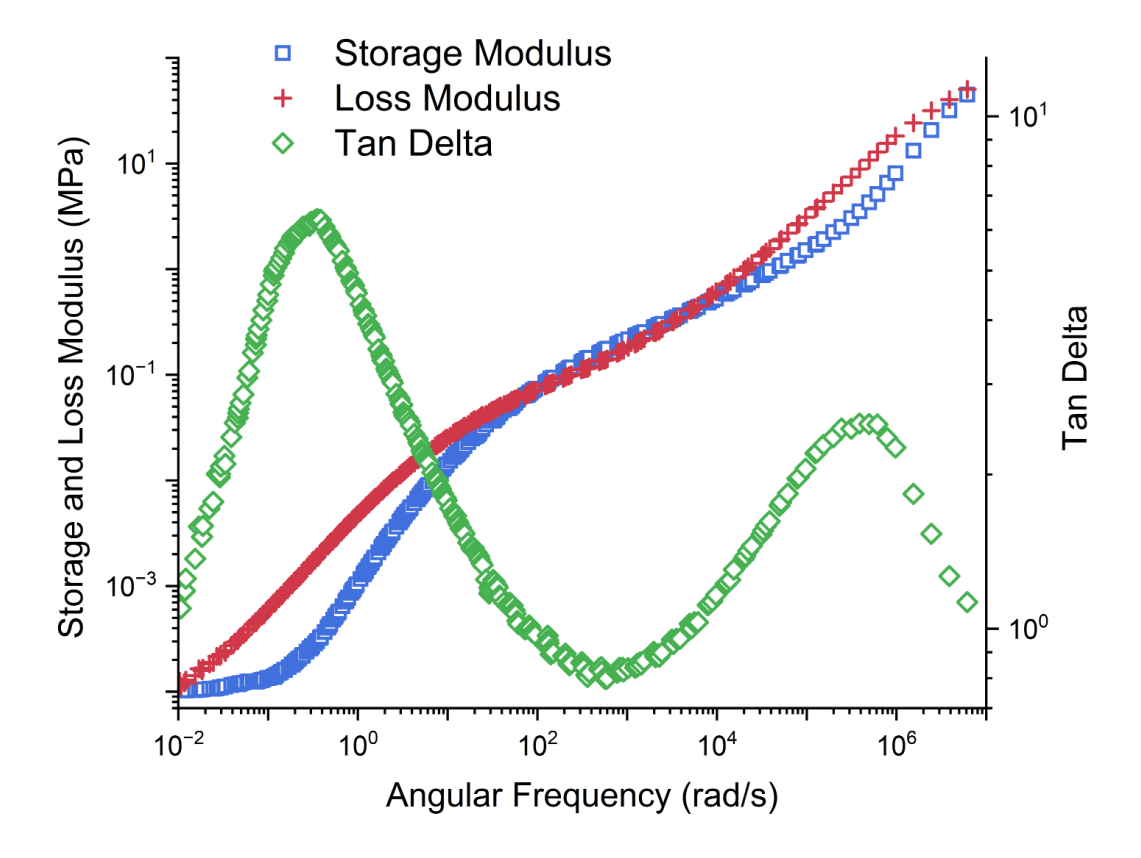


Figure 2.4: TTS master curve of PiPP.

Instead, the plateau modulus was estimated using two methods. First, the minimum of the $\tan(\delta)$ and the storage modulus at the same frequency $(G^0_{N \tan(\delta)} = G'(\omega)_{\tan(\delta) \to \min})$ was used.⁵² As an additional comparison, the crossover modulus $(G' = G'' = G_C)$ was used to solve for the plateau modulus according to the method proposed by Wu (Equation 2.1).⁵³ This method relates the crossover modulus and D to solve for G^0_N , which will be referred to as $G^0_{N,Wu}$.

$$\log\left(\frac{G_{N,Wu}^{0}}{G_{C}}\right) = 0.380 + \frac{2.63 \cdot \log(\Theta)}{1 + 2.45 \cdot \log(\Theta)}$$

Equation 2.1

In 1994, Fetters *et al.*^{54, 55} presented the following relationship between the plateau modulus G^{0}_{N} and entanglement molecular weight, M_{e}^{G} (Equation 2.2):

$$G_N^0 = \frac{4\rho RT}{5M_e^G}$$

Equation 2.2

From M_e^G and the experimentally determined melt density (ρ), the packing length (p) can also be determined (Equation 2.3):

$$\frac{M_e^G}{\rho} = 218p^3$$

Equation 2.3

The packing length is a measure of chain bulkiness and flexibility and describes how tightly or loosely a polymer can arrange itself, and the amount of space (in Å) required by a polymer chain in the melt between other chains. A higher packing length often indicates greater free volume around the polymer chain and is typically associated with a more flexible polymer backbone.

Finally, with the values above, it was possible to calculate the characteristic ratio (C_{∞}) of the polymers in this study using the following relationship (Equation 2.4):⁵⁶

$$C_{\infty} = \frac{10 \cdot \rho^{-2/3} \cdot M_e^{-1/3} \cdot M_b}{L^2}$$

Equation 2.4

Where ρ is the polymer melt density (determined using melt flow index), M_b is the relative molecular weight per backbone bond, and L is the length of each monomer unit (calculated using Chem 3D software).

The C_{∞} describes the ratio between the experimental end-to-end length of a polymer and that of the freely jointed chain model. A higher C_{∞} indicates a stiffer polymer with greater rotational and/or steric hindrances, relative to the idealized model. From the equations above, values for G^0_N using Wu's method ($G^0_{N, Wu}$) were calculated, as well as values for packing length (p) and characteristic ratio (C_{∞}) (Table 2.2). Comparisons are made within this polymer class for tacticity, different substituents, structural isomerism, and regioisomerism.

Table 2.2: Summary of rheological characteristics derived and calculated from TTS master curves.

Name	Ð	ρ (g/cm ³)	Gc, (MPa)	G ⁰ N, Wu (MPa)	T _{ref} (°C)	Me, Wu (kDa)	<i>p</i> Wu (Å)	C∞, Wu
PiPP	1.3	1.12	0.065	0.267	80	9.92	3.43	4.30
o-PiPP	1.6	1.14	0.038	0.209	80	12.79	3.72	5.28
(R)-PiPP	1.4	1.13	0.219	1.007	90	2.71	2.22	6.61
PEMP	2.8	1.13	0.085	0.742	80	3.59	2.44	6.38
PiPMP	1.7	1.11	0.597	3.493	60	0.71	1.43	11.12
ΡαΒΡ	1.3	1.15	0.182	0.747	60	3.41	2.39	6.43
PIPHF	1.7	1.14	0.184	1.074	90	2.57	2.18	7.57

Tacticity effects:

Tacticity plays a significant role in the chain flexibility of polyesters. Previous work by Randall *et al.* investigated the tacticity effects of PLAs using melt rheology. ⁵⁶ Poly(*meso*-lactide), an atactic PLA that is completely amorphous, had the highest chain flexibility with $C_{\infty} = 5.9$, p = 3.0 Å. This contrasts with isotactic poly(*L*-lactide), which exhibited stiffer chains, with $C_{\infty} = 7.5$, p = 2.3 Å. A similar trend was observed in the case of atactic PiPP ($C_{\infty} = 4.3$, p = 3.43 Å) compared to isotactic (*R*)-PiPP ($C_{\infty} = 6.6$, p = 2.22 Å). The decrease in chain flexibility observed from atactic PiPP to isotactic (*R*)-PiPP may correlate with the significant differences in the polymer tensile

properties. Despite PiPP and (R)-PiPP having similar M_w and T_g , PiPP exhibits more than double the ε_b of (R)-PiPP.

Substituent Effects:

The effects of varying pendant groups were also investigated. In a computational study of poly(propylene), poly (n-butene), poly(n-hexene), and poly(n-octene), based on the rotational isomeric state model, it was predicted that the chain stiffness increases as the side chain length of the polymer increases.⁵⁷ The same trend was observed for PiPP ($C_{\infty} = 4.3$, p = 3.43 Å) and P α BP ($C_{\infty} = 6.4$, p = 2.39 Å). However, despite the stiffer chain, P α BP exhibited significantly greater ϵ_b in this study than PiPP, at > 3800 % compared to 843 %. This is likely due to the differences in T_g between the two polymers. Introducing a bulkier pendant group on the aromatic moiety of the polymer backbone increases chain stiffness as observed when comparing PiPP ($C_{\infty} = 4.3$, p = 3.43 Å) to PiPHF ($C_{\infty} = 7.6$, p = 2.2 Å). This structural change increases the T_g from 25°C (PiPP) to 29°C (PiPHF). The resulting decrease in ϵ_b , from 843 % (PiPP) to 188 % (PiPHF), stems from a combination of higher T_g and increased chain stiffness.

Structural Isomeric Effects:

In the case of PEMP and PiPP, the impact of methyl group position was investigated. The location of the methyl group at the α -position of the carbonyl has a greater effect on the chain stiffness than adjacent to the alcohol, as observed when comparing PEMP ($C_{\infty} = 6.4$, p = 2.44 Å) and PiPP ($C_{\infty} = 4.3$, p = 3.43 Å). Although the T_g of PEMP (21°C) is lower than that of PiPP

(25°C), it still exhibited reduced ε_b at 350 % (PEMP) relative to 843% (PiPP), possibly due to the increased chain stiffness of the polyester. Additionally, the structural isomers PiPMP and P α BP were analyzed. The presence of two methyl groups in PiPMP ($C_{\infty} = 11.1, p = 1.43$ Å) appear to have a more significant impact on the stiffness of the polymer chain than the ethyl pendant group of P α BP ($C_{\infty} = 6.4, p = 2.39$ Å). The increase in chain stiffness may correspond to the increased T_g of PiPMP (26°C) and subsequent reduction in ε_b (886%) when compared to P α BP (T_g : 16°C, ε_b : >3800%).

Regioisomeric Effects:

It was observed that regioisomerism has the least significant effect when comparing rheological properties of this polymer series. The difference in chain stiffness between o-PiPP ($C_{\infty} = 5.3$, p = 3.72 Å) and PiPP ($C_{\infty} = 4.3$, p = 3.43 Å) is present, but to a lesser degree than previous examples. However, even with the slight increase in chain stiffness, the T_g of o-PiPP is increased to 27 °C and likely contributes to the decrease in ε_b from 843% (PiPP) to 400% (o-PiPP).

Chemical Recycling:

Previously, we demonstrated that PiPP and other amorphous polyesters can degrade under industrial composting conditions.³⁹ We have also observed in unreported work that these polyesters are chemically-recyclable *via* base hydrolysis. In contrast to semi-aromatic, AABB-type polyesters such as PET, PBT, and PEF, these lignin-derived AB-type polyesters do not contain water soluble and volatile glycols in the polymeric backbone. Because of this, chemically

recycling the polymers in aqueous conditions is straightforward and can be accomplished in high yields.

For this study, (R)-PiPP was chosen as a model polyester, although this strategy may be applied to others in this series. The polymer (Figure 2.5b, M_w : 27.0 kDa, D = 1.4) was degraded rapidly at 150 °C using a sealed system in 2M KOH in ethanol and water. The sealed pressure vessel is not a necessity but does allow for higher temperatures that increase the rate of depolymerization, with an 80 % yield of monomer achieved after a reaction time of 60 minutes. The recycled monomer (Figure 2.5c) exhibited excellent purity via ¹H-NMR with a comparable spectrum to the starting monomer (Figure 2.5a). Matching the reaction times between the two batches resulted in a slightly higher molecular weight of the second batch, with $M_w = 42.3$ kDa; D = 1.5 (Figure 2.5d). This experiment demonstrates that chemical recycling to monomer is another viable end-of-life strategy for this polymer series.

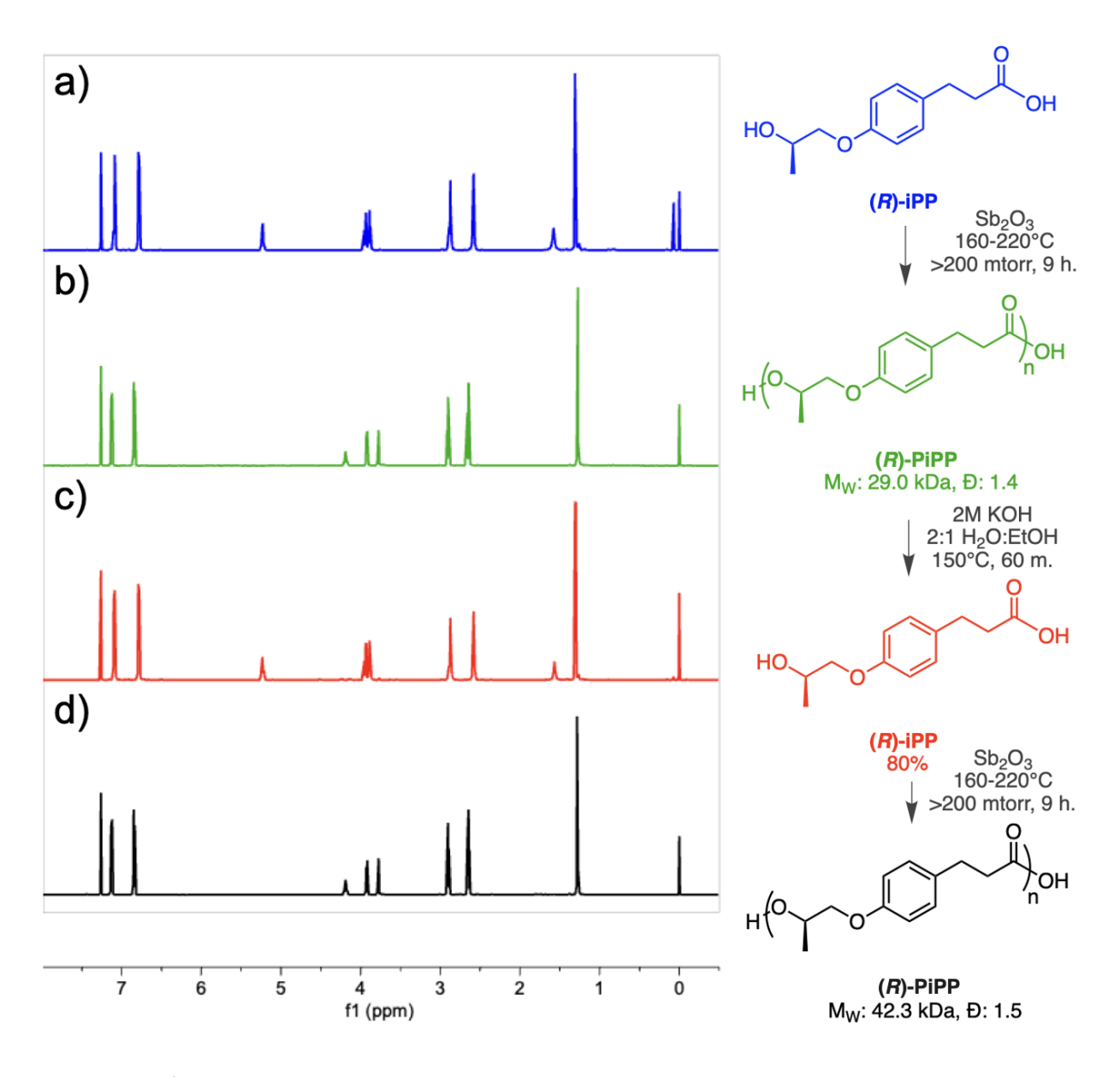


Figure 2.5: ¹H NMR Spectra of (*R*)-iPP monomer (a), (*R*)-PiPP polymer (b), recycled (*R*)-iPP monomer (c), and repolymerized (*R*)-PiPP (d) in chloroform-*d*.

Conclusions:

In this study, nine potentially lignin-derived monomers were synthesized using sustainable, highyield reactions that were easily scalable to produce polymers at greater than 50 g scale. Comprehensive characterization of thermal and mechanical properties revealed excellent thermal stability, with T_g ranging from 16 °C to 63 °C. Mechanical properties ranged from polymers that were too brittle to test to those with strain at break exceeding 3800%. Through iterative monomer design, rheological properties of subsequent polymers were evaluated using TTS master curves, demonstrating a diverse range of polymer properties, with packing length varying from 1.43 to 3.43 Å and C_∞ ranging from 4.30 to 11.12. Finally, using (R)-PiPP as a case study, it was demonstrated that these polyesters can be efficiently depolymerized to monomer via base hydrolysis, achieving rapid conversion with high yield. Subsequent repolymerization resulted in polymers with equal or greater molecular weights compared to the initial polyester.

References:

- (1) Xie, Y.; Gao, S.; Zhang, D.; Wang, C.; Chu, F. Bio-based polymeric materials synthesized from renewable resources: A mini-review. *Resources Chemicals and Materials* **2023**, *2* (3), 223-230. DOI: https://doi.org/10.1016/j.recm.2023.05.001.
- (2) MacLeod, M.; Arp, H. P. H.; Tekman, M. B.; Jahnke, A. The global threat from plastic pollution. *Science* **2021**, *373* (6550), 61-65. DOI: doi:10.1126/science.abg5433.
- (3) Geyer, R.; Jambeck, J. R.; Law, K. L. Production, use, and fate of all plastics ever made. *Science Advances* **2017**, *3* (7), e1700782. DOI: doi:10.1126/sciadv.1700782.
- (4) Zhang, Q.; Song, M.; Xu, Y.; Wang, W.; Wang, Z.; Zhang, L. Bio-based polyesters: Recent progress and future prospects. *Progress in Polymer Science* **2021**, *120*, 101430.
- (5) Cywar, R. M.; Rorrer, N. A.; Hoyt, C. B.; Beckham, G. T.; Chen, E. Y. X. Bio-based polymers with performance-advantaged properties. *Nature Reviews Materials* **2022**, *7* (2), 83-103. DOI: 10.1038/s41578-021-00363-3.
- (6) Vidal, F.; van der Marel, E. R.; Kerr, R. W. F.; McElroy, C.; Schroeder, N.; Mitchell, C.; Rosetto, G.; Chen, T. T. D.; Bailey, R. M.; Hepburn, C.; et al. Designing a circular carbon and plastics economy for a sustainable future. *Nature* **2024**, *626* (7997), 45-57. DOI: 10.1038/s41586-023-06939-z.
- (7) Miller, S. A. Sustainable Polymers: Opportunities for the Next Decade. *ACS Macro Lett* **2013**, *2* (6), 550-554. DOI: 10.1021/mz400207g From NLM PubMed-not-MEDLINE.
- (8) Reddy, C.; Ghai, R.; Kalia, V. C. Polyhydroxyalkanoates: an overview. *Bioresource technology* **2003**, *87* (2), 137-146.

- (9) Sin, L. T.; Tueen, B. S. *Polylactic acid: a practical guide for the processing, manufacturing, and applications of PLA*; William Andrew, 2019.
- (10) Aliotta, L.; Seggiani, M.; Lazzeri, A.; Gigante, V.; Cinelli, P. A Brief Review of Poly (Butylene Succinate) (PBS) and Its Main Copolymers: Synthesis, Blends, Composites, Biodegradability, and Applications. *Polymers (Basel)* **2022**, *14* (4). DOI: 10.3390/polym14040844 From NLM.
- (11) Jian, J.; Xiangbin, Z.; Xianbo, H. An overview on synthesis, properties and applications of poly(butylene-adipate-co-terephthalate)–PBAT. *Advanced Industrial and Engineering Polymer Research* **2020**, *3* (1), 19-26. DOI: https://doi.org/10.1016/j.aiepr.2020.01.001.
- (12) Loos, K.; Zhang, R.; Pereira, I.; Agostinho, B.; Hu, H.; Maniar, D.; Sbirrazzuoli, N.; Silvestre, A. J.; Guigo, N.; Sousa, A. F. A perspective on PEF synthesis, properties, and end-life. *Frontiers in chemistry* **2020**, *8*, 585.
- (13) Lund, F.; Gorwa-Grauslund, M. Production of bio-based adipic acid using a combination of engineered Pseudomonas putida strains. *Sustainable Chemistry for the Environment* **2024**, 8, 100154. DOI: https://doi.org/10.1016/j.scenv.2024.100154.
- (14) Toray Invents 100% Bio-Based Adipic Acid from Sugars Derived from Inedible Biomass, Scaling Up for Application to Eco-Friendly Nylon 66. Toray Industries, 2022. (accessed 2024 November 4th).
- (15) Burk, M. J.; Van Dien, S. J.; Burgard, A. P.; Niu, W. Compositions and methods for the biosynthesis of 1,4-butanediol and its precursors. U.S. Patent US 8,067,214 B2 2011.
- (16) He, Y.; Luo, Y.; Yang, M.; Zhang, Y.; Zhu, L.; Fan, M.; Li, Q. Selective catalytic synthesis of bio-based terephthalic acid from lignocellulose biomass. *Applied Catalysis A: General* **2022**, 630, 118440. DOI: https://doi.org/10.1016/j.apcata.2021.118440.

- (17) Tachibana, Y.; Kimura, S.; Kasuya, K.-i. Synthesis and Verification of Biobased Terephthalic Acid from Furfural. *Scientific Reports* **2015**, *5* (1), 8249. DOI: 10.1038/srep08249.
- (18) Volanti, M.; Cespi, D.; Passarini, F.; Neri, E.; Cavani, F.; Mizsey, P.; Fozer, D. Terephthalic acid from renewable sources: early-stage sustainability analysis of a bio-PET precursor. *Green Chem* **2019**, *21* (4), 885-896.
- (19) Delidovich, I.; Hausoul, P. J. C.; Deng, L.; Pfützenreuter, R.; Rose, M.; Palkovits, R. Alternative Monomers Based on Lignocellulose and Their Use for Polymer Production. *Chemical Reviews* **2016**, *116* (3), 1540-1599. DOI: 10.1021/acs.chemrev.5b00354.
- (20) Vermaas, J. V.; Crowley, M. F.; Beckham, G. T. Molecular Lignin Solubility and Structure in Organic Solvents. *ACS Sus. Chem. Eng.* **2020**, *8* (48), 17839-17850. DOI: 10.1021/acssuschemeng.0c07156.
- (21) Sun, Z.; Fridrich, B.; De Santi, A.; Elangovan, S.; Barta, K. Bright side of lignin depolymerization: toward new platform chemicals. *Chemical reviews* **2018**, *118* (2), 614-678.
- (22) Pollegioni, L.; Tonin, F.; Rosini, E. Lignin-degrading enzymes. *Febs j* **2015**, *282* (7), 1190-1213. DOI: 10.1111/febs.13224 From NLM.
- (23) Fang, Z.; Smith, J. R. L. *Production of Biofuels and Chemicals from Lignin*, 1st ed.; Springer Singapore: Imprint: Springer,, 2016. DOI: 10.1007/978-981-10-1965-4.
- (24) Zhong, R.; Cui, D.; Ye, Z.-H. Secondary cell wall biosynthesis. *New Phytologist* **2019**, *221* (4), 1703-1723. DOI: https://doi.org/10.1111/nph.15537.
- (25) Martínková, L.; Grulich, M.; Pátek, M.; Křístková, B.; Winkler, M. Bio-Based Valorization of Lignin-Derived Phenolic Compounds: A Review. *Biomolecules* **2023**, *13* (5), 717.
- (26) Qiang, H.; Wang, J.; Liu, H.; Zhu, Y. From vanillin to biobased aromatic polymers. *Polymer Chemistry* **2023**, *14* (37), 4255-4274.

- (27) Libretti, C.; Correa, L. S.; Meier, M. A. From waste to resource: advancements in sustainable lignin modification. *Green Chem* **2024**.
- (28) Andriani, F.; Lawoko, M. Oxidative Carboxylation of Lignin: Exploring Reactivity of Different Lignin Types. *Biomacromolecules* **2024**.
- (29) Subbotina, E.; Souza, L. R.; Zimmerman, J.; Anastas, P. Room temperature catalytic upgrading of unpurified lignin depolymerization oil into bisphenols and butene-2. *Nature Communications* **2024**, *15* (1), 5892. DOI: 10.1038/s41467-024-49812-x.
- (30) Hafezisefat, P.; Qi, L.; Brown, R. C. Lignin Depolymerization and Esterification with Carboxylic Acids to Produce Phenyl Esters. *ACS Sus. Chem. Eng.* **2023**, *11* (48), 17053-17060. DOI: 10.1021/acssuschemeng.3c05221.
- (31) Upton, B. M.; Kasko, A. M. Strategies for the Conversion of Lignin to High-Value Polymeric Materials: Review and Perspective. *Chemical Reviews* **2016**, *116* (4), 2275-2306. DOI: 10.1021/acs.chemrev.5b00345.
- (32) Tana, T.; Zhang, Z.; Beltramini, J.; Zhu, H.; Ostrikov, K. K.; Bartley, J.; Doherty, W. Valorization of native sugarcane bagasse lignin to bio-aromatic esters/monomers via a one pot oxidation–hydrogenation process. *Green Chem* **2019**, *21* (4), 861-873.
- (33) Kim, S.; Chung, H. Biodegradable Polymer: From Synthesis Methods to Applications of Lignin-graft-Polyester. *Green Chem* **2024**.
- (34) Duval, A.; Benali, W.; Avérous, L. Turning lignin into a recyclable bioresource: transesterification vitrimers from lignins modified with ethylene carbonate. *Green Chem* **2024**, *26* (14), 8414-8427.
- (35) Bilal, M.; Qamar, S. A.; Qamar, M.; Yadav, V.; Taherzadeh, M. J.; Lam, S. S.; Iqbal, H. M. N. Bioprospecting lignin biomass into environmentally friendly polymers—Applied perspective

- to reconcile sustainable circular bioeconomy. *Biomass Conversion and Biorefinery* **2024**, *14* (4), 4457-4483. DOI: 10.1007/s13399-022-02600-3.
- (36) Huang, J.; Wang, H.; Liu, W.; Huang, J.; Yang, D.; Qiu, X.; Zhao, L.; Hu, F.; Feng, Y. Solvent-free synthesis of high-performance polyurethane elastomer based on low-molecular-weight alkali lignin. *International Journal of Biological Macromolecules* **2023**, *225*, 1505-1516. DOI: https://doi.org/10.1016/j.ijbiomac.2022.11.207.
- (37) Ana, L.; Helena, P. Compositional Variability of Lignin in Biomass. In *Lignin*, Matheus, P. Ed.; IntechOpen, 2017; p Ch. 3.
- (38) Mialon, L.; Vanderhenst, R.; Pemba, A. G.; Miller, S. A. Polyalkylenehydroxybenzoates (PAHBs): Biorenewable aromatic/aliphatic polyesters from lignin. *Macromolecular Rapid Communications* **2011**, *32* (17), 1386-1392.
- (39) Winfield, D.; Ring, J.; Horn, J.; White, E. M.; Locklin, J. Semi-aromatic biobased polyesters derived from lignin and cyclic carbonates. *Green Chem* **2021**, *23* (23), 9658-9668. DOI: 10.1039/d1gc03135j.
- (40) Xanthopoulou, E.; Terzopoulou, Z.; Zamboulis, A.; Koltsakidis, S.; Tzetzis, D.; Peponaki, K.; Vlassopoulos, D.; Guigo, N.; Bikiaris, D. N.; Papageorgiou, G. Z. Poly(hexylene vanillate): Synthetic Pathway and Remarkable Properties of a Novel Alipharomatic Lignin-Based Polyester. *ACS Sus. Chem. Eng.* **2023**, *11* (4), 1569-1580. DOI: 10.1021/acssuschemeng.2c06507.
- (41) Grossman, A.; Vermerris, W. Lignin-based polymers and nanomaterials. *Current opinion in biotechnology* **2019**, *56*, 112-120.
- (42) Dessbesell, L.; Paleologou, M.; Leitch, M.; Pulkki, R.; Xu, C. C. Global lignin supply overview and kraft lignin potential as an alternative for petroleum-based polymers. *Renewable and Sustainable Energy Reviews* **2020**, *123*, 109768.

- (43) Alinejad, M.; Henry, C.; Nikafshar, S.; Gondaliya, A.; Bagheri, S.; Chen, N.; Singh, S. K.; Hodge, D. B.; Nejad, M. Lignin-based polyurethanes: Opportunities for bio-based foams, elastomers, coatings and adhesives. *Polymers* **2019**, *11* (7), 1202.
- (44) Laurichesse, S.; Avérous, L. Chemical modification of lignins: Towards biobased polymers. *Progress in polymer science* **2014**, *39* (7), 1266-1290.
- (45) Llevot, A.; Grau, E.; Carlotti, S.; Grelier, S.; Cramail, H. From lignin-derived aromatic compounds to novel biobased polymers. *Macromolecular rapid communications* **2016**, *37* (1), 9-28.
- (46) Duval, A.; Lawoko, M. A review on lignin-based polymeric, micro-and nano-structured materials. *Reactive and Functional Polymers* **2014**, *85*, 78-96.
- (47) Pescarmona, P. P. Cyclic carbonates synthesised from CO2: Applications, challenges and recent research trends. *Current Opinion in Green and Sustainable Chemistry* **2021**, *29*, 100457. DOI: https://doi.org/10.1016/j.cogsc.2021.100457.
- (48) Anastas, P. T.; Warner, J. C. *Green chemistry: theory and practice*; Oxford university press, 2000.
- (49) D638, A. S. Standard Test Method for Tensile Properties of Plastics. American Society for Testing and Materials: 2015.
- (50) Papadopoulos, L.; Zamboulis, A.; Kasmi, N.; Wahbi, M.; Nannou, C.; Lambropoulou, D. A.; Kostoglou, M.; Papageorgiou, G. Z.; Bikiaris, D. N. Investigation of the catalytic activity and reaction kinetic modeling of two antimony catalysts in the synthesis of poly(ethylene furanoate). *Green Chem* **2021**, *23* (6), 2507-2524, 10.1039/D0GC04254D. DOI: 10.1039/D0GC04254D.

- (51) Sung, S.-J.; Cho, K.-Y.; Hah, H.; Lee, J.; Shim, H.-K.; Park, J.-K. Two different reaction mechanisms of cinnamate side groups attached to the various polymer backbones. *Polymer* **2006**, 47 (7), 2314-2321. DOI: https://doi.org/10.1016/j.polymer.2006.02.003.
- (52) Liu, C.; He, J.; Ruymbeke, E. v.; Keunings, R.; Bailly, C. Evaluation of different methods for the determination of the plateau modulus and the entanglement molecular weight. *Polymer* **2006**, *47* (13), 4461-4479. DOI: https://doi.org/10.1016/j.polymer.2006.04.054.
- (53) Wu, S. Chain structure and entanglement. *Journal of Polymer Science Part B: Polymer Physics* **1989**, *27* (4), 723-741. DOI: https://doi.org/10.1002/polb.1989.090270401 (accessed 2024/11/12).
- (54) Larson, R. G.; Sridhar, T.; Leal, L. G.; McKinley, G. H.; Likhtman, A. E.; McLeish, T. C.
 B. Definitions of entanglement spacing and time constants in the tube model. *Journal of Rheology* 2003, 47 (3), 809-818. DOI: 10.1122/1.1567750 (accessed 11/12/2024).
- (55) Fetters, L. J.; Lohse, D. J.; Richter, D.; Witten, T. A.; Zirkel, A. Connection between Polymer Molecular Weight, Density, Chain Dimensions, and Melt Viscoelastic Properties. *Macromolecules* **1994**, *27* (17), 4639-4647. DOI: 10.1021/ma00095a001.
- (56) Randall, J.; Flodquist, M.; Schroeder, J.; Valentine, J. R.; Owusu, O.; McCarthy, K.; Weed, J.; Hennen, J.; Heuzey, M. C.; Carreau, P. J. Comparing the Structural, Thermal, and Rheological Properties of Poly(meso-lactide) to Poly(l-lactide) and Poly(rac-lactide).

 Macromolecules 2024, 57 (6), 2715-2728. DOI: 10.1021/acs.macromol.3c02029.
- (57) Madkour, T. M.; Goderis, B.; Mathot, V. B.; Reynaers, H. Influence of chain microstructure on the conformational behavior of ethylene-1-olefin copolymers. Impact of the comonomeric mole content and the catalytic inversion ratio. *Polymer* **2002**, *43* (9), 2897-2908.

CHAPTER 3

IMPROVEMENT OF ELASTOMERIC RECOVERY IN LIGNIN-DERIVED THERMOPLASTIC POLYESTERS \emph{VIA} THE INCORPORATION OF AABB-TYPE CROSSLINKERS

Ryan K. Maynard, Kush G. Patel, Huiming Wu, Maximo T. Reyes, Frida C. Knudsen, Imrie C. Ross, Nohora P. Manovacia Moreno, and Jason J. Locklin. To be submitted to *ACS Biomacromolecules*.

Abstract

Crosslinked elastomers are a very important class of materials but are rarely recyclable. In this work, the synthesis of two novel AABB crosslinkers is described. Subsequent polymerization of various loadings of crosslinker with α -butylene phloretate at small scales using antimony catalysis yielded crosslinked elastomers. The crosslinked polymers were subjected to rheological analysis, which indicated via Cole-Cole plots that lower loadings of both materials favored short-chain branching, while higher loadings led to fully crosslinked systems. Tensile testing showed that low MBPE loadings outperformed higher loadings in terms of Y, ϵ b, and σ b, whereas HEMT exhibited increased Y and ϵ b with higher loadings until a limit of 5%. To demonstrate the elastomeric performance of these elastomers, cyclic tensile testing was conducted which demonstrated superior elastomeric recovery in MBPE-based systems, with 0.25% and 2.5% MBPE loadings retaining \sim 60% elastic recovery over 10 cycles. Finally, we demonstrate that these crosslinked systems can be rapidly chemically recycled to monomers with excellent retention of the original feed ratios.

Introduction

In Chapter 1, nine amorphous elastomers were characterized for their thermal and mechanical properties. However, above T_g , amorphous polymers will begin to flow, and the rate increases proportionally with temperature. To counter this, most elastomers are crosslinked. In a continuation of the previous work, two AABB crosslinkers, both derived from lignin, were synthesized. The first crosslinker is derived from erythritol, a natural sugar, and phloretic acid, an abundant molecule that can be isolated from lignin valorization. The second was derived from p-coumaric acid, which can be dimerized upon exposure to UV light. Subsequent

alkylation via the ring opening of ethylene carbonate can provide a fully biobased, AABB structure that can be incorporated into polyesters. P α BP was chosen as a candidate polyester to crosslink due to a lower T_g (16 °C) and crosslinking was accomplished with the addition of various loadings of AABB comonomers. Conventional rubber-based elastomers are not easily chemically-recyclable. For this work, two chemical recycling experiments are performed to demonstrate the end-of-life options for these crosslinked polyesters.

Materials and Methods

Phloretic acid (98%), ethylene carbonate (98%), potassium carbonate (99%), DMSO-d6 (99.8%), CDCl₃ (99.8%), D₂O (99.9%) and MeOD (99.9%) were purchased from Oakwood Chemical. α-Butylene carbonate (99%) was purchased from Ambeed, Inc. (*E*)-*p*-coumaric acid was purchased from TCI and found to be >99% trans *via* ¹H NMR. Dimethylformamide was purchased from VWR (99%), dried using an SPS 5 (MBRAUN, USA), and stored under nitrogen. KOD was prepared by dissolving 200 mg of KOH in 1.0 mL of D₂O under nitrogen. Distillation under vacuum (< 100 mTorr) removed D₂O, leaving behind mostly deuteroxide. This process was repeated four more times to yield KOD which was subsequently dissolved in dry MEOD at a concentration of 2M and stored under nitrogen. All other solvents and reagents were purchased from commercial suppliers and used as received.

Synthesis of Crosslinkers and Monomers:

Scheme 3.1: Synthesis of *meso-*1,4-bis(phloretic acid) erythritol (BPE).

21.76 g of erythritol bis-carbonate (0.125 mol) was prepared as previously reported using the trans-carbonation route⁵ and added to a 1L 3-neck flask which fitted with a nitrogen inlet and pressure relief valve. Following this, 67.56 g of methyl phloretate (0.375 mol, 3 eq.), and 1.73 g of K₂CO₃ (0.1 eq) were added. The flask was purged and backfilled five times with nitrogen and heated to 160 °C with an oil bath. The evolution of gas began rapidly, and the colorless, heterogenous solution turned to nearly black in about 30 minutes. The reaction was monitored by the evolution of CO₂ using a bubbler, which indicated stalled conversion at 12 hours. After this, 500 mL of aqueous 3M NaOH was added and the heterogenous mixture was refluxed. Solids completely dissolved after 15 minutes, and the refluxing was continued for another 45 minutes. After this, the solution was cooled to room temperature and acidified using 6M HCl until pH = 2. The brown colloidal suspension was concentrated via centrifuge, and the supernatant liquid was decanted away. The pellet was washed three times with acetone until it became colorless and was dried overnight under vacuum at 70°C to yield 7.96 g of a fine white powder. (15%). M.P. 246 °C. ¹H NMR (600 MHz, DMSO-*d6*): δ 11.82 (s, 2H, COO*H*), 7.12 (d, 4H, Ar-*H*), 6.84 (d, 4H, Ar-H), 5.13 (s, 2H, CH-OH), 4.14 (d, 2H, CH), 3.92 (m, 2H, CHH), 3.81 (m, 2H, CHH), 2.75 (t, 4H, CH₂), 2.47 (t, 4H, CH₂). ¹³C NMR (600 MHz, 5:1 CDCl₃: TDA-d): δ 181.20, 156.14, 133.38, 129.41, 114.79, 70.90, 67.94, 35.48, 29.38.

Scheme 3.2: Synthesis of *meso-*1,4-bis(methyl phloretate) erythritol (MBPE).

5.50 g of *meso*-1,4-bis(phloretic acid) erythritol (0.013 mol), 500 mL of methanol, and 5 mL of concentrated sulfuric acid were added to a 1L single-neck flask fitted with a reflux condenser. The contents were heated under reflux for 12 hours and then cooled to room temperature. The reaction mixture remained cloudy during the entire reaction. The solvent was removed under reduced pressure at 30 °C so that about 1/3 volume remained. The residual solution was poured into ice water (500 mL) and filtered. The filter cake was washed one time with a 200 mL portion of water, once with 200 mL of saturated sodium bicarbonate solution, and twice with water again. The filter cake was dried in a vacuum oven overnight at 60°C to yield 5.67 g of a white powder (97%). M.P. 180 °C. ¹H NMR (600 MHz, CDCl₃; 10 μL TFA-*d*): 7.11 (d, 4H, Ar-*H*), 6.84 (d, 4H, Ar-*H*), 4.39 (s, 2H, C*H*), 4.26 (m, 2H, C*H*H), 3.74 (s, 6H, OC*H*₃), 2.91(t, 4H, C*H*₂), 2.69 (t, 4H, C*H*₂). ¹³C NMR (600 MHz, 5:1 CDCl₃: TDA-*d*): δ 177.79, 156.15, 133.33, 129.38, 114.77, 70.85, 67.93, 53.88, 36.13, 29.88.

Scheme 3.3: Synthesis of 4,4' dihydroxytruxillic acid.

10 g of (*E*)-*p*-coumaric acid were added to a 500 mL glass single-neck round bottom flask. 350 mL of D.I. water were added and the heterogenous contents were irradiated at 365 nm for 72 h with a mercury lamp. After completion of the reaction as indicated by ¹H NMR, the heterogenous slurry was filtered and dried at 50°C for 24 h. to yield 9.88 g of a white powder (99%). ¹H NMR (600 MHz, DMSO-*d6*): δ 11.97 (s, 2H, COO*H*), 9.27 (s, 2H, Ar-O*H*), 7.12 (d, 4H, Ar-*H*), 6.69 (d, 4H, Ar-*H*), 4.12 (q, 2H, C*H*), 3.64 (q, 2H, C*H*).

Scheme 3.4: Synthesis of 4,4' dihydroxy-dimethyltruxillate.

8.5 g of 4,4' dihydroxytruxillic acid were added to a 1L single-neck flask. 500 mL of methanol and 10 mL H₂SO₄ were added to the flask. The high amount of sulfuric acid was to aid in solubility of the truxillic acid. The heterogenous mixture quickly became clear upon heating and was refluxed for 10 hours. After completion of the reaction, the solvent was removed by rotary evaporation. The crude residue was taken up in ethyl acetate and the organic layer was washed three times with water, twice with saturated sodium bicarbonate solution, and once with brine before being dried over magnesium sulfate. Filtration and removal of solvent under reduced pressure yielded 8.1 g of an off-white solid (88%). ¹H NMR (600 MHz, DMSO-*d6*): δ 9.29 (s, 2H, Ar-O*H*), 7.10 (d, 4H, Ar-*H*), 6.70 (d, 4H, Ar-*H*), 4.20 (q, 2H, C*H*), 3.79 (q, 2H, C*H*), 3.25 (s, 6H, COOC*H*₃).

Scheme 3.5: Synthesis of 4,4' bis(2-hydroxyethoxy)dimethyltruxillate (HEMT).

To a 250 mL flame-dried Schlenk flask, 2.67 g of 4,4' dihydroxy-dimethyltruxillate (1.0 eq.), 7.93 g of ethylene carbonate, (12 eq.), and 4.14 g potassium carbonate (4 eq) were added under nitrogen. The flask was purged and backfilled an additional three times with nitrogen and 100 mL of anhydrous DMF were added. The heterogenous mixture was heated to 100°C. TLC

indicated consumption of starting material after 2 hours, but evolution of carbon dioxide was still observed. After 16 hours, no more gas evolution was observed, and the solvent was removed under reduced pressure at 60°C. The residue was taken up in ethyl acetate (500 mL), washed five times with water (300 mL portions) and once with brine (300 mL portion). The organic layer was dried over magnesium sulfate and the solvent was removed under reduced pressure. The crude solid was purified via flash chromatography (silica gel; CyHex:EtOAc 1:4; Rf: 0.33) and yielded 2.52 g of a white, waxy solid (76%). Although chromatographically pure by both TLC and GC-MS, the product isomerized during the reaction at about 30% abundance. It was stored at -20 °C prevent further isomerization. ¹H NMR (600 MHz, CDCl₃): δ 7.24 (d, 4H, Ar-*H*), 6.90 (d, 4H, Ar-*H*), 4.40 (q, 2H, C*H*), 4.09 (s, 4H, C*H*₂), 3.98 (s, 4H, C*H*₂), 3.93 (q, 2H, C*H*), 3.36 (s, 6H, COOC*H*₃). ¹³C NMR (600 MHz, CDCl₃): δ 172.45, 157.70, 131.25, 129.38, 128.64, 127.63, 114.42, 69.15, 61.50, 51.55, 47.04, 40.73.

Scheme 3.6: Synthesis of α -Butylene Phloretate.

The synthesis was adapted from our previous work. 240 g of methyl phloretate (1.33 mol), 170.1 g of a-butylene carbonate (1.1 eq), and 9.19 g of K₂CO₃ (0.05 eq) were added to a 2L 3-neck flask fitted with a nitrogen inlet and a gas relief valve. The flask was purged and

backfilled 3X under nitrogen before being heated to 160 °C for 5 hours until the evolution of CO₂ stalled. The flask was cooled to 80 °C and 1.25L of 3M NaOH was added and the flask was fitted with a reflux condenser under air. The heterogenous solution was refluxed for 2 hours, at which point it became a clear solution Refluxing was continued for another 10 hours before the contents were cooled to 10°C and acidified to pH = 2. The white precipitate was isolated by filtration, washed with cold water at pH = 3, and then dried at 60°C for 48 h to yield 278 grams of pure monomer (>99% by 1 H NMR), which was used without further purification (88%). 1 H NMR (600 MHz, CDCl₃): δ 7.12 (d, 2H, H_{Ar}), 6.85 (d, 2H, H_{Ar}), 3.97 (dd, 1H, CHH), 3.82 (dd, 1H, CHH), 2.90 (t, 2H, C H_2), 2.65 (t, 2H, C H_2), 2.06 (p, 2H, C H_2), 1.03 (t, 3H, C H_3).

Synthesis of Polyesters and Crosslinked Polyesters:

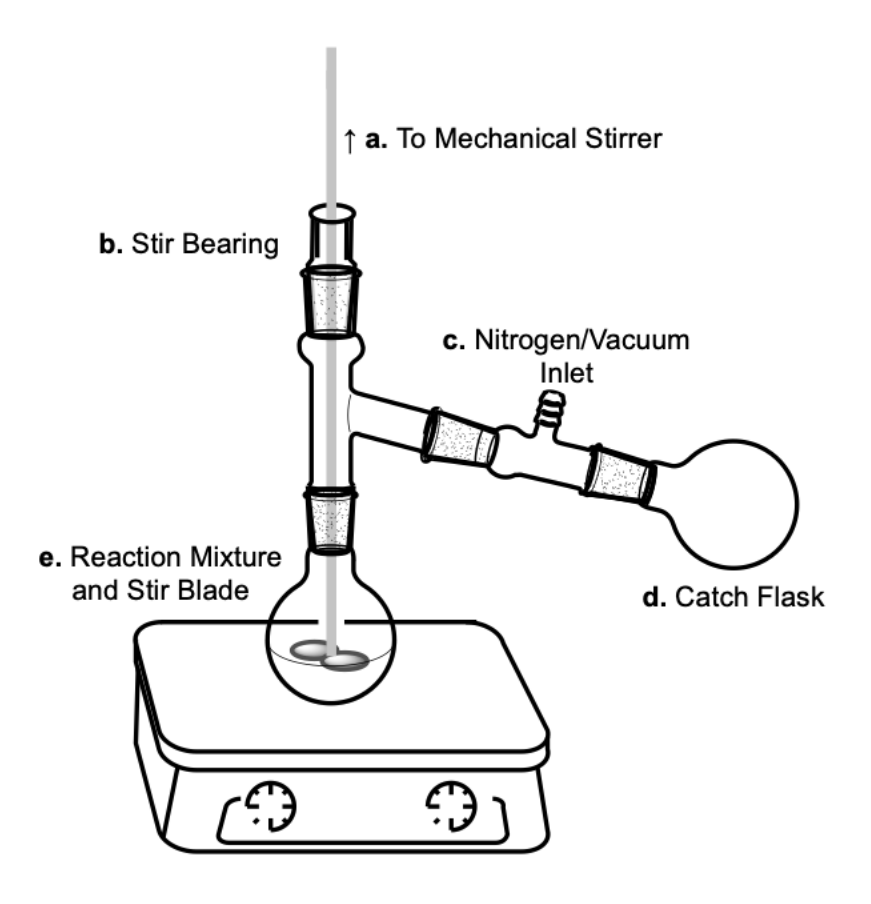


Figure 3.1: Polycondensation apparatus used in this study.

 $10.0~{\rm g}$ of α -butylene phloretate, 1 mol% antimony trioxide, and 10 mg of 4-methoxyphenol (as an antioxidant) were added to a 25 mL round-bottom flask with heating to reduce the volume of the powder. The appropriate percentage of crosslinker was added, where $X_{\alpha BP} + X_{Crosslinker} = 1.0$. After this, the flask was fitted with a 24/40 distillation adaptor, through which a Teflon stir blade was guided (Figure 3.1e). A stir bearing (Figure 3.1b) was added, and the stir shaft was connected to a mechanical stirrer (Figure 3.1a). Finally, a vacuum distillation adaptor was used as a nitrogen/vacuum inlet (Figure 3.1c) and a catch flask was added (Figure 3.1d) which was cooled with an ice bath during normal distillation, and dry ice/isopropanol during vacuum distillation. The flask was purged and backfilled seven times with gentle vacuum

(~25 Torr) followed by nitrogen, then heated to 180°C with an oil bath with stirring at 150 rpm under a nitrogen atmosphere. After one hour, the temperature was increased to 200°C. Finally, after another hour, the temperature was increased to 220°C and vacuum was applied to the system (<300 mTorr) until the reaction became too vicious to stir, or for 6 hours - whichever came first. As the reaction became more viscous, stirring was reduced to 30 rpm as needed to maintain effective mixing. A summary of vacuum times and resultant molecular weights are summarized in Table 3.1.

Table 3.1: Summary of reaction times, molecular weight, and glass transition data for crosslinked polymers in this study. A vacuum time of less than 6 hours indicates that the material was too viscous to be stirred.

Polymer	Vacuum Duration:	M _w (kDa):	Đ:	T _g (°C):
PαBP with 0% crosslinker	6 h.	35.1	1.51	16
PαBP with 0.25% MBPE	6 h.	178	3.60	17
PαBP with 0.25% HEMT	6 h.	50.2	1.60	15
PαBP with 1.0% MBPE	3 h.	118	3.25	15
PαBP with 1.0% HEMT	6 h.	22.8	1.54	16
PαBP with 2.5% MBPE	1.5 h.	107	4.58	16
PαBP with 2.5% HEMT	6 h.	23.3	2.07	17
PαBP with 5.0% MBPE	0.7 h.	69.9	3.12	17
PαBP with 5.0% HEMT	3 h.	163	4.53	16

Structural Characterization:

¹H NMR and ¹³C NMR spectra were recorded at room temperature (unless otherwise noted) with an Avance Neo 600 MHz instrument (Bruker, USA) at a concentration of 10 mg/mL. Peak shifts in parts per million (ppm) were reported relative to the signal of chloroform-*d* at 7.26 ppm or DMSO-*d*6 at 2.50 ppm for ¹H NMR and chloroform-*d* at 77.16 ppm or DMSO-*d*6 at 39.52 ppm for ¹³C NMR spectra.

Thermal Characterization:

Thermal transitions were determined using a DSC 250 equipped with an RCS 90 chilling system (TA Instruments, USA). Samples were cooled to -20 °C before being heated to 120 °C for two cycles. Data reported is from the second heating cycle.

Rheological Characterization:

Rheological experiments were conducted on a TA instruments Discovery Hybrid Rheometer (USA) using an 8 mm parallel plate geometry with a 850 micron trim gap and 750 micron running gap. A series of temperature ramps from -10 °C to 110 °C with oscillation frequency of 1 Hz and strain at 0.01% were conducted with a ramp rate of 10°C/min. Cole-Cole plots were created after frequency sweeps were conducted at the same trim and running gap with 1% strain and frequencies from 600 to 0.1 rad/s.

Density Characterization:

The true polymer density was obtained using a helium pycnometer (Micromeritics, AccuPyc II 1340, USA). For all samples, approximately 0.03 - 0.05 g of each sample was tested using the 0.1 cm³ insert. Gas pressure was 19.5 psi and equilibration was set at 0.005

psi/min. For each sample, ten purge cycles and ten measurement cycles were performed, and the test was stopped when the variation between five consecutive measurements was below 0.05%. The average of those five measurements was reported.

Mechanical Characterization:

Tensile specimens were prepared by melt-pressing films. 2.0 g of polymer was pressed at at 100°C using 0.20 mm shims with 5000 psi of force using a heated stage hydraulic press (Carver, Inc., USA). Films were then cut using an ATSM Type 1708 film cut die. Tensile testing was subsequently performed using a Shimadzu AGX Tensile Tester (Shimadzu, USA) pulling at a rate of 200mm/min. Modulus values were reported by the slope of the curve between 0 and 1% strain. Cyclic tensile testing was performed to 150% strain at 5mm/min with 10 cycles.

Chemical Recycling to Monomer:

2.0 g of MBPT was added to a 25 mL round-bottom flask with a stir bar. 10 mL of 2.25 M KOH in ethanol was added, and the flask contents were brought to reflux for 15 minutes until homogenous. The flask contents were cooled to 5 °C with an ice bath, acidified to pH = 2 with 2M HCl, and a white precipitate formed. The precipitate was filtered and washed with three 50 mL portions of cold, acidified water (pH = 3) before being dried in a vacuum oven to yield 2.32 g of a white powder (96%) which contained the ethyl esters of the crosslinker and monomer at at 2.53% and 97.47% abundance, respectively. This reaction was repeated with ¹H NMR monitoring. 7.50 mg of polymer and 750 μL OF 2M KOD in MeOD were added to a 5mm NMR tube (VWR, USA) which was sealed with a tube cap. The probe temperature was maintained at

40°C and the sample spinning was enabled. 32 scan spectra were taken in 10-minute intervals for 120 minutes total, until more than 98% of residual polymer peak had disappeared.

Results and Discussion

Monomer and Crosslinker Synthesis:

The synthesis of the P α BP monomer followed the same synthesis as previously reported in this dissertation (See Chapter 2). The results were equally excellent at a significant larger scale (> 200 g) and recrystallization was avoided in this case. A crosslinker was proposed that utilized two phloretic acid monomers and joined them by ring opening of cyclic carbonates. Erythritol dicarbonate was an excellent candidate for this, since it can be derived wholly from biobased meso-erythritol and synthesized in high yields. This procedure was attempted in solution, but the best results were obtained when an excess of methyl phloretate was used to solvate the reaction mixture, with a catalytic amount of K₂CO₃ present to initiate deprotonation of the methyl phloretate phenol. Using this method, complete conversion of erythritol dicarbonate was observed via ¹H NMR. Purification of the compound with column chromatography proved difficult due to a very large number of species present and low solubility. Because of this, the procedure was modified to include a deprotection step, which cleaved the esters, and any small oligomers present in the reaction that can form through transesterification. With this, a homogenous solution was obtained. After subsequent acidification, a crude brown powder was isolated that contained roughly 25% desired product. The BPE monomer was completely insoluble in most common solvents, so several washed with acetone were sufficient to remove impurities. This yielded pure BPE in very poor yield (15%), but in sufficient quantities to

synthesize all crosslinked polymer systems in this study. To ensure incorporation during polycondensation, the BPE monomer (mp: 246 °C) was protected as its methyl ester via a high-yielding Fischer esterification, reducing the melting point to 180 °C.

It was proposed that a second crosslinker be synthesized that can be used to compare properties directly, thus gaining an understanding of the effectiveness of one solution vs another for these systems. As discussed in Chapter 2, hindrances at the α -methyl position vs. adjacent to the alcohol on AB monomers seemed to have different effects on the reactivity of substrates. TO investigate this, a second crosslinker was synthesized that had less hindered substrates on the alcohol moiety, but more hindrances closer to the carbonyl of the molecule. Truxillic acid derivatives were found to be an excellent candidate, since they can be derived from completely biobased sources such as coumaric acid derivatives and are also found in various natural sources.^{4,6} The synthesis conditions of the HEMT crosslinker was largely inspired by the success of our previous syntheses, specifically the high-yielding syntheses of phenolic cinnamate derivatives with ethylene carbonate. However, to maximize the yield, the conditions were modified to include DMF as a solvent, which prolongs the reaction time but is milder to the substrates due to the lower reaction temperatures. Interestingly, although TLC indicated complete conversion of the starting material and gas evolution completely ceased, there appeared to be two species in the ¹H NMR spectrum of the product. Because of this, the product mixture was subjected to column chromatography, which isolated a single spot on TLC (by UV and Iodine stains) and a single peak on Gas Chromatography. However, once again, there appeared to be multiple species present by both ¹H NMR and ¹³C NMR. Careful analysis of COSY and HMBC experiments suggested that there were multiple isomers of the truxillic-acid derivative present, which has already been well-reported to happen under thermal heating of 4,4' truxillic

acids and their derivatives.⁷ This is still under investigation in our laboratory, both in terms of reaction conditions to avoid isomerization, as well as the determination of specific isomers that are present in the mixture. Even with this, we justified that regardless of the isomers present, the HEMT monomer should perform well as a crosslinker and used it as-is until further investigations can be completed.

Polymerization:

To reduce reaction times and use of monomer, polymerization was conducted at small scales. In contrast to the previously described procedure (Chapter 2), an oil bath was utilized with a distillation adaptor. This allowed efficient mixing of small batches of polymer (~10 g) even when high melt viscosity was obtained. Antimony trioxide was used as a catalyst as it has been observed in previous work in our group to produce high molecular-weight polyesters with minimal side products. Since many polymers can darken when exposed to high temperatures for extended reaction times, MEHQ was added as an antioxidant. A test polymerization was first conducted using αBP monomer, and the reaction was stalled with a thick polymer melt at 6 hours of vacuum (< 300 mTorr). Consequently, subsequent polymerizations were conducted for a maximum of 6 hours or until stirring became impractical, as indicated by the reaction mixture fully adhering to the stir shaft and blade, resulting in a polymer gel. The reaction times decreased with increasing MBPE crosslinker content. However, with HEMT, gelling of the reaction did not occur until 5% loading was achieved (Error! Reference source not found.). This could possibly be due to reduced reactivity of the HEMT crosslinker when compared to the MBPE crosslinker, which aligns with data we have previously observed with the reactivity of α - carbonyl substituted monomers compared to substitution adjacent to the terminal hydroxy group (Chapter 2.)

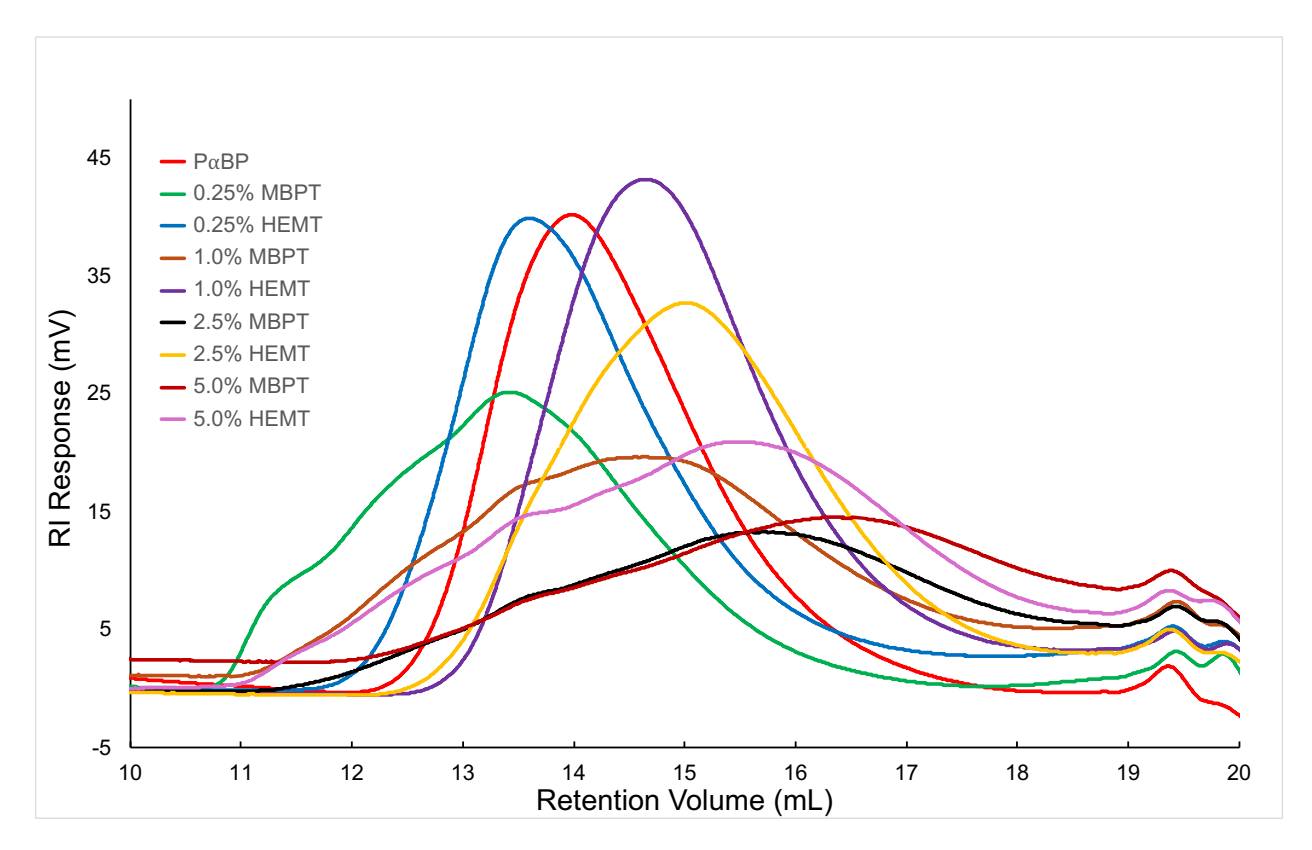


Figure 3.2: GPC curve overlay of control and crosslinked polyesters in this study.

The possibility of reduced reactivity of the HEMT crosslinker was also strengthened by GPC data (Figure 3.2). MBPE curves consistently demonstrated higher M_w and higher Đ (Table 3.1) in comparison to those with HEMT crosslinker. The very broad signals in GPC are likely due to crosslinking of the materials causing significant increases in hydrodynamic radius in comparison to the control, rather than a true increase in molecular weight.

Crosslinking vs Branching of Truxillates and Covalent Linkers:

To investigate this further, frequency sweeps and Cole-Cole plots were conducted for the polymers in this study (Figure 3.3).

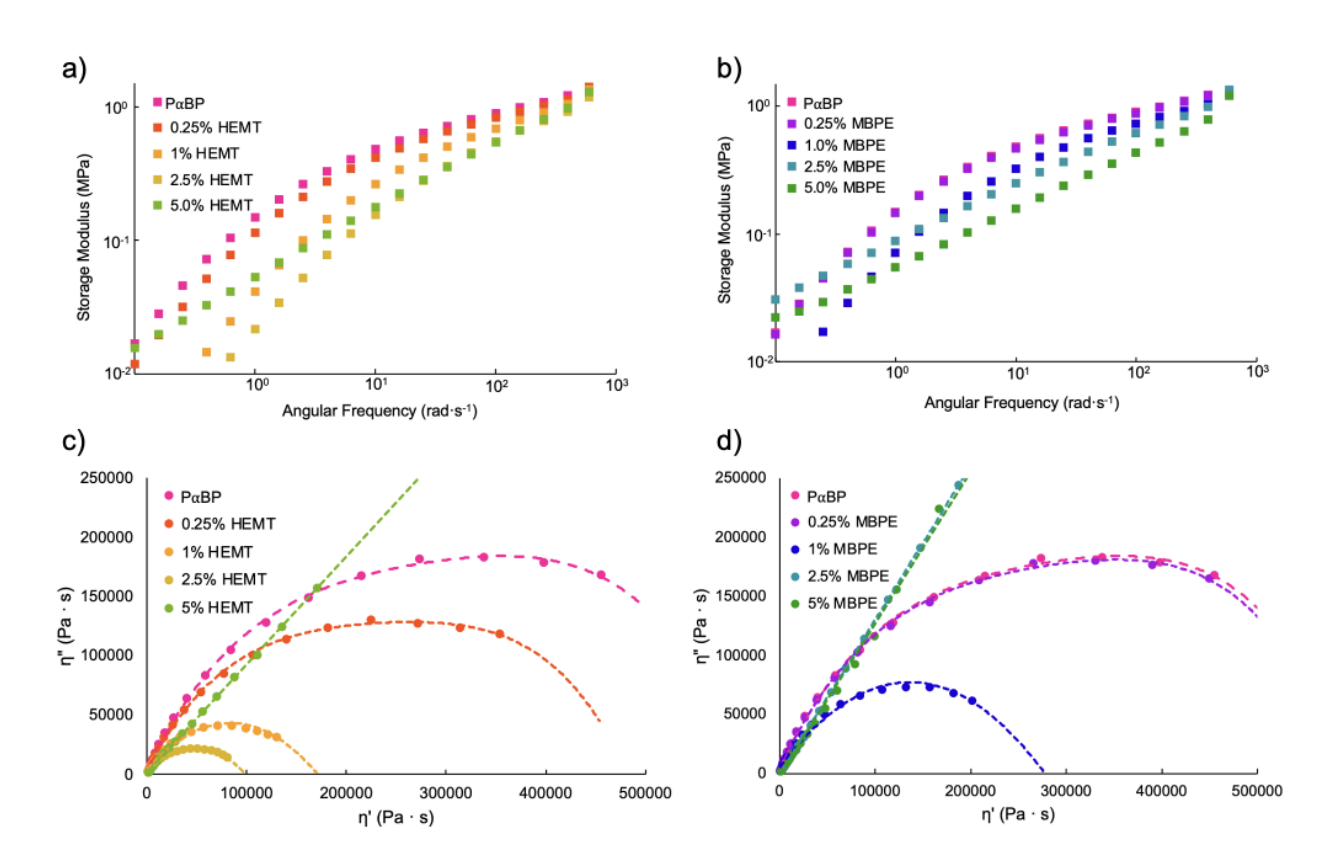


Figure 3.3: Rheological frequency sweeps (G' v. ω) for P α BP with HEMP (a) and MBPE (b) and Cole-Cole plots for HEMP (c) and MBPE (d).

In Cole-Cole plots, as a material undergoes increasing short-chain branching, a smaller "half moon" plot is obtained. This is extremely apparent in Figure 3.3c, in the case of HEMT. As HEMT is added, up to 2.5%, the amount of short chain branching increases significantly. However, at 5% addition, HEMT gels, and the line becomes linear. The same trend is observed in MBPE (Figure 3.3d), but at a lower concentration. At 0.25% loading of MBPE, some

branching is indicated in the plot. 1% indicates increased branching, and 2.5% and 5% loadings are both completely linear, indicating a strongly crosslinked system. With this, it is indicated that HEMT may have a better tendency to impart branching into the substrate, whereas MBPE will impart crosslinking at lower loadings or quicker reaction times.

Characterization of M_c:

Further rheological investigation was conducted using temperature sweeps to probe G' and G" over a range of temperatures. Using these plots, it is possible to relate the density of the polymer to the plateau modulus, $G'_{plateau}$. The determination of $G'_{plateau}$ was accomplished by the determination of the corresponding storage modulus (G') at the minimum tan δ above the T_g of the polymers ($G'_{plateau} = G'_{tan(\delta) = min}$). This value, as well as the temperature at this point, were used to calculate molecular weight between crosslinks (M_c) using the relationship described in Equation 3.1.

$$M_c = \frac{R \cdot T \cdot \rho}{G'_{plateau}}$$

Equation 3.1: Relationship between M_c , temperature at tan δ minimum (T), density of polymer as determined by helium pycnometery (ρ), and $G'_{plateau}$.

With this, temperature sweeps of all polymers were conducted. Sweeps of highly crosslinked materials did not exhibit a crossover of the storage modulus and the loss modulus after T_g of the polymers (Figure 3.4; S3.18 – S3.26).

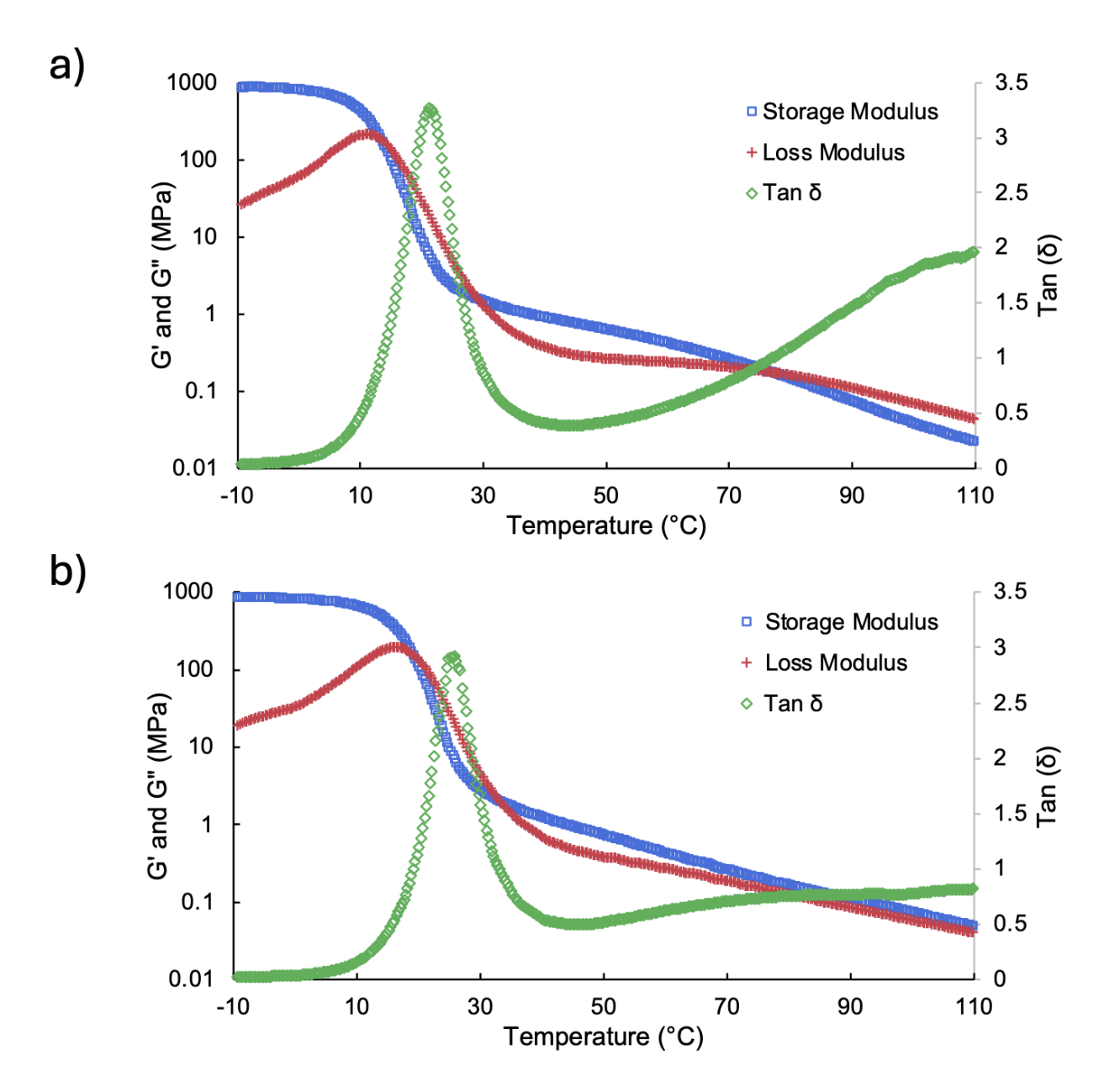


Figure 3.4: Rheology temperature sweeps of P α BP (a) and P α BP polymerized with 2.5% MBPE (b).

Using these plots, data was transformed using the density of the polymer and the rheological properties at the minimum value of tan δ above the T_g of the polymer. Summarized data for each polymer is outlined in Table 3.2.

Table 3.2: Summary of data required to calculate M_c.

Polymer	Density (g/cm ³):	T _{ref} (°C):	G'plateau (MPa):	M _c (g/mol):
PαBP with 0% crosslinker	1.188 ± 0.001	44.0	0.786	3950
PαBP with 0.25% MBPE	1.1832 ± 0.0005	49.5	0.767	4120
PαBP with 0.25% HEMT	1.181 ± 0.001	48.5	0.974	3240
PαBP with 1.0% MBPE	1.183 ± 0.002	41.0	0.890	3470
PαBP with 1.0% HEMT	1.180 ± 0.001	41.2	0.879	3510
PαBP with 2.5% MBPE	1.183 ± 0.002	45.6	0.934	3350
PαBP with 2.5% HEMT	1.180 ± 0.001	40.4	0.707	4350
PαBP with 5.0% MBPE	1.187 ± 0.001	46.1	0.596	5280
PαBP with 5.0% HEMT	1.198 ± 0.002	44.0	0.551	5730

Interestingly, there is not a clear trend observed for crosslinker loading and M_c. At high loadings of HEMT and MBPE, M_c is significantly higher than the control for both. This could possibly be related to high loadings of crosslinkers causing significant gelation of the material, preventing complete reaction of the remaining species. This possibility and others are currently under investigation in our laboratory.

Tensile Performance of Different Loadings:

The tensile performance of the polymers was evaluated using pressed film samples testing at 25.4°C. Agreeing with our previous work, even as pressed films, $P\alpha BP$ exhibited significant ductility and was unable to be pulled to sample rupture within the stroke distance of our instrument. (Figure 3.5).

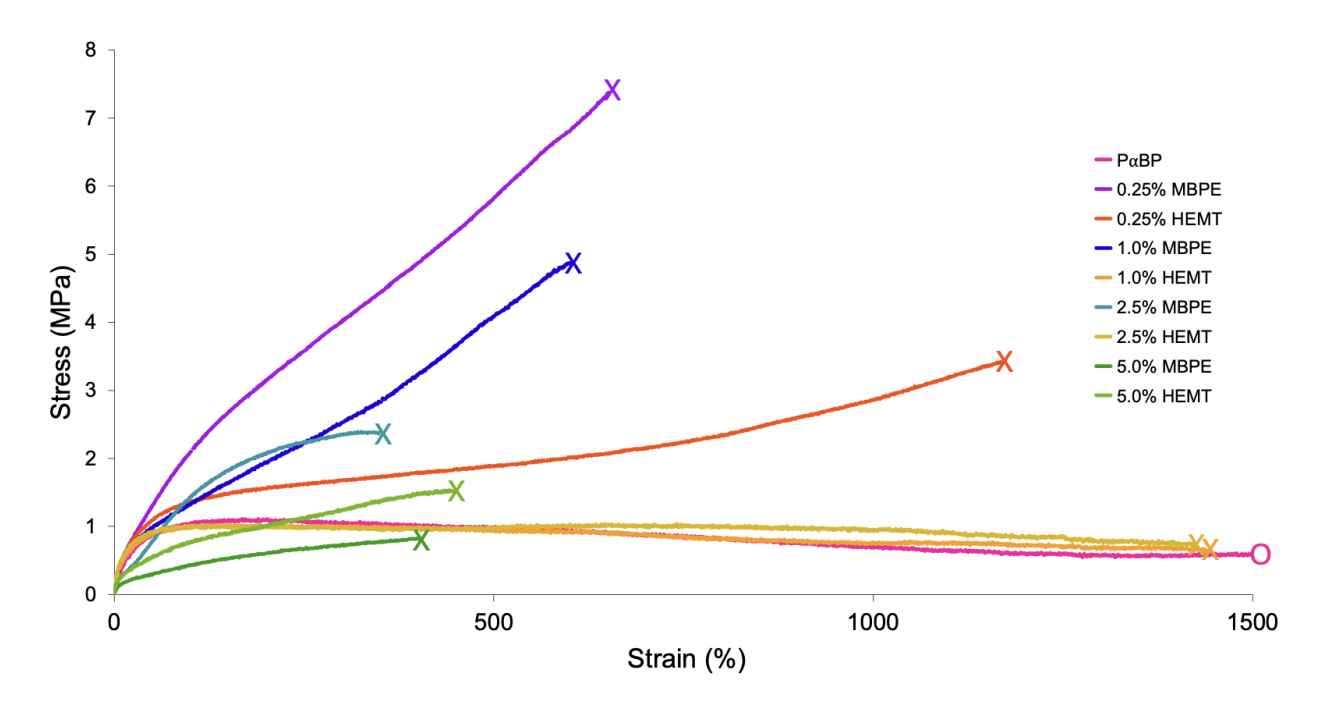


Figure 3.5: Stress v. strain for representative tensile specimens for each polymer in this study.

The addition of crosslinkers reduced the strain at break of the sample, and until very high loadings of material, also increased the modulus in turn. Interestingly, the σ_b for MBPE samples was obtained in the lowest loadings of crosslinker. As crosslinker loading increased, the σ_b decreased as well (Figure 3.5; Table 3.33. Perhaps correlated to earlier observations about M_c (Table 3.2), the 5% loading of MBPE exhibited a lower modulus than the control polymer. This could indicate that lower loadings of MBPE crosslinker can lead to improved, ϵ_b , and σ_b compared to higher loadings. For polymers containing HEMT crosslinkers, 0.25% loadings did improve Y in comparison to the control. As crosslinking content was increased to 1% and 2.5%, Y increased and ϵ_b also increased. Similarly to with MBPE, the addition of 5% HEMT decreased Y and ϵ_b , but still offered an improvement over the control.

Table 3.3: Summary of mechanical properties for polymers in this study

Polymer	Y (MPa):	ε _b (%)	σ _b (MPa):
PαBP with 0% crosslinker	8.7 ± 2.1	> 3800	n.d.
PαBP with 0.25% MBPE	12 ± 2.8	646 ± 41	7.4 ± 1.1
PαBP with 0.25% HEMT	12.0 ± 3.3	1100 ± 165	3.19 ± 0.13
PαBP with 1.0% MBPE	13.1 ± 3.6	679 ± 103	$4.62 \pm .97$
PαBP with 1.0% HEMT	15.3 ± 3.5	1124 ± 470	0.844 ± 0.32
PαBP with 2.5% MBPE	11.6 ± 2.2	350 ± 34	2.2 ± 0.50
PαBP with 2.5% HEMT	17.6 ± 4.4	1478 ± 28	1.01 ± 0.05
PαBP with 5.0% MBPE	$6.11 \pm .80$	442 ± 54.8	0.94 ± 0.18
PαBP with 5.0% HEMT	12.7 ± 2.8	461 ± 73	1.4 ± 0.37

Cyclic Tensile Performance of Different Loadings:

To quantify the elastomeric performance of the various crosslinked polyesters, r using cyclic tensile testing. First, films of the crosslinked polyesters underwent 10 cycles to 150%

strain. A comparison of uncrosslinked polymer to a high-performing example are shown in Figure 3.6.

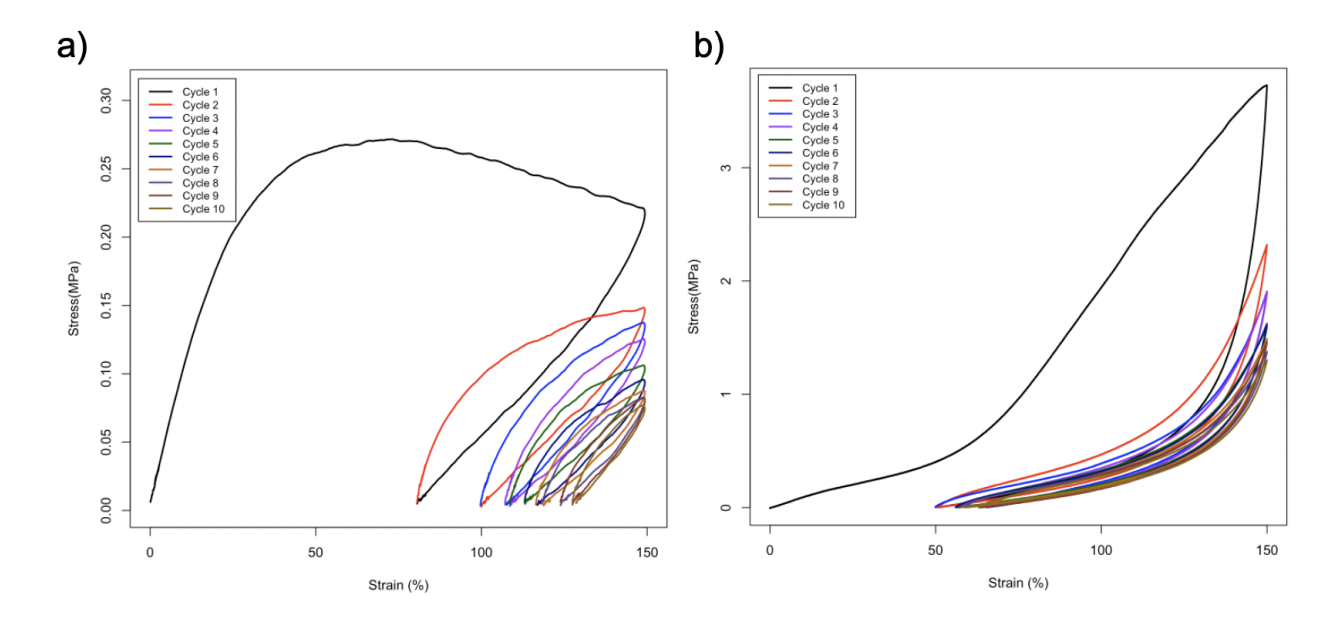


Figure 3.6: Cyclic tensile testing of P α BP (a) and P α BP that was crosslinked with 2.5% MBPE (b). Cyclic tensile testing data for all crosslinked polyesters may be found in the Appendix.

A qualitative look at the data above demonstrates significantly less hysteresis in the crosslinked sample than the control sample. To quantify the performance, relative recovery (R_r) and total recovery (R_t) were calculated using Equations 3.2 and 3.3. Relative recovery describes the amount the specimen recovered its dimensions compared to the previous final deformation (Equation 3.2).

$$R_r = \frac{|D_n - D_{n-1}|}{D_{n-1}}$$

Equation 3.2: R_r where D_n is the travel distance of the cycle n, and D_{n-1} is the travel distance of cycle n-1.

Total recovery describes the amount of recovery attained compared to total deformation (150 %). This is represented by Equation 3.3.

$$R_t = \left(1 - \frac{D_n}{D_{max}}\right) \cdot 100 \%$$

Equation 3.3: R_t where D_n is the stroke distance for cycle n, and D_{max} is the stroke value at the maximum ram travel; in the case of this experiment, 150%.

All relevant data for cyclic testing and the values obtained for these samples is summarized in Table S3.1. The most relevant parameter for comparisons to ideal elastomers is R_t , since an R_t value of 100% indicates perfect elastomeric recovery, and a plateau of R_t values at a strain above 50% indicates good elastomeric performance. Because of this, the values of R_t for each cycle were plotted.

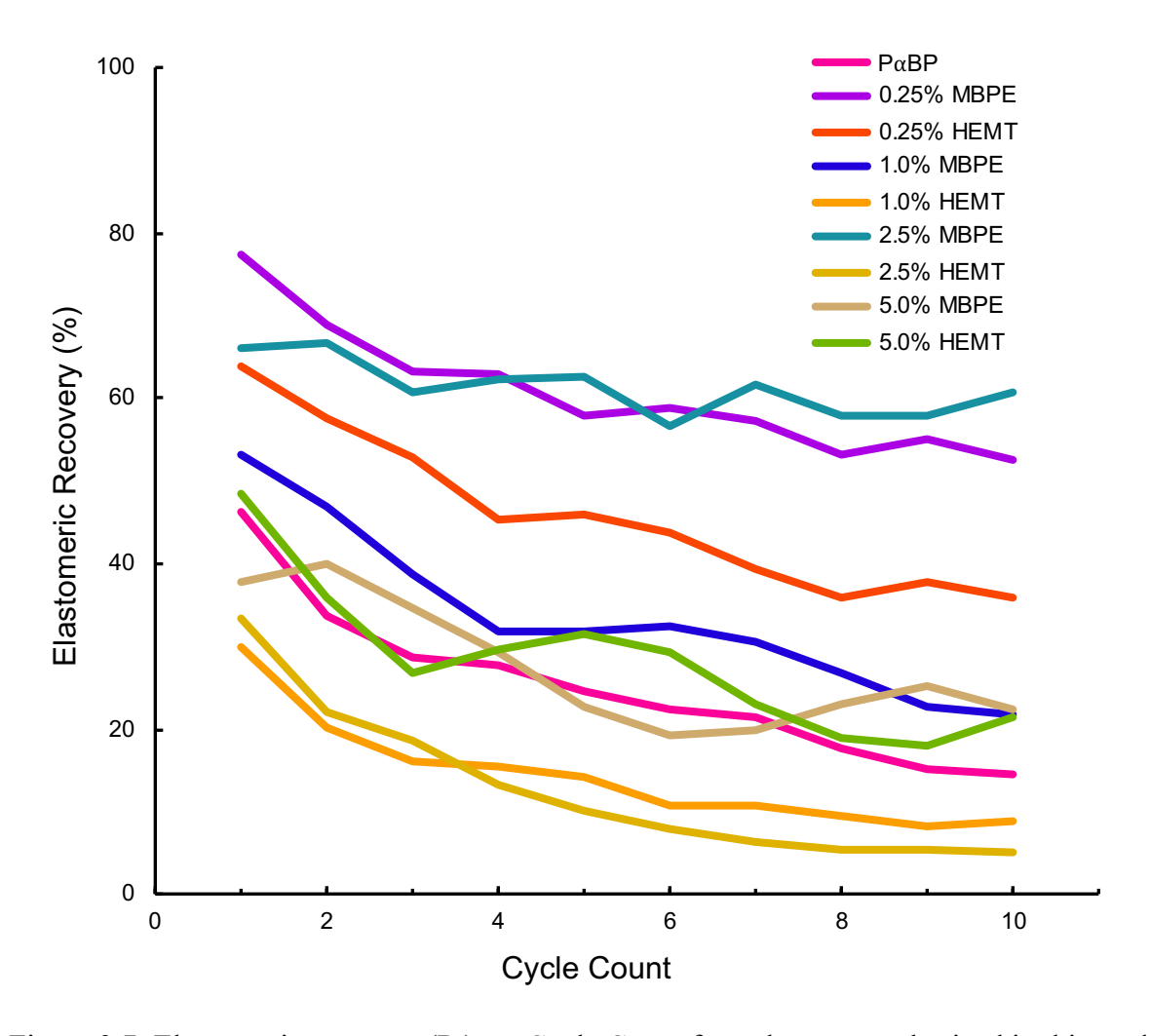


Figure 3.7: Elastomeric recovery (R_t) vs. Cycle Count for polymers synthesized in this study.

As shown in Figure 3.7, the incorporation of even very low loadings of MBPE (0.25% and 2.5%) offered a dramatic improvement to cyclic recovery when compared to the control. High loadings (5.0%) had a negligible difference in cyclic recovery when compared to the control. Interestingly, low loadings of HEMT (0.25%) also offered improvement in elastomeric performance, but higher loadings (1.0 %, 2.5%, and 5.0%) had negligible or deleterious effects on elastomeric recovery compared to the control. In the future, lower loadings of crosslinkers (of

both types) should be investigated to determine at which point elastomeric recovery reaches the maximum value, which could be at loadings lower than studied in this work.

Chemical Recycling to Monomer of 2.5% Crosslinked Samples:

One of the primary motivators for the design of the MBPE crosslinker was hypothesized ease of chemical recycling to monomer (CRM). To test this, a high-performing crosslinked polymer (2.5% MTBE, which exhibited excellent elastomeric recovery) was chosen as a test example. To our excitement, we found this polymer to degrade exceptionally rapidly in basic ethanol under reflux, with full conversion to the ethyl ester of the monomer and crosslinker occurring in 15 minutes (Figure 3.8).

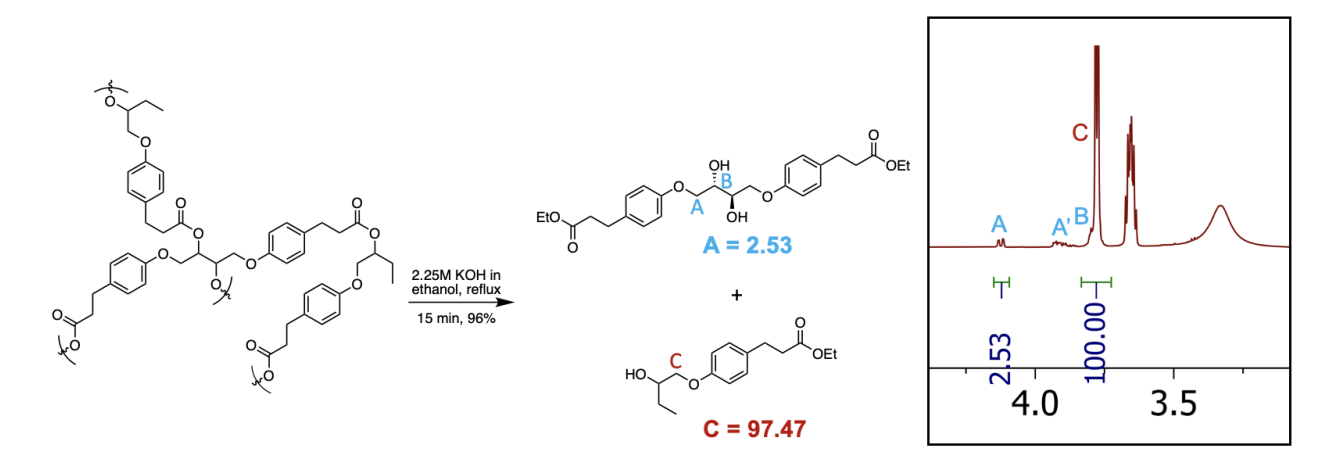


Figure 3.8: CRM scheme of 2.5% MBPE in basic ethanol.

Since this conversion was so rapid at reflux temperatures, similar conditions were replicated using deuterated base and solvent at the temperature of 40 °C, which could be observed in an NMR instrument. The results for this are demonstrated in a 120-minute long experiment, the data summarized in Figure 3.9.

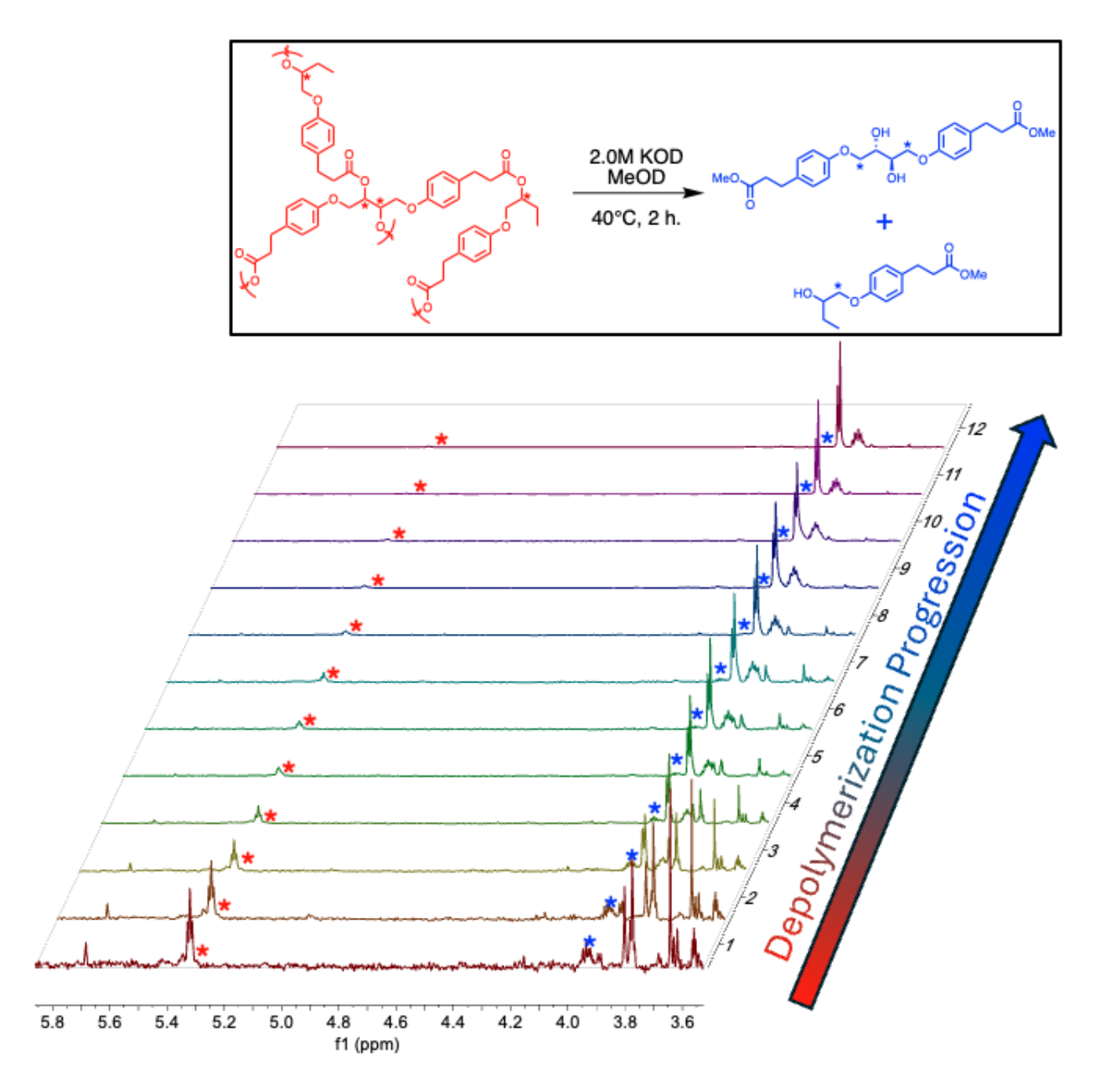


Figure 3.9: ¹H NMR monitoring of the conversion of polymer (bottom of overlay) to monomer and crosslinker (top of graph) at 40 °C in 2M KOD in MeOD. Scans were taken in 10 minute cycles for 2 hours.

With this experimental design, >98% depolymerization was achieved in two hours at relatively low temperatures. This indicates that these polymers may be excellent candidates for chemical recycling since they are rapidly depolymerized with excellent retention of original feed ratios.

Conclusions

Two crosslinker architectures were polymerized with α-butylene phloretate at small scales using antimony catalysis. The incorporation of MBPE crosslinker, which has hindered alcohols on the backbone, produced more highly crosslinked polymers compared to HEMT, which has more hindered carbonyls. Cole-Cole plots indicated that lower loadings of both materials favored short-chain branching, while higher loadings led to fully crosslinked systems. Tensile testing showed that low MBPE loadings outperformed higher loadings in terms of Y, εb, and σb, whereas HEMT exhibited increased Y and εb with higher loadings. Overall tensile performance decreased at 5% loadings of both crosslinkers. Cyclic tensile testing demonstrated superior elastomeric recovery in MBPE-based systems, with 0.25% and 2.5% MBPE loadings retaining ~60% elastic recovery over 10 cycles. Finally, these crosslinked systems can be rapidly chemically recycled to monomers with retention of the original feed ratios, highlighting their potential for sustainable materials design

References

- (1) Rzechonek, D. A.; Dobrowolski, A.; Rymowicz, W.; Mirończuk, A. M. Recent advances in biological production of erythritol. *Critical reviews in Biotechnology* **2018**, *38* (4), 620-633.
- (2) Sun, Z.; Fridrich, B.; De Santi, A.; Elangovan, S.; Barta, K. Bright side of lignin depolymerization: toward new platform chemicals. *Chemical reviews* **2018**, *118* (2), 614-678.
- (3) Martínková, L.; Grulich, M.; Pátek, M.; Křístková, B.; Winkler, M. Bio-Based Valorization of Lignin-Derived Phenolic Compounds: A Review. *Biomolecules* **2023**, *13* (5), 717.
- (4) Morrison, W. H.; Hartley, R. D.; Himmelsbach, D. S. Synthesis of substituted truxillic acids from p-coumaric and ferulic acid: simulation of photodimerization in plant cell walls. *Journal of Agricultural and Food Chemistry* **1992**, *40* (5), 768-771. DOI: 10.1021/jf00017a012.
- (5) Schmidt, S.; Gatti, F. J.; Luitz, M.; Ritter, B. S.; Bruchmann, B.; Mülhaupt, R. Erythritol
 Dicarbonate as Intermediate for Solvent- and Isocyanate-Free Tailoring of Bio-Based
 Polyhydroxyurethane Thermoplastics and Thermoplastic Elastomers. *Macromolecules* 2017, 50
 (6), 2296-2303. DOI: 10.1021/acs.macromol.6b02787.
- (6) Tachibana, S.; Ohkubo, K.; Towers, G. H. N. 4,4'-Dihydroxytruxillic acid as a component of the cell walls of the bambooPhyllostachys edulis. *Phytochemistry* **1992**, *31* (1), 81-83. DOI: https://doi.org/10.1016/0031-9422(91)83010-I.
- (7) Cohen, M. D.; Schmidt, G. M. J.; Sonntag, F. I. 384. Topochemistry. Part II. The photochemistry of trans-cinnamic acids. *Journal of the Chemical Society (Resumed)* **1964**, (0), 2000-2013, 10.1039/JR9640002000. DOI: 10.1039/JR9640002000.

CHAPTER 4

SYNTHESIS AND CHARACTERIZATION OF LIGNIN-DERIVED POLY(ESTER AMIDE)S.

Abstract

Finding alternative feedstocks to synthesize thermally stable polymers with excellent mechanical properties is increasingly important. In this work, a novel polyester was synthesized from potentially biobased 6-chloro-1-hexanol and phloretic acid, an abundant valorization product of lignin. Two previously reported polyesters were also synthesized, as well as copolymers of all three polyesters with ϵ -caprolactam and 11-aminoundecanonic acid to produce a suite of three biobased polyesters and six potentially-biobased poly(ester amide)s. Investigation of thermal stability of the polyesters and poly(ester amide)s indicated exceptional performance, with the lowest onset of degradation being 368 °C. Thermal properties varied greatly, with a range of T_g -14 °C – 79 °C, and T_m from 49 °C – 214 °C, suiting a variety of applications. Mechanical properties similarly covered a wide array, with polymers too brittle to test to those with significant elongation at break (Y = 27 MPa and ϵ_b = 1104 %.) One poly(ester amide) exhibited excellent elastomeric recovery, with R_r as low as 0.2% once initial permanent deformation had been achieved. This study reports the synthesis, thermal characterization and mechanical characterization of nine novel polyesters and poly(ester amide)s.

Introduction

Plastics are a critical component of modern society, but their increasing production will eventually cause difficulties with dwindling fossil fuel feedstocks. To counter this, significant work has been done to identify alternate feedstocks form polymers that can be derived from sustainable sources. One area of particular interest is finding biosourced feedstocks that can be polymerized into materials that exhibit high thermal stability while still maintaining excellent mechanical properties. Polyamides, while exhibiting excellent thermal stability and potentially

bioderived, are completely nondegradable in normal conditions.⁴ Additionally, very few of the most common nylon precursors are bioderived. One class of materials that is particularly interesting, combining both the processibility of esters and the thermal stability of nylons are poly(ester amide)s.⁵ Poly(ester amide)s can be synthesized to include various ester components, which can be completely bioderived, alongside amide comonomers.^{6,7} Through variation of the ester and amide components, the properties of poly(ester amide)s can be tuned to balance thermal stability and mechanical performance while still retaining biobased comonomer content.^{8,9} Additionally, characterizing the structure-property relationships of these materials is crucial for optimizing their performance and expanding their potential applications in sustainable plastics.

In this work, lignin-derived monomers were synthesized using sustainable, high-yielding reactions to be subsequently polymerized into both polyesters and poly(ester amide)s. The incorporation of lignin-derived monomers offers a promising route to sustainable comonomers while also potentially introducing unique structural features that can influence their thermal and mechanical behavior. By systematically varying the ester and amide monomer structures, specifically the length of alkyl chains in the polymer backbones, we aimed to characterize how these factors impact the resulting polymer properties. Thermal stability, mechanical performance, and processability were evaluated to assess the viability of these lignin-derived poly(ester amide)s as sustainable alternatives to conventional polymers. Additionally, cyclic recovery experiments for a highly elastic poly(ester amide) were conducted. These experiments provide insight into the structure-property relationships of lignin-derived poly(ester amide)s, highlighting their potential for applications requiring both high performance and sustainably-sourced materials.

Materials and Methods

Materials:

Phloretic acid (98%), ethylene carbonate (99%), 1-chloro-6-hexanol (98%), and potassium carbonate (99%) were purchased from Oakwood Chemical. 11-amino undecanoic acid and ε-caprolactam were purchased from Ambeed, Inc. Methyl-4-hydroxybenzoate was kindly supplied by Essential Ingredients, Inc. All other solvents and reagents were purchased from commercial suppliers and used as received.

Synthesis of Monomers:

1.
$$K_2CO_3$$
, $160^{\circ}C$

OMe

 K_2CO_3 , $160^{\circ}C$

OH

OH

75%

Scheme 4.1: Synthetic scheme of 4-(2-hydroxyethoxy)benzoic acid *via* the ring-opening of ethylene carbonate.

The synthesis of 4-(2-hydroxyethoxy)benzoic acid was adapted from our previously reported synthesis of 3-(4-(2-hydroxyethoxy)phenyl)propanoic acid (EP). ¹⁰ 239.3 g of methyl-4-hydroxybenzoate (1.57 mol), 152.0 g of ethylene carbonate (1.75 mol, 1.1 seq.), and 10.85 g of anhydrous K₂CO₃ (0.079 mol, 0.05 eq.) were added to a 2L 3-neck flask fitted with a nitrogen

inlet and a septum. The flask was purged and backfilled three times with nitrogen, and the septum was fitted with several 18-gauge needles to allow gas to vent, including a very slightly pressurized stream of nitrogen passing through the flask. After this, the flask was heated to 160 °C in an oil bath for 4 hours, until the evolution of CO_2 ceased. After this, the flask was cooled and 1L 3M NaOH was added. The turbid solution was refluxed overnight until the reaction was clear then cooled to 5 °C before acidifying with 6M HCl until pH = 2. The resulting precipitate was filtered and washed with water to yield 213 g (75%) of a white powder which was found to be >99% pure by ¹H NMR. ¹H NMR (600 MHz, CDCl₃; 10μ L TFA-*d* added): δ 8.07 (d, 2H, Ar-*H*), 6.98 (d, 2H, Ar-*H*), 4.22 (d, 2H, C*H*₂), 4.16 (d, 2H, C*H*₂).

HO CI
$$\rightarrow$$
 OH \rightarrow OH \rightarrow

Scheme 4.2: Synthetic scheme of 4-(6-hydroxyhexoxy)phloretic acid *via* the Williamson Ether Synthesis of 6-chlorohexanol and phloretic acid.

200 g of phloretic acid (1.2 mol, 1.0 eq.) and 200 g of potassium hydroxide (3.6 mol, 3 eq.) were added to a 3L, 3-neck flask followed by 1.25 L of 4:1 MeOH:H₂O. The homogenous solution was brought to reflux, and 246 g of 6-chloro-1-hexanol (1.8 mol, 1.5 eq.) were added dropwise over the course of two hours. After this addition, reflux was continued overnight. Reaction monitoring by ¹H NMR indicated only 85% conversion of phloretic acid, so an additional 82 g

(0.6 mol, 0.5 eq) of 6-chloro-1-hexanol was added dropwise. After 4 hours, all phloretic acid was consumed and the product mixture was cooled to room temperature and diluted with 1L of water. After dilution, the solution was cooled to 5 °C, acidified with 6M HCl until pH = 2, filtered, and washed with acidified water. The crude product was dried in a vacuum oven, and then recrystallized three times from 1:4 EtOH:Toluene to yield 237 g of a white powder (74%). 1 H NMR (600 MHz, CDCl₃): δ 7.11 (d, 2H, Ar-*H*), 6.82 (d, 2H, Ar-*H*), 3.95 (t, 2H, C*H*₂), 3.66 (t, 2H, C*H*₂), 2.90 (t, 2H, C*H*₂), 2.64 (t, 2H, C*H*₂), 1.78 (p, 2H, C*H*₂), 1.60 (p, 2H, C*H*₂), 1.46 (m, 2H, C*H*₂). 13 C NMR (600 MHz, CDCl₃): δ 157.56, 132.04, 129.14, 114.51, 67.76, 62.87, 35.54, 32.57, 29.74, 29.16, 25.81, 25.44.

Synthesis of Poly(ester amide)s:

General synthesis of homopolyesters and 11-amino-undecanoic acid copolymers:

Powdered monomers (120 grams total), 120 mg of MEHQ, and 1 mol% of catalyst relative to total monomer content was added to a 200 mL 3-neck round-bottom flask. The flask usually required some heating to reduce the volume of the powdery monomer. After loading, the flask was equipped with a short-path condenser with catch flask, a stir bearing with stir shaft and Teflon stir blade (SP Bel-Art), and a thermocouple. The flask was purged and backfilled three times with full vacuum and nitrogen, then heated to 160 °C with stirring at 150 rpm. A heating ramp of 5 °C/hr. was applied to the flask until the contents reached 220 °C. (12 h.). Full vacuum was applied to the flask (<200 mTorr) until the reaction was too viscous to accomplish adequate stirring. After this, the pressure was equalized with nitrogen, and the crude polymer was

collected from the flask using silicon release paper. The residual material was dissolved in solvent, precipitated, and dried in a vacuum oven at 80°C for three days to provide polymers in quantitative yields.

General Synthesis of 6-aminohexanoate copolymers:

Hydroxy (ether)acid monomers and ε-caprolactam (1:1 molar ratio; 120 g of total monomer) were added to a 200 mL 3-neck flask. The flasks required heating to reduce the volume of the powdery monomers. After loading, the flask was equipped with a short-path condenser with catch flask, a stir bearing with stir shaft and Teflon stir blade (SP Bel-Art), and a thermocouple. The flask was purged and backfilled three times with full vacuum and nitrogen, then heated to 160 °C with stirring at 150 rpm. The temperature was ramped to 220 °C at 10 °C/h. at which point the distillation apparatus was removed under positive nitrogen pressure and replaced with a reflux condenser. The condenser was not added initially due to difficulty maintaining temperature at >200 °C due to excess water in the reaction vessel. The solution was refluxed for 12 hours, after which the condenser was replaced once again by the distillation apparatus under positive nitrogen pressure. The flask was carefully put under vacuum (< 200 mTorr) and reacted at 220 °C until the contents were too viscous to attain adequate mixing. The crude polymer was removed from the flask and the residue was dissolved in solvent, precipitated, filtered, and then dried in a vacuum oven at 80 °C for three days to provide polymers in quantitative yields.

Structural Characterization:

¹H NMR and ¹³C NMR spectra were recorded at 25 °C on a Bruker Avance Neo 600 MHz instrument (USA) at a concentration of 10 mg/mL. Peak shifts in parts per million (ppm) were reported relative to the signal of chloroform-*d* at 7.26 ppm or DMSO-*d*6 at 2.50 ppm. For polyesters that were soluble in chloroform, molecular weight and dispersity (*Đ*) analyses were conducted on a Malvern OMNISEC RESOLVE gel permeation chromatography system (Malvern, USA) with a refractometer detector. Samples were dissolved in chloroform at a concentration of 1 mg/mL and filtered through a 0.2 μm PTFE filter. Viscotek® T-Series Columns (T3000, T4000, and T6000) columns were regulated at 35 °C and were eluted with HPLC-grade chloroform at a rate of 1 mL/min. The resulting molecular weight data is reported relative to polystyrene standards. Molecular weight data was unable to be collected for the copolymers in this study, as well as poly(ethylene benzoate) due to poor solubility.

Thermal Characterization:

The thermal stability of the polymers was determined *via* thermogravimetric analysis (TGA) using a Discovery TGA (TA Instruments, USA). Approximately 7-12 mg of sample was heated from room temperature to 600°C at 10°C/min in a nitrogen atmosphere. The thermal transitions of the polymers were determined using a Discover DSC 250 equipped with an RCS 90 cooling system (TA Instruments, USA). Samples were cooled to -40 °C, then heated to 220°C for two cycles. Data reported is from the first heating cycle unless otherwise noted.

Melt Extrusion:

Polymers were processed using melt extrusion with a Haake MiniLab II (Thermo-Fisher, USA). Injection molding was accomplished using a Haake Minijet Pro injection molding

machine (Thermo-Fisher, USA). The polymers were extruded at the endset of T_M by DSC + $\sim 20^{\circ}$ C. The injection molding ram was held at the extrusion temperature. A summary of the injection molding conditions may be found in **Error! Reference source not found.**

Table 4.1: Summary of injection molding conditions.

Polymer Name:	Extrusion/Barrel Temperature:	Mold Temperature:	Mold Treatment Prior to Sample Removal:
PEB	220 °C	80 °C	Ambient conditions
PCEB	160 °C	60 °C	Ambient conditions
PUEB	180 °C	70 °C	Ambient conditions
PEP	135 °C	25 °C	Ambient conditions
PCEP	130 °C	27 °C	Cooled in brine/ice bath (-15°C) before removing from mold.
PUEP	160 °C	50 °C	Ambient conditions
PHP	100 °C	40 °C	Cooled in brine/ice bath (-15°C) before removing from mold.
РСНР	160 °C	40 °C	Ambient conditions
PUHP	160 °C	50 °C	Ambient conditions

Mechanical Characterization:

Tensile performance of polyesters was evaluated using a Shimadzu AGS-X Universal Testing Machine (Shimadzu, USA). Samples were tested at 25.6 ± 0.3 °C with a rate of 50 mm/min for polymer and copolymers containing HP and EP monomers. For polymers containing EB monomers, a rate of 5mm/min was used. Data reported is the statistical average of 3

specimens. Cyclic tensile testing of PCEP was accomplished at a rate of 5 mm/min with a max strain of 300% and 10 cycles.

Results and Discussion

Synthesis of Monomers:

The synthesis of 4-(2-hydroxyethoxy)benzoic acid (EB) was adapted from our previous work. ¹⁰ Although EB has been synthesized previously using haloalcohols in the literature, ¹¹⁻¹³ to our knowledge this is the first report of the synthesis using the cyclic carbonate route. The advantages of this process are the ability to use ethylene carbonate, which can be derived from biorenewable feedstocks and carbon dioxide. ¹⁴ The reaction was straightforward to accomplish in these conditions and provided the desired monomer in high purity and good yield.

The synthesis of 4-(6-hydroxy-n-hexoxy)phloretic acid (HP) was accomplished using a traditional Williamson Ether-type reaction, starting with 6-chloro-1-hexanol. Although traditionally derived from petroleum, 6-chloro-1-hexanol may be derived by halogenation of 1,6-hexanediol, which can be synthesized from resources like cellulose and levoglucosenone. With condition optimization, the synthesis of potentially-biobased HP was accomplished in good yields with simple purification *via* recrystallization at greater than 200g scales.

Synthesis of Polyesters:

HO
$$\times$$
 OH

1) 1% Sb₂O₃, 0.1% MEHQ
160°C - 220°C, N₂, 12 h.

2) 220°C, < 200 mTorr, 3 - 12 h.

 \times = 1-5; \times = 0-2

HO

PEB

PEP

Vacuum Duration: 12 h.

Vacuum Duration: 3 h.

 \times Wacuum Duration: 4 h.

 \times M_w: 84.8 kDa; \times 1.9

New Yacuum Duration: 4 h.

M_w: 92.7 kDa; \times 1.9

Scheme 4.3: Synthesis of polyesters *via* antimony-catalyzed melt polycondensation.

The synthesis of polyesters in this study largely followed procedures that have yielded high-molecular weight polymers in our previous work. Antimony trioxide was chosen as a catalyst due to its relatively low activity which reduces side reactions that can cause substantial darkening of semi-aromatic polyesters. ¹⁰ Undesired oxidation was mitigated through the addition of 1000 ppm MEHQ. An initial heating ramp from 160 °C- 220 °C was conducted at a rate of 5 °C/h., during which most of the calculated water for the polycondensation was collected. This initial ramp is useful to build low-molecular weight oligomers, as these monomers can co-distill with water at elevated temperatures under vacuum otherwise. After the heating ramp and subsequent vacuum application, polyesters were afforded in excellent molecular weights for lab scale polycondensation reactions in the case of poly(ethylene phloretate) (PEP) (M_w: 84.8 kDa; Đ: 1.9) and poly(hexamethylene phloretate) (PHP) (M_w: 92.7 kDa; Đ: 1.9), both of which were soluble in chloroform and suitable for GPC analysis (Error!

Reference source not found.). However, PEB was found to be insoluble in chloroform and molecular weight data was unable to be collected using available instrumentation.

Synthesis of Ester-*co*-11-aminoundecanoate Polyesters:

HO
$$\begin{pmatrix} 1 \\ \\ \\ \\ \end{pmatrix}$$
 OH + $\begin{pmatrix} 1 \\ \\ \\ \\ \end{pmatrix}$ 1) 1% Sb₂O₃, 0.1% MEHQ
160°C - 220°C, N₂, 12 h.
2) 220°C, < 200 mTorr, 2 - 4 h.
$$x = 1-5; y = 0-2$$
PUEB
Vacuum Duration: 3 h.

PUEP
Vacuum Duration: 4 h.

PUEP
Vacuum Duration: 2 h.

Scheme 4.4: Synthesis of poly(ester amide)s with 11-UDA as comonomer *via* antimony-catalyzed melt polycondensation.

The synthesis of poly(ester amide)s with 11-aminoundecanoic acid (11-UDA) comonomer followed the same procedure as with the polyesters with good results. 11-UDA reacted well under these conditions, and distillation proceeded smoothly. These polymers were insoluble in chloroform and therefore molecular weight analyses were unable to be performed using instrumentation available.

Synthesis of Ester-*co*-6-aminohexanoate Polyesters:

HO
$$\begin{pmatrix} 1 \\ \\ \\ \\ \\ \end{pmatrix}$$
 OH + $\begin{pmatrix} 1 \\ \\ \\ \end{pmatrix}$ NH

$$\begin{pmatrix} 1 \\ \\ \\ \\ \end{pmatrix}$$
 1) 1% Sb₂O₃, 0.1% MEHQ
$$\begin{pmatrix} 160^{\circ}\text{C} - 220^{\circ}\text{C}, N_2, 6 \text{ h., -H}_2\text{O} \\ 2 \end{pmatrix}$$
 220°C, N₂, ref., 12 h.

$$\begin{pmatrix} 1 \\ \\ \\ \\ \end{pmatrix}$$
 3) 220°C, < 200 mTorr, 4 - 9 h.
$$x = 1-5; y = 0-2$$

$$\begin{pmatrix} 1 \\ \\ \\ \\ \\ \end{pmatrix}$$
PCEB
$$\begin{pmatrix} 1 \\ \\ \\ \\ \\ \\ \end{pmatrix}$$
PCEP
$$\begin{pmatrix} 1 \\ \\ \\ \\ \\ \\ \\ \end{pmatrix}$$
PCEP
$$\begin{pmatrix} 1 \\ \\ \\ \\ \\ \\ \\ \\ \end{pmatrix}$$
Vacuum Duration: 4 h.

Vacuum Duration: 4 h.

Scheme 4.5: Synthesis of poly(ester amide)s with 6-AH as comonomer *via* antimony-catalyzed ring opening of ε-caprolactam and subsequent melt polycondensation.

The synthesis of 6-aminohexanoate (6-AH) containing copolymers required more optimization. Initial attempts followed the same procedure as previously described, with a 12-hour ramp from 160 °C to 220 °C, followed by immediate application of vacuum. However, it was found that the ring-opening of ε -caprolactam (ε -CL) did not fully occur under these timeframes under these conditions. Rather, residual ε -CL remained in the reaction vessel and was slowly distilled out with water, leading to extended reaction times and uneven monomer incorporation. To reduce this, a reflux stage was utilized in which the water evolved during the initial reaction would be retained in order to continue the initiation of ε -CL hydrolytic ring-opening. This method worked very well and seemed to allow complete incorporation of 6-AH into the polymer with no evidence of monomer distillation. These polymers were also insoluble in chloroform and therefore molecular weight analyses were unable to be performed using instrumentation available.

Thermal Stability:

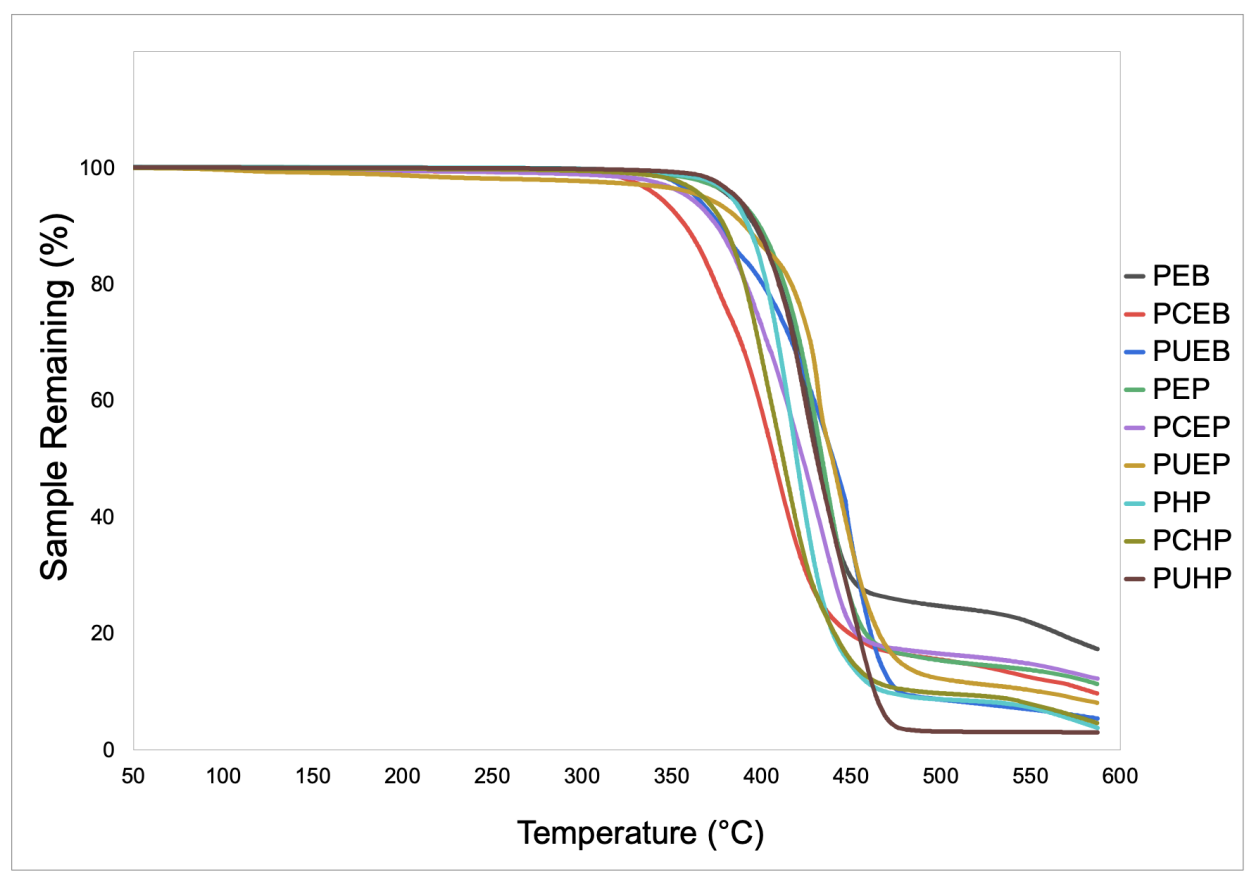


Figure 4.1: Thermogravimetric analysis data of all polymers synthesized in this study.

The thermal stability of the polyesters and poly(ester amides) was investigated using thermal gravimetric analysis (TGA) (Figure 4.1). Both the polyesters and poly(ester amide)s synthesized in this study exhibited excellent thermal stability, with the lowest onset of degradation exhibited by the copolymer PCEB ($T_{d95\%} = 368^{\circ}$ C) and the highest exhibited by the copolymer PUEP ($T_{d95\%} = 416^{\circ}$ C). There was no clear trend toward increasing or decreasing thermal stability observed in this study when comparing polyesters to the poly(ester amide) counterparts. Overall, the thermal stability of each polymer and copolymer was found to far exceed the minimum requirements for thermal processing *via* melt extrusion.

Thermal Transitions:

The glass transition temperatures (T_g) of the polyesters and copolymers synthesized followed the trend: PEB > PEP > PHP, as expected due to the hypothesized increase in chain flexibility offered by the increasing aliphatic moieties on the backbones of PEP and PHP polymers and copolymers (Table 4.2, Figure 4.2).

Table 4.2: Summary of thermal and mechanical data for polymers synthesized in this study.

Entry:	Polymer:	M _w (kDa):	Đ :	Y (MPa):	σ _y (MPa):	ε at break (%):	T _g (°C):	T _m (°C):	T _{d95%} (°C):
1	PEB	-	-	n.d.	n.d.	n.d.	79	214	402
2	PCEB	-	-	1290 ± 98	16 ± 3.1	2.8 ± 0.4	54	118	368
3	PUEB	-	-	830 ± 130	25.3 ± 0.4	38.0 ± 1.2	46	150	381
4	PEP	84.8	1.85	240 ± 54	0.51 ± 0.12	705 ± 17	22	127	406
5	PCEP	-	-	210 ± 35	0.42 ± 0.11	661 ± 30	20	112	380
6	PUEP	-	-	77 ± 3.8	4.4 ± 0.1	360 ± 19	1	121	416
7	PHP	92.7	1.94	90 ± 6.1	4.4 ± 0.5	641 ± 23	-14	49	396
8	PCHP	-	-	27 ± 4.7	1.6 ± 0.14	1104 ± 38	1	120	379
9	PUHP	-	-	77.9 ± 0.3	5.02 ± 0.05	248 ± 21	-4	119	400

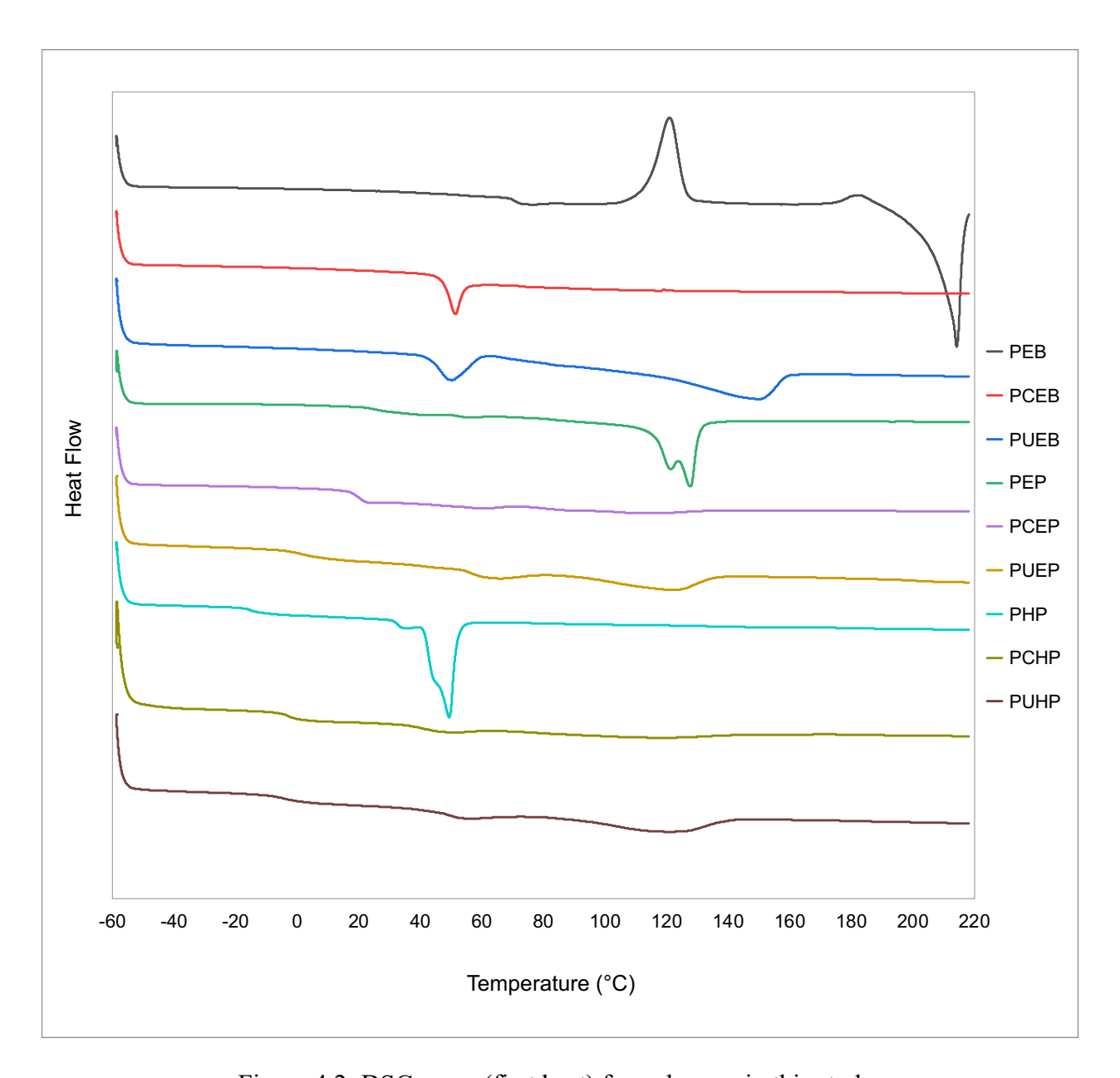


Figure 4.2: DSC scans (first heat) for polymers in this study.

PEB exhibited a high T_g of 79 °C, and a peak of melt (T_m) of 214 °C. This data agrees with the findings previously reported by Miller. ¹² For , the incorporation of amino comonomers reduced the T_g and T_m , with the larger reduction for both with 11-aminoundecanoate comonomer incorporation. PCEB exhibited reduced thermal transitions compared to the homopolymer (T_g :

54 °C, T_m : 118 °C) while PUEB displayed reduced T_g (46 °C) and a less-reduced T_m (150 °C) when compared to the reduction observed in PCEB. PEP as a homopolymer has already been reported in our group. Similarly to the case with PEB, incorporation of 6-AH comonomers reduced the T_g from 22 °C (PEP) to 20 °C (PCEP). The T_m was reduced from 127 °C with a bimodal melt transition to 112 °C with a very broad melting transition. The incorporation of 11-UDA comonomer in PUEP reduced the T_g further to 1 °C and the copolymer exhibited a very broad melting transition at 121 °C. PHP is a previously unreported polyester, with a T_g of -14 °C and a T_m of 49 °C. In contrast to the other six copolymers in this study, the incorporation of 6-AH and 11-UDA comonomers increased the T_g (PCHP: 1 °C; PUHP: -4 °C) and T_m (PCHP: 120 °C; PUHP: 119 °C). This is likely due to increased chain stiffness imparted by the amide groups increasing the T_g , as opposed to the very flexible backbone of the PHP homopolymer. Similarly, the hydrogen bond donating character of the amide backbones may increase the ΔH_m, which is directly correlated to the T_m of macromolecules. T_g

Melt Broadening and Reduction in Melting Enthalpy:

The copolymers in this study were synthesized at a 1:1 molar ratio. The melt enthalpy (ΔH_m) and change in temperature from onset of melt and endset of melt ($\Delta T_{o.e.} = T_{endset} - T_{onset}$) for the polymers synthesized in this study are summarized in **Error! Reference source not** found. Table 4.3: Description of melt transitions for polymers in this study.

Table 4.3: Description of melt transitions for polymers in this study.

Entry:	Polymer:	T _m (°C):	$\Delta H_m (J/g)$:	ΔT _{0.e} (°C):
1	PEB	214	48.5	36
2	PCEB	118	6.3	125

3	PUEB	150	37.8	89
4	PEP	127	35.9	93
5	PCEP	112	15.8	160
6	PUEP	121	38.4	130
7	PHP	49	31.8	51
8	PCHP	120	26.5	149
9	PUHP	119	38.14	132

For EB-containing polymers, the incorporation of amide comonomers significantly broadened the melting transition as compared to the polyester. The incorporation of 6-AH comonomer decreased the melt enthalpy by a significant amount, from 48.5 J/g to 6.3 J/g. The incorporation of the 11-UDA comonomer with EB reduced the enthalpy by a less significant amount to 37.8 J/g with less of a broadening effect when compared to 6-AH incorporation. While adding 6-AH comonomer to EP decreased the T_m and ΔH_m compared to the polyester of EP, the incorporation of 11-UDA increased the melt enthalpy compared to PEP (35.9 J/g vs. 38.4 J/g) with broadening of the melt. The addition of amide copolymers increased the T_m of HP containing polymers, with a change in PHP from 49 °C to 120°C for PCHP and 119 °C for PUHP.

With all copolymers in this study, the melt was significantly broadened when compared to the polyester counterpart. This is expected in copolymers, especially those with 1:1 molar ratios, and has been observed in other studies with 6-AH and 11-UDA copolymers. This phenomenon may be caused by crystal-lattice exclusion of one monomer's crystal from the other comonomer. This can cause a wide variation in the lamellar thickness and therefore can produce an exceptionally broad melting transition, which is usually most pronounced in 1:1 copolymers. This phenomenon is under investigation in our group by studying the effects of varying comonomer ratios upon the T_m , the ΔH_m , and the onset and endset of the melt.

Mechanical Properties:

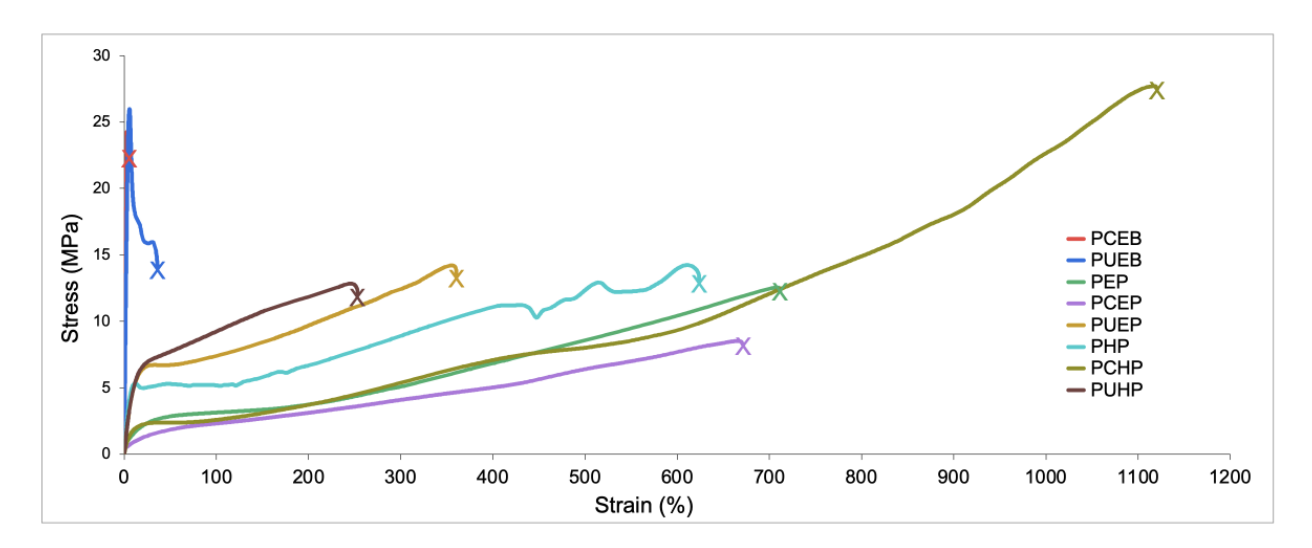


Figure 4.3: Stress/Strain data for all polymers except PEB (which was too brittle to test).

Mechanical properties of the polyesters and copolymers in this study varied widely (Figure 4.3). The least ductile polymers in this study were those containing EB moieties. PEB was too brittle to test, as sample specimens shattered before testing could begin. The incorporation of 6-AH comonomers improved the mechanical properties slightly, resulting in the brittle copolymer PCEB with Y = 1290 MPa and ε_b = 2.8. The incorporation of 11-UDA comonomers (PUEB) led to significantly increased mechanical performance compared to the polyester, with Y = 830 MPa and ε_b = 38.0 %.

PEP has been reported previously in our group.¹⁰ Compared to our previous work, an increase in modulus (Y = 240 MPa) and slight decrease in ε_b was observed (705 %) possibly due to the higher molecular weight achieved in this study due to longer polycondensation under vacuum. Incorporation of 6-AH comonomer in PCEP interestingly had little effect on Y or ε_b when compared to PEP (Y = 210 MPa; ε_b = 661 %). However, PCEP interestingly gained both

elastomeric and self-healing behavior, which will be discussed later. PUEP was both a softer material and lower strain at break with compared with PEP (Y = 77 MPa; ε_b = 360 %).

PHP was a softer polyester with (Y = 90 MPa; ε_b = 641 %). Interestingly, stress oscillation (SO) behavior was observed in PHP (Error! Reference source not found.) which was not observed in any other polyester in this study. SO is observed as an oscillatory response as opposed to a regular constant stress increase with strain. This behavior also occurs in a number of other polyesters, including poly(butylene succinate),²¹ poly(butylene succinate-*co*-cyclohexanedimethylene succinate),²² and poly(ethylene terephthalate)²³ and is considered difficult to replicate. It was observed for each sample of PHP when pulling at a rate of 50 mm/minute in this study. The incorporation of 6-AH comonomers to synthesize PCHP resulted in the softening of the polymer and increased ductility, with Y = 27 MPa and ε_b = 1104 %. The incorporation of 11-UDA as a comonomer reduced the ductility while maintaining the modulus of the parent polyester for PUHP (Y = 77.9 MPa and ε_b = 248 %).

Cyclic Recovery of PCEP

Upon tensile testing of PCEP, it was discovered that tensile specimens of PCEP recovered nearly completely to the original dimensions as demonstrated in Figure 4.4.

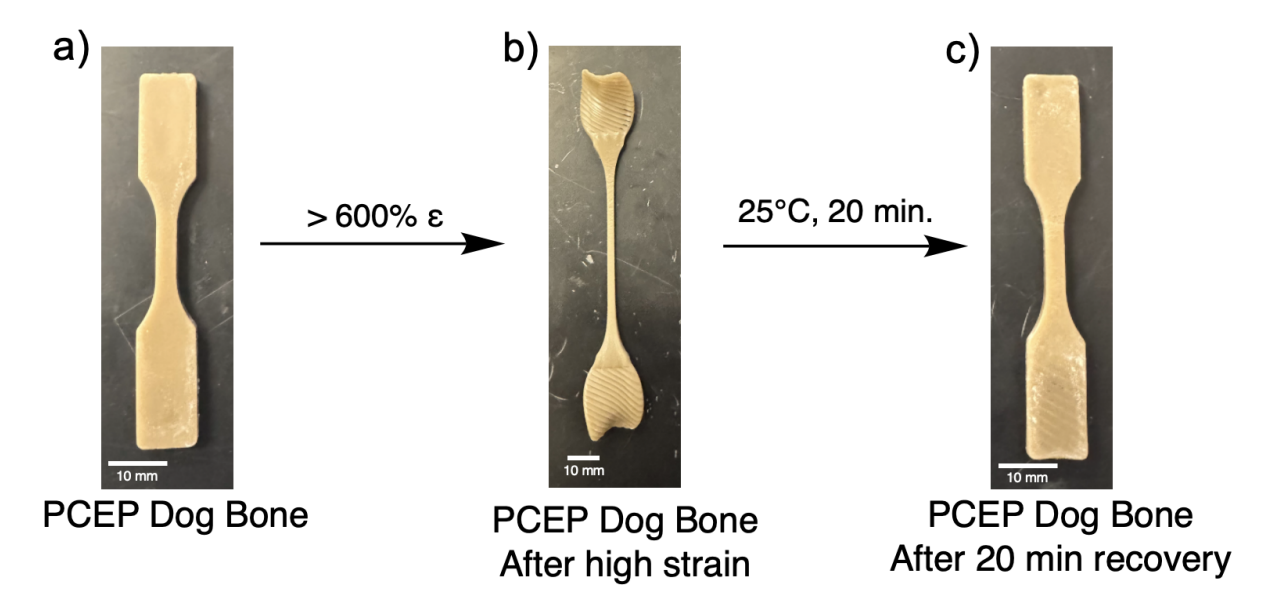


Figure 4.4: PCEP tensile specimen after injection molding (a), after high strain (b), and after 20 minutes of recovery at room temperature (c).

This behavior was intriguing, and was similar to what we have observed in previous work in our group, as well as that in other groups with semi-aromatic polymers and polymer additives. ^{10, 24, 25} To probe this behavior, PCEP was subjected to cyclic tensile loading at 5 mm/min as shown in Figure 4.5.

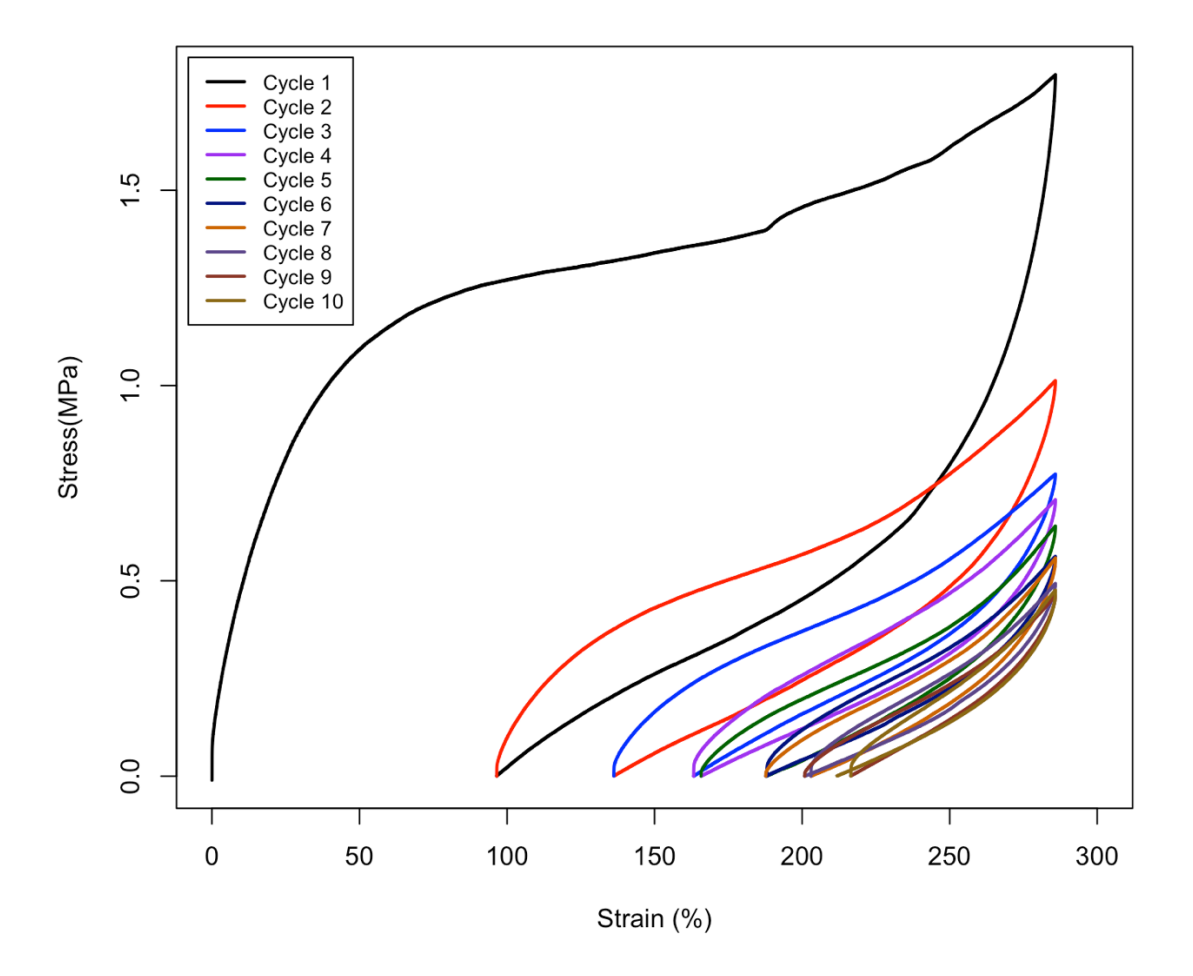


Figure 4.5: Cyclic tensile testing of PCEP at 5mm/min to 300% strain for 10 cycles.

This material exhibits excellent cyclic recovery performance. To quantify the performance, relative recovery (R_r) and total recovery (R_t) were quantified. Relative recovery describes the amount the specimen recovered its dimensions compared to the previous final deformation (Equation 4.1).

$$R_r = \frac{|D_n - D_{n-1}|}{D_{n-1}}$$

Equation 4.1: R_r where D_n is the travel distance of the cycle n, and D_{n-1} is the travel distance of cycle n-1.

Total recovery describes the amount of recovery attained compared to total deformation (300 %). This is represented by **Error! Reference source not found.**.

$$R_t = \left(1 - \frac{D_n}{D_{max}}\right) \cdot 100 \%$$

Equation 4.2: R_t where D_n is the stroke distance for cycle n, and D_{max} is the stroke value at the maximum ram travel; in the case of this experiment, 300%.

Using these equations, final values for R_r and R_t were calculated for PCEP and summarized in Table 4.4.

Table 4.4: Summarized cyclic tensile data for PCEP.

Cycle	E Final	R_r	R_t
1	97 %	66.1 %	66.1 %
2	136 %	40.6 %	52.3%
3	163 %	19.9 %	42.9 %
4	166 %	1.5 %	42.0 %
5	188 %	13.4 %	34.2 %
6	188 %	0.2 %	34.3 %
7	203 %	8.1 %	28.9 %
8	201 %	1.1 %	29.7 %
9	217 %	7.8 %	24.3 %
10	211 %	2.1 %	25.9 %

With cyclic loading, an elastomer is loaded to a maximum strain, and then relaxed until the stress reaches zero. For an ideal elastomer, this point would be where the strain is zero as well. However, in most materials there is some amount of permanent deformation that occurs that can cause loss of elastomeric performance and hysteresis. In the case of PCEP, significant irreversible deformation occurs in cycles 1-3. However, after this initial deformation, there is a plateau where performance maintains relative stability for the remaining cycles, indicating good elastomeric recovery which aligns well with other data in the literature for thermoplastic elastomers. Although the exact mechanism of elastomeric behavior for this material is unknown, contributing factors could be the T_g, which is near room temperature, the low crystallinity of then material, or potentially ideal spacing between 6-AH and EP comonomer units allowing for favorable hydrogen bonding interactions. The mechanism of elastomeric behavior is currently under investigation in our laboratory.

Conclusions

With sustainable methodology, three aromatic monomers were synthesized in high-yielding reactions. Using these lignin-derived monomers, three polyesters and six poly(ester amides) were polymerized under polycondensation conditions using antimony catalysis, which yielded high molecular weight polyesters and also poly(ester amides) that were too viscous in the melt to maintain sufficient mixing, indicating similarly-suitable molecular weights. The thermal stability of the polyesters and poly(ester amide)s was high, with the lowest onset of degradation being $368 \, ^{\circ}$ C for PCEB. Thermal properties varied greatly, with a range of T_g -14 $^{\circ}$ C - 79 $^{\circ}$ C, and T_m from 49 $^{\circ}$ C - 214 $^{\circ}$ C. Mechanical properties covered a wide array, with polymers too brittle to test (PEB) to those with significant elongation at break (PCHP; Y = 27 MPa and ϵ_b = 1104 %.)

PCEP exhibited excellent elastomeric recovery, with R_r as low as 0.2% after permanent deformation occurred. Overall, this study reports the synthesis of novel poly(ester amide)s with excellent thermal and mechanical properties that could be used for a variety of applications.

References

- (1) Geyer, R.; Jambeck, J. R.; Law, K. L. Production, use, and fate of all plastics ever made. *Science Advances* **2017**, *3* (7), e1700782. DOI: doi:10.1126/sciadv.1700782.
- (2) Rosenboom, J.-G.; Langer, R.; Traverso, G. Bioplastics for a circular economy. *Nature Reviews Materials* **2022**, *7* (2), 117-137. DOI: 10.1038/s41578-021-00407-8.
- (3) The multifaceted challenges of bioplastics. *Nature Reviews Bioengineering* **2024**, *2* (4), 279-279. DOI: 10.1038/s44222-024-00181-6.
- (4) Vagholkar, P. Nylon (Chemistry, Properties and Uses). *International Journal of Scientific Research* **2016**, *5*, 349-351.
- (5) Winnacker, M.; Rieger, B. Poly(ester amide)s: recent insights into synthesis, stability and biomedical applications. *Polymer Chemistry* **2016**, *7* (46), 7039-7046, 10.1039/C6PY01783E. DOI: 10.1039/C6PY01783E.
- (6) Martino, L.; Basilissi, L.; Farina, H.; Ortenzi, M. A.; Zini, E.; Di Silvestro, G.; Scandola, M. Bio-based polyamide 11: Synthesis, rheology and solid-state properties of star structures. *European Polymer Journal* **2014**, *59*, 69-77. DOI: https://doi.org/10.1016/j.eurpolymj.2014.07.012.
- (7) Botines, E.; Rodríguez-Galán, A.; Puiggalí, J. Poly(ester amide)s derived from 1,4-butanediol, adipic acid and 1,6-aminohexanoic acid: characterization and degradation studies. *Polymer* **2002**, *43* (23), 6073-6084. DOI: https://doi.org/10.1016/S0032-3861(02)00577-3.

- (8) Ferré, T. s.; Franco, L.; Rodríguez-Galán, A.; Puiggalí, J. Poly(ester amide)s derived from 1,4-butanediol, adipic acid and 6-aminohexanoic acid. Part II: composition changes and fillers. *Polymer* **2003**, *44* (20), 6139-6152. DOI: https://doi.org/10.1016/S0032-3861(03)00679-7.
- (9) Lozano, M.; Franco, L.; Rodríguez-Galán, A.; Puiggalí, J. Poly(ester amide)s derived from 1,4-butanediol, adipic acid and 6-aminohexanoic acid: Part III: substitution of adipic acid units by terephthalic acid units. *Polymer Degradation and Stability* **2004**, *85* (1), 595-604. DOI: https://doi.org/10.1016/j.polymdegradstab.2003.11.018.
- (10) Winfield, D.; Ring, J.; Horn, J.; White, E. M.; Locklin, J. Semi-aromatic biobased polyesters derived from lignin and cyclic carbonates. *Green Chem* **2021**, *23* (23), 9658-9668. DOI: 10.1039/d1gc03135j.
- (11) Gao, Y.; Yao, W.; Sun, J.; Zhang, H.; Wang, Z.; Wang, L.; Yang, D.; Zhang, L.; Yang, H. A novel soft matter composite material for energy-saving smart windows: from preparation to device application. *Journal of Materials Chemistry A* **2015**, *3* (20), 10738-10746, 10.1039/C4TA06347C. DOI: 10.1039/C4TA06347C.
- (12) Mialon, L.; Vanderhenst, R.; Pemba, A. G.; Miller, S. A. Polyalkylenehydroxybenzoates (PAHBs): Biorenewable aromatic/aliphatic polyesters from lignin. *Macromolecular Rapid Communications* **2011**, *32* (17), 1386-1392.
- (13) Xu, X.-X.; Chao, C.-Y.; Yao, X.-J. Synthesis, structure, and mesomorphism of novel liquid crystalline acrylate monomers and polymers. *Molecular Crystals and Liquid Crystals* **2016**, *624* (1), 1-10. DOI: 10.1080/15421406.2015.1017295.
- (14) Ng, W. L.; Er, Z. X.; Chandrakumar, D.; Loy, A. C. M.; Vongsvivut, J.; Bhattacharya, S. Sustainable Route of Ethylene Carbonate Production via CO2 Carboxylation: Process

- Development, Process Integration, and Economic Analysis. *ACS Sus. Chem. Eng.* **2024**, *12* (51), 18320-18334. DOI: 10.1021/acssuschemeng.4c06519.
- (15) Becker, R., Machenroth, W., Seufert, W. Preparation of haloalcohols. 1994.
- (16) Kim, H.; Lee, S.; Won, W. System-level analyses for the production of 1,6-hexanediol from cellulose. *Energy* **2021**, *214*, 118974. DOI: https://doi.org/10.1016/j.energy.2020.118974.
- (17) Allgeier, A. M.; Corbin, D. R.; De Silva, W. I. N.; Korovessi, E.; Menning, C. A.; Ritter, J. C.; Sengupta, S. K. Process for preparing 1, 6-hexanediol. Google Patents: 2014.
- (18) Fang, H.; Su, S.; Luo, Y.; Jiang, Y.; Luo, Z. Unveiling the Mechanisms of Hydrolytic Ring-Opening Polymerization of Caprolactam and Amino-Assisted Ring Opening of Cyclic Dimers: A DFT Study. *Industrial & Engineering Chemistry Research* **2023**, *62* (1), 136-144. DOI: 10.1021/acs.iecr.2c03328.
- (19) Ornstein, R. L.; Fresco, J. R. Correlation of Tm and sequence of DNA duplexes with delta H computed by an improved empirical potential method. *Biopolymers* **1983**, *22* (8), 1979-2000. DOI: 10.1002/bip.360220811 From NLM.
- (20) Zierdt, P.; Mitzner, E.; Gomoll, A.; Theumer, T.; Lieske, A. Synthesis of polyamide 6/11 copolymers and their use as matrix polymer in wood-plastic composites. *Journal of Applied Polymer Science* **2016**, *133* (46).
- (21) Wan, C.; Heeley, E. L.; Zhou, Y.; Wang, S.; Cafolla, C. T.; Crabb, E. M.; Hughes, D. J. Stress-oscillation behaviour of semi-crystalline polymers: the case of poly(butylene succinate). *Soft Matter* **2018**, *14* (45), 9175-9184, 10.1039/C8SM01889H. DOI: 10.1039/C8SM01889H. (22) Wan, T.; Zhang, J.; Liao, S.; Du, T. An investigation of stress oscillation in poly(butylene succinate-co-cyclohexanedimethylene succinate). *Polymer Engineering & Science* **2015**, *55* (4), 966-974. DOI: https://doi.org/10.1002/pen.23966.

- (23) Heeley, E. L.; Smith, J.; Wan, C.; Huband, S.; Brambley, E.; Hughes, D. J. Revisiting stress-oscillation in cold drawing of poly(ethylene terephthalate). *Polymer* **2023**, *285*, 126364. DOI: https://doi.org/10.1016/j.polymer.2023.126364.
- (24) Xanthopoulou, E.; Terzopoulou, Z.; Zamboulis, A.; Koltsakidis, S.; Tzetzis, D.; Peponaki, K.; Vlassopoulos, D.; Guigo, N.; Bikiaris, D. N.; Papageorgiou, G. Z. Poly(hexylene vanillate): Synthetic Pathway and Remarkable Properties of a Novel Alipharomatic Lignin-Based Polyester. *ACS Sus. Chem. Eng.* **2023**, *11* (4), 1569-1580. DOI: 10.1021/acssuschemeng.2c06507.
- (25) Gallos, A.; Crowet, J.-M.; Michely, L.; Raghuwanshi, V. S.; Mention, M. M.; Langlois, V.; Dauchez, M.; Garnier, G.; Allais, F. Blending Ferulic Acid Derivatives and Polylactic Acid into Biobased and Transparent Elastomeric Materials with Shape Memory Properties.

 Biomacromolecules 2021, 22 (4), 1568-1578. DOI: 10.1021/acs.biomac.1c00002.

CHAPTER 5

CONCLUSIONS AND FUTURE DIRECTIONS

Conclusions

A significant number of novel, bioderived and semi-aromatic polyesters were synthesized from sustainably-sourced monomers. Starting with fundamental studies of polymers in this class, incremental changes to polymer microstructure were performed and the resulting polymers were compared. With this came novel reports of the effects of polymer structure on mechnical, thermal, and rheological properties. Furthermore, it was demonstrated that these lignin-derived AB polyesters could be very simply chemically-recycled in rapid timeframes and in good yields. However, one significant downside of these polymers was their completely amorphous nature. Because of this, when heated above their Tg, the polyesters will have a tendency to flow, with more rapid flow rate occurring the higher the temperature of the material.

To counter this, novel AABB crosslinkers were designed using the same fundamental ideas as presented in Chapter 2. In contrast to traditional crosslinking or branching agents that are freely water soluble, these crosslinkers were designed to be specifically insoluble to encourage the possibility of chemical-recycling. Using p-coumaric acid, a truxillate-based crosslinker was designed using the ring opening of biobased ethylene carbonate in good yields. A second AABB crosslinker from phloretic acid and erythritol dicarbonate was also designed and synthesized. These crosslinkers, when incorporated with aBP monomers in small-scale

polycondensations, produced a significant range of tunable crosslinked polyesters, some of which exhibited remarkable elastomeric recovery. Additionally, agreeing with the original goal of the project, the crosslinked polymers were rapidly chemically-recycled to monomer in complete conversion and high yields.

Finally, in moving toward biobased materials that require higher moduli, a novel polyester PHP was synthesized and characterized. Additionally, two previously-reported polyesters, PEB and PEP were sythesizer, alongside copolymers of all three polyesters with caprolactam comonomers and 11-aminoundecanoic acid comonomers. The nine polymer series was characterized to exhibit high thermal stability and was processed via melt-extrusion.

Subsequent tensile testing demonstrated a significant variance in mechanical performance of the polymers, from extremely brittle to very ductile while still retaining high stress at break. One polymer, PCEP, was found to exhibit excellent elastomeric recovery when deformed to 300% strain.

Future Directions

For the first project, an important direction for improvement was the addition of crosslinkers to enhance elasticity. However, the exact cause of the elasticity (as thermoplastics) has not been thoroughly investigated. Some literature evidence has pointed toward π - π stacking as a possible contributing factor to this recovery. X-ray diffraction experiments could be conducted on the polyesters to see to what extent these effects may be imparting elastomeric recovery in these systems.

In the second chapter, the isomerization of HEMT during synthesis may be systematically investigated. Reaction optimization through solvent selection, base selection, total concentration, and reaction duration could be investigated to either prevent isomerization, or to deliberately completely isomerize the truxillate. This would allow for the synthesis of a isomerically pure crosslinker. Subsequent polymerization could help determine if there is a change in reactivity for one isomer or another depending on the steric orientation of the carboxylate group.

Another important addition would be to investigate lower loadings of crosslinkers.

Excellent tensile and elastomeric properties were achieved with both crosslinkers at the lowest loading. This is a potential indication that the most optimized performance may be at lower loadings of crosslinkers than were tested in this work. Further investigations could also include the synthesis of these polymers at larger scales, which would potentially offer better mixing and prevent the poor performance observed in the highest percent loadings.

Finally, the applications of the lignin-derived poly(ester amide)s gave not been thoroughly characterized. The first starting point will be the investigation of 3D printing of PCHP, which is currently in ongoing investigation in our lab. Optimization of this process will present the opportunity to create functional materials that can be used to demonstrate applicability outside of the laboratory setting.

Literature Cited

(1) Gallos, A.; Crowet, J.-M.; Michely, L.; Raghuwanshi, V. S.; Mention, M. M.; Langlois, V.; Dauchez, M.; Garnier, G.; Allais, F. Blending Ferulic Acid Derivatives and Polylactic Acid into Biobased and Transparent Elastomeric Materials with Shape Memory Properties.

Biomacromolecules 2021, 22 (4), 1568-1578. DOI: 10.1021/acs.biomac.1c00002.

APPENDICES

APPENDIX A

SUPPLEMENTAL INFORMATION FOR CHAPTER 2

Synthesis of Hydroxyacids, Hydroxyesters, and Monomers:

Synthesis of methyl 3-(2-hydroxyphenyl)propanoate:

100 g of dihydrocoumarin (665 mmol), 1 L of methanol, and 1 mL of concentrated sulfuric acid were added to a 2 L, single neck flask. The solution was heated to reflux for 12 h. before being cooled to room temperature. The solvent was removed under reduced pressure and the residue was taken up into ethyl acetate. The organic layer was washed with water, a saturated solution of sodium bicarbonate, then brine, followed by drying over magnesium sulfate. After filtration, the solvent was removed under reduced pressure to afford 116 g of a slowly crystallizing white solid (95%). The resulting ¹H NMR spectrum agreed with previously published results. ¹ H NMR (600 MHz, CDCl₃): δ 7.11 (m, 2H, H_{Ar}), 7.01 (s, 1H, OH), 6.87 (t, 2H, H_{Ar}), 3.69 (s, 3H, OCH₃), 2.91 (t, 2H, CH₂), 2.73 (t, 2H, CH₂).

Synthesis of 3-(4-hydroxyphenyl)-2-methylacrylic acid:

Adapted from published procedure. 2 260 g of 4-hydroxybenzaldehyde (2.13 mol) and 435 g of sodium propionate (4.5 mol) were added to a 5 L 3-neck flask. The flask was purged with full vacuum and backfilled with dry nitrogen three times. 790 mL of propionic anhydride (6 mol) were added under positive nitrogen flow and the mixture was heated to 140 °C, becoming a homogenous, light brown solution. The solution was kept at this temperature for 48 h, during which it became extremely dark in color. After this, the solution was cooled to room temperature and 3 L of deionized water were added. The heterogenous mixture was filtered, and the cake was washed with water. The collected solid was dissolved in 3 L of 2 M NaOH solution and filtered once again. The small amount of collected solid was discarded, and the filtrate was acidified to pH = 1. A final filtration was conducted, and the collected solid was once again washed very thoroughly with water. The solid was dried under vacuum at 60 °C for 24 h. to yield 370 g of a light tan solid (98%). Spectra agreed with the previously published result. 1 H NMR (600 MHz, DMSO-d₆): δ 12.27 (s, 1H, COOH), 9.89 (s, 1H, OH), 7.50 (s, 1H, =CH), 7.34 (d, 2H, H_{Ar}), 6.83 (d, 2H, H_{Ar}), 2.02 (s, 3H, CH₃).

Synthesis of methyl 3-(4-hydroxyphenyl)-2-methylacrylate:

120 g (0.67 mol) of 3-(4-hydroxyphenyl)-2-methylacrylic acid, 1 L methanol, and 1 mL concentrated H₂SO₄ were added to a 2 L single neck flask and refluxed for 14 hours. After completion of the reaction, the solvent was removed under reduced pressure and the residue was

taken up in ethyl acetate. The organic layer was washed once with water, three times with saturated aqueous sodium bicarbonate solution, and once with brine. The organic layer was dried over magnesium sulfate and then filtered into a flask. Excess solvent was removed under reduced pressure to afford 127 g of product as a light tan solid (98%). ¹H NMR (600 MHz, DMSO-d₆): δ 9.86 (s, 1H, OH), 7.53 (s, 1H, =CH), 7.36 (d, 2H, H_{Ar}), 6.82 (d, 2H, H_{Ar}), 3.72 (s, 3H, OCH₃), 2.06, (s, 3H, CH₃).

Synthesis of 3-(4-hydroxyphenyl)-2-methylpropanoic acid:

134 g of 3-(4-hydroxyphenyl)-2-methylacrylic acid (752 mmol), 7.98 g of 10 % pd/C (0.01 eq.), and 1.5 L of ethyl acetate were added to a 3 L three-necked flask under a nitrogen atmosphere. The atmosphere of the flask was gently evacuated and backfilled 5 times with hydrogen. The mixture was kept under a hydrogen atmosphere for 48 h and monitored by ¹H NMR spectroscopy. After this time, complete conversion was not observed. The atmosphere was flushed with nitrogen and a second equivalent of catalyst (7.98 g) was added. Once again, the atmosphere was gently evacuated and backfilled 5 times with hydrogen. The mixture was stirred in a hydrogen atmosphere for another 48 hours until ¹H NMR spectroscopy indicated complete conversion. The solid catalyst was removed via filtration, and the filtrate was further purified by passing through a short column of celite. The solvent was removed under reduced pressure to

yield 120 g of a slowly crystallizing yellow solid (90%). ¹H NMR (600 MHz, DMSO-d₆): δ 12.07 (s, 1H, COOH), 9.16 (s, 1H, s, OH), 6.96 (d, 2H, H_{Ar}), 6.66 (d, 2H, H_{Ar}), 2.79 (q, 1H, CHH), 2.54 (m, 1H, CHH), 2.47 (m, 1H, CH), 1.01 (d, 3H, CH₃).

Synthesis of methyl 3-(4-hydroxyphenyl)-2-methylpropanoate:

120 g (0.67 mol) of 3-(4-hydroxyphenyl)-2-methylpropanoic acid, 1 L methanol, and 1 mL concentrated H₂SO₄ were added to a 2 L single neck flask and refluxed under air for 16 hours. After completion of the reaction, the solvent was removed under reduced pressure and the residue was taken up in ethyl acetate. The organic layer was washed once with water, three times with saturated aqueous sodium bicarbonate solution, and once with brine. The organic layer was dried over magnesium sulfate and then filtered into a flask. Excess solvent was removed under reduced pressure to afford 124 g of product as a brown, slowly-crystallizing solid (95%). ¹H NMR (600 MHz, DMSO-d₆): δ 9.18 (s, 1H, OH), 6.94 (d, 2H, H_{Ar}), 6.65 (d, 2H, H_{Ar}), 3.54 (s, 3H, OCH₃), 2.76 (q, 1H, CH), 2.64 (m, 1H, CH), 2.53 (q, 1H, CH), 1.02 (d, 3H, CH₃).

General synthesis for alkylation of phenols from ring-opening of cyclic carbonates:

1.
$$R_1 = H, OMe$$
 $R_2 = H, CH_3$
 $R_3 = H, CH_3, CH_2CH_3$

The procedure outlined in our previous work was followed. 55-90 g of starting phenol were added to a 1 L 3-neck flask. 0.05 eq. of anhydrous potassium carbonate was added to the flask, which was purged under full vacuum and backfilled with nitrogen three times. 1.1 eq. of the appropriate cyclic carbonate was added under positive nitrogen pressure, and the entire flask was heated to 160 °C while stirring for 90 minutes. During this time, the mixture increased in viscosity and significant quantities of carbon dioxide evolved. After the reaction was complete (as evidenced in a lack of carbon dioxide evolution), the mixture was cooled to roughly 40 °C upon which 500 mL of 3 M NaOH were added. The solution was heated to reflux until the entire solution became homogenous, usually between 12-48 h. After the solution became homogenous, it was cooled to room temperature and acidified carefully with 6M HCl until the pH = 2. The precipitate was filtered, and the filter cake was washed thoroughly with acidified water (pH = 2) and dried in a vacuum oven at 60°C for 24 h. to afford the products in good to excellent yields.

Synthesis of 3-(2-(2-hydroxypropoxy)phenyl)propanoic acid:

90 g of methyl 3-(2-hydroxyphenyl)propanoate (0.5 mol) were added to a 1 L 3-neck flask with 56.1 g of propylene carbonate (1.1 eq.). The general synthesis procedure outlined above was followed and after alkylation the mixture was refluxed in 500 mL 3 M NaOH for 48 h. An undissolved precipitate was removed by filtration. Acidification and filtration as described above yielded 87.9 g of a white solid (78%). ¹H NMR (600 MHz, CDCl₃): δ 7.17 (m, 2H, H_{Ar}), 6.90 (t, 1H, H_{Ar}), 6.81 (d, 1H, H_{Ar}), 4.24 (m, 1H, CH), 3.96 (dd, 1H, CHH), 3.81 (dd, 1H, CHH), 3.00 (m, 2H, CH₂), 2.63 (m, 2H, CH₂), 1.30 (d, 3H, CH₃). ¹³C NMR (400 MHz, DMSO-d6): 174.01, 156.41, 129.50, 128.81, 127.39, 120.16, 111.42, 73.05, 64.59, 33.66, 25.41, 20.23.

Synthesis of (R)-3-(4-(2-hydroxypropoxy)phenyl)propanoic acid:

90 g of methyl 3-(4-hydroxyphenyl)propanoate (0.5 mol) was synthesized as previously described³ and added to a 1 L 3-neck flask with 56.1 g of (R)-propylene carbonate (1.1 eq.). The general synthesis procedure outlined above was followed and after alkylation the mixture was

refluxed in 500 mL 3 M NaOH for 48 h. Acidification and filtration as described above yielded an impure solid that was crystallized from water to yield 98.0 g of a white powder (87%). ¹H NMR (600 MHz, CDCl₃): δ 7.11 (d, 2H, H_{Ar}), 6.84 (d, 2H, H_{Ar}), 4.18 (m, 1H, CH), 3.91 (dd, 1H, CHH), 3.77 (dd, 1H, CHH), 2.90 (t, 2H, CH₂), 2.65 (t, 2H, CH₂), 1.28 (d, 3H, CH₃). ¹³C NMR (400 MHz, DMSO-d6): 173.74, 156.99, 132.70, 129.13, 115.52, 114.32, 73.18, 64.49, 35.55, 29.47, 20.13.

Synthesis of 3-(4-(2-hydroxyethoxy)phenyl)-2-methylpropanoic acid:

60 g of methyl 3-(4-hydroxyphenyl)-2-methylpropanoate (0.31 mol) were added to a 1 L 3-neck flask with 29.9 g of ethylene carbonate (1.1 eq.). The general synthesis procedure outlined above was followed and after alkylation the mixture was refluxed in 500 mL 3 M NaOH for 24 h. The aqueous solution was added to a 2 L separatory funnel and slowly acidified with 2 M HCl until pH = 2. The aqueous layer was extracted three times with ethyl acetate, and the combined organic fractions were washed with brine, dried over magnesium sulfate, filtered into a flask, and the solvent removed with rotary evaporation. The color of the product was unexpectedly dark, so it was further purified by dissolving in 500 mL dichloromethane and spinning over activated charcoal for 2 h. The charcoal was removed via filtration over a short pad of celite and the solvent was removed via rotary evaporation. 58.9 g of a slowly crystallizing yellow solid were collected (85%). ¹H NMR (600 MHz, CDCl₃): δ 7.09 (d, 2H, H_{Ar}), 6.83 (d, 2H, H_{Ar}), 4.05 (t, 2H, CH₂), 3.95 (t, 2H, CH₂), 2.98 (q, 1H, CHH), 2.71 (m, 1H, CH), 2.64 (q, 1H, CHH), 1.17 (d, 3H,

CH₃). ¹³C NMR (400 MHz, DMSO-d6): 176.82, 157.05, 131.33, 129.80, 114.16, 69.37, 59.58, 40.76, 38.07, 16.55.

Synthesis of 3-(4-(2-hydroxypropoxy)phenyl)-2-methylpropanoic acid:

60 g of methyl 3-(4-hydroxyphenyl)-2-methylpropanoate (0.31 mol) were added to a 1 L 3-neck flask with 34.7 g of propylene carbonate (1.1 eq.). The general synthesis procedure outlined above was followed and after alkylation the mixture was refluxed in 500 mL 3M NaOH for 24 h. The aqueous solution was added to a 2 L separatory funnel and acidified with 2 M HCl until pH = 2. The aqueous layer was extracted three times with ethyl acetate, and the combined organic fractions were washed with brine, dried over magnesium sulfate, filtered into a flask, and the solvent removed with rotary evaporation to isolate 68.0 g of a light brown, viscous liquid (92%). ¹H NMR (600 MHz, CDCl₃): δ 7.10 (d, 2H, H_{Ar}), 6.83 (d, 2H, H_{Ar}), 5.30 (s, 1H, OH), 4.19 (m, 1H, CH), 3.92 (dd, 1H, CHH), 3.77 (t, 1H, CHH), 2.99 (q, 1H, CHH), 2.75 (m, 1H, CH), 2.64 (q, 1H, CHH), 1.28 (d, 3H, CH₃), 1.17 (d, 3H, CH₃). ¹³C NMR (400 MHz, DMSO-d6): 176.81, 157.07, 131.35, 129.79, 114.19, 73.15, 64.50, 40.77, 38.07, 20.13, 16.55

Synthesis of 3-(4-(2-hydroxybutoxy)phenyl)propanoic acid:

90 g of methyl 3-(4-hydroxyphenyl)propanoate (0.5 mol) was synthesized as previously described³ and added to a 1 L 3-neck flask with 63.9 g of α-butylene carbonate (1.1 eq.). The general synthesis procedure outlined above was followed and after alkylation the mixture was refluxed in 500 mL 3M NaOH for 48 h. Acidification and filtration as described above yielded a crude solid that was recrystallized in toluene to yield 103 g of a white powder (86%). ¹H NMR (600 MHz, CDCl₃): δ 7.12 (d, 2H, H_{Ar}), 6.85 (d, 2H, H_{Ar}), 3.97 (dd, 1H, CHH), 3.82 (dd, 1H, CHH), 2.90 (t, 2H, CH₂), 2.65 (t, 2H, CH₂), 2.06 (p, 2H, CH₂), 1.03 (t, 3H, CH₃). ¹³C NMR (400 MHz, DMSO-d6): 173.74, 157.04, 132.67, 129.12, 114.32, 71.82, 69.64, 35.53, 29.46, 26.45, 9.77.

Synthesis of 3-(4-(2-hydroxypropoxy)-3-methoxyphenyl)propanoic acid:

55 g of methyl 3-(4-hydroxy-3-methoxyphenyl)propanoate (0.26 mol) was synthesized as previously described³ and added to a 1 L 3-neck flask with 29.5 g of propylene carbonate (1.1 eq.). The general synthesis procedure outlined above was followed and after alkylation the mixture was refluxed in 500 mL 3M NaOH for 16 h. Acidification and filtration as described above yielded 56.2 g of a white powder (85%). ¹H NMR (600 MHz, DMSO-d₆): δ 12.09 (s, 1H,

COOH), 6.83 (dd, 2H, H_{Ar}), 6.69 (dd, 1H, H_{Ar}), 4.79 (d, 1H, OH), 3.91 (m, 1H, CH), 3.78 (q, 1H, CHH), 3.73 (s, 3H, OCH₃), 3.67 (q, 1H, CHH), 2.74 (t, 2H, CH₂), 2.50 (t, 2H, CH₂), 1.13 (d, 3H, CH₃). ¹³C NMR (400 MHz, DMSO-d6): 174.43, 149.59, 147.16, 134.27, 120.65, 114.33, 113.30, 74.90, 65.18, 56.15, 36.12, 30.59, 20.91.

Synthesis of (E)-3-(4-(2-hydroxyethoxy)phenyl)-2-methylacrylic acid:

60 g of methyl 3-(4-hydroxyphenyl)-2-methylacrylate (0.34 mol) was added to a 1 L 3-neck flask with 30.2 g of ethylene carbonate (1.1 eq.). The general synthesis procedure outlined above was followed and after alkylation the mixture was refluxed in 500 mL 3M NaOH for 38 h. Acidification and filtration as described above yielded 74.1 g of a tan powder (98%). ¹H NMR (600 MHz, DMSO-d₆): δ 12.35 (s, 1H, COOH), 7.55 (s, 1H, =CH), 7.44 (d, 2H, H_{Ar}), 7.00 (d, 2H, H_{Ar}), 4.88 (s, 1H, OH), 4.02 (t, 2H, CH₂), 3.72 (m, 2H, CH₂), 2.03 (s, 3H, CH₃). ¹³C NMR (400 MHz, DMSO-d₆): 169.54, 158.84, 137.46, 131.40, 127.87, 126.10, 114.50, 69.58, 59.48, 13.90.

Synthesis of 3-(4-(2-hydroxypropoxy)phenyl)acrylic acid:

60 g of methyl (3-(4-hydroxyphenyl)acrylate (0.34 mol) were added to a 1 L 3-neck flask with 37.8 g of propylene carbonate (1.1 eq.). The general synthesis procedure outlined above was followed and after alkylation the mixture was refluxed in 500 mL 3M NaOH for 48 h, after which an insoluble mass was removed by filtration. Acidification and filtration as described above yielded a mixture of monomers and dimers as 61.4 g (81%) of a brown solid which was used in the following step without further purification. ¹H NMR (600 MHz, DMSO-d₆): δ 12.20 (s, 1H, COOH), 7.62 (d, 2H, H_{Ar}), 7.53 (d, 1H, =CH), 6.96 (d, 2H, H_{Ar}) 6.36 (d, 1H, =CH), 4.89 (d, 1H, OH), 3.95 (m, 1H, CH), 3.84 (m, 2H, CH₂), 1.15 (d, 3H, CH₃). ¹³C NMR (400 MHz, DMSO-d₆): 167.76, 160.40, 143.70, 129.88, 126.73, 116.42, 114.86, 73.29, 64.41, 20.02.

Polyester Synthesis:

Polyester synthesis was conducted according to the procedure outlined in the main body of this text. The polyesters are named according first to their parent glycol (ethylene, iso-propylene, and α -butylene) and then their parent carboxylic acid (phloretic acid, methyl-phloretic acid, hydroferulic acid, coumaric acid, methyl-coumaric acid).

Synthesis of poly-isopropyl phloretate (PiPP):

$$\mathsf{HO} \underbrace{\hspace{1cm} 0}_{\mathsf{n}} \mathsf{OH}$$

PiPP

Mw: 27.2 kDa, PDI 1.3 Gel content: 0; Tg: 25°C

3-(4-(2-hydroxypropoxy)phenyl)propanoic acid was synthesized as previously reported and added to a 200 mL 3-neck flask. After following the general procedure, vacuum was applied to the system for 6 h before reaction completion. The resulting brown polymer was collected in quantitative yield on silicon release paper. Spectra agreed with our previously published results.³

Synthesis of poly-ortho-isopropyl phloretate (o-PiPP):

Mw: 90.6 kDa, PDI 1.6 Gel content: 0; Tg: 27°C Following the addition of 60 g of monomer, 1 mol % Sb₂O₃, and 1000 ppm MEHQ to a 200 mL 3-neck flask, the previously described heating ramp from 160-220°C at 10°C/h. was followed. After completion of the heating ramp, vacuum was maintained for 5 h until reaction completion and the resultant light grey polymer was collected in quantitative yield on silicon release paper. ¹H NMR (600 MHz, CDCl₃): δ 7.11 (m, 2H, H_{Ar}), 6.81 (t, 1H, H_{Ar}), 6.74 (d, 1H, H_{Ar}), 5.24 (m, 1H, CH), 3.94 (m, 1H, CHH), 3.85 (m, 1H, CHH), 2.89 (m, 2H, CH₂), 2.59 (m, 2H, CH₂), 1.30 (d, 3H, CH₃). ¹³C NMR (400 MHz, CDCl₃): δ 172.72, 156.49, 130.29, 129.06, 120.93, 111.28, 69.96, 68.69, 34.35, 26.32, 17.02.

Synthesis of (R)-poly-isopropyl phloretate ((R)-PiPP):

(R)-PiPP Mw: 29.0 kDa, PDI 1.4 Gel content: 0; Tg: 25°C

Following the addition of 180 g of monomer, 1 mol % Sb₂O₃, and 1000 ppm MEHQ to a 500 mL 3-neck flask, the previously described heating ramp from 160-220°C at 10°C/h. was followed. After completion of the heating ramp, vacuum was maintained for 9 h until reaction completion and the resultant grey polymer was collected in quantitative yield on silicon release paper. ¹H NMR (600 MHz, CDCl₃): δ 7.10 (d, 2H, H_{Ar}), 6.79 (d, 2H, H_{Ar}), 5.23 (m, 1H, CH), 3.92 (dd, 2H, CHH), 2.87 (t, 2H, CH₂), 2.58 (t, 2H, CH₂), 1.31 (d, 3H, CH₃). ¹³C NMR (400 MHz, CDCl₃): δ 172.53, 157.29, 133.17, 129.44, 114.83, 70.27, 69.02, 36.45, 30.27, 16.84.

Synthesis of poly-ethylene methyl phloretate (PEMP):

PEMP

Mw: 103 kDa, PDI 2.8 Gel content: 0; Tg: 21°C

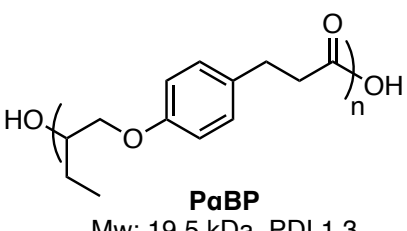
Following the addition of 50 g of monomer, 1 mol % Sb₂O₃, and 1000 ppm MEHQ to a 100 mL 3-neck flask, the previously described heating ramp from 160-220°C at 10°C/h. was followed. After completion of the heating ramp, vacuum was maintained for 10 h until reaction completion and the resultant dark brown polymer was collected in quantitative yield on silicon release paper. ¹H NMR (600 MHz, CDCl₃): δ 7.07 (d, 2H, H_{Ar}), 6.76 (d, 2H, H_{Ar}), 4.35 (m, 2H, CH₂), 4.04 (m, 2H, CH₂), 2.95 (q, 1H, CHH), 3.73 (m, 1H, CH), 2.63 (q, 1H, CHH), 1.14 (d, 3H, CH₃). ¹³C NMR (400 MHz, CDCl₃): δ 176.11, 157.25, 131.97, 130.18, 114.67, 66.06, 62.85, 41.69, 38.90, 16.81.

Synthesis of poly-isopropyl methyl phloretate (PiPMP):

PiPMP

Mw: 22.0 kDa, PDI 1.7 Gel content: 0; Tg: 26°C Following the addition of 60 g of monomer, 1 mol % Sb₂O₃, and 1000 ppm MEHQ to a 200 mL 3-neck flask, the previously described heating ramp from 160-220°C at 10°C/h. was followed. After completion of the heating ramp, vacuum was maintained for 15 h until reaction completion and the resultant brown polymer was collected in quantitative yield on silicon release paper. ¹H NMR (600 MHz, CDCl₃): δ 7.10 (m, 2H, H_{Ar}), 6.79 (m, 2H, H_{Ar}), 5.22 (m, 1H, CH), 3.91 (m, 2H, CH₂), 2.95 (m, 1H, CHH), 2.70 (p, 1H, CH), 2.62 (m, 1H, CHH), 1.29 (m, 3H, CH₃), 1.14 (m, 3H, CH₃). ¹³C NMR (400 MHz, CDCl₃): δ 175.68, 157.36, 132.01, 130.14, 114.65, 70.19, 68.77, 41.92, 41.74, 38.99, 38.86, 16.84.

Synthesis of poly- α -butylene phloretate (P α BP):



Mw: 19.5 kDa, PDI 1.3 Gel content: 1%; Tg: 16°C

Following the addition of 60 g of monomer, 1 mol % Sb₂O₃, and 1000 ppm MEHQ to a 200 mL 3-neck flask, the previously described heating ramp from 160-220°C at 10°C/h. was followed. After completion of the heating ramp, vacuum was maintained for 8.3 h until reaction completion and the resultant light grey polymer was collected in quantitative yield on silicon release paper. ¹H NMR (600 MHz, CDCl₃): δ 7.10 (d, 2H, H_{Ar}), 6.78 (d, 2H, H_{Ar}), 5.11 (m, 1H, CHH), 3.93 (m, 2H, CH₂), 2.88 (m, 2H, CH₂), 2.60 (t, 2H, CH₂), 1.70 (m, 2H, CH₂), 0.90 (t, 3H,

CH₃). ¹³C NMR (400 MHz, CDCl₃): δ 172.75, 157.35, 133.13, 129.40, 114.83, 73.53, 68.69, 36.39, 30.32, 24.04, 9.67.

Synthesis of poly-isopropyl dihydroferulate (PiPHF):

Mw: 67.5 kDa, PDI 1.7 Gel content: 0; Tg: 29°C

Following the addition of 50 g of monomer, 1 mol % Sb₂O₃, and 1000 ppm MEHQ to a 100 mL 3-neck flask, the previously described heating ramp from 160-220°C at 10°C/h. was followed. After completion of the heating ramp, vacuum was maintained for 8.5 h until reaction completion and the resultant light tan polymer was collected in quantitative yield on silicon release paper. ¹H NMR (600 MHz, CDCl₃): δ 6.79(d, 1H, H_{Ar}), 6.71 (m, 2H, H_{Ar}), 5.25 (m, 1H, CH), 4.00 (m, 2H, CH₂), 3.80 (s, 3H, OCH₃), 2.88 (t, 2H, CH₂), 2.60 (t, 2H, CH₂), 1.31 (d, 3H, CH₃). ¹³C NMR (400 MHz, CDCl₃): δ 172.54, 150.09, 146.85, 134.68, 120.51, 115.30, 112.92, 72.05, 69.24, 56.17, 36.43, 30.76, 16.88.

Synthesis of poly-ethylene methyl cinnamate (PEMC):

PEMC

Mw: 22.5 kDa, PDI 1.4 Gel content: 6%; Tg: 53°C

Following the addition of 50 g of monomer, 1 mol % Sb₂O₃, and 1000 ppm MEHQ to a 100 mL 3-neck flask, the previously described heating ramp from 160-220°C at 10°C/h. was followed. After completion of the heating ramp, vacuum was maintained for 10 h until reaction completion and the resultant brown, brittle polymer was collected in quantitative yield on silicon release paper. ¹H NMR (600 MHz, CDCl₃): δ 7.65 (s, 1H, =CH), 7.37 (d, 2H, H_{Ar}), 6.96 (d, 2H, H_{Ar}), 4.56 (approximately t, 2H, CH₂), 4.29 (approximately t, 2H, CH₂), 2.12 (s, 3H, CH₃). ¹³C NMR (400 MHz, CDCl₃): δ 168.88, 158.99, 139.27, 131.68, 128.94, 126.17, 114.79, 66.29, 63.27, 14.24.

Synthesis of poly-isopropyl cinnamate (PiPC):

PiPC

Mw: 41.6 kDa, PDI 3.7 Gel content: 36; Tg: 65°C

Following the addition of 60 g of monomer, 1 mol % Sb₂O₃, and 1000 ppm MEHQ to a 200 mL 3-neck flask, the previously described heating ramp from 160-220°C at 10°C/h. was followed. After completion of the heating ramp, vacuum was maintained for 12 h until reaction completion and the resultant dark brown, brittle polymer was collected in quantitative yield on silicon

release paper. Spectral data was extremely poor quality due to the high gel content and low solubility of the crosslinked polyester. Several solvent systems were attempted (CDCl₃, TFA-d, DMSO, and cosolvents) with equally poor spectral resolution.

Thermal Characterization of Polymers:

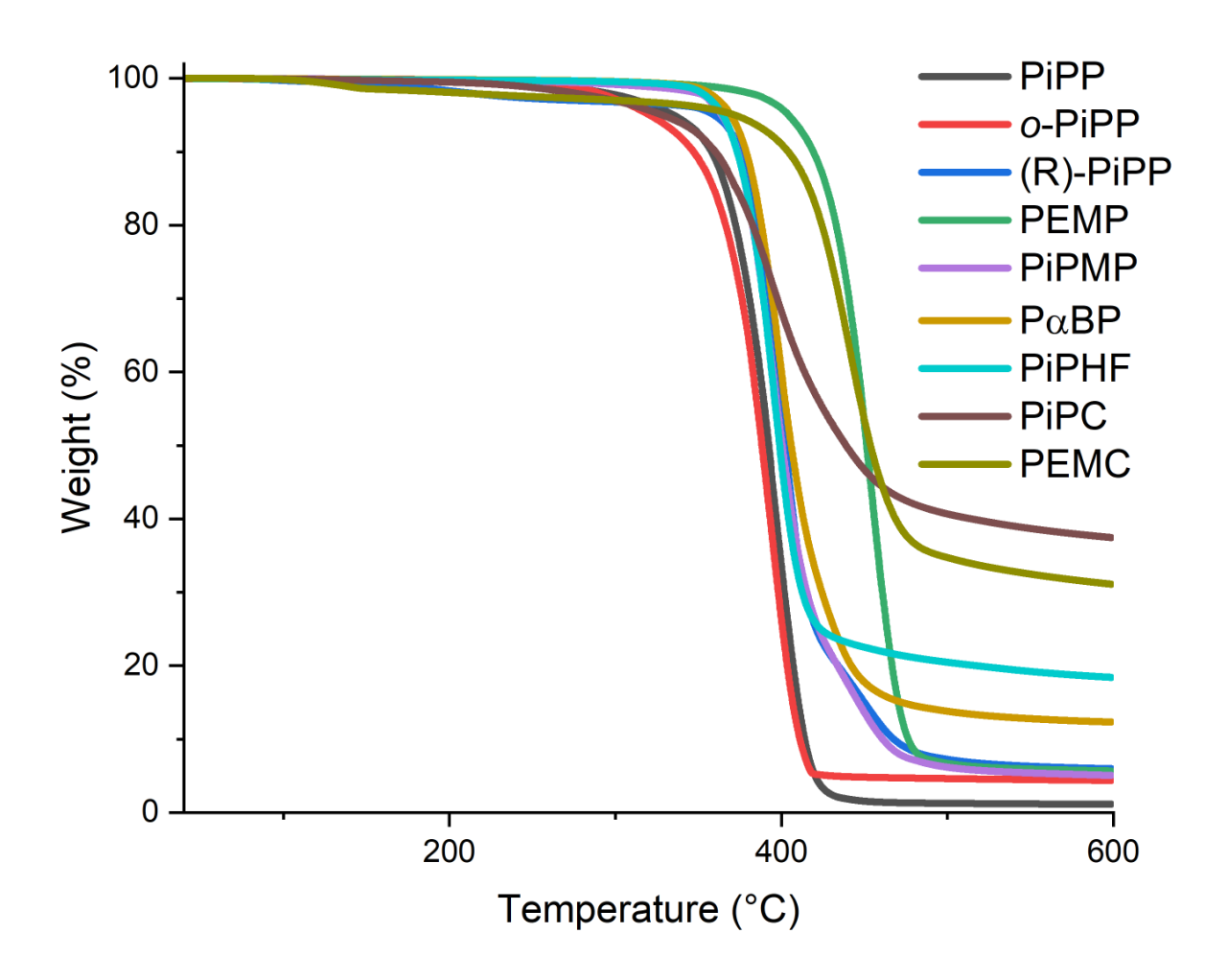


Figure S2.1. TGA Overlay of polyesters synthesized in this study.

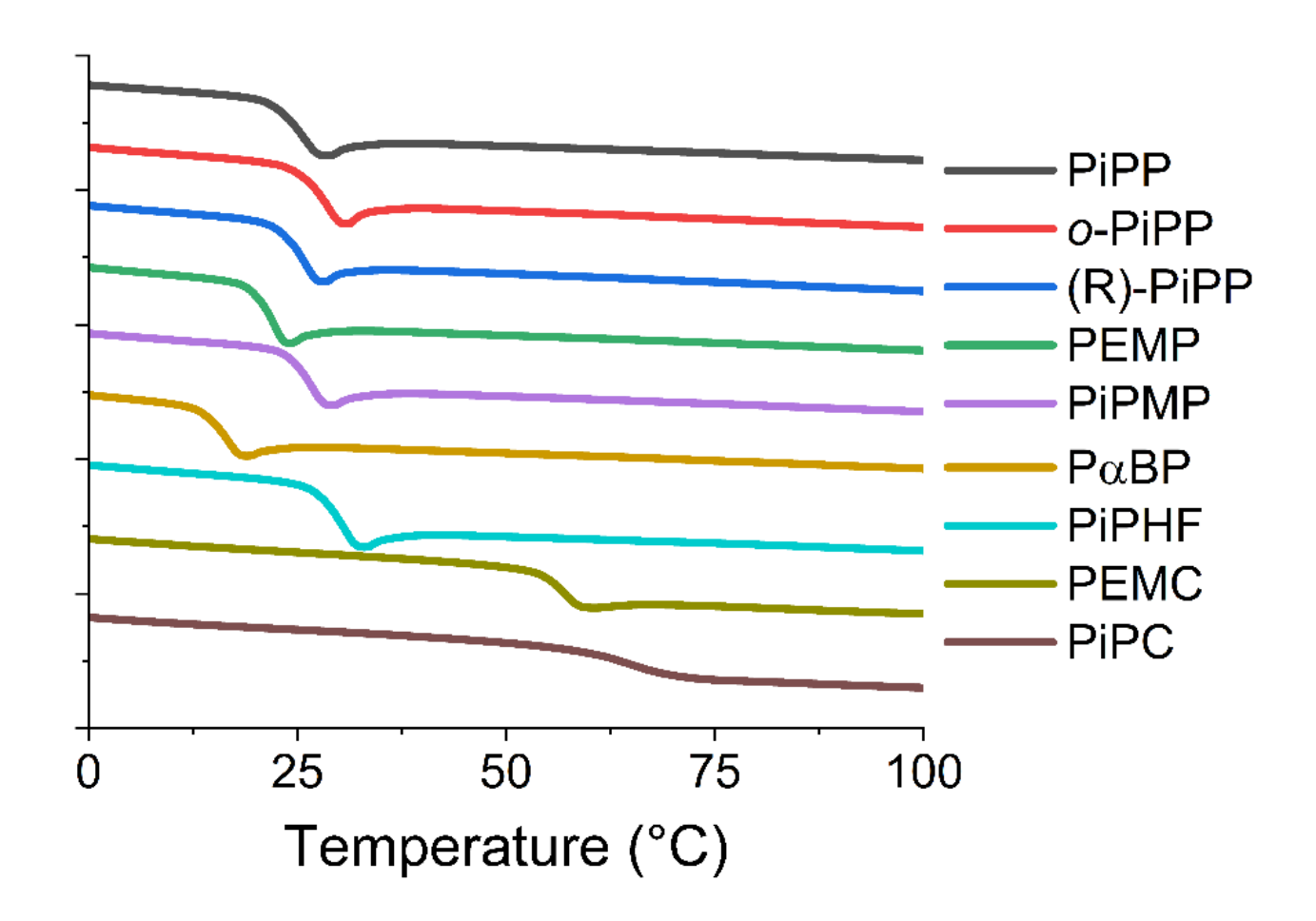


Figure S2.2: DSC Overlay of polyesters synthesized in this study.

<u>Injection Molding of Polymers:</u>

Table S2.1. Summary of extrusion and injection molding conditions

Polymer	Extrusion Temp (°C)	Mold Temp (°C)	Pressure (bar)
$P_{\alpha}BP$	100	RT then Ice Bath	350
(R)-PiPP	120	23 (RT)	350
PiPMP	120	25 (RT)	350
PiPP	120	25 (RT)	350
PiPHF	140	24 (RT)	350
o-PiPP	140	28	350
PEMC	160	58	350
PiPC	170	90	350
PEMP	120	24 (RT)	350

Rheological Characterization of Polyesters:

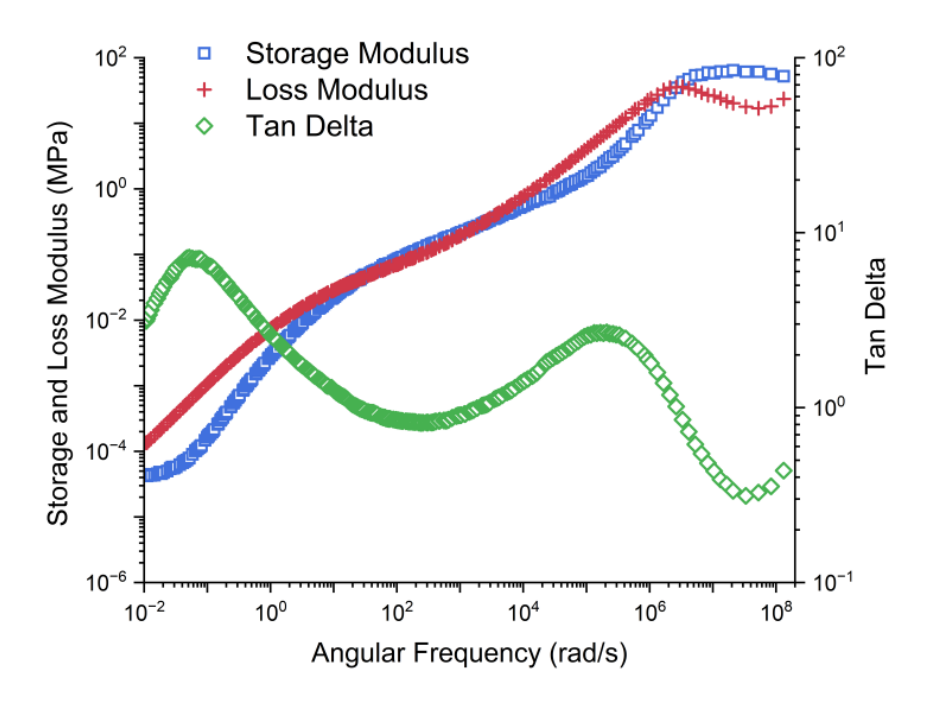


Figure S2.3. TTS master curve of o-PiPP.

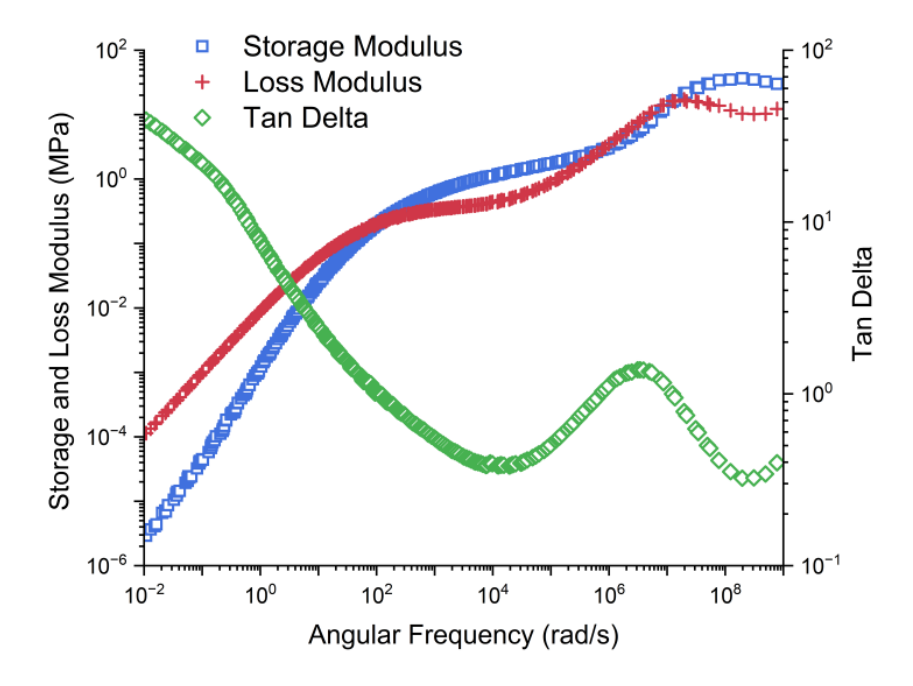


Figure S2.4. TTS master curve of (R)-PiPP.

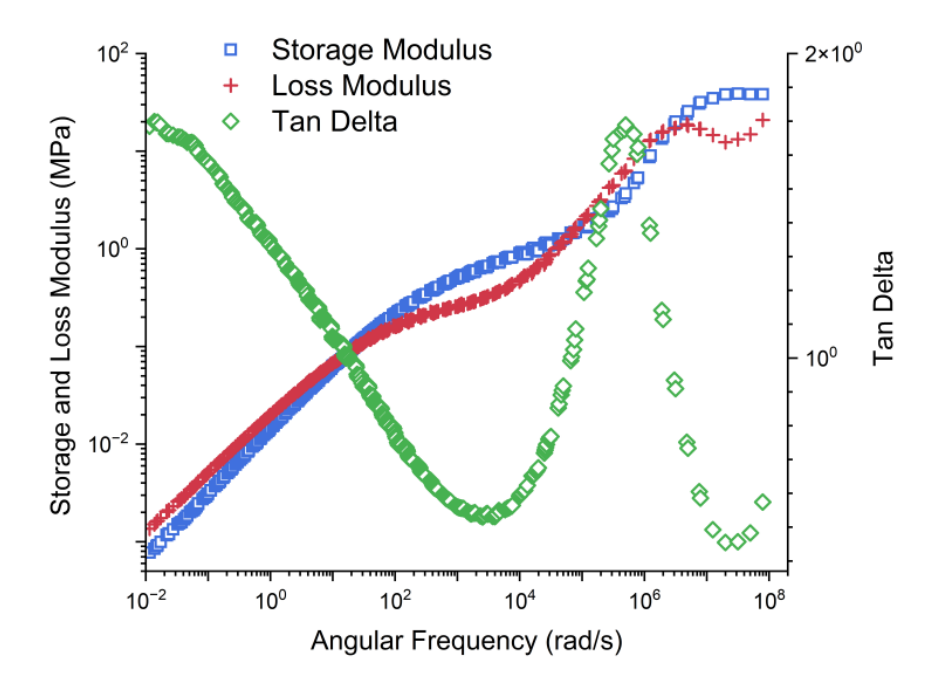


Figure S2.5. TTS master curve of PEMP.

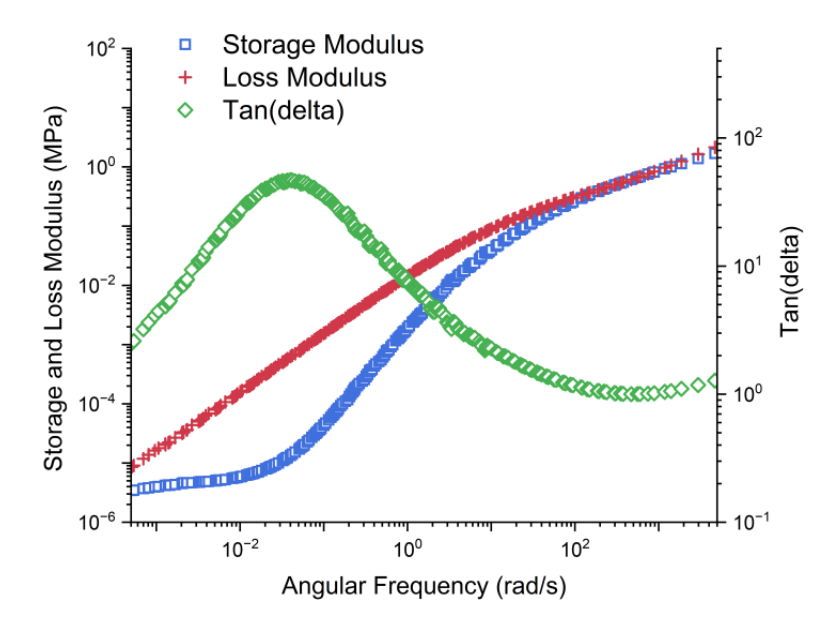


Figure S2.6. TTS master curve of PiPMP.

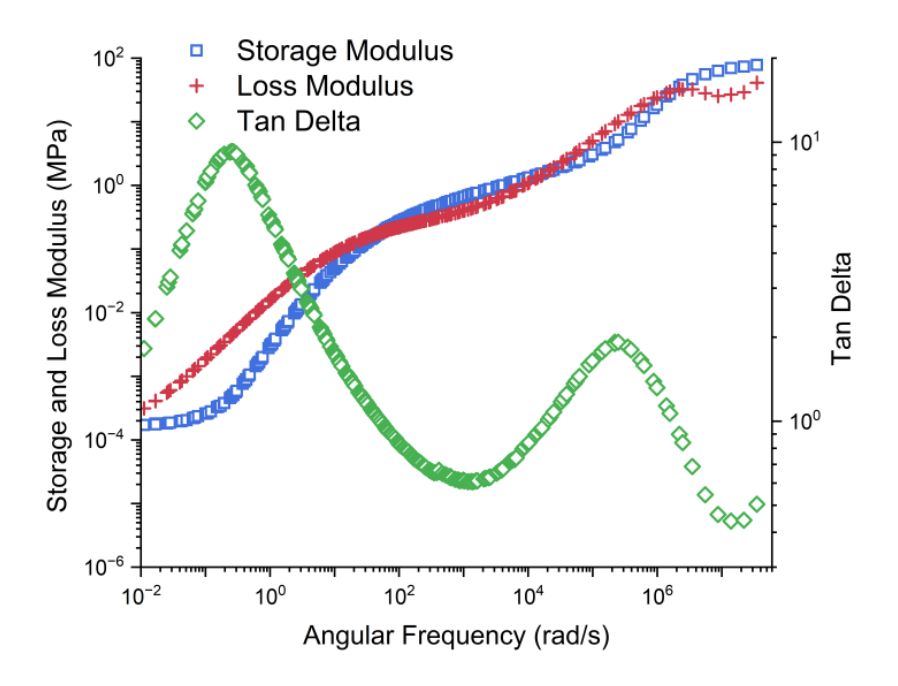


Figure S2.7. TTS master curve of $P\alpha BP$.

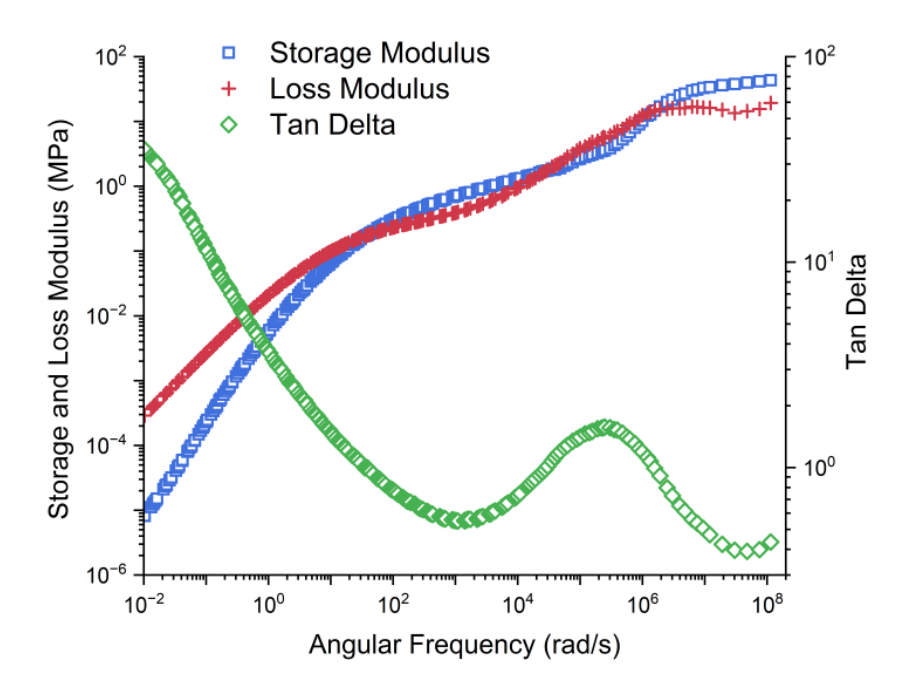
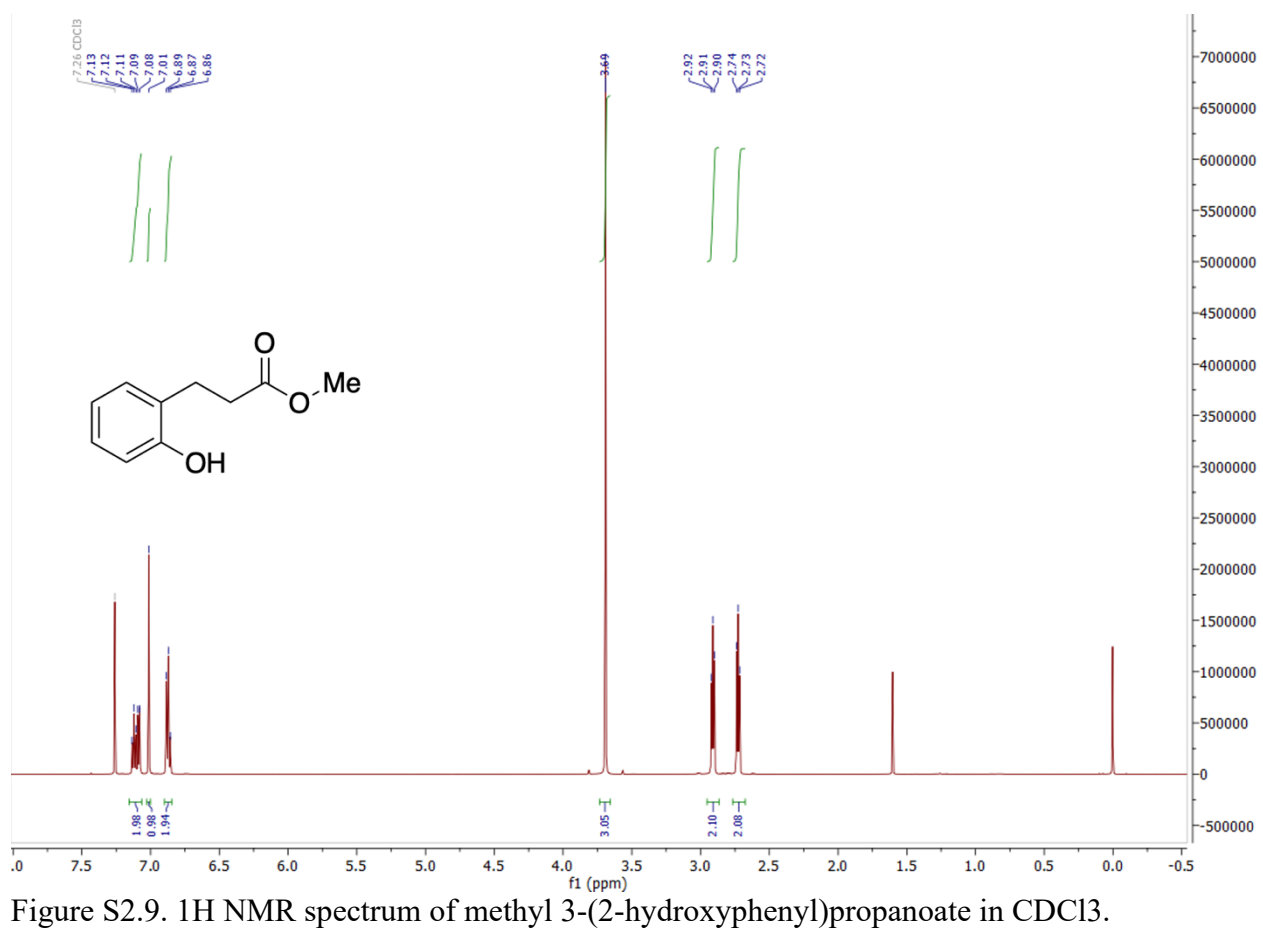
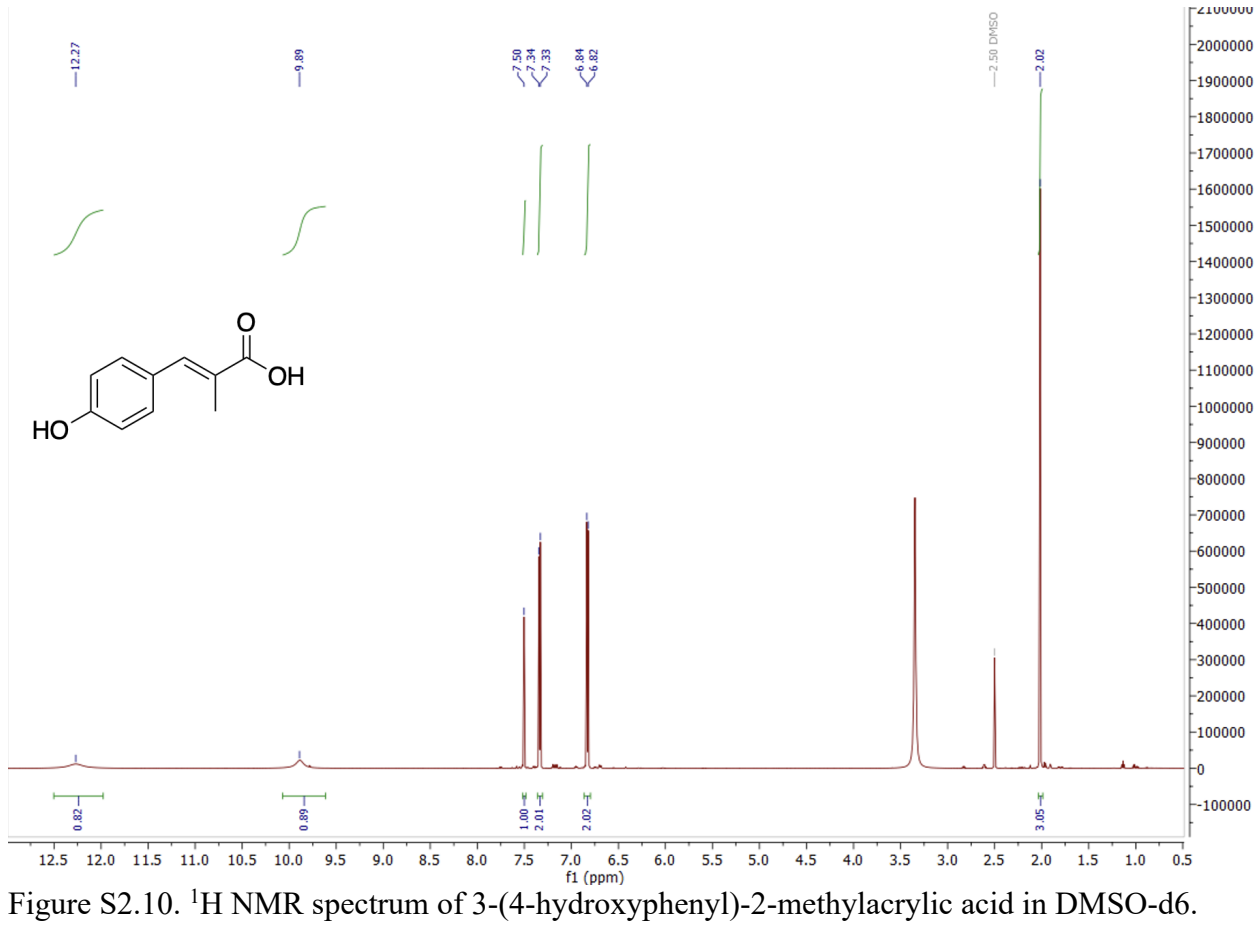
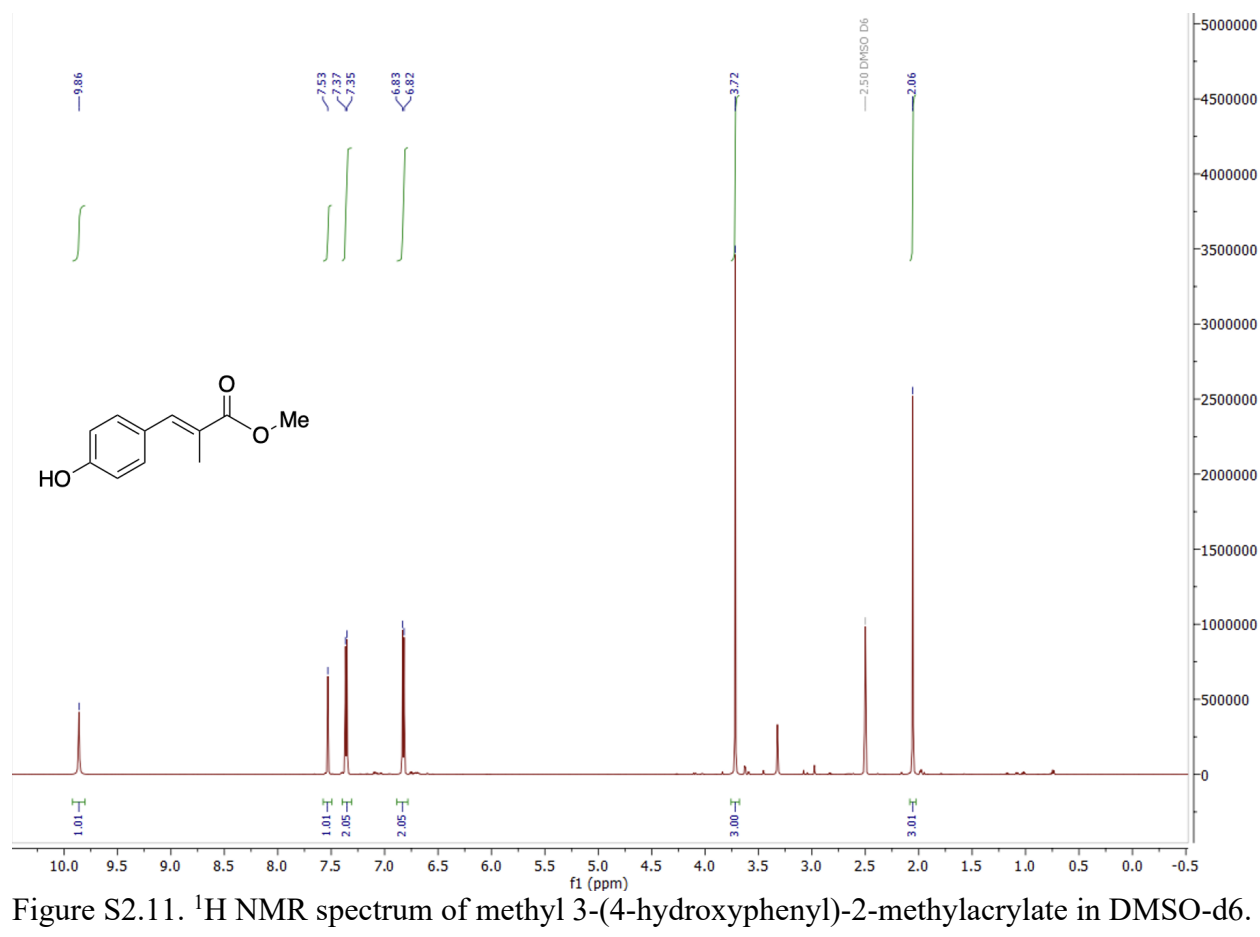


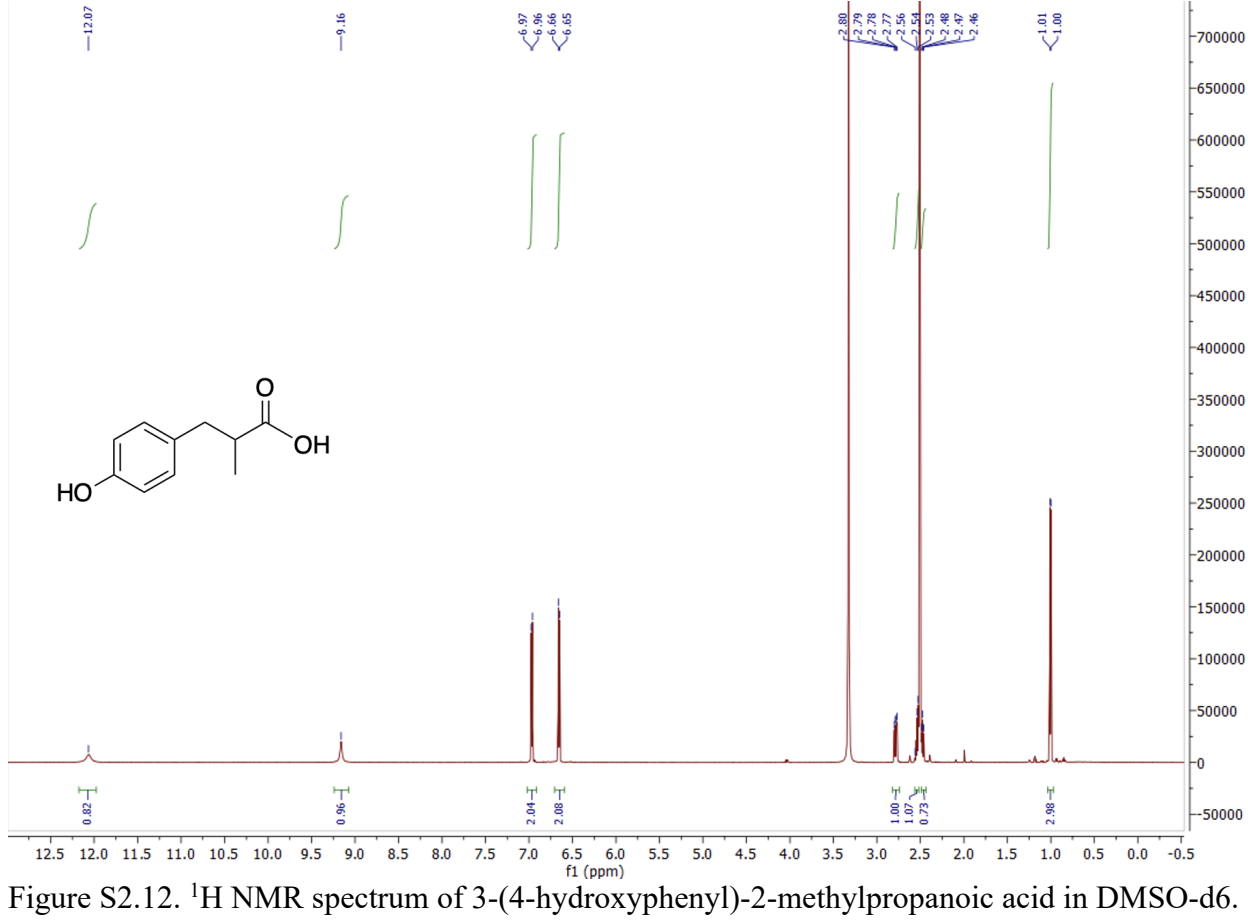
Figure S2.8. TTS master curve of PiPHF.

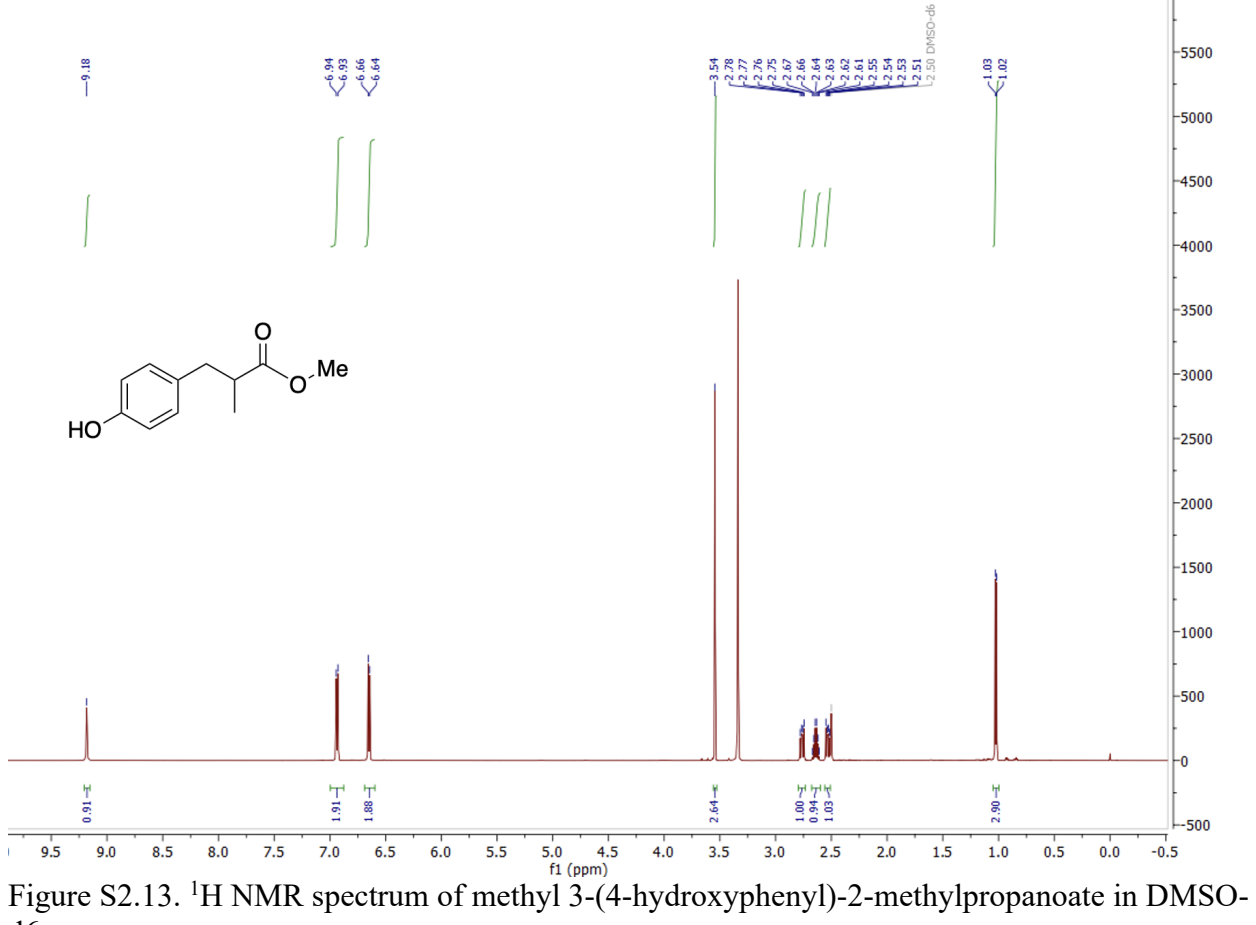
¹H NMR Spectra of Synthesized Precursors, Monomers, and Polymers:



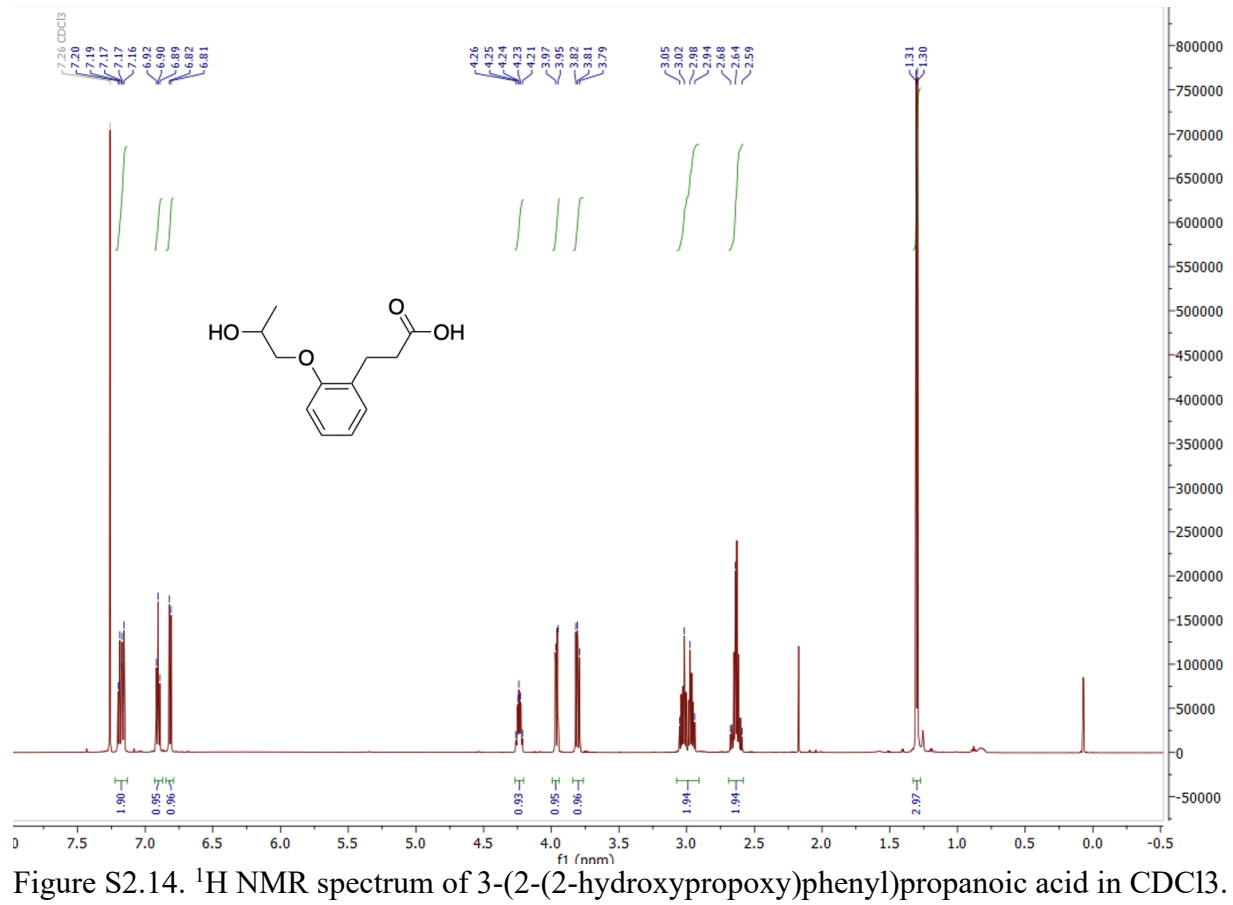


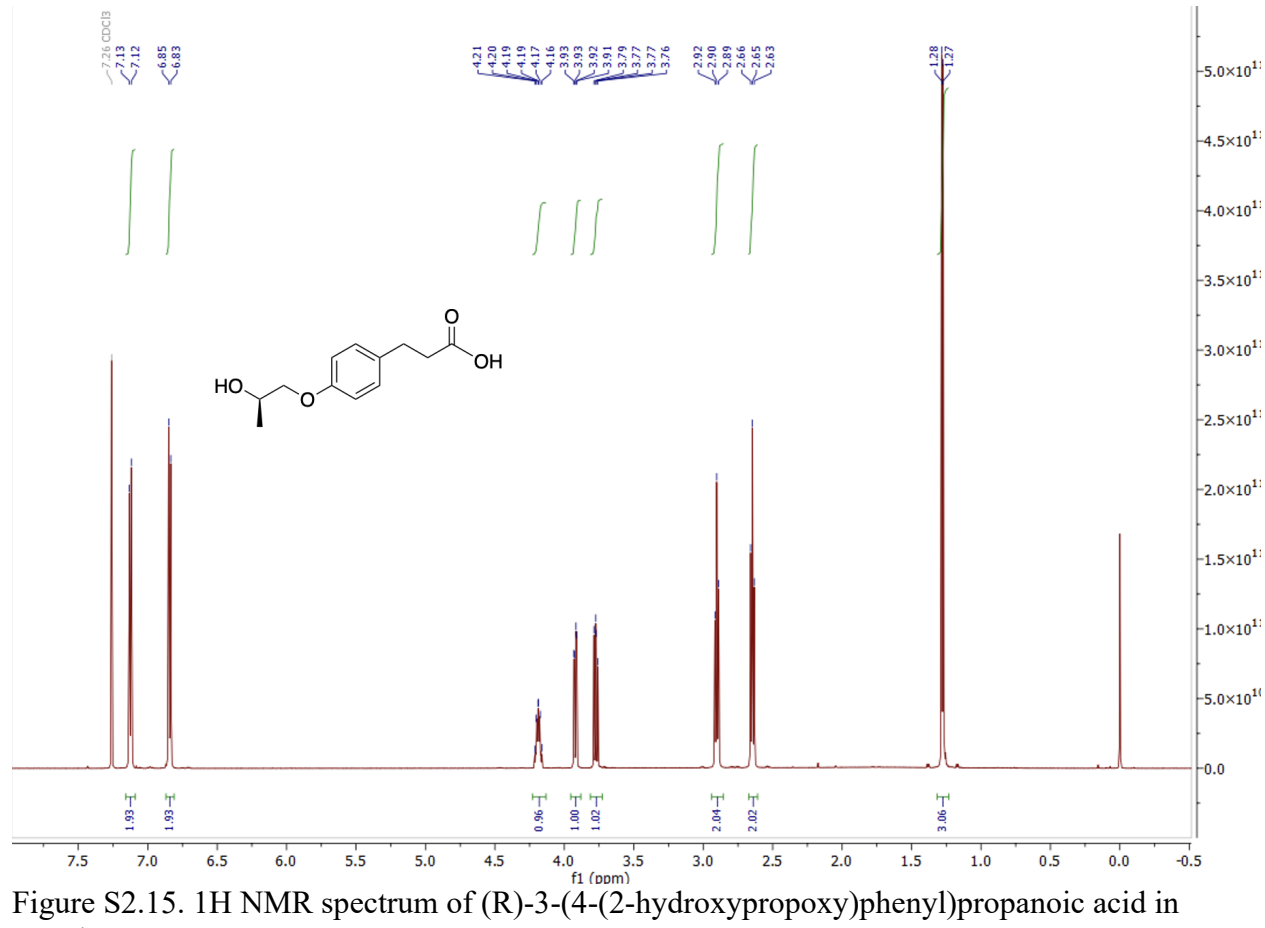




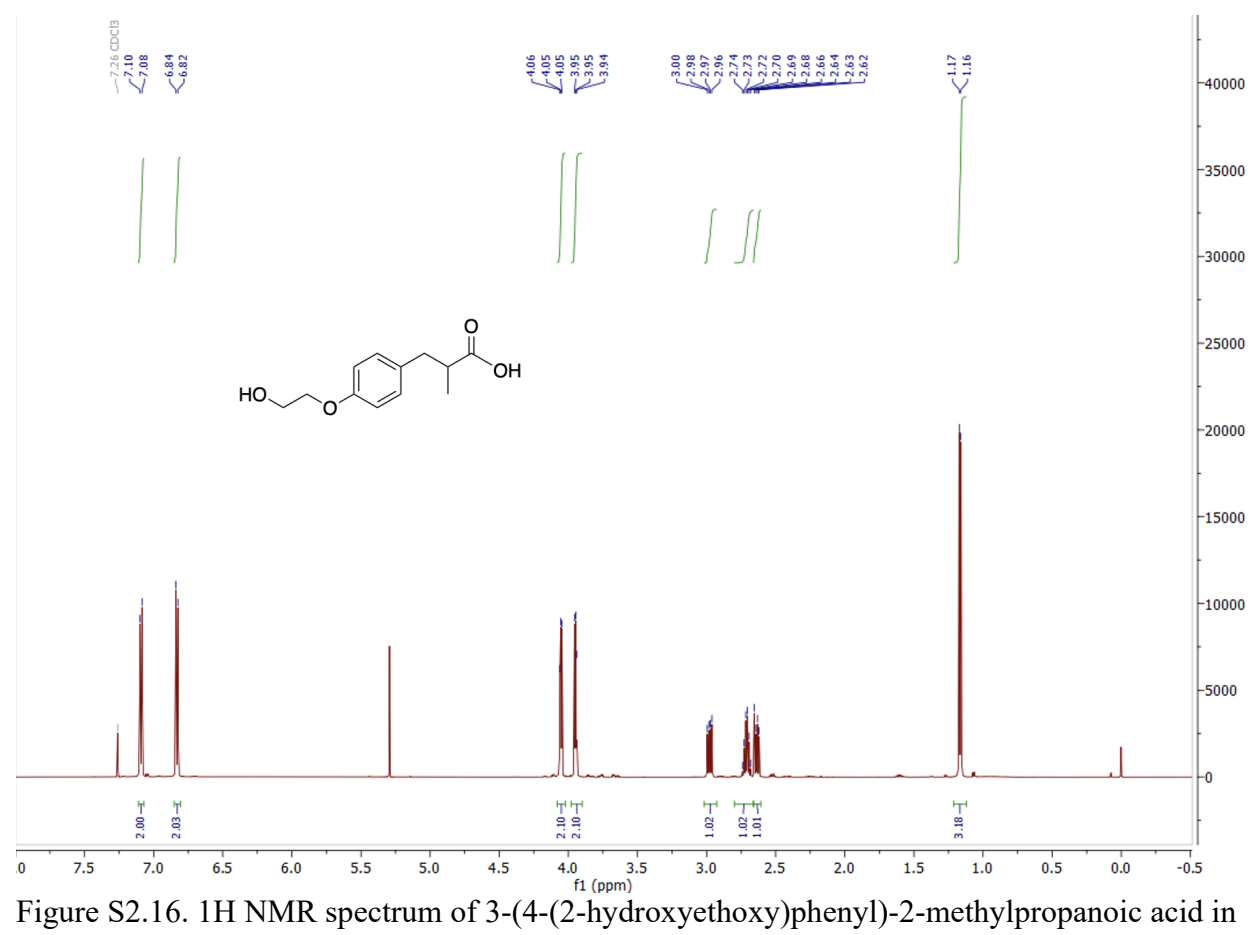


d6.

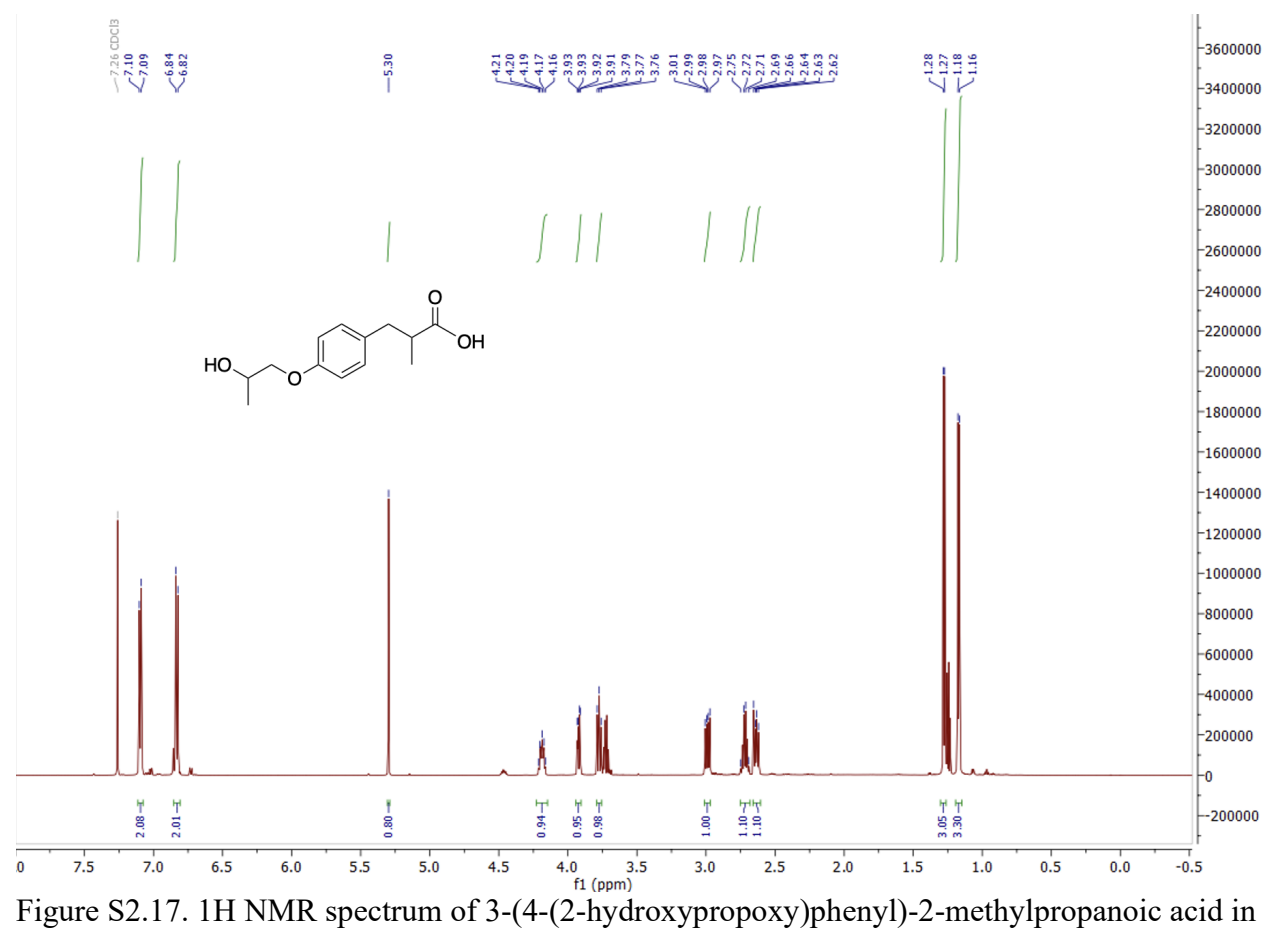




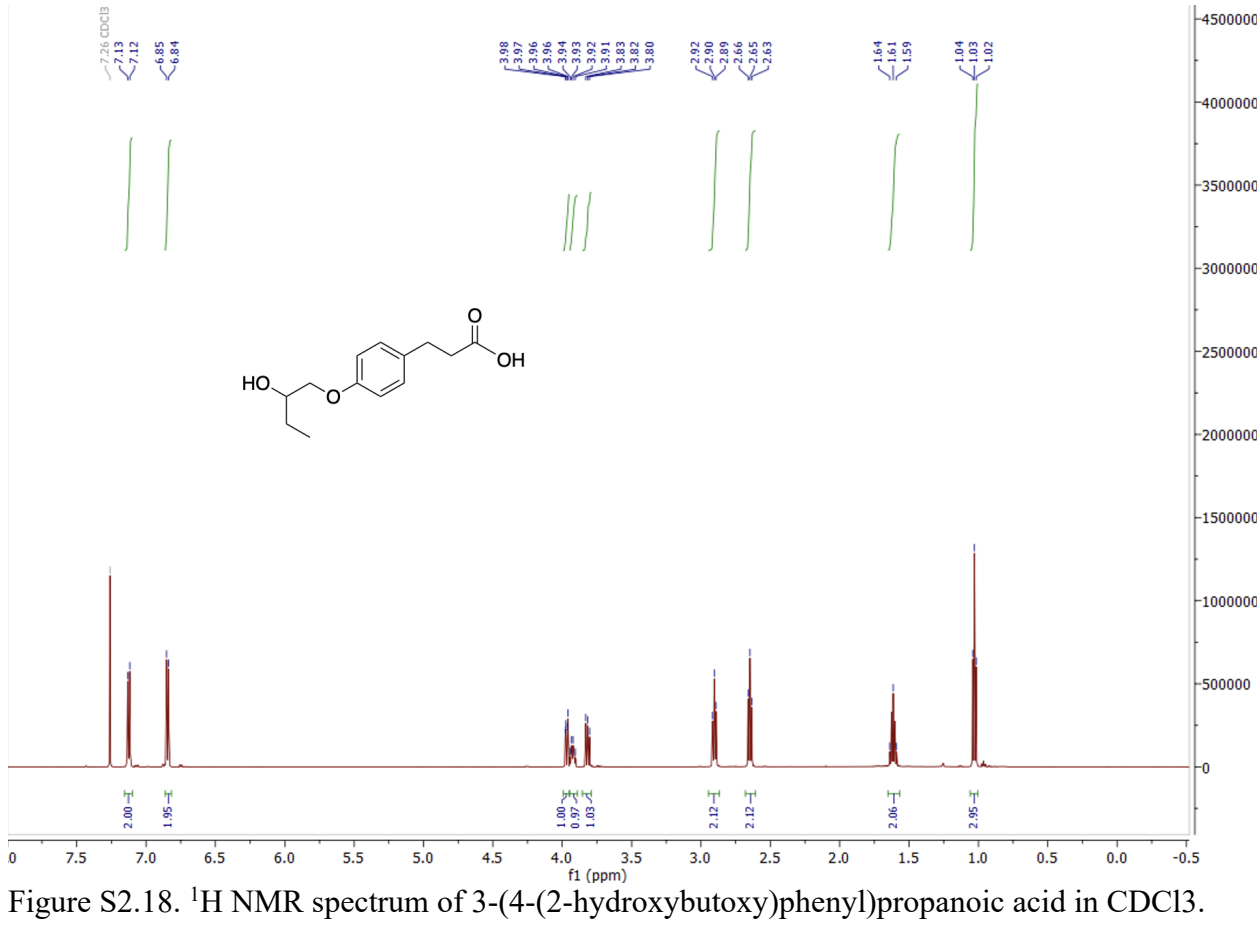
CDC13.

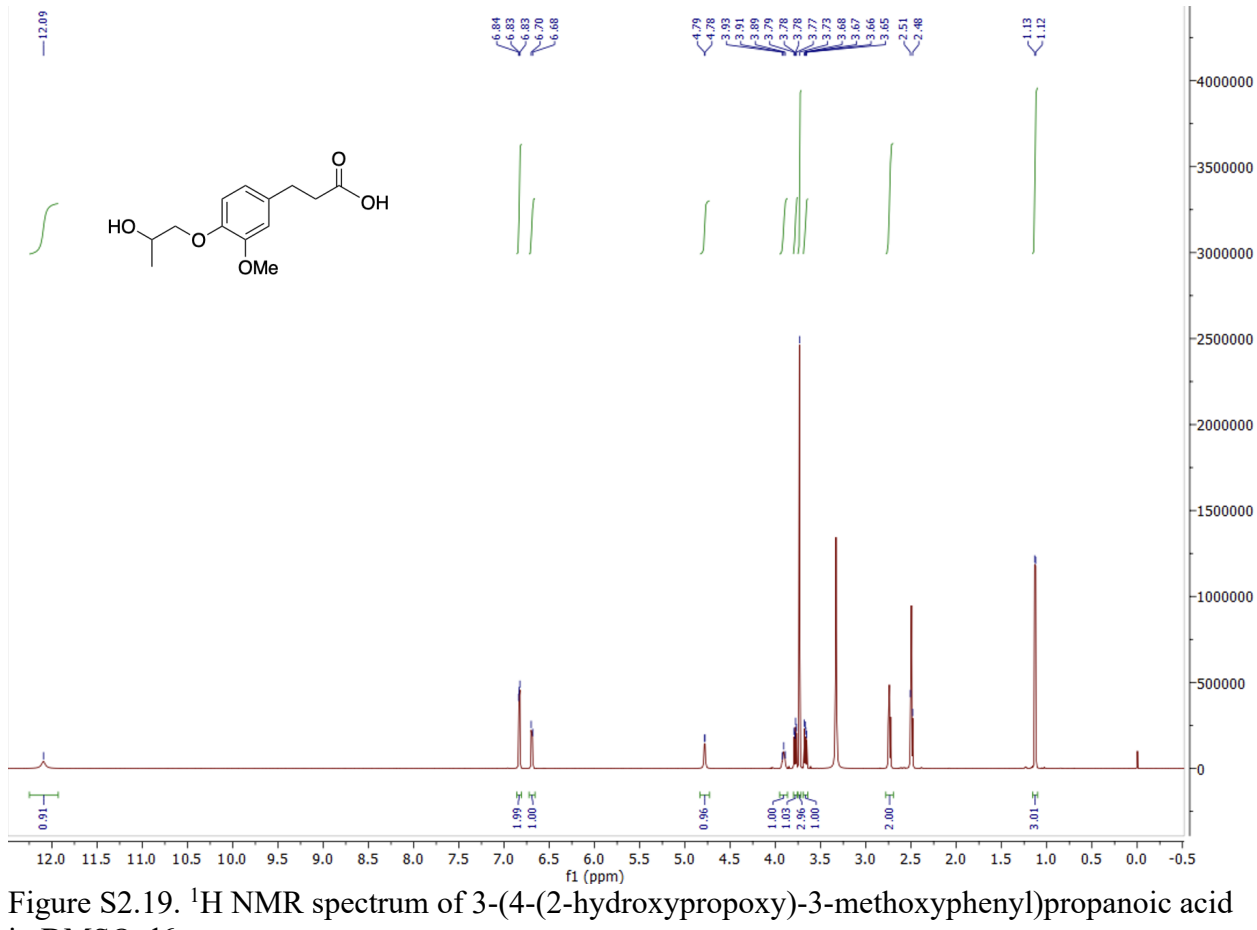


CDC13.

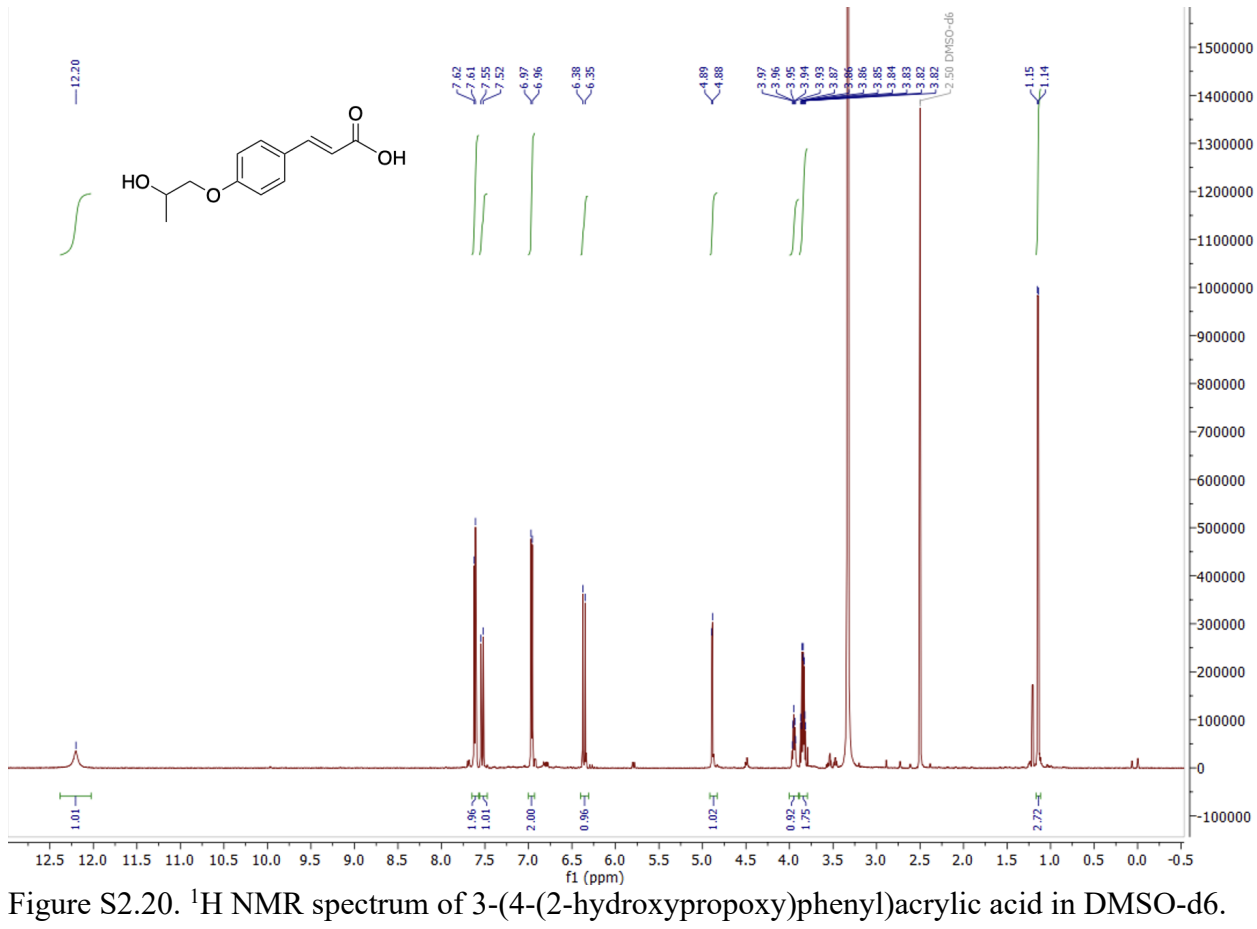


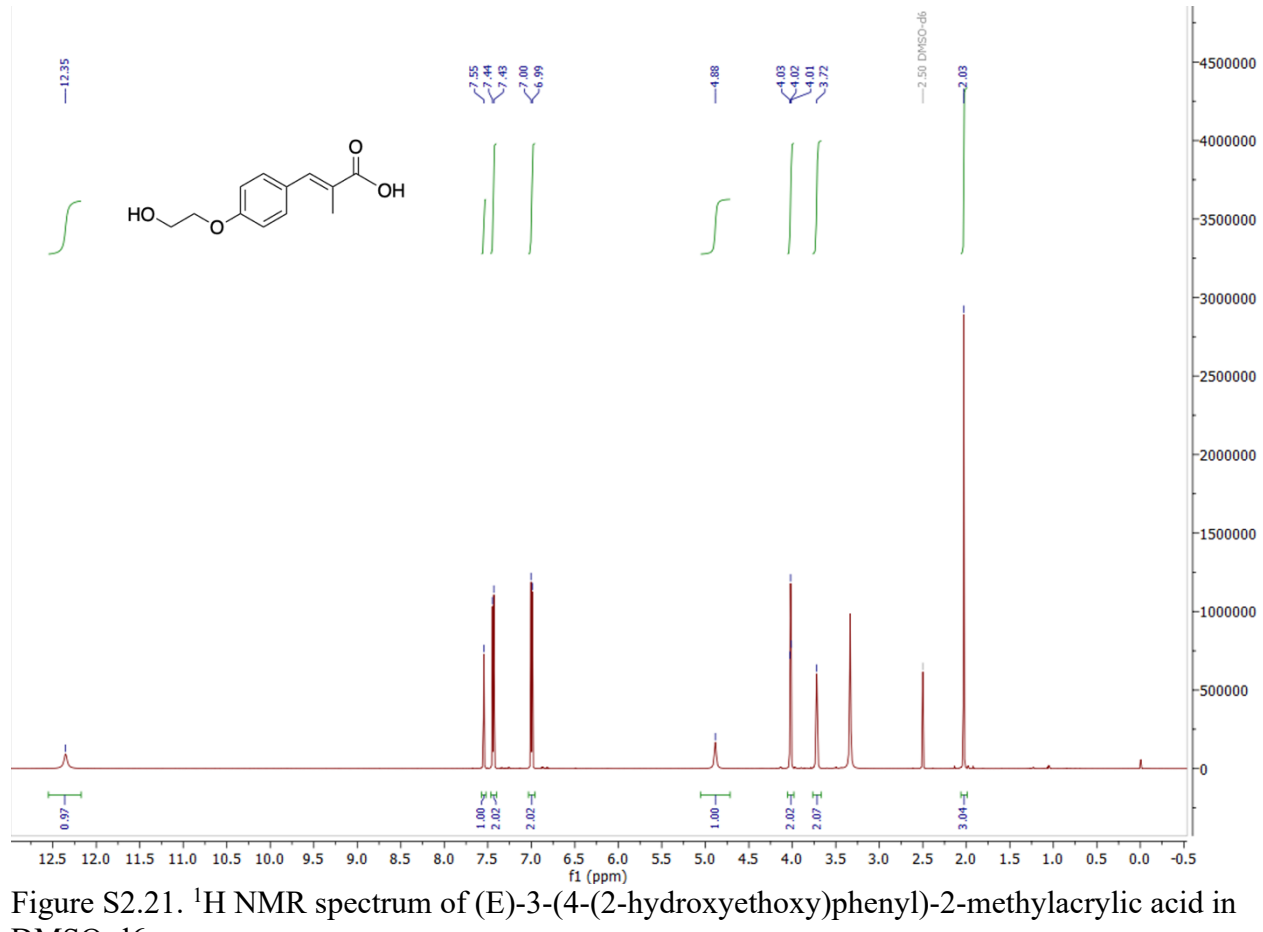
CDCl3.



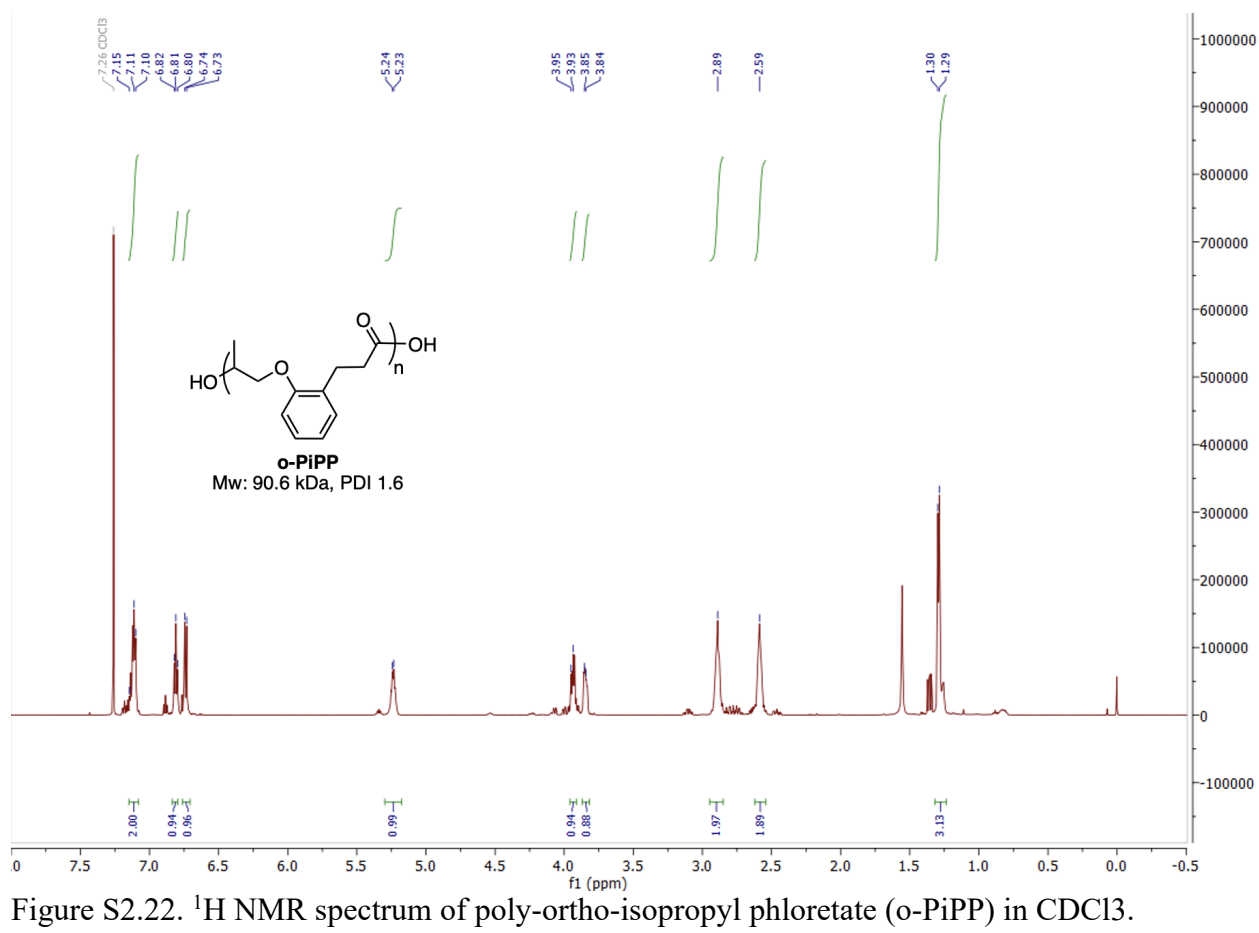


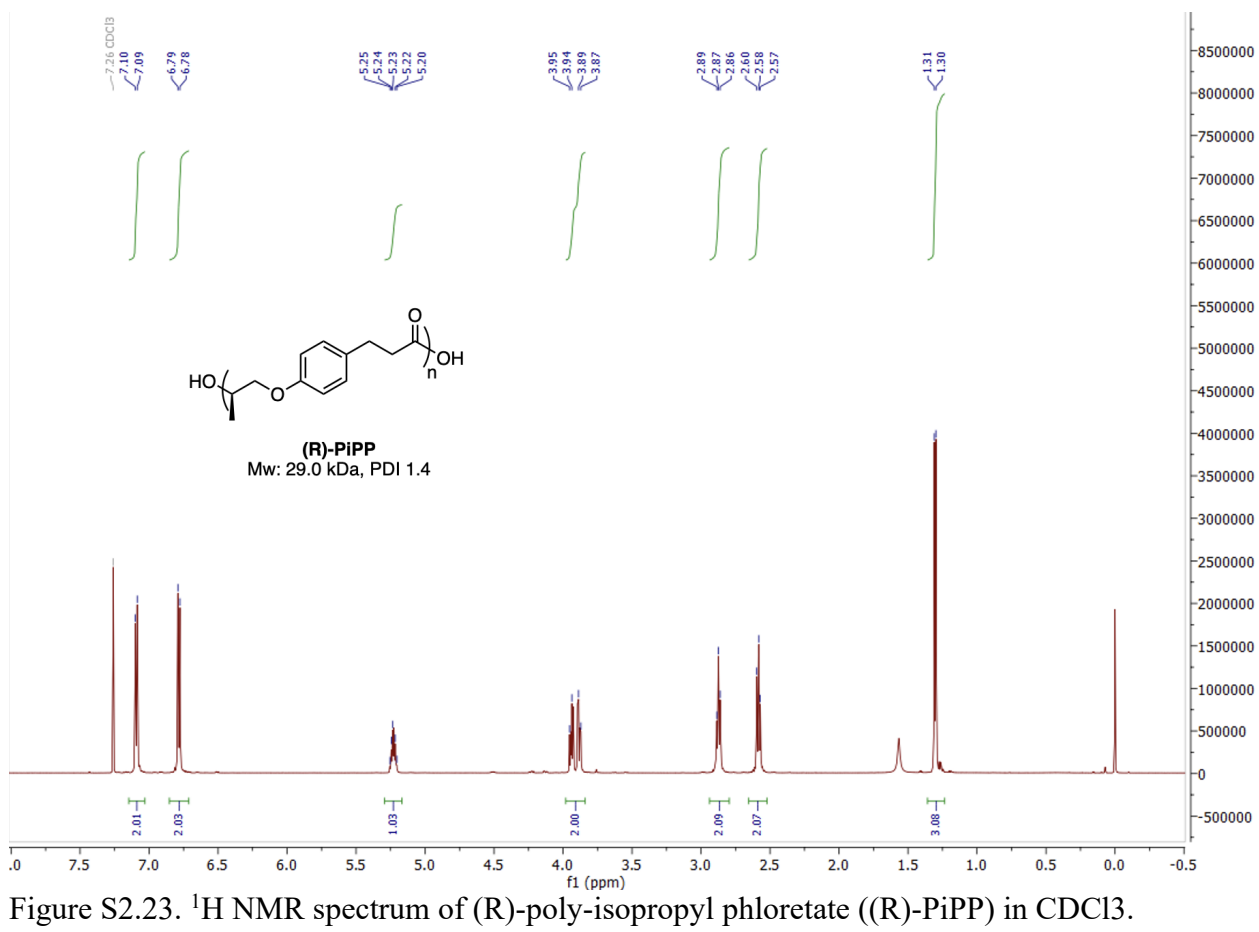
in DMSO-d6.

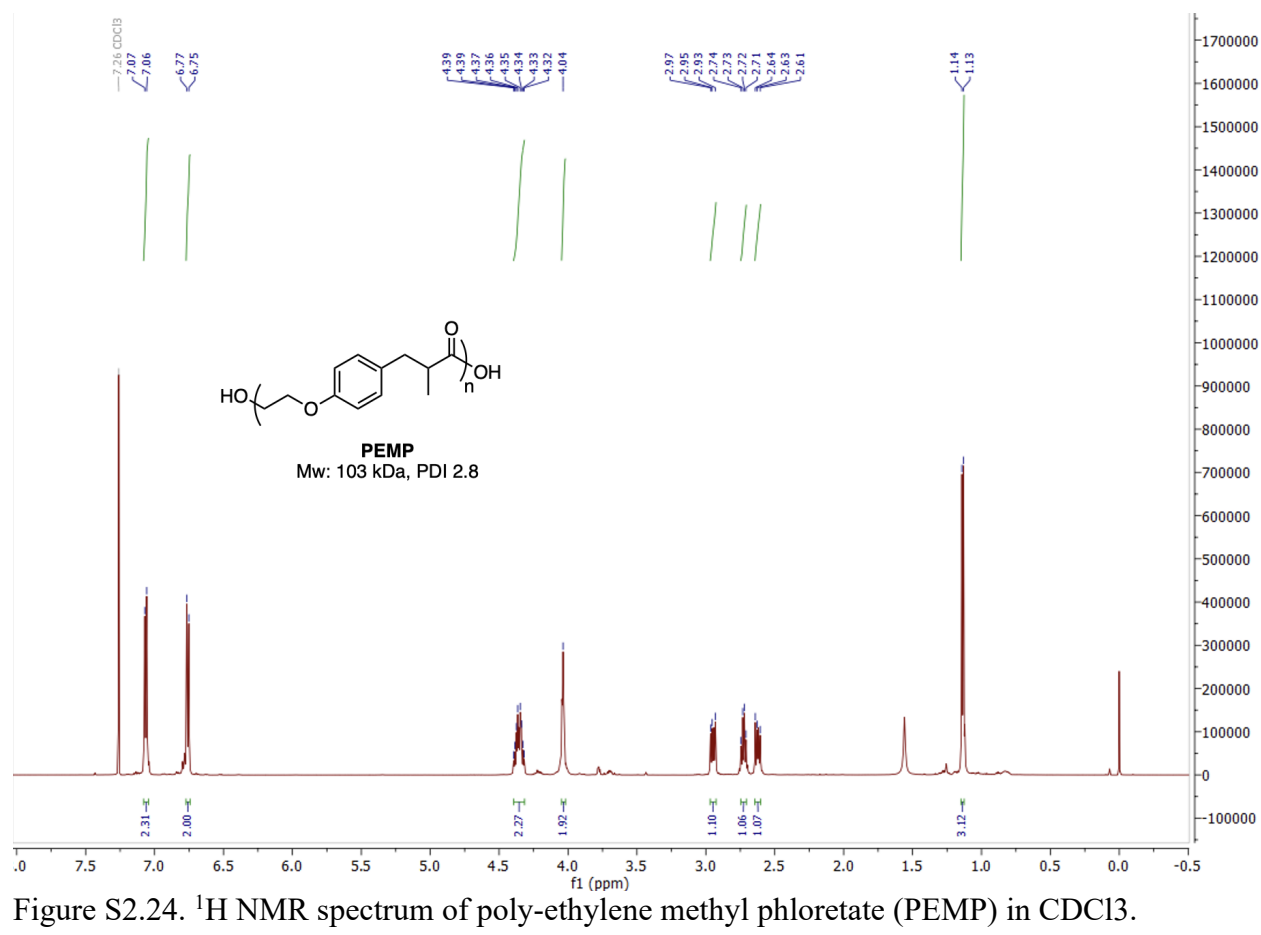


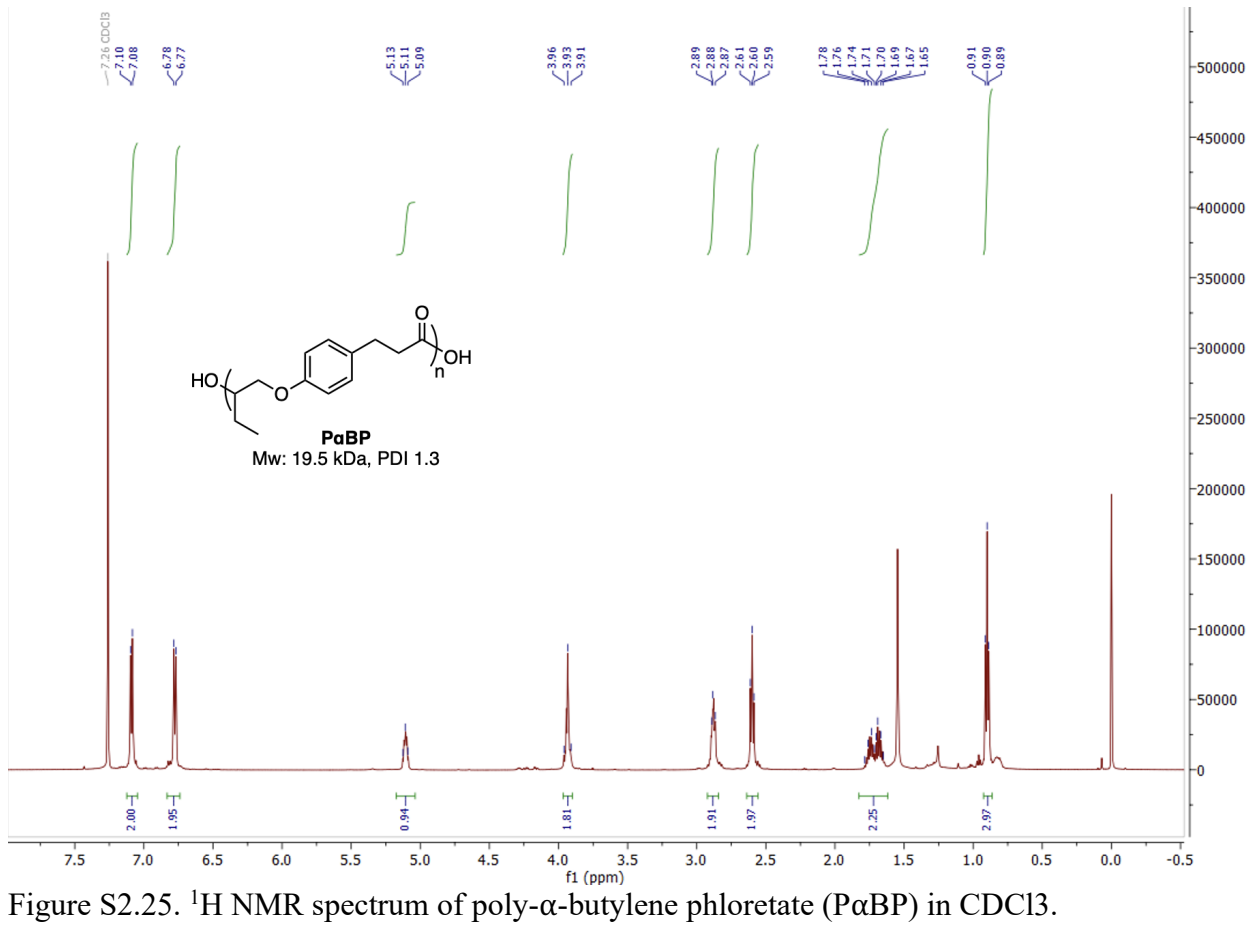


DMSO-d6.









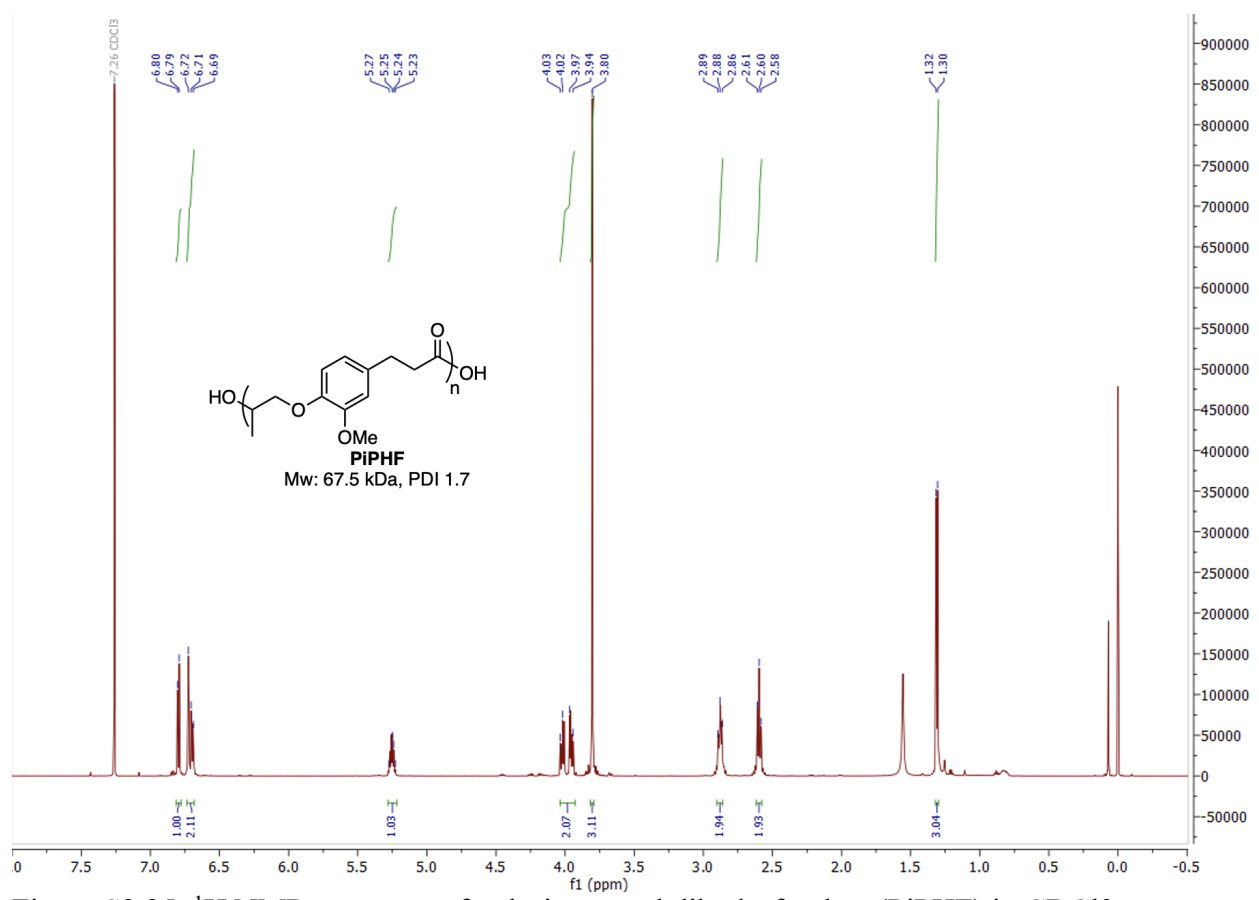


Figure S2.25. ¹H NMR spectrum of poly-isopropyl dihydroferulate (PiPHF) in CDC13.

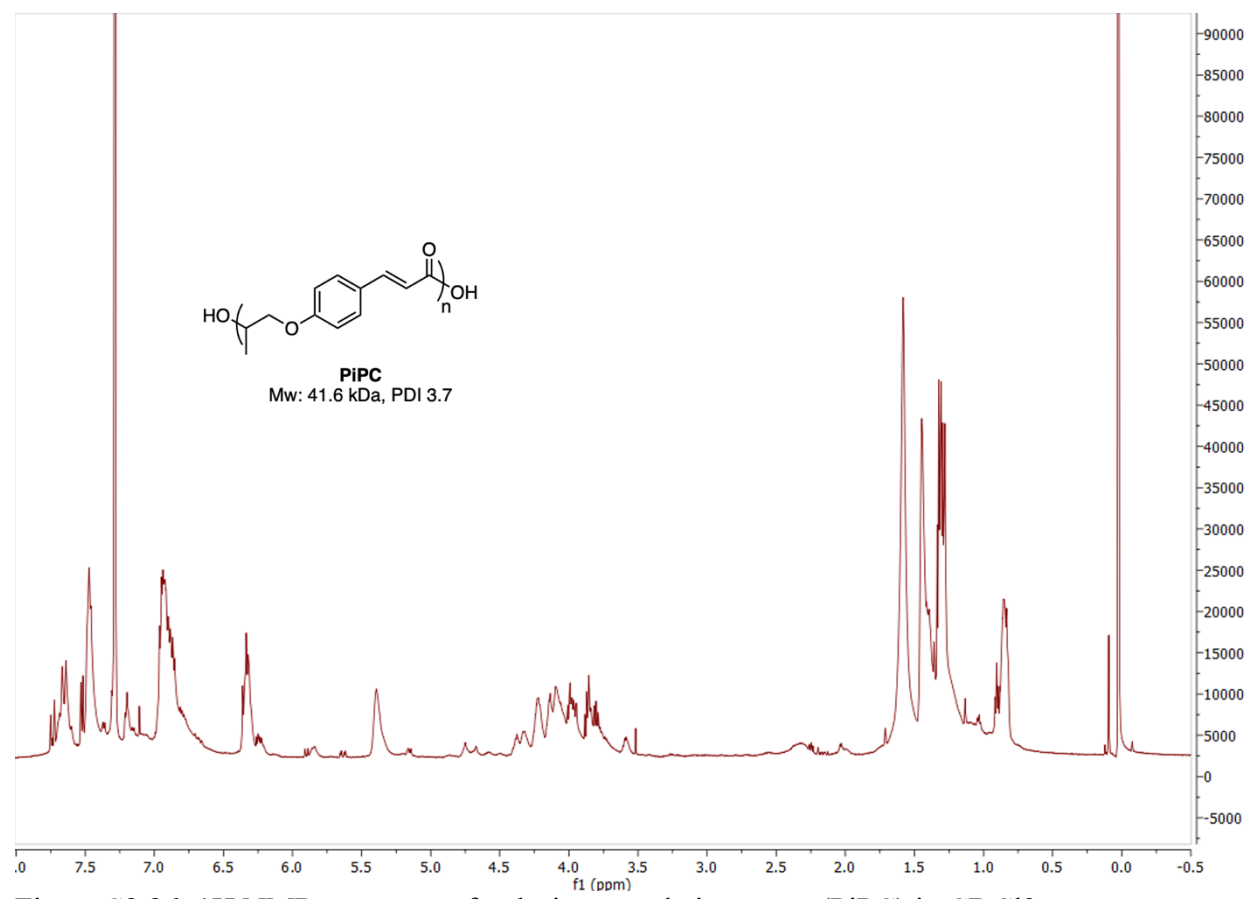
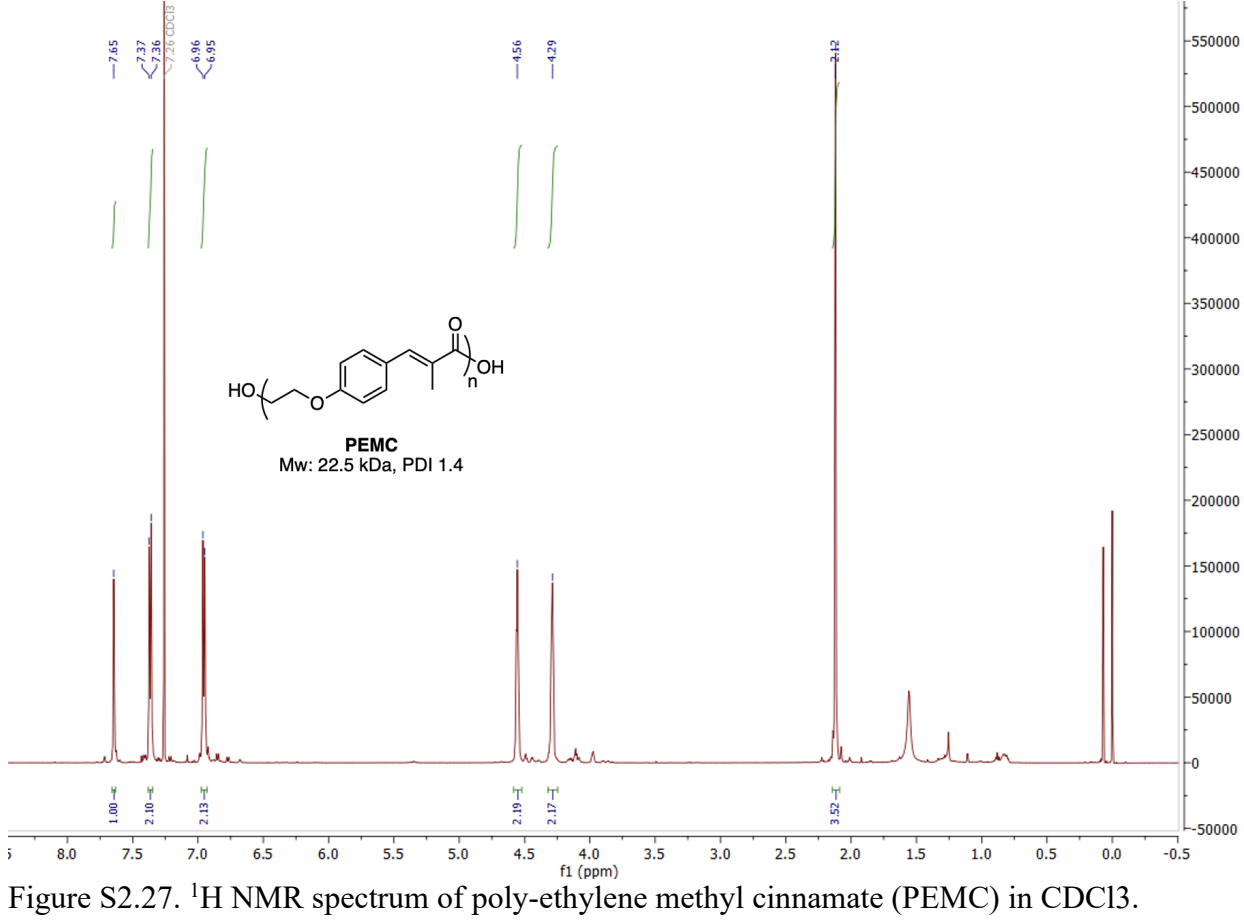


Figure S2.26. 1H NMR spectrum of poly-isopropyl cinnamate (PiPC) in CDCl3.



¹³C NMR Spectra of Monomers and Polymers:

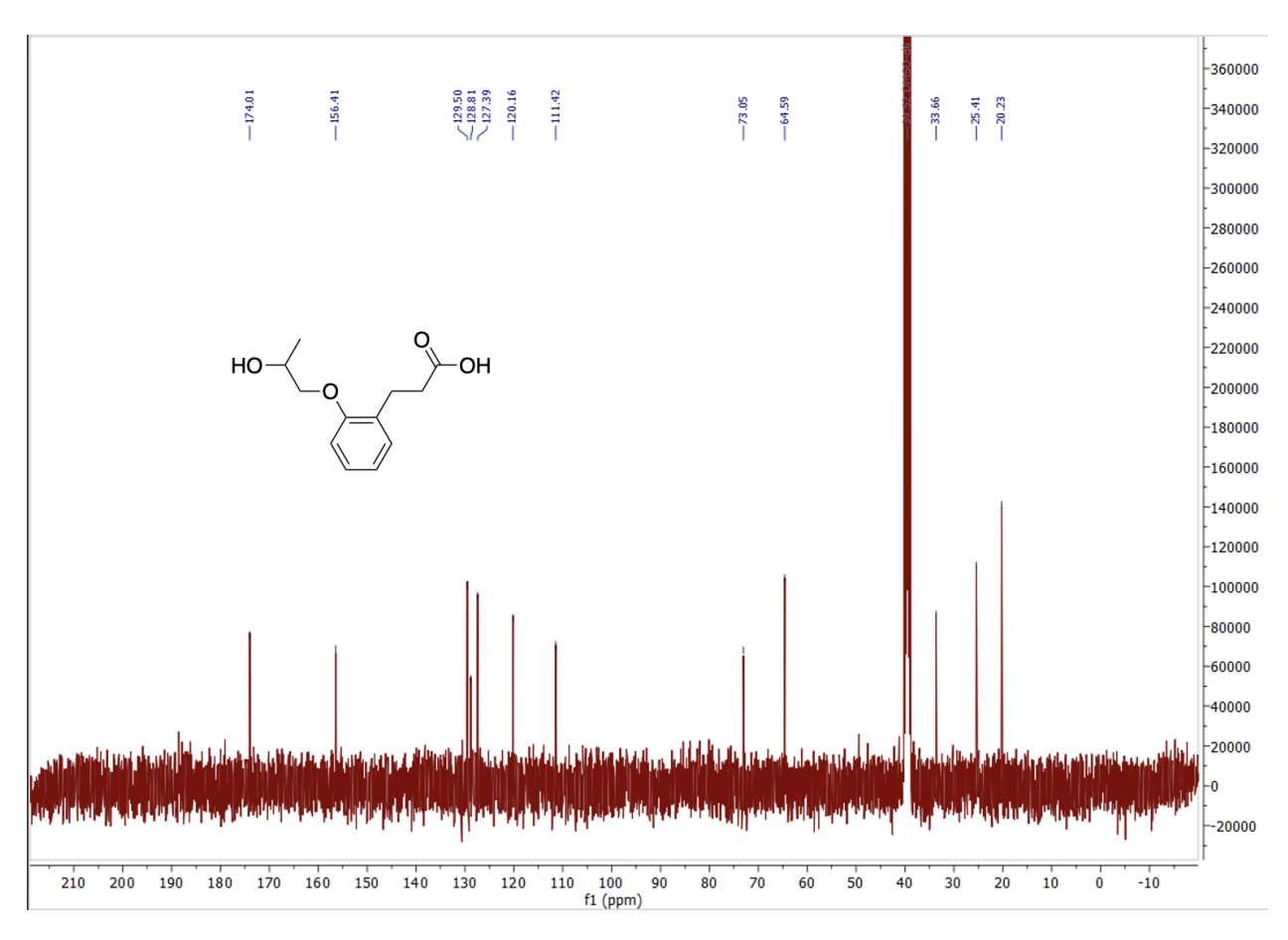


Figure S2.28. ¹³C NMR spectrum of 3-(2-(2-hydroxypropoxy)phenyl)propanoic acid in DMSO-d6.

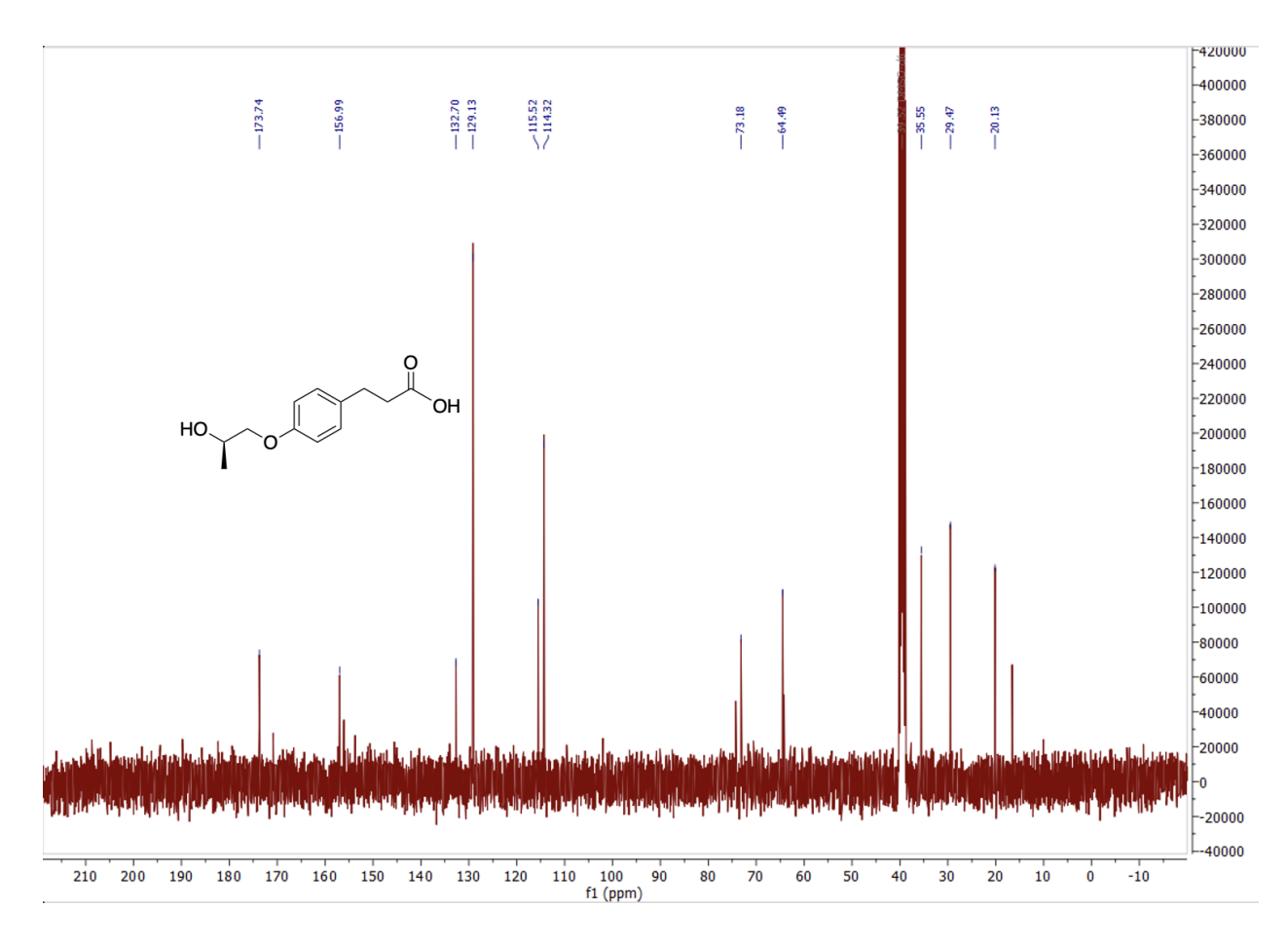


Figure S2.29. ¹³C NMR spectrum of (R)-3-(4-(2-hydroxypropoxy)phenyl)propanoic acid in DMSO-d6.

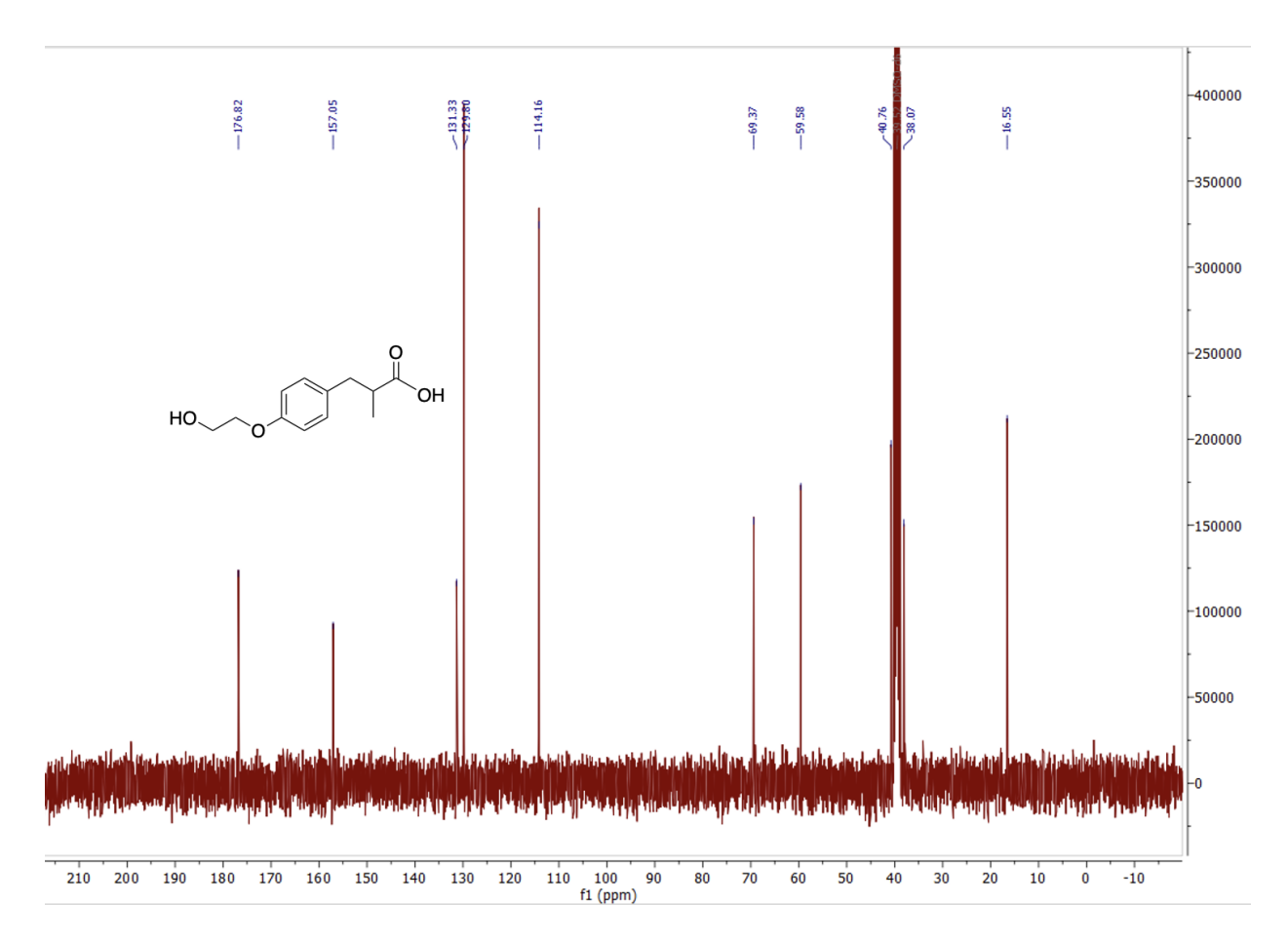


Figure S2.30. 13 C NMR spectrum of 3-(4-(2-hydroxyethoxy)phenyl)-2-methylpropanoic acid in DMSO-d6.

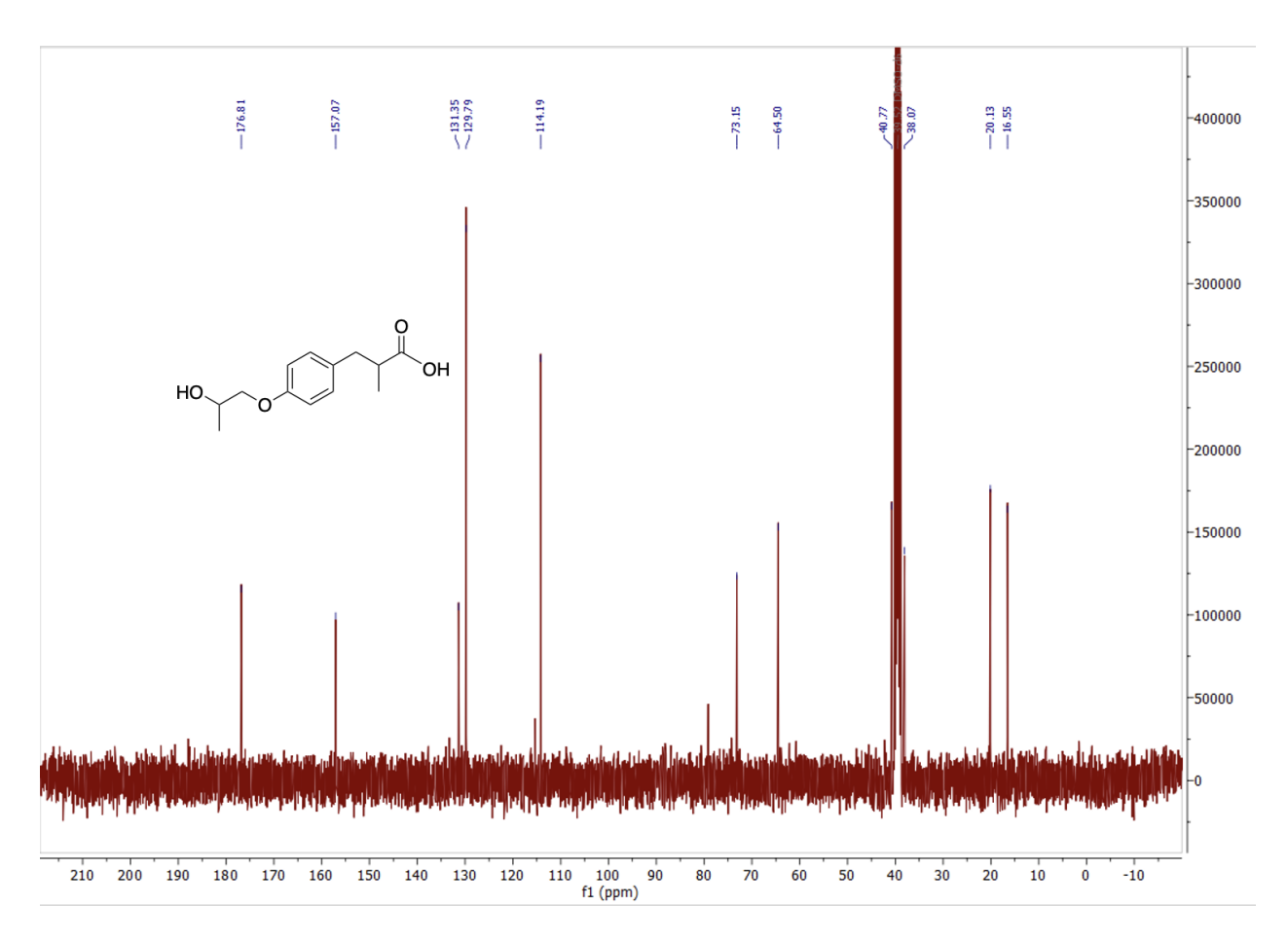


Figure S2.31. 13 C NMR spectrum of 3-(4-(2-hydroxypropoxy)phenyl)-2-methylpropanoic acid in DMSO-d6.

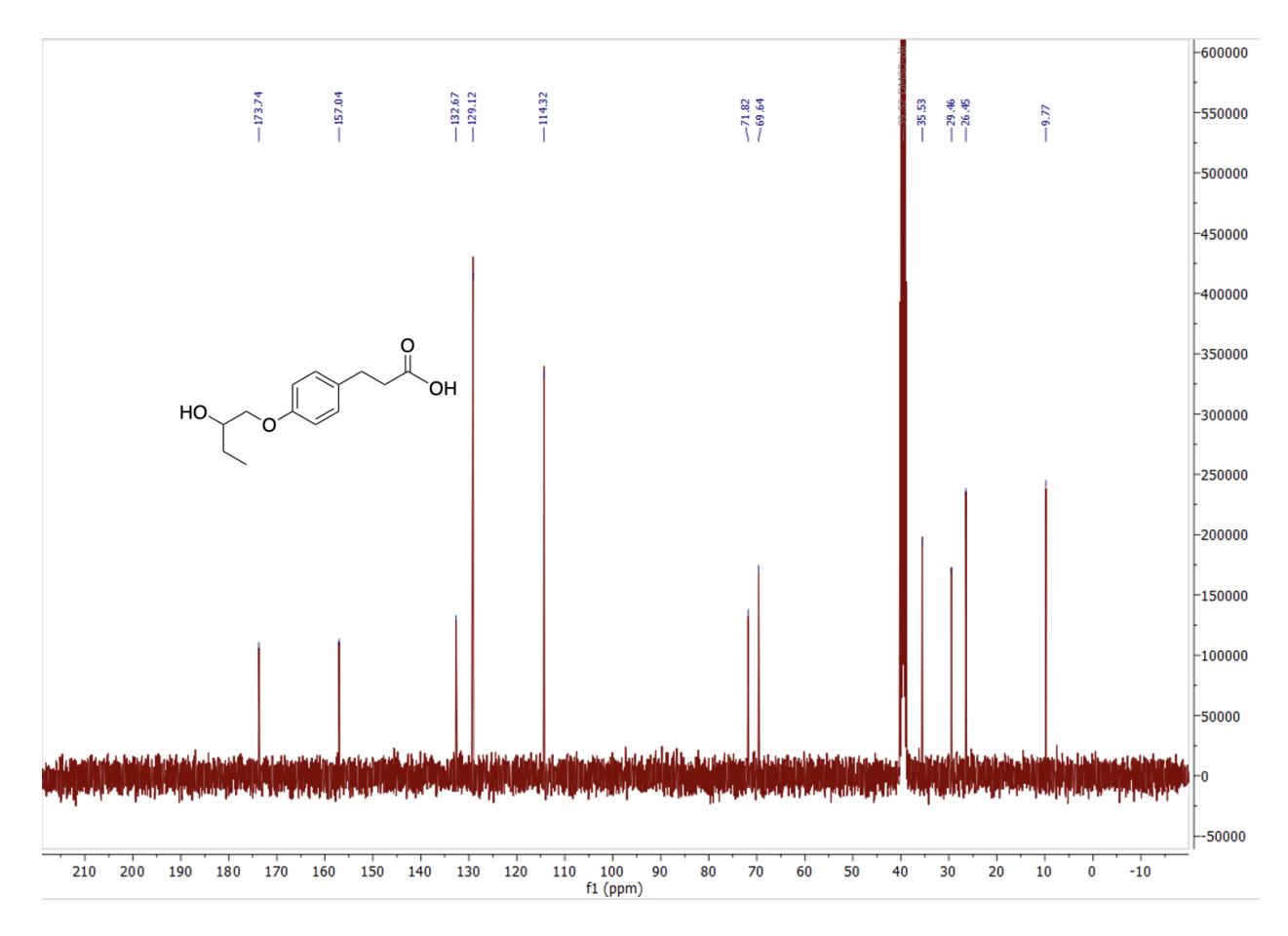


Figure S2.32. ¹³C NMR spectrum of 3-(4-(2-hydroxybutoxy)phenyl)propanoic acid in DMSO-d6.

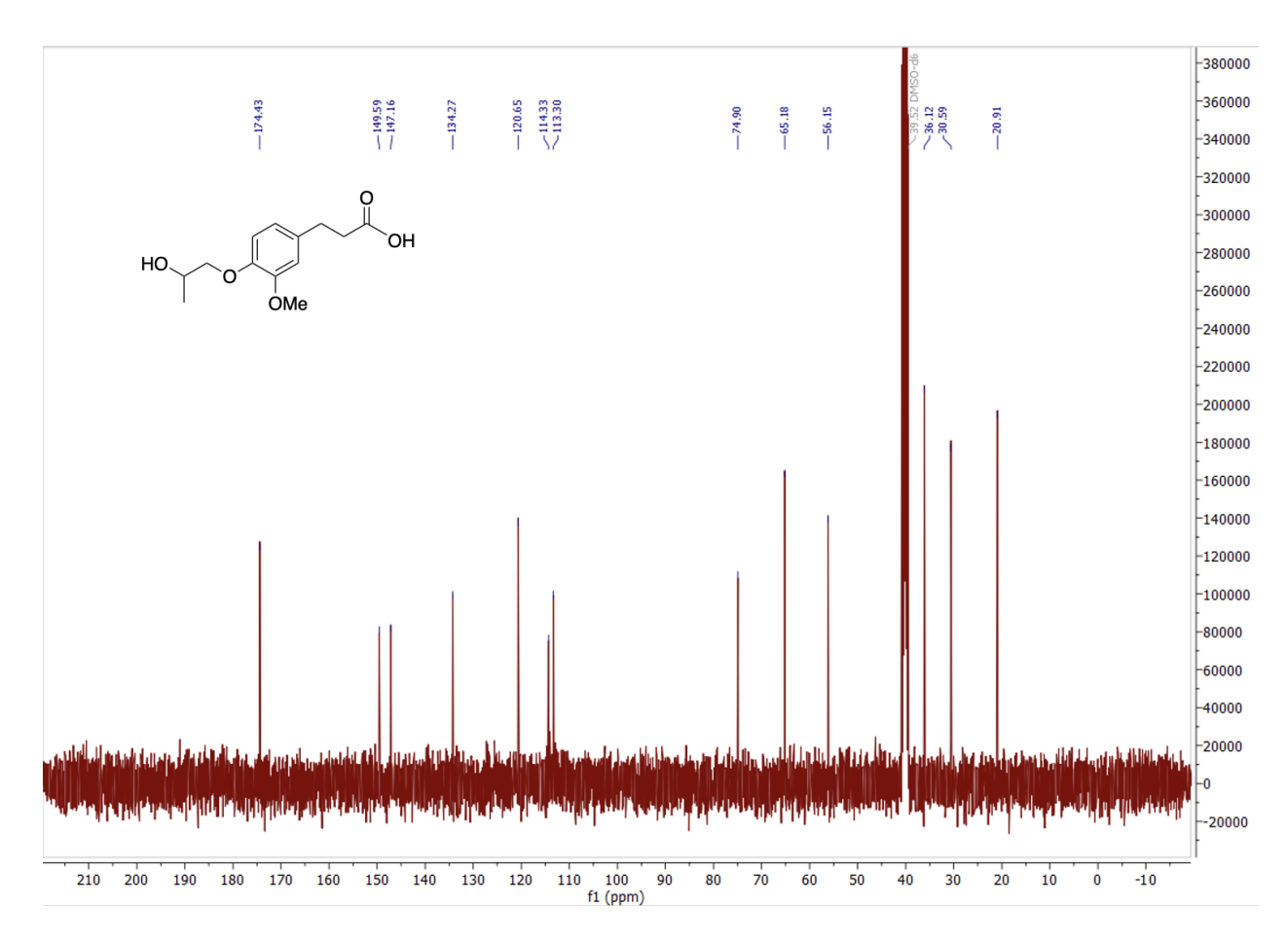


Figure S2.33. ¹³C NMR spectrum of 3-(4-(2-hydroxypropoxy)-3-methoxyphenyl)propanoic acid in DMSO-d6.

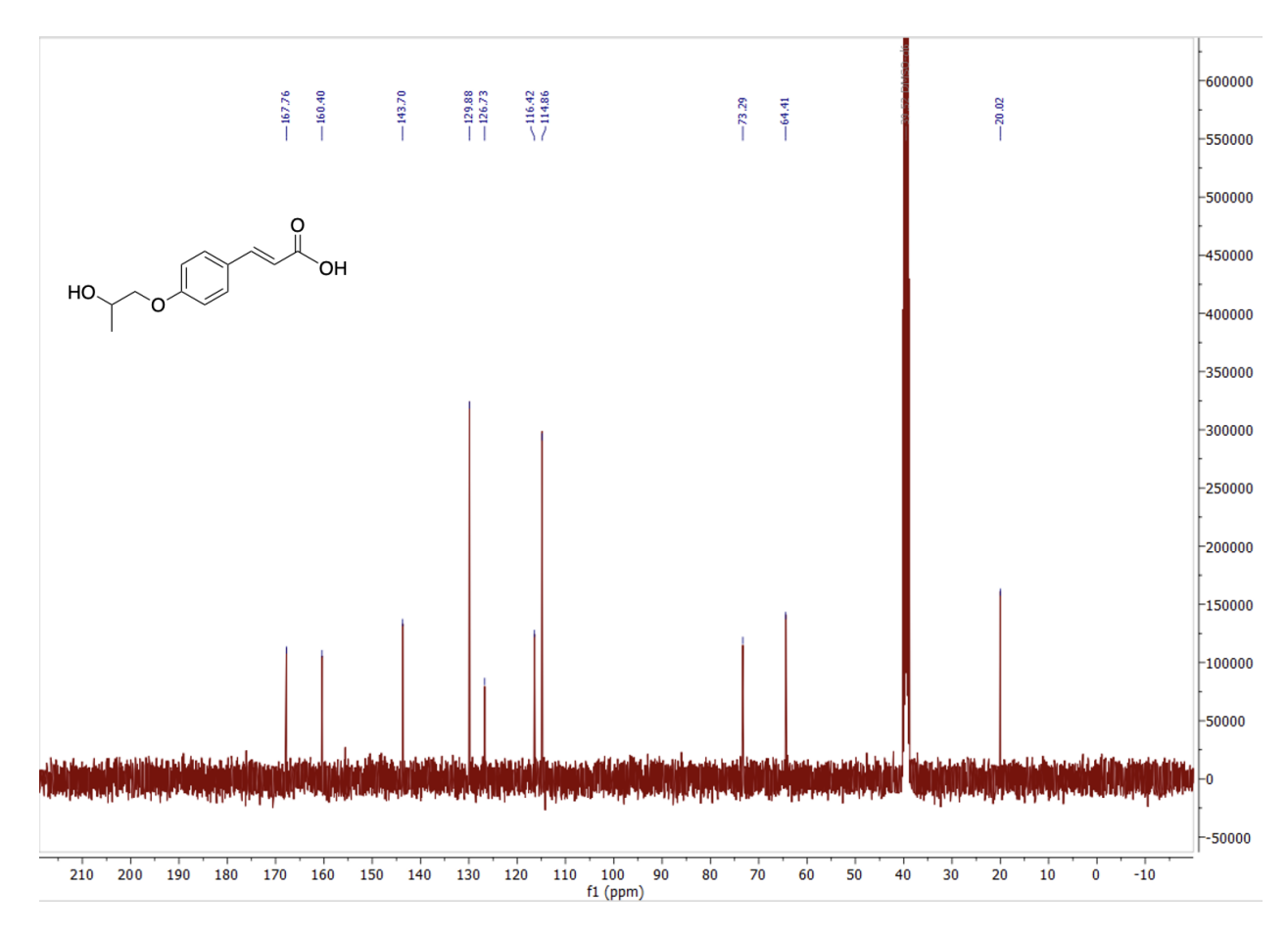


Figure S2.34. ¹³C NMR spectrum of 3-(4-(2-hydroxypropoxy)phenyl)acrylic acid in DMSO-d6.

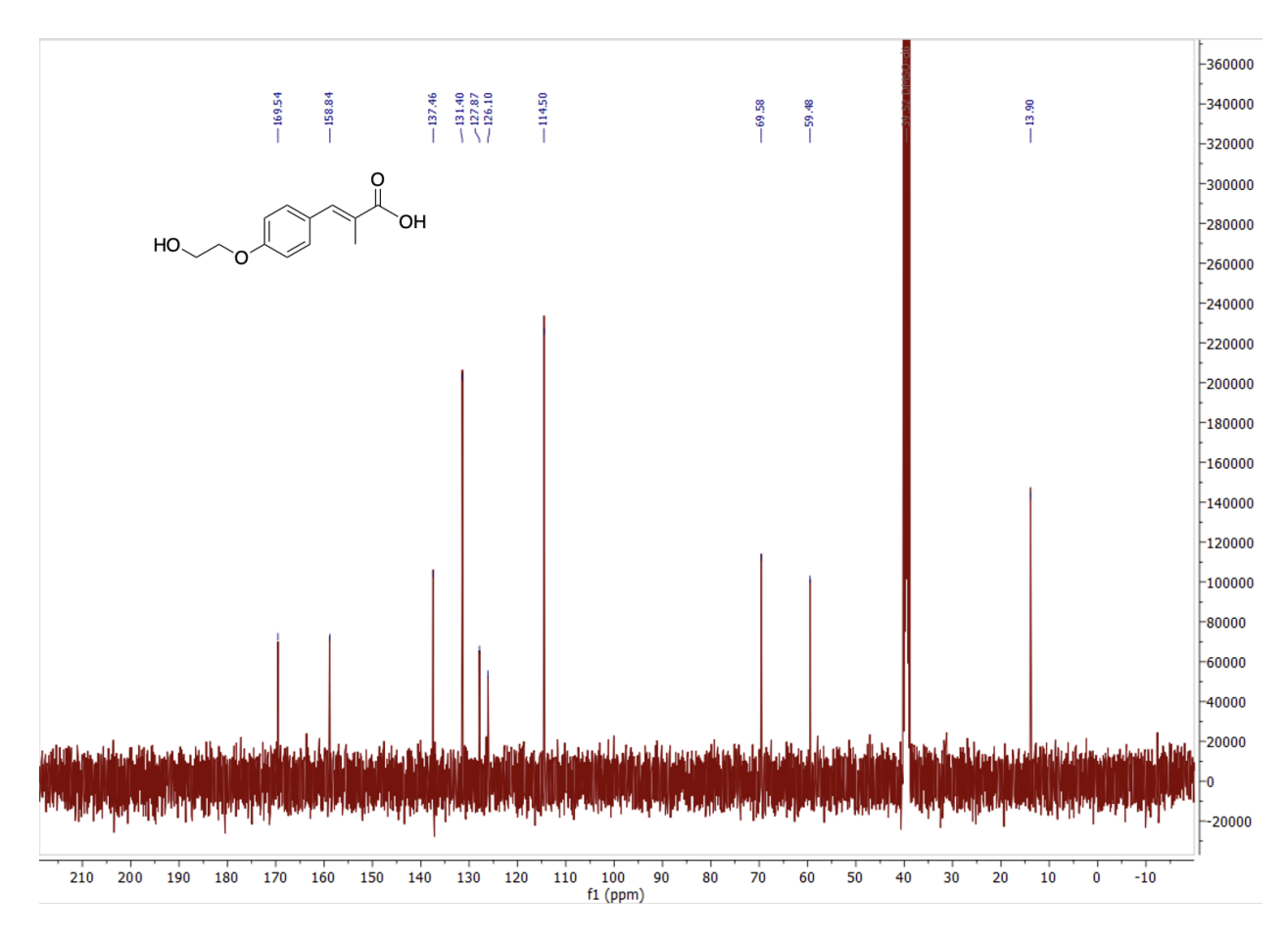


Figure S2.35. 13 C NMR spectrum of (E)-3-(4-(2-hydroxyethoxy)phenyl)-2-methylacrylic acid in DMSO-d6.

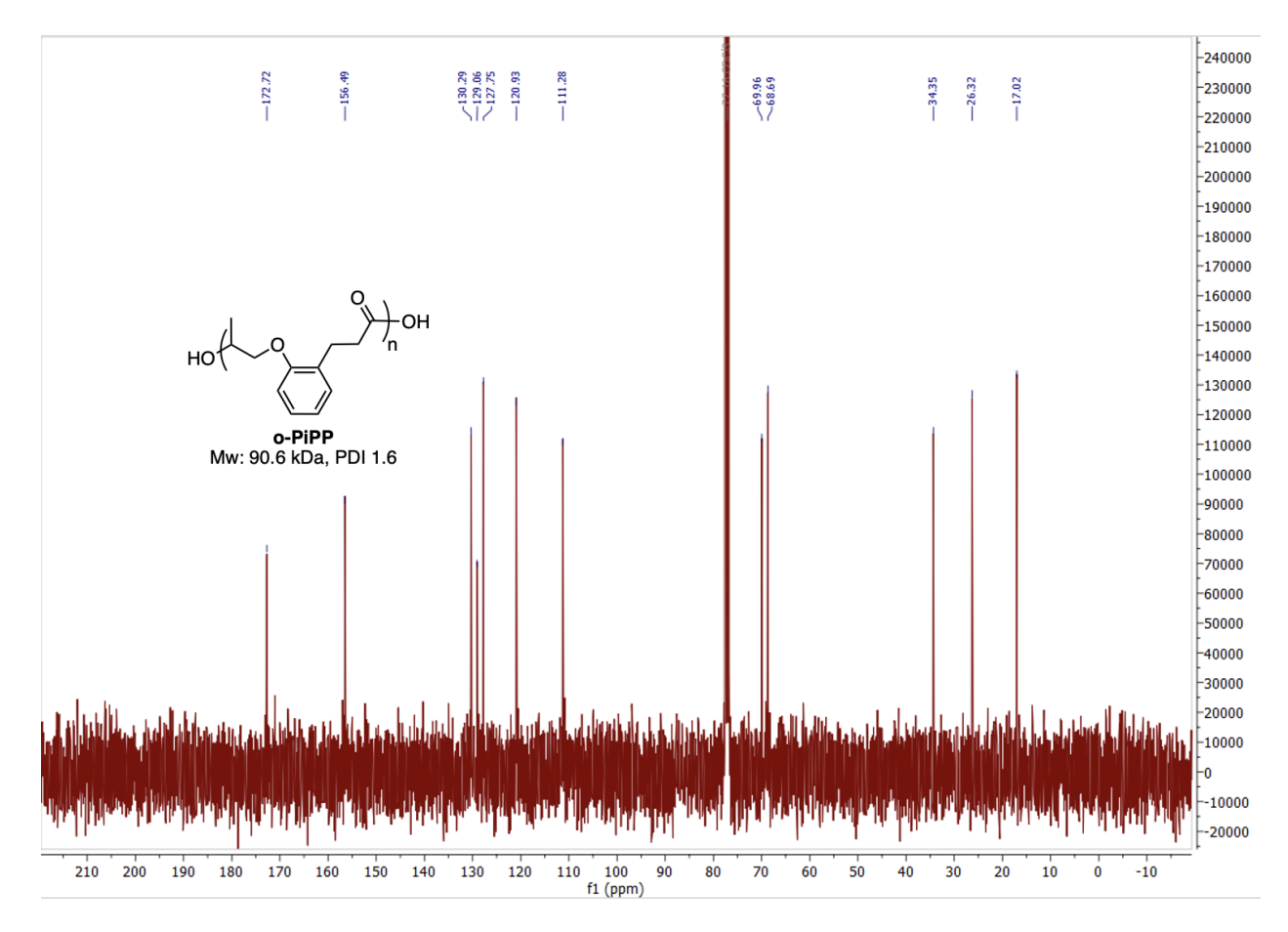


Figure S2.36. ¹³C NMR spectrum of poly-ortho-isopropyl phloretate (o-PiPP) in CDCl₃.

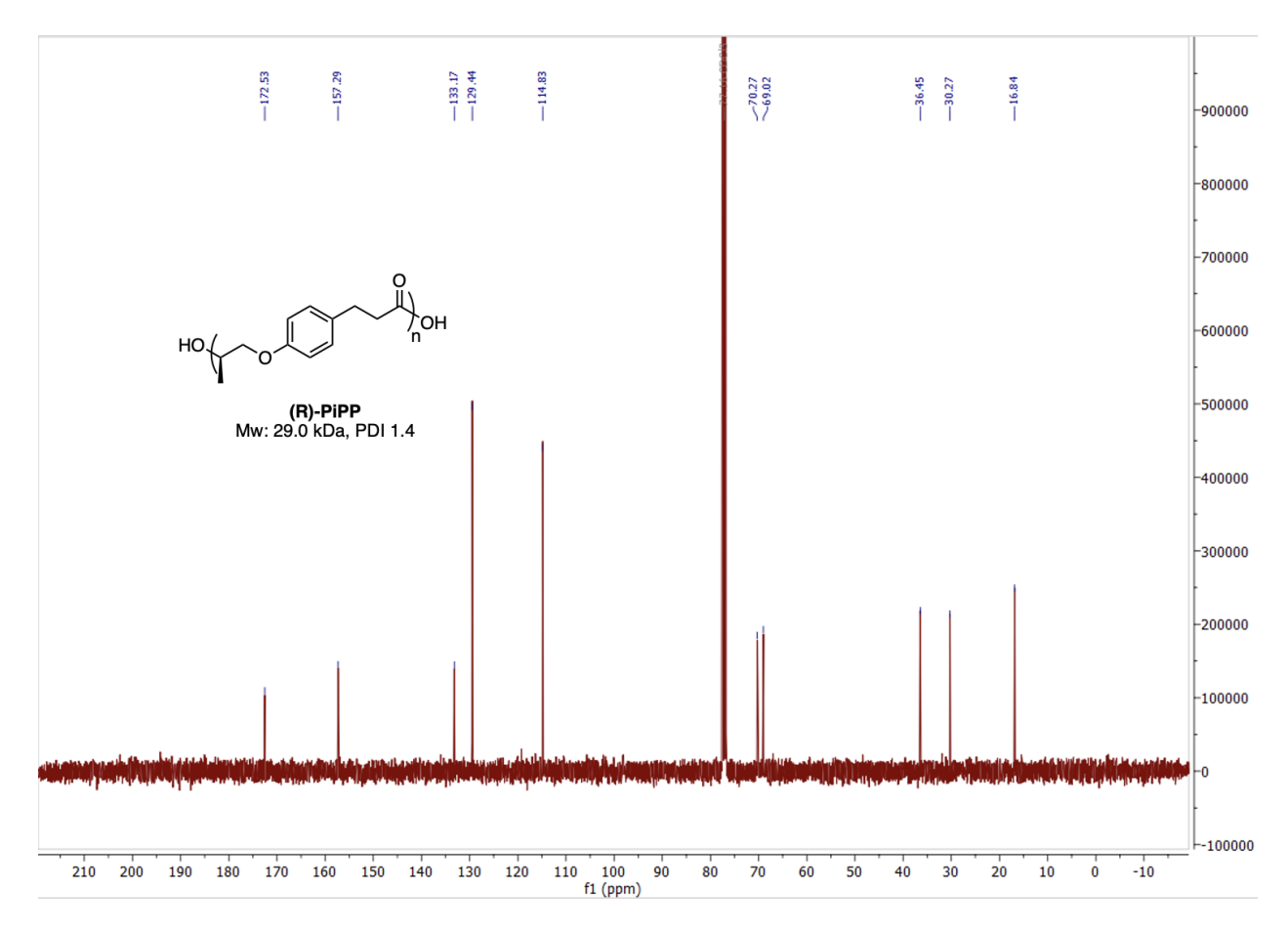


Figure S2.37. ¹³C NMR spectrum of (R)-poly-isopropyl phloretate ((R)-PiPP) in CDCl₃.

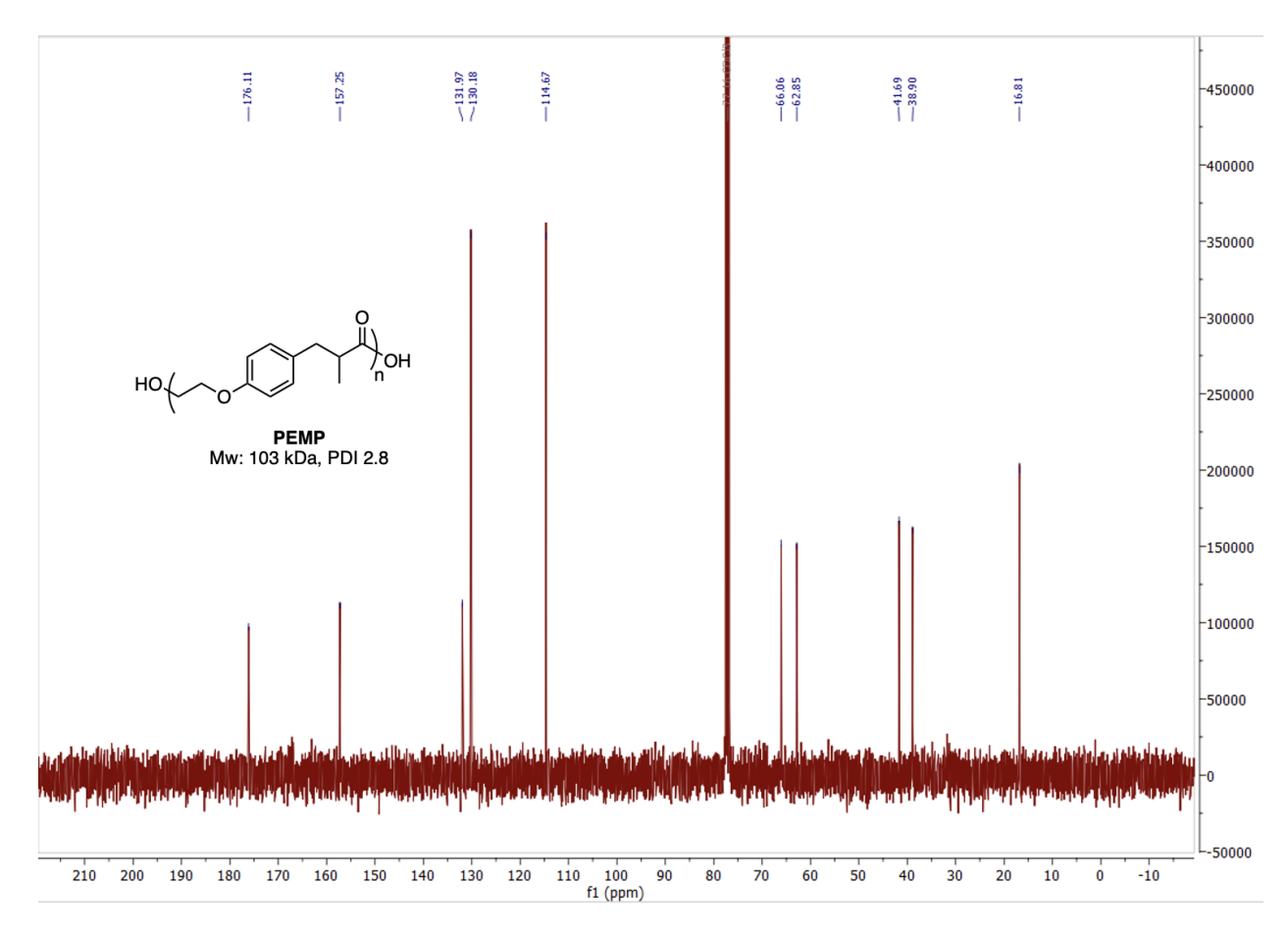


Figure S2.38. ¹³C NMR spectrum of poly-ethylene methyl phloretate (PEMP) in CDCl₃.

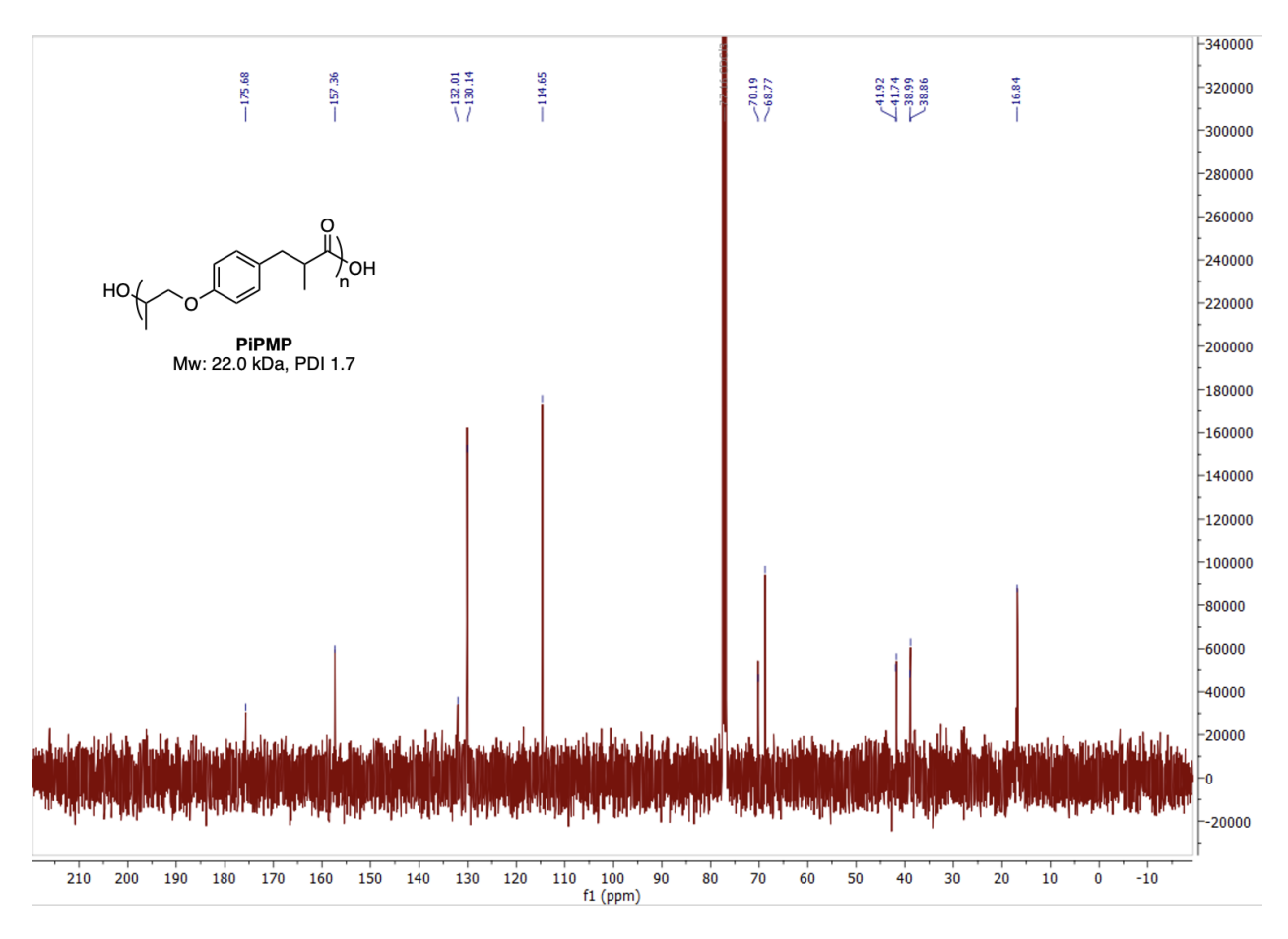


Figure S2.39. ¹³C NMR spectrum of poly-isopropyl-methyl-phloretate (PiPMP) in CDCl₃.

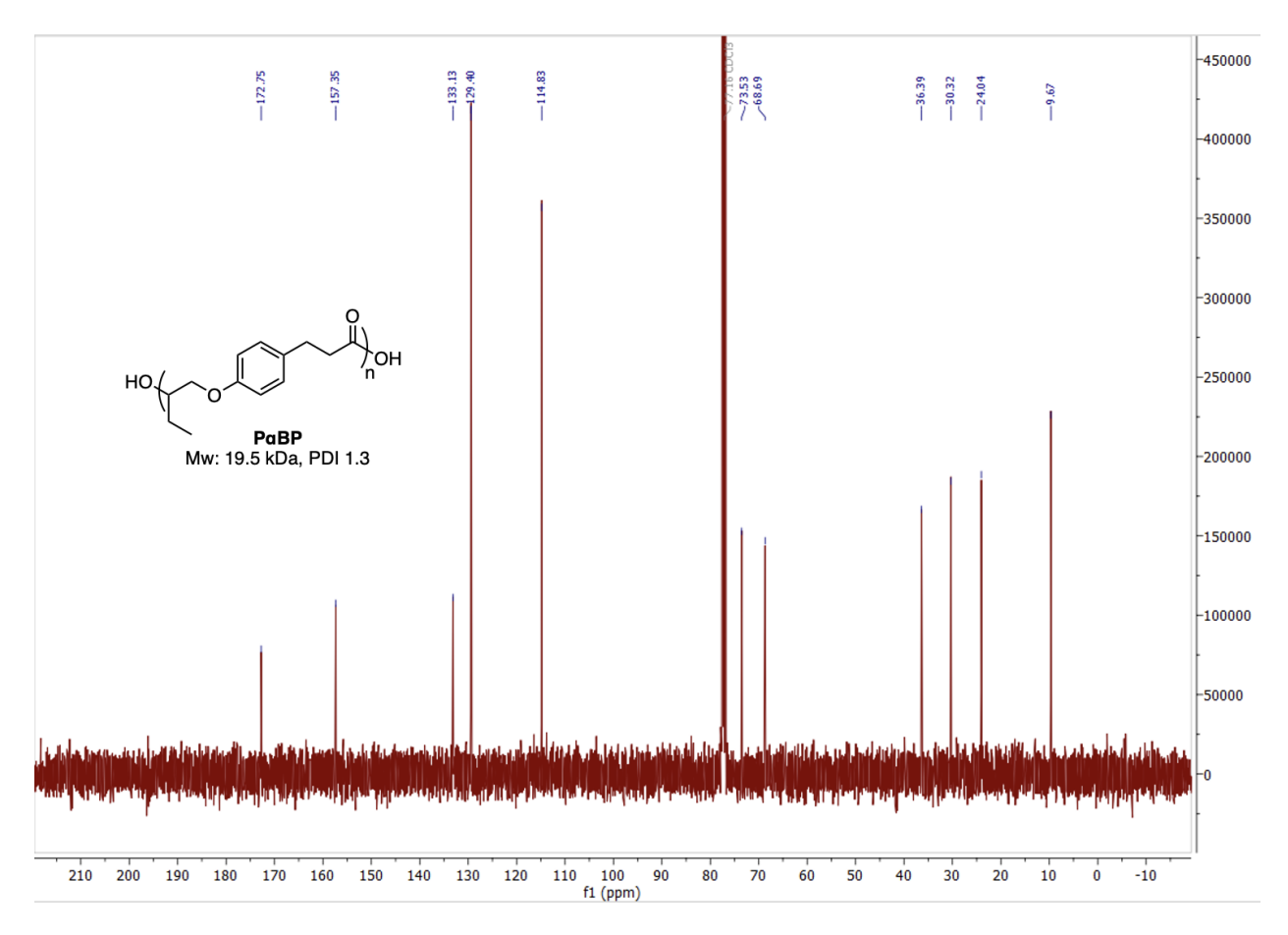


Figure S2.40. 13 C NMR spectrum of poly- α -butylene phloretate (P α BP) in CDCl₃.

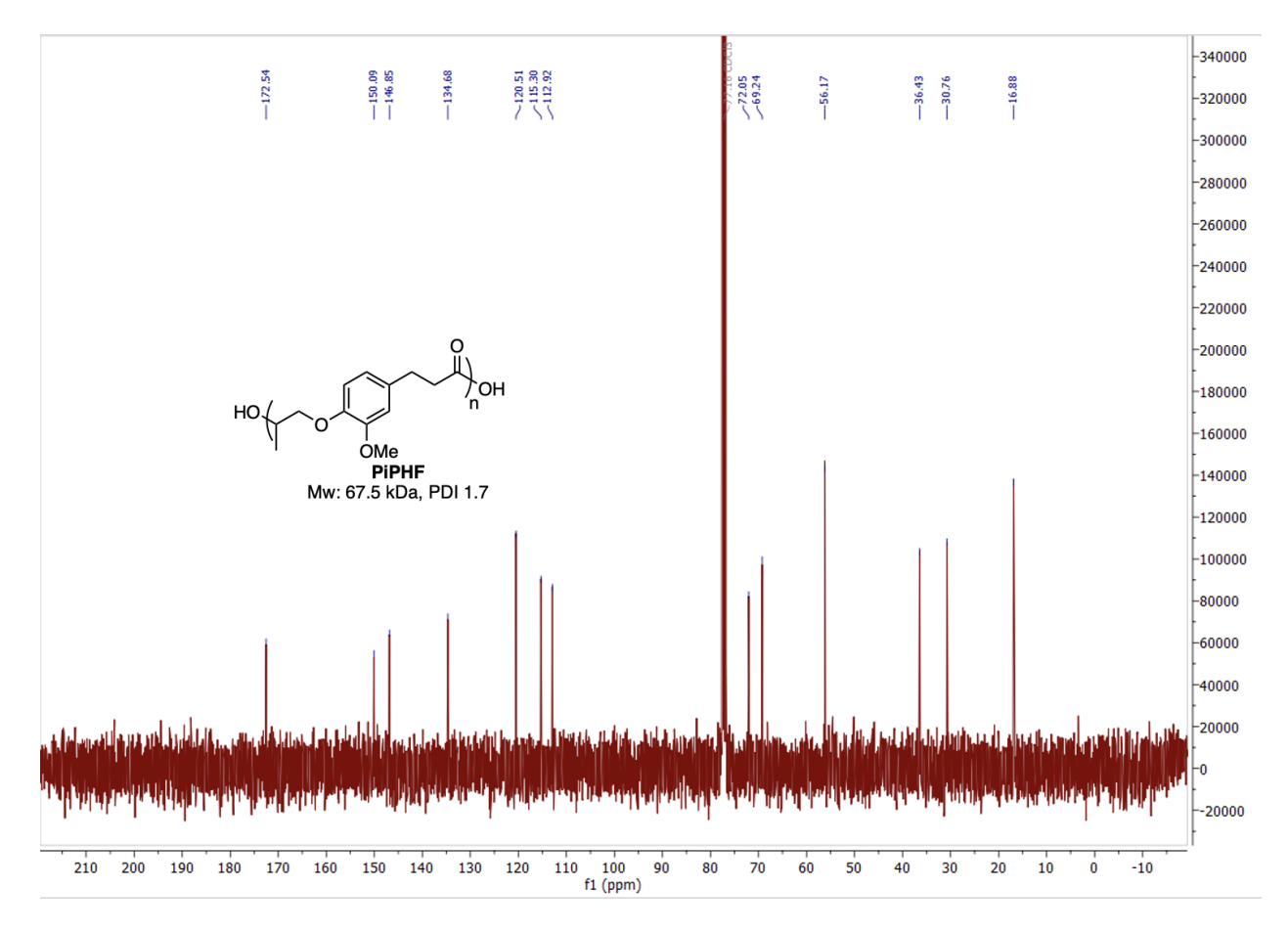


Figure S2.41. ¹³C NMR spectrum of poly-isopropyl dihydroferulate (PiPHF) in CDCl₃.

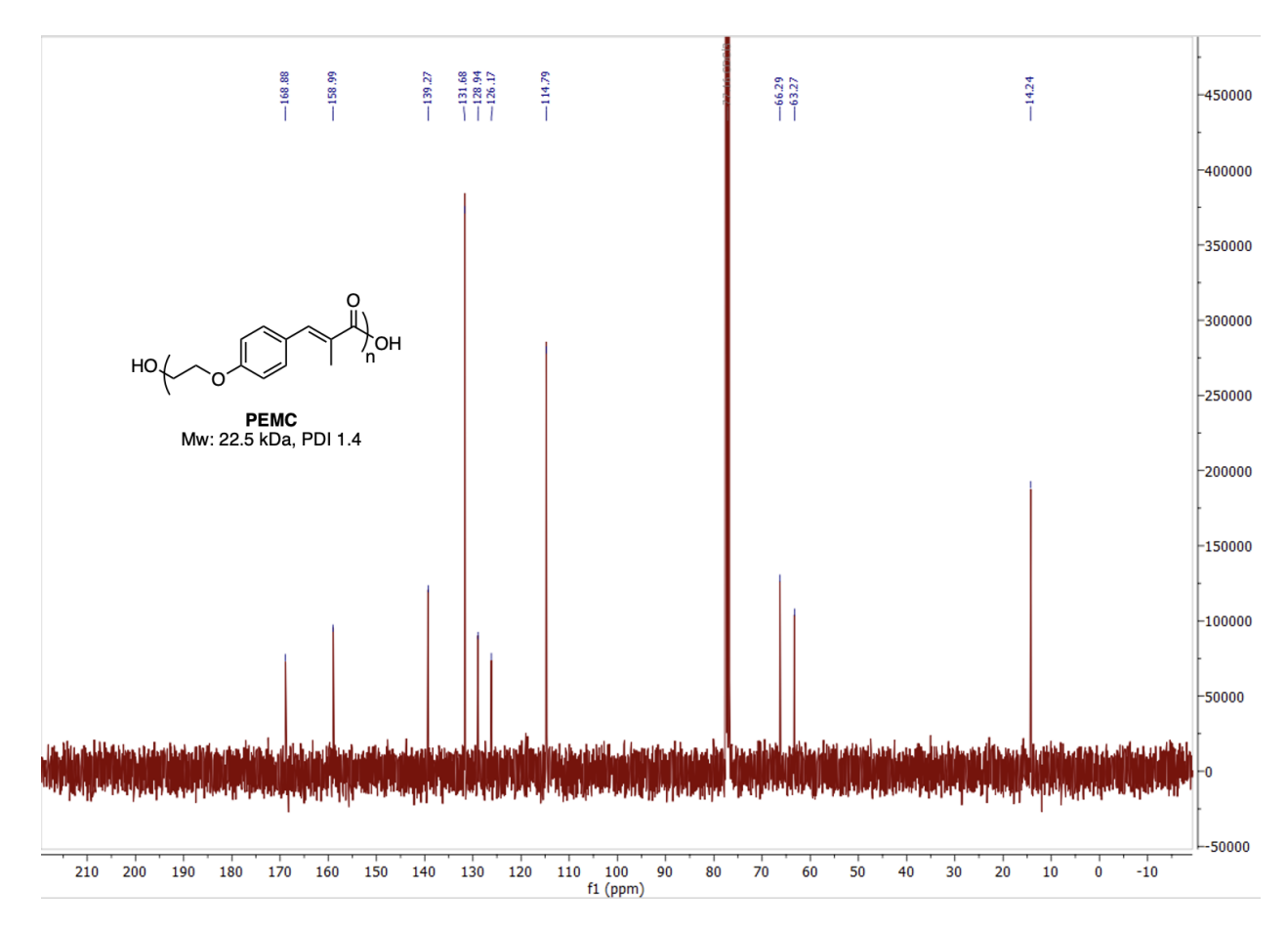


Figure S2.42. ¹³C NMR spectrum of poly-ethylene methyl cinnamate (PEMC) in CDCl₃.

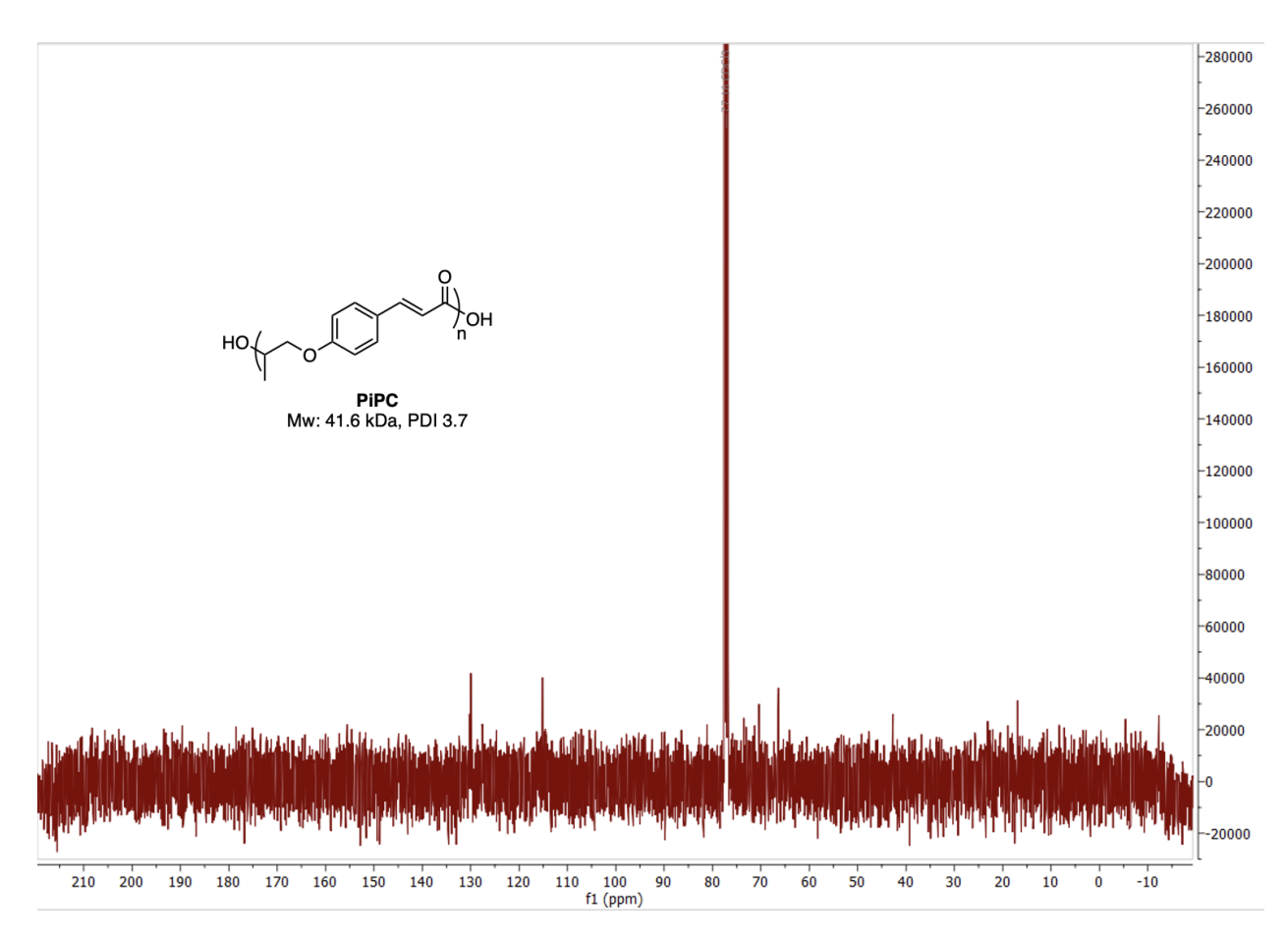


Figure S2.43. ¹³C NMR spectrum of poly-isopropyl cinnamate (PiPC) in CDCl₃.

References:

- (1) Marumoto, S.; Miyazawa, M. Microbial reduction of coumarin, psoralen, and xanthyletin by Glomerella cingulata. *Tetrahedron* **2011**, *67* (2), 495-500. DOI: https://doi.org/10.1016/j.tet.2010.10.089.
- (2) Fujii, S. K., H.; Wantanabe, S. Phenylcarboxylic Acid Derivatives. USA 1989.
- (3) Winfield, D.; Ring, J.; Horn, J.; White, E. M.; Locklin, J. Semi-aromatic biobased polyesters derived from lignin and cyclic carbonates. *Green Chem* **2021**, *23* (23), 9658-9668. DOI: 10.1039/d1gc03135j.

APPENDIX B

SUPPLEMENTAL INFORMATION FOR CHAPTER 3

NMR Spectra of Crosslinker Molecules:

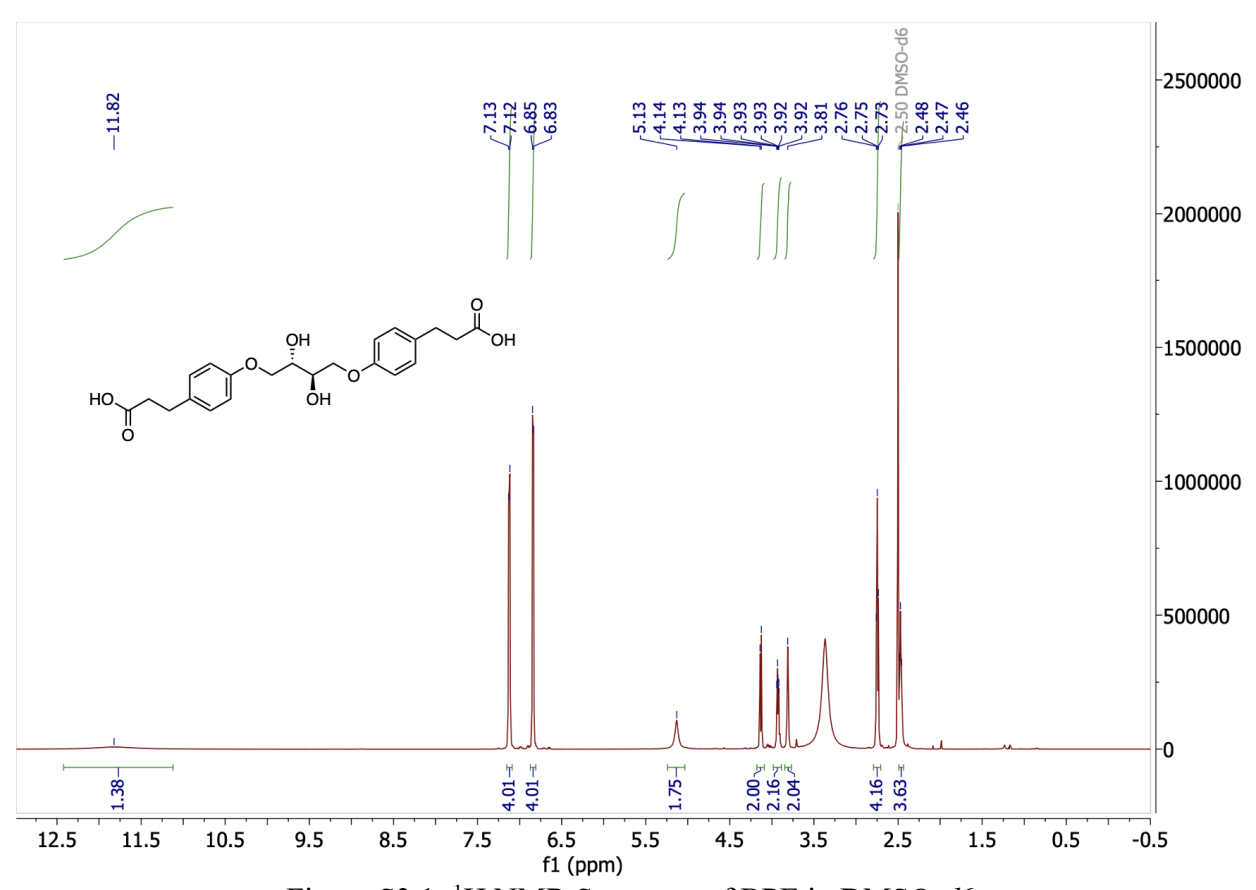


Figure S3.1: ¹H NMR Spectrum of BPE in DMSO-d6

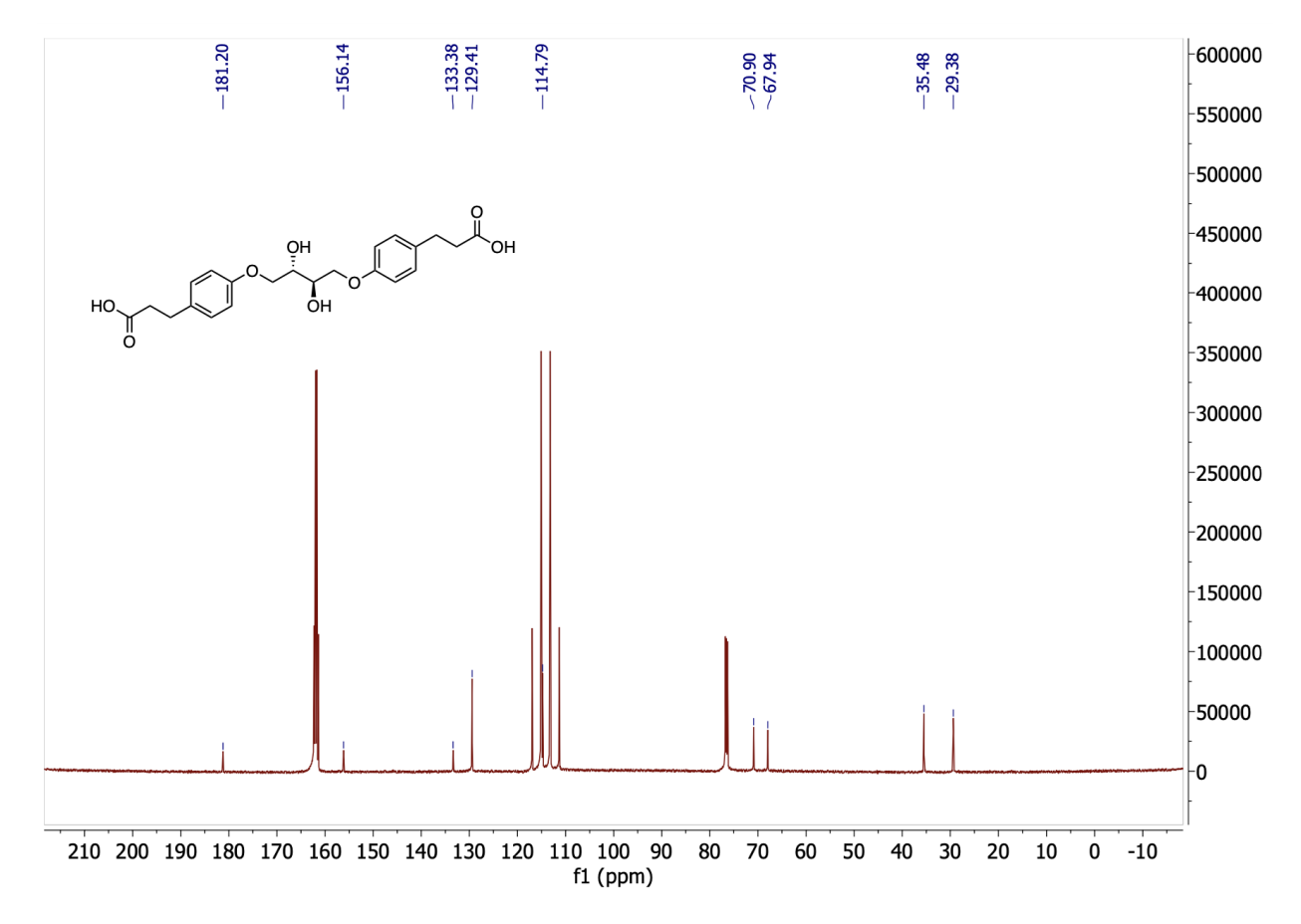


Figure S3.2: ¹³C NMR Spectrum of BPE in CDCl₃: TFA-d (6:4)

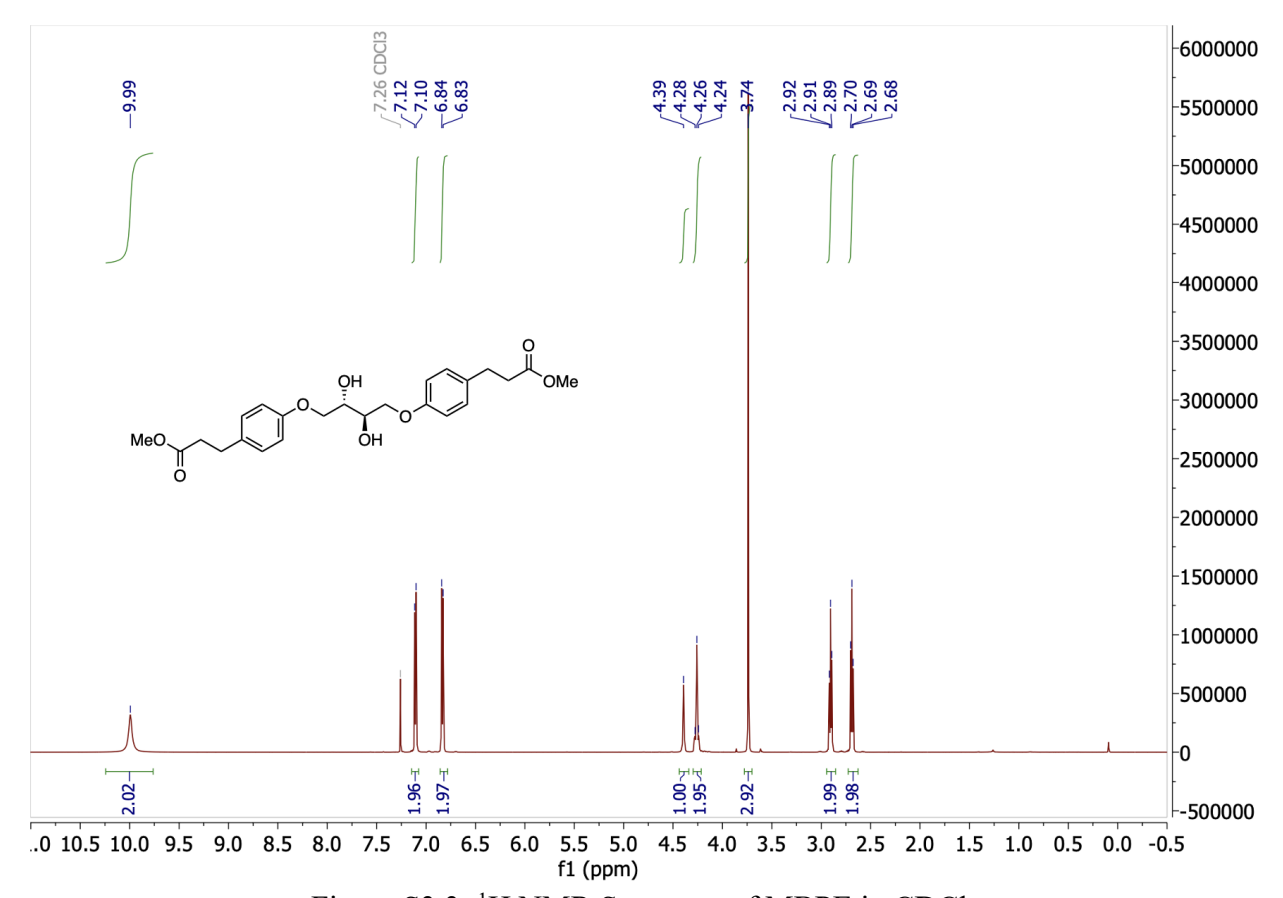


Figure S3.3: ¹H NMR Spectrum of MBPE in CDCl₃

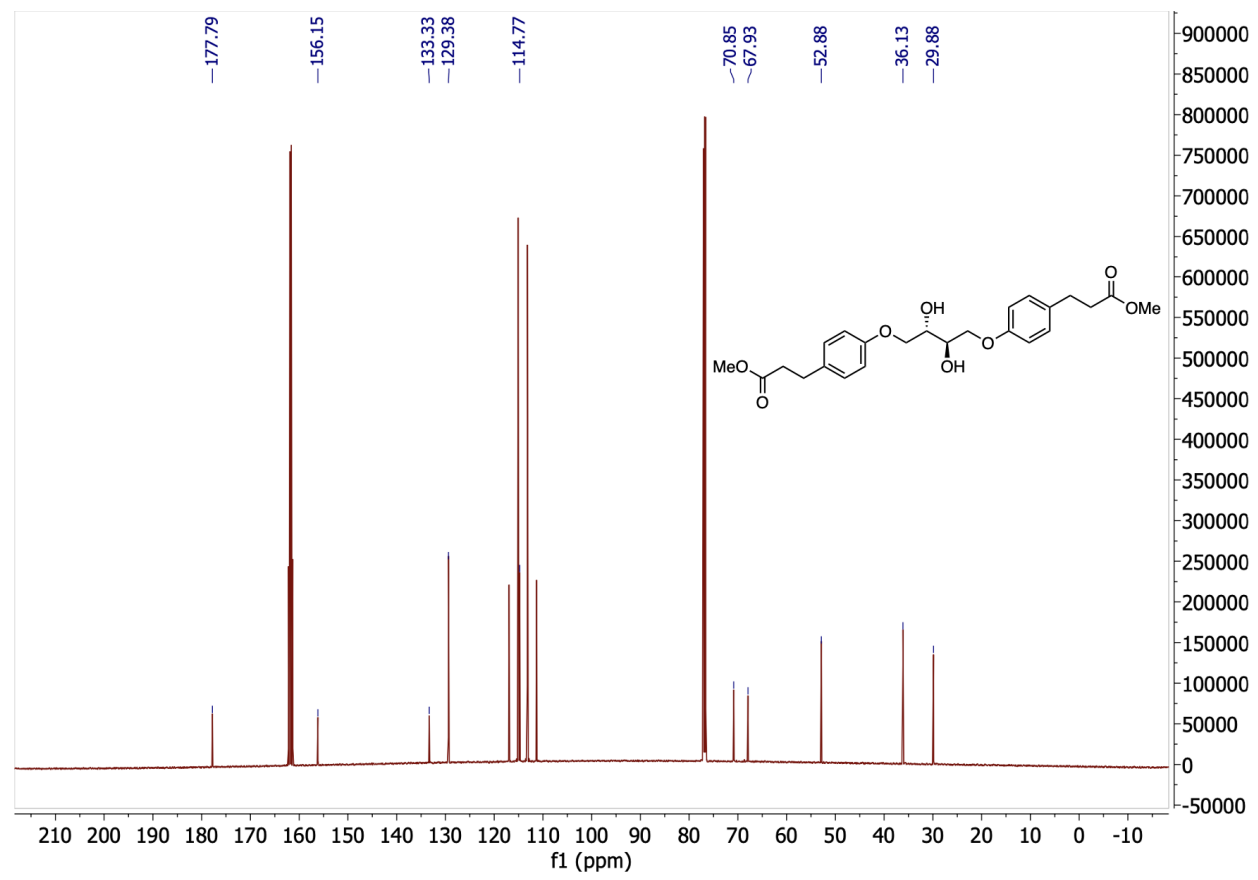


Figure S3.4: ¹³C NMR Spectrum of MBPE in CDCl₃ with a drop of TFA-d.

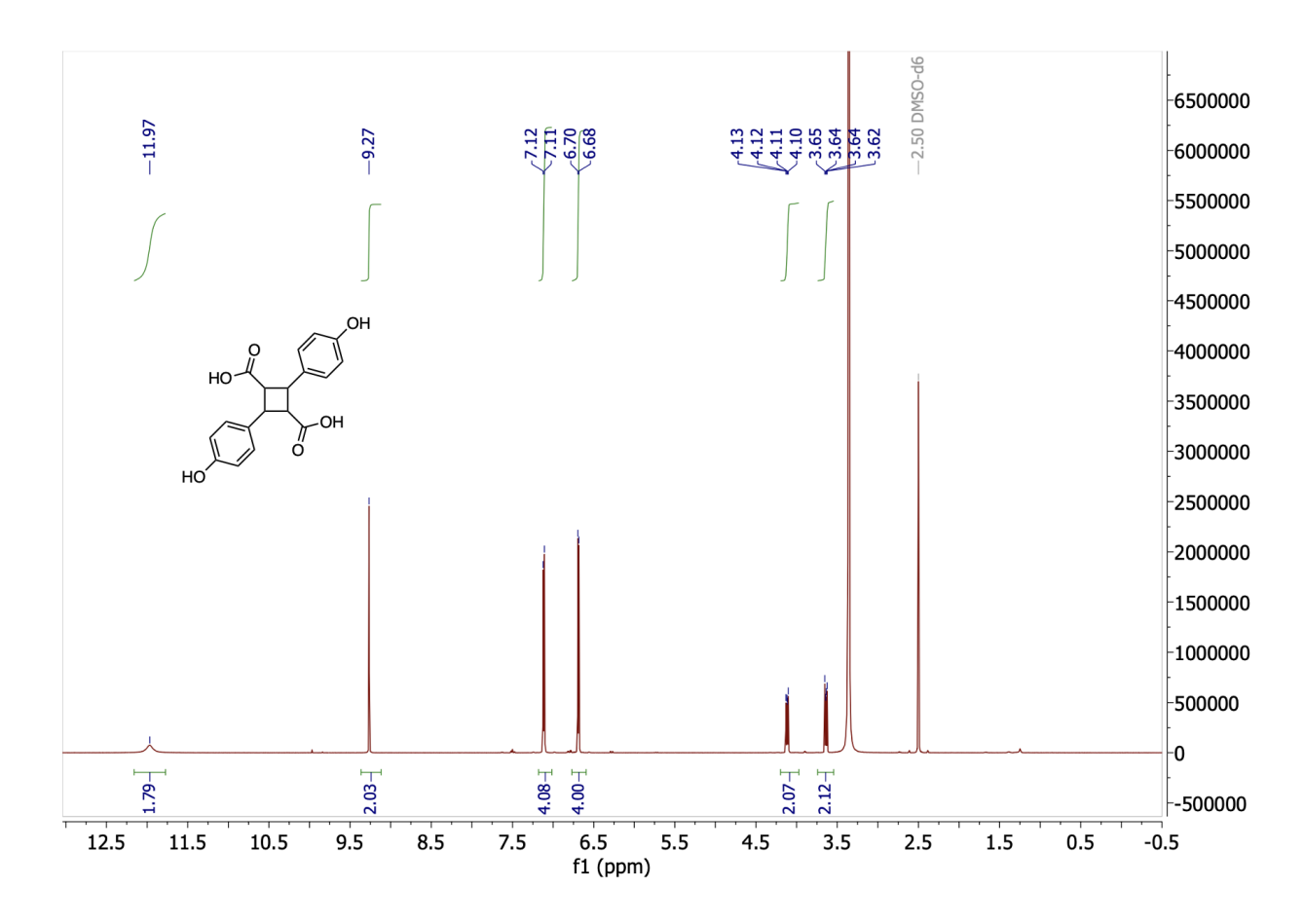


Figure S3.5: ¹H NMR spectrum of 4,4' dihydroxytruxillic acid in DMSO-d6

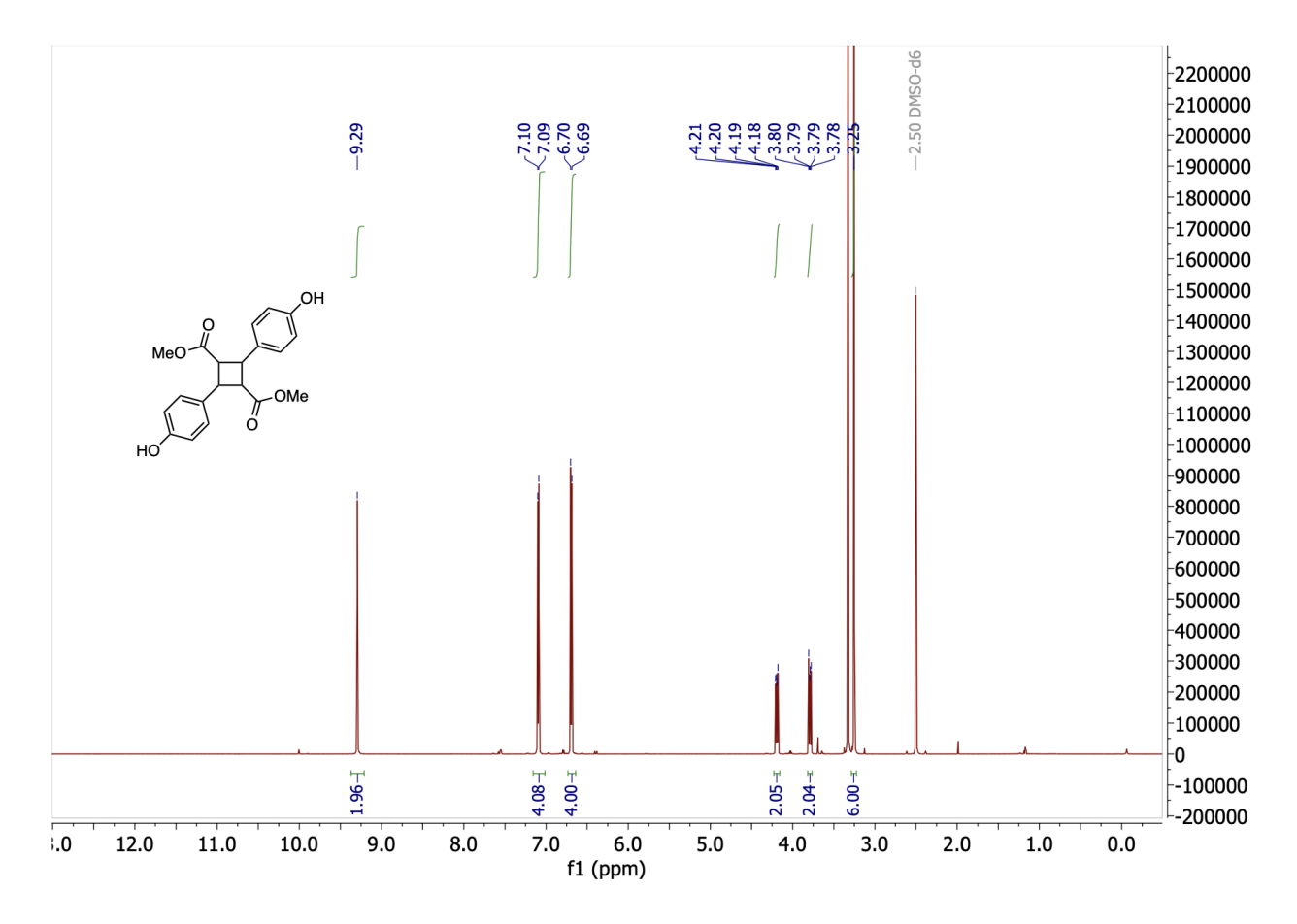


Figure S3.6: ¹H NMR spectrum of dimethyl 4,4' dihydroxytruxillate in DMSO-d6

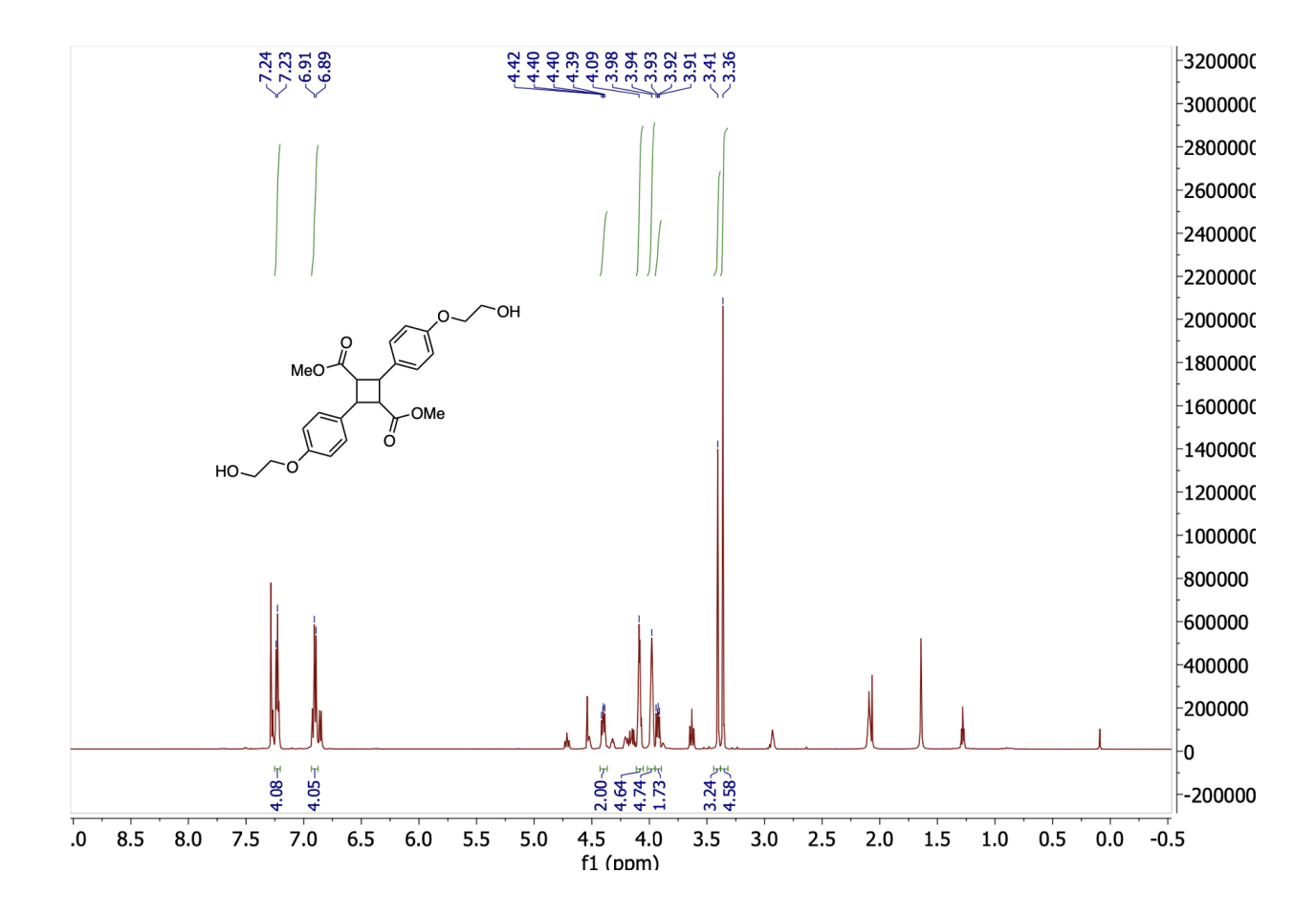


Figure S3.7: ¹H NMR spectrum of HEMT in CDCl₃

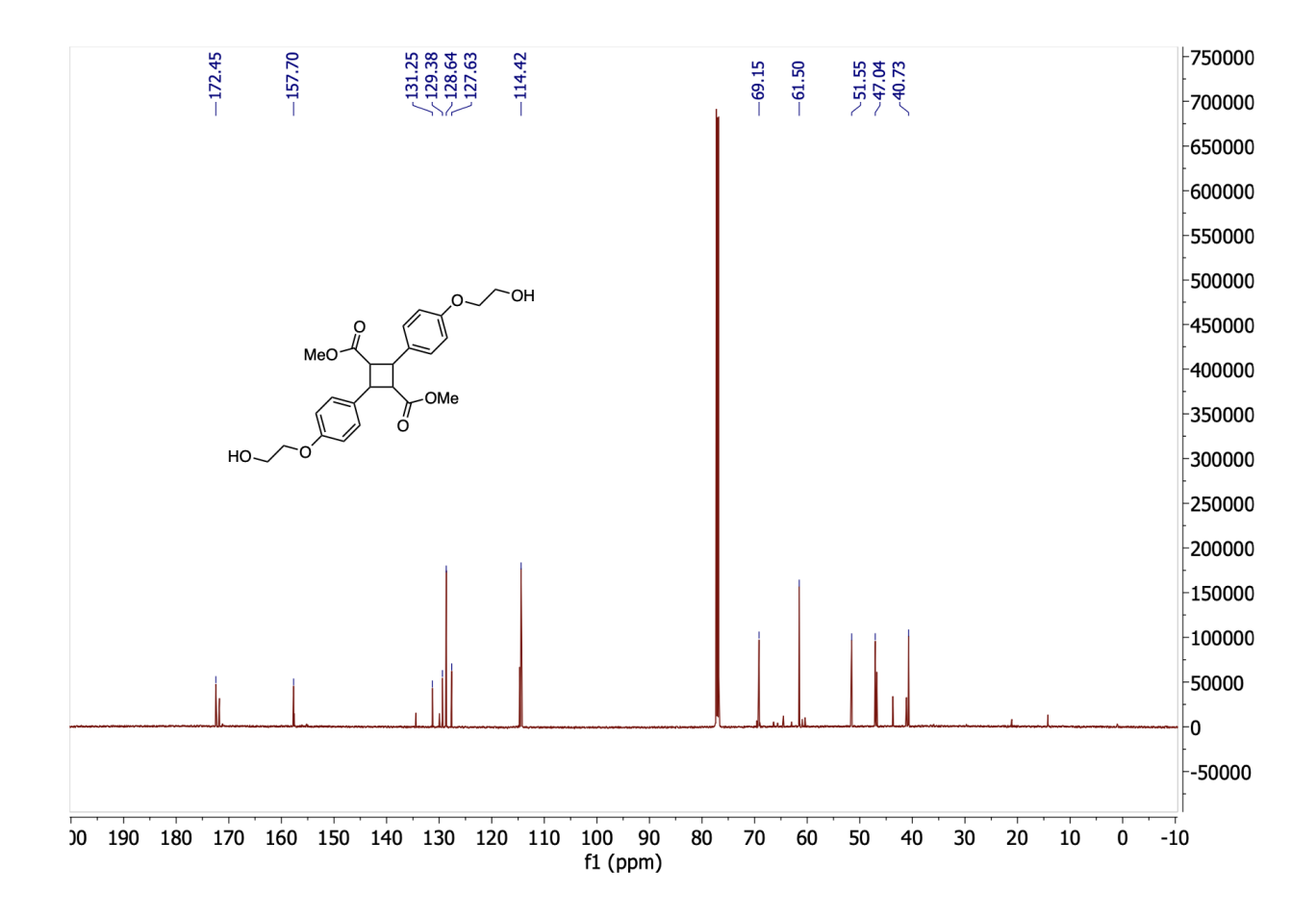


Figure S3.8: ¹³C NMR spectrum of HEMT in CDCl₃

Cyclic tensile plots and data:

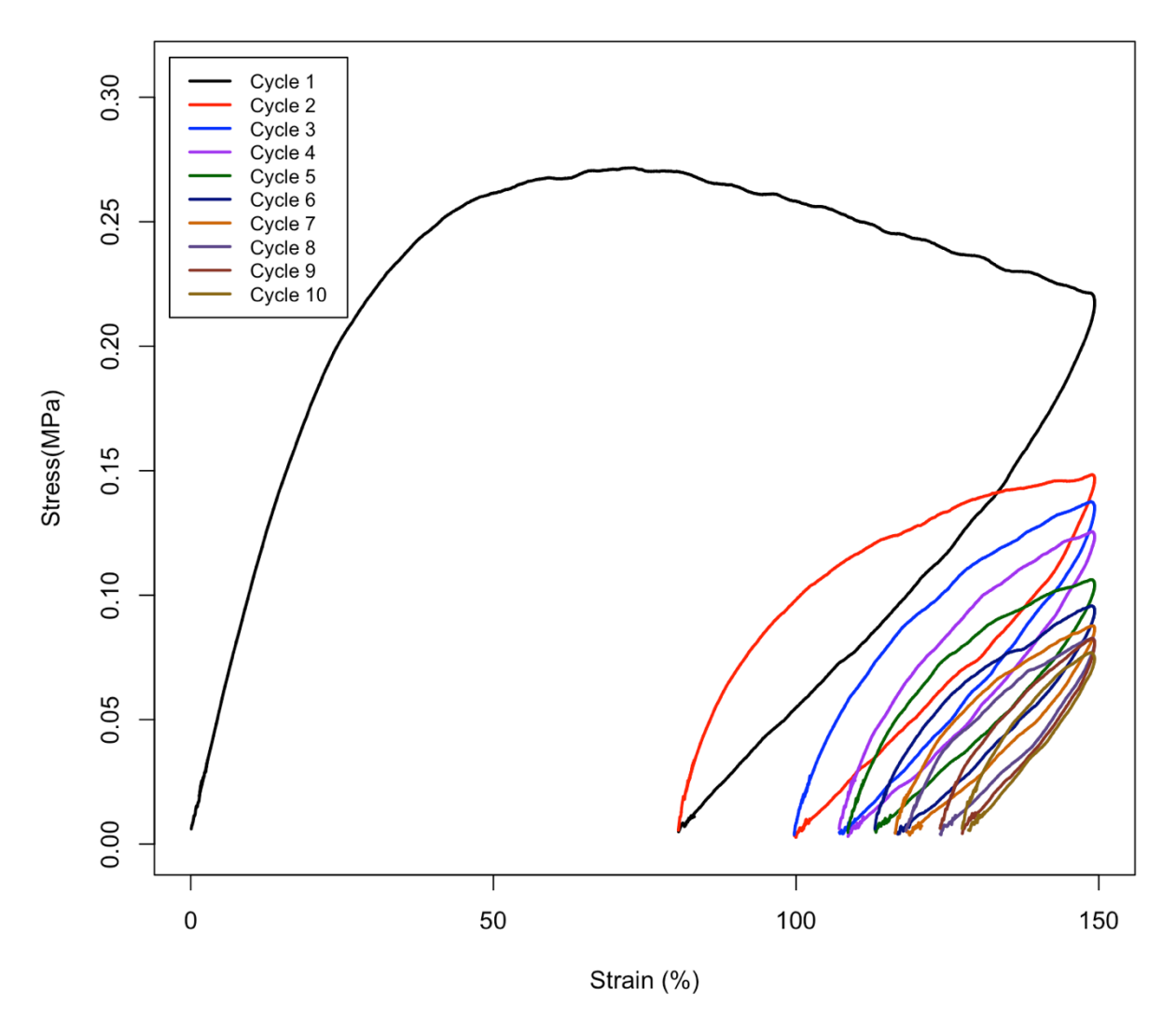


Figure S3.9: Cyclic tensile testing of P α BP to 150% strain at 5mm/min for 10 cycles.

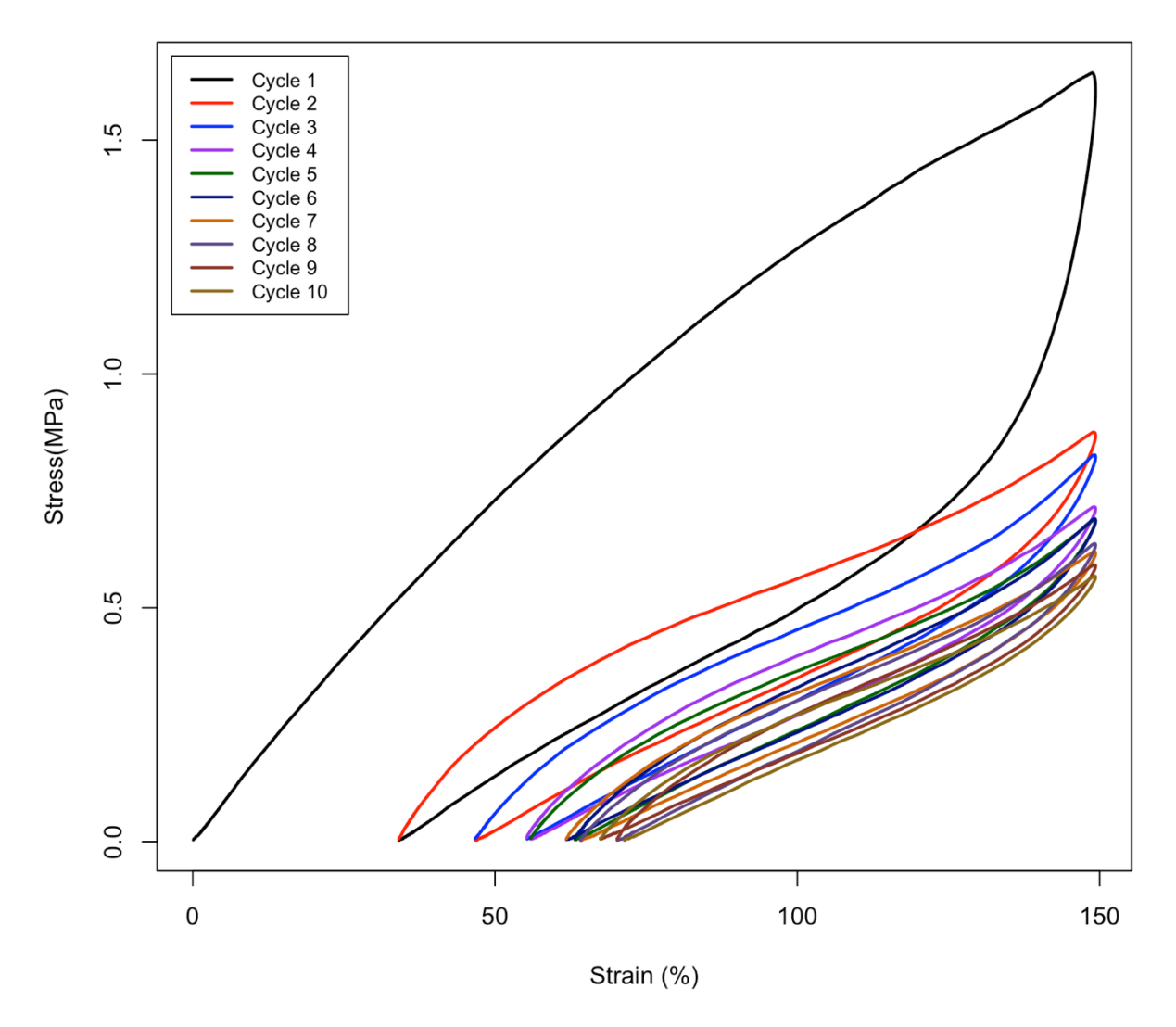


Figure S3.10: Cyclic tensile testing of P α BP polymerized with 0.25% MBPE to 150% strain at 5mm/min for 10 cycles.

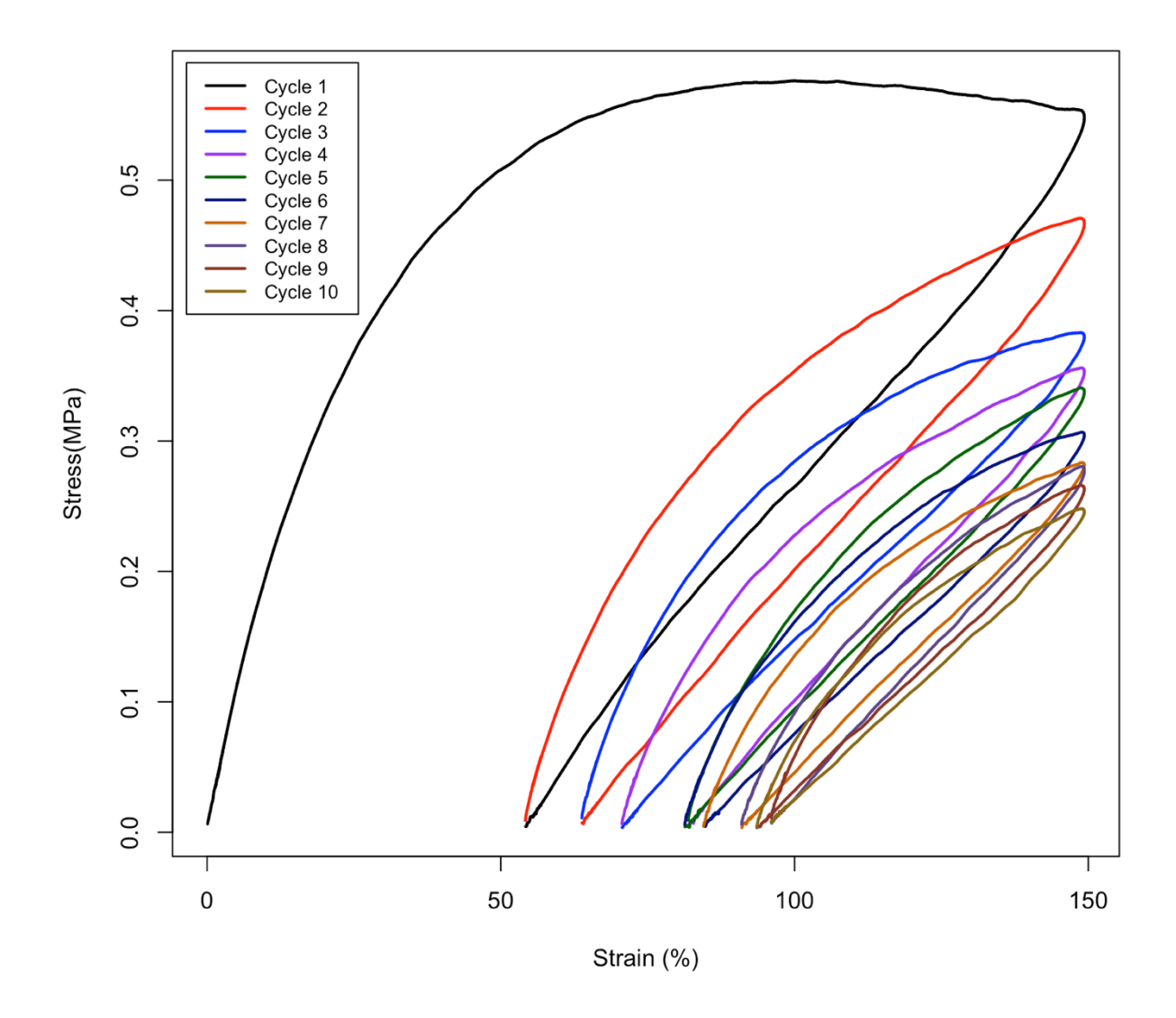


Figure S3.11: Cyclic tensile testing of P α BP polymerized with 0.25% HEMT to 150% strain at 5mm/min for 10 cycles.

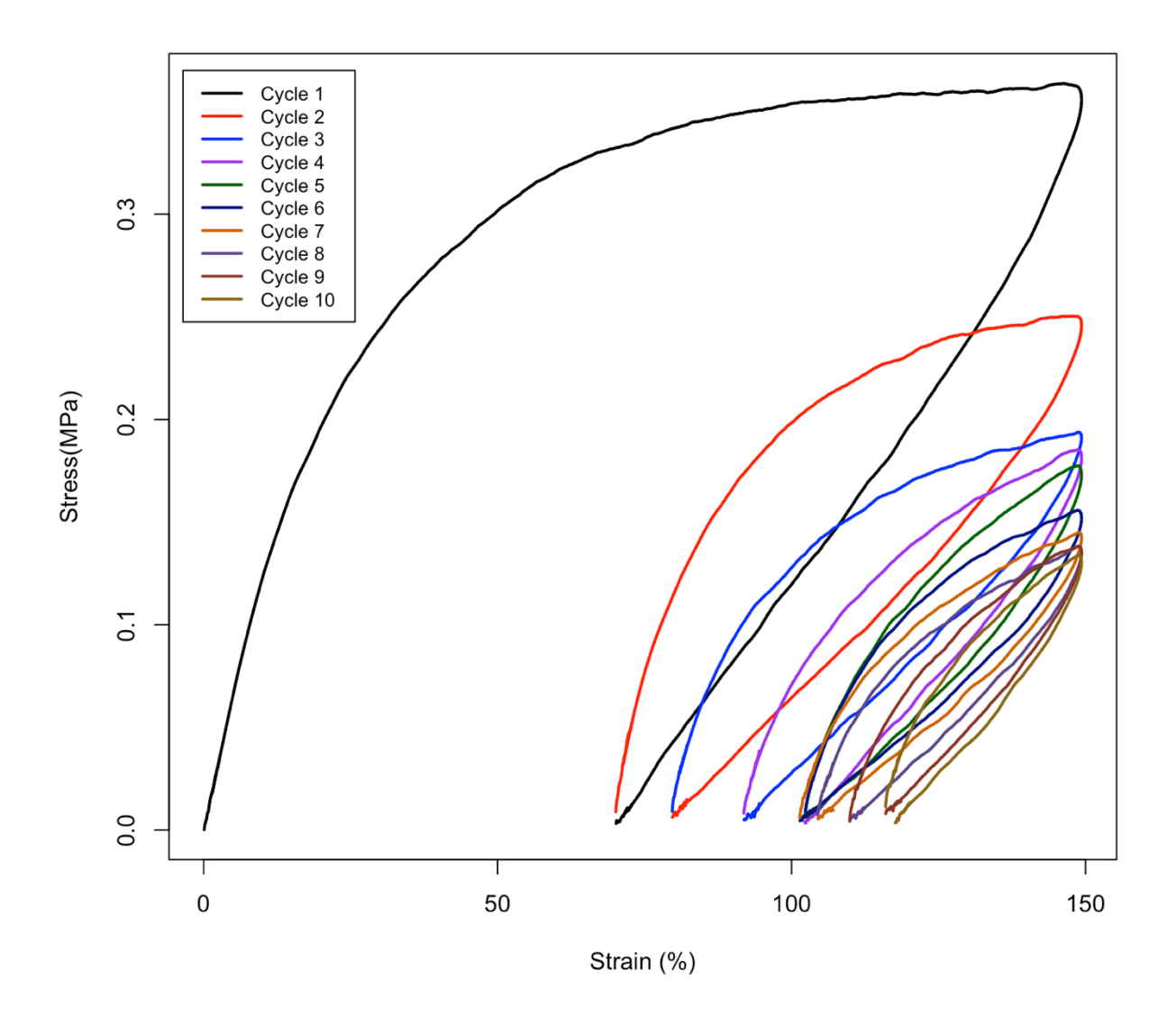


Figure S3.12: Cyclic tensile testing of P α BP polymerized with 1.0% MBPE to 150% strain at 5mm/min for 10 cycles.

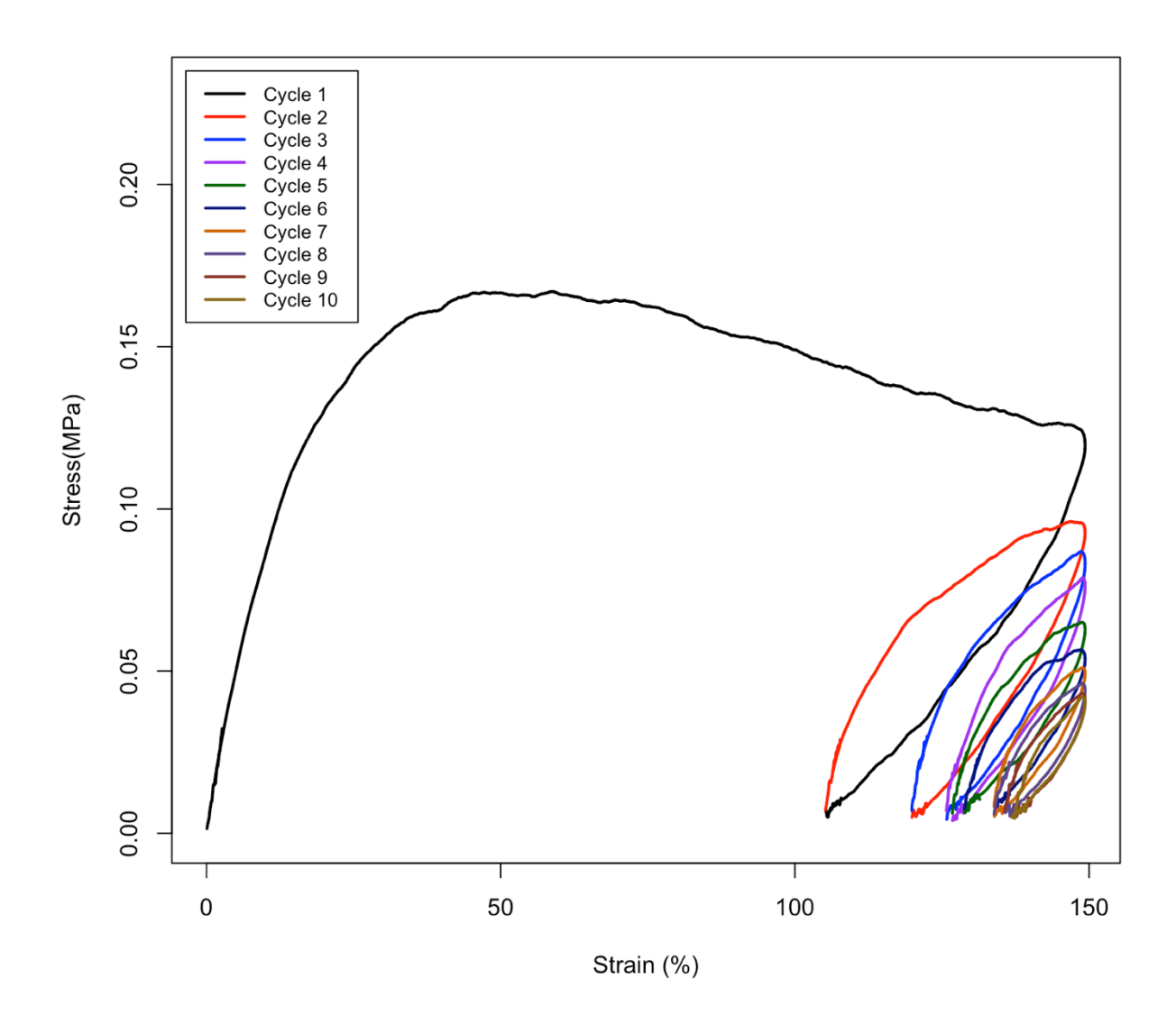


Figure S3.13: Cyclic tensile testing of P α BP polymerized with 1.0% HEMT to 150% strain at 5mm/min for 10 cycles.

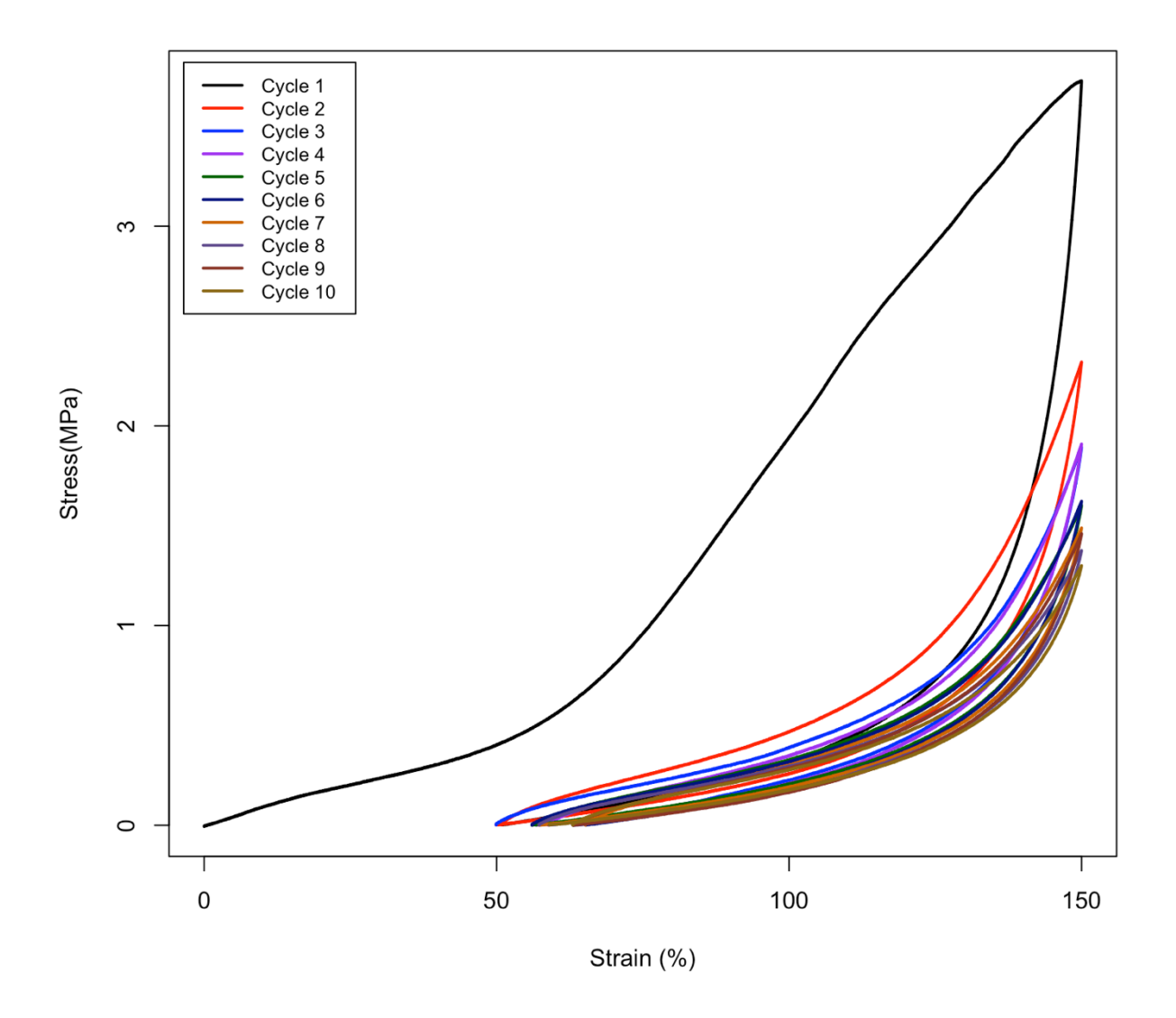


Figure S3.14: Cyclic tensile testing of P α BP polymerized with 2.5% MBPE to 150% strain at 5mm/min for 10 cycles.

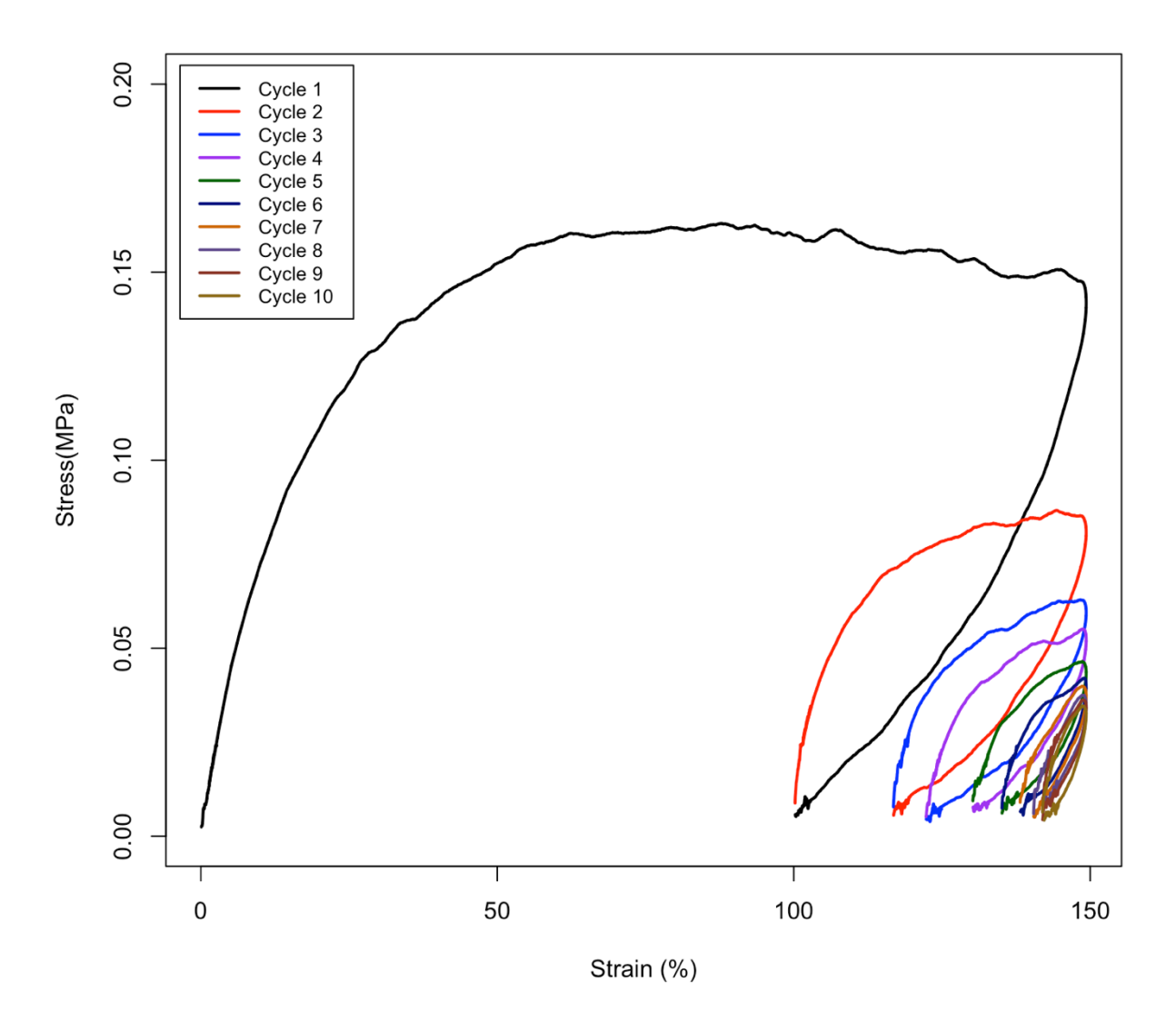


Figure S3.15: Cyclic tensile testing of P α BP polymerized with 2.5% HEMT to 150% strain at 5mm/min for 10 cycles.

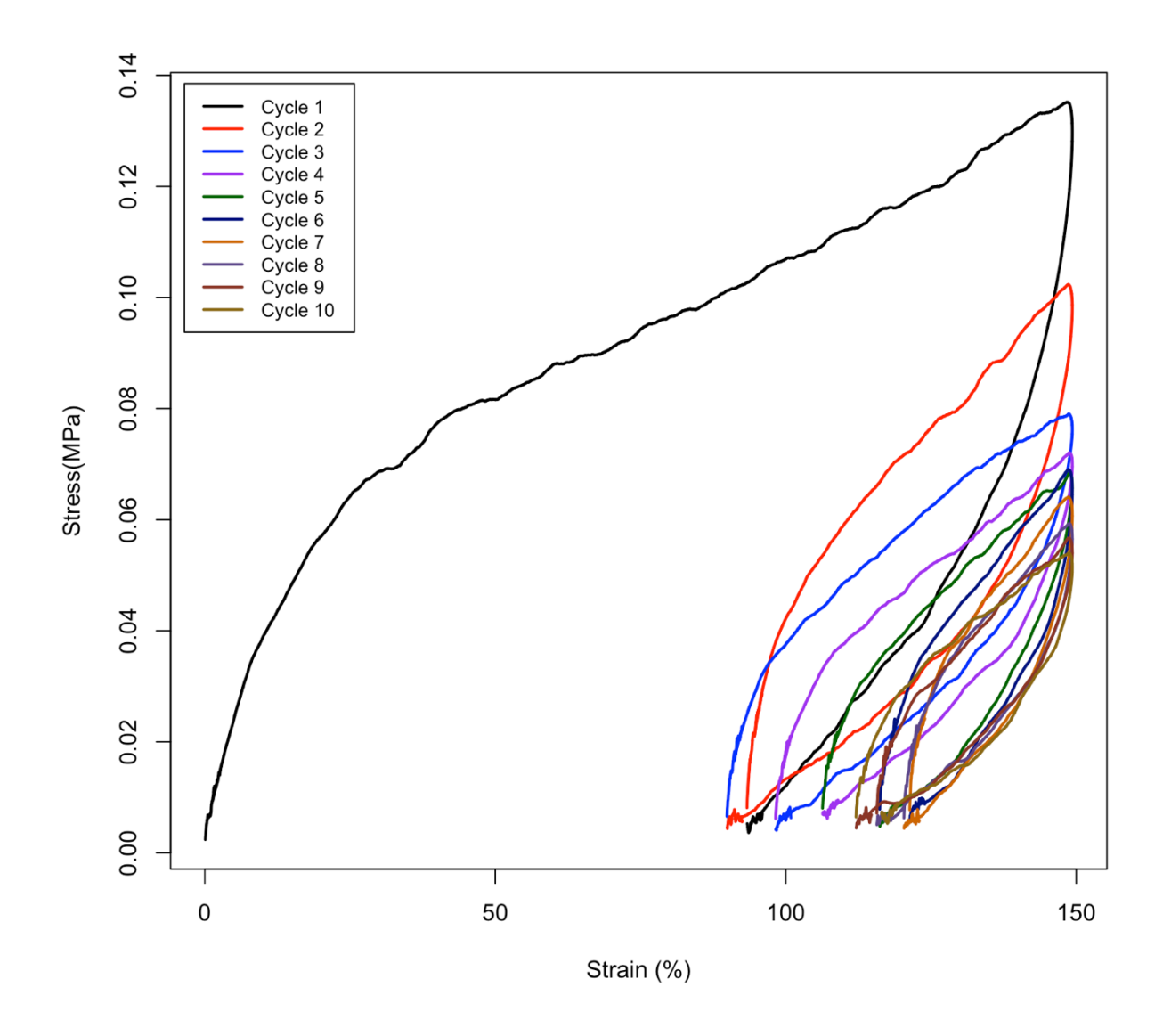


Figure S3.16: Cyclic tensile testing of P α BP polymerized with 5.0% MBPE to 150% strain at 5mm/min for 10 cycles.

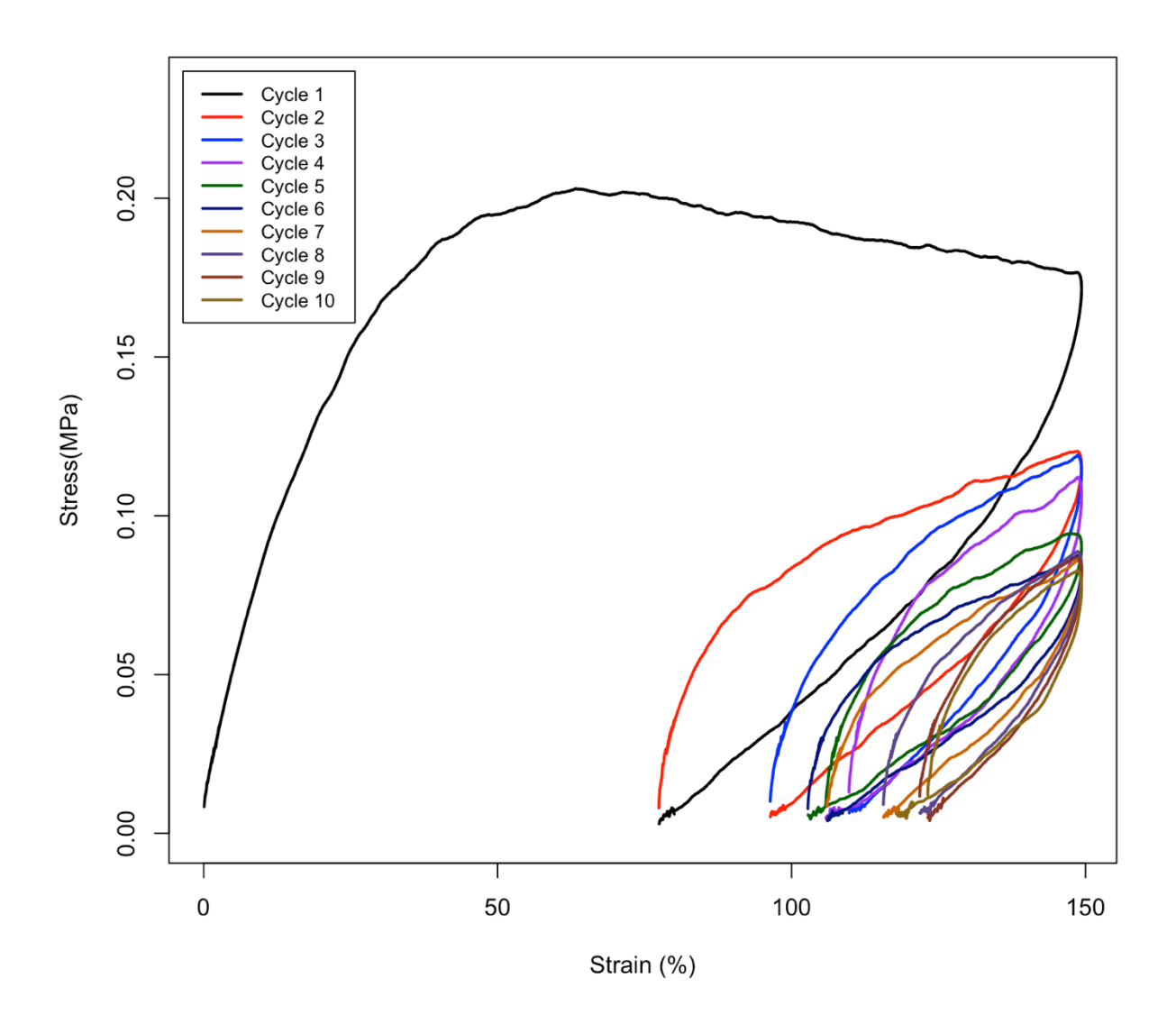


Figure S3.17: Cyclic tensile testing of P α BP polymerized with 5% HEMT to 150% strain at 5mm/min for 10 cycles.

Table S3.1: Summary of elastomeric recovery for all samples and all cycles. R_T is shown in the top rows, R_R is shown in the bottom.

	R _T								
CYCLE	ΡαΒΡ	0.25% MBPE	0.25% HEMT	1.0% MBPE	1.0% HEMT	2.5% MBPE	2.5% HEMT	5.0% MBPE	5.0% HEMT
1	46.3	77.3	63.9	53.3	29.9	66.1	33.2	37.8	48.4
2	33.6	68.9	57.5	46.9	20.1	66.7	22.2	40.1	35.8
3	28.6	63.2	53.0	38.8	16.2	60.8	18.5	34.5	26.9
4	27.7	62.8	45.4	31.9	15.5	62.1	13.2	29.1	29.5
5	24.7	57.9	45.8	31.8	14.2	62.6	10.0	22.6	31.5
6	22.5	58.8	43.7	32.4	10.8	56.5	7.9	19.2	29.3
7	21.3	57.3	39.4	30.4	10.8	61.8	6.4	19.8	23.0
8	17.5	53.3	36.0	26.8	9.6	57.9	5.3	22.9	18.8
9	15.1	55.1	37.7	22.7	8.4	58.0	5.4	25.3	17.9
10	14.4	52.5	36.0	21.6	8.8	60.7	5.2	22.4	21.4
	R _R								
1	46.3	77.3	63.9	53.3	29.9	66.1	33.2	37.8	48.4
2	23.8	37.2	17.7	13.7	13.9	1.8	16.6	3.7	24.5
3	7.5	18.3	10.7	15.3	4.9	17.8	4.7	9.3	13.9
4	1.3	1.2	16.0	11.3	0.8	3.5	6.5	8.2	3.6
5	4.1	13.1	0.7	0.1	1.6	1.3	3.8	9.3	2.9
6	3.0	2.2	3.9	0.9	3.9	16.3	2.3	4.4	3.2
7	1.5	3.8	7.7	3.0	0.0	12.1	1.6	0.8	9.0
8	4.8	9.4	5.6	5.2	1.3	10.2	1.2	3.9	5.3
9	2.9	3.9	2.6	5.6	1.4	0.2	0.1	3.1	1.1
10	0.8	5.9	2.6	1.4	0.5	6.4	0.2	3.9	4.2

Temperature Sweeps of Polymers:

PαBP Temperature Sweep

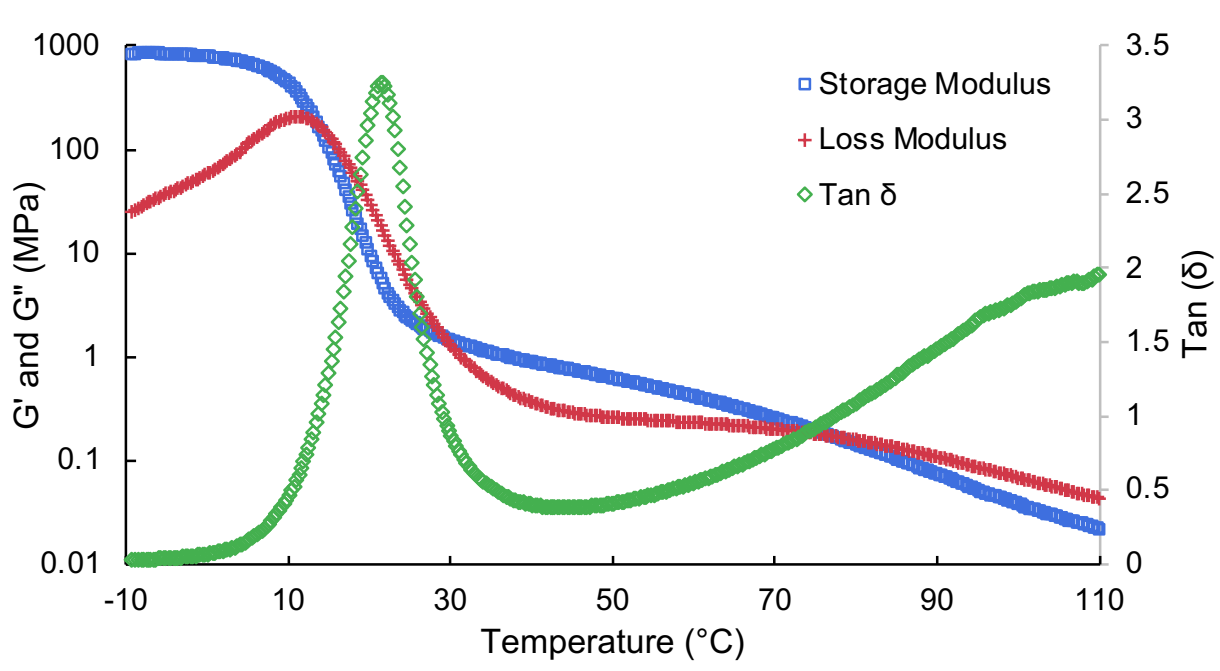


Figure S3.18: Temperature sweep of PαBP

0.25% MBPE

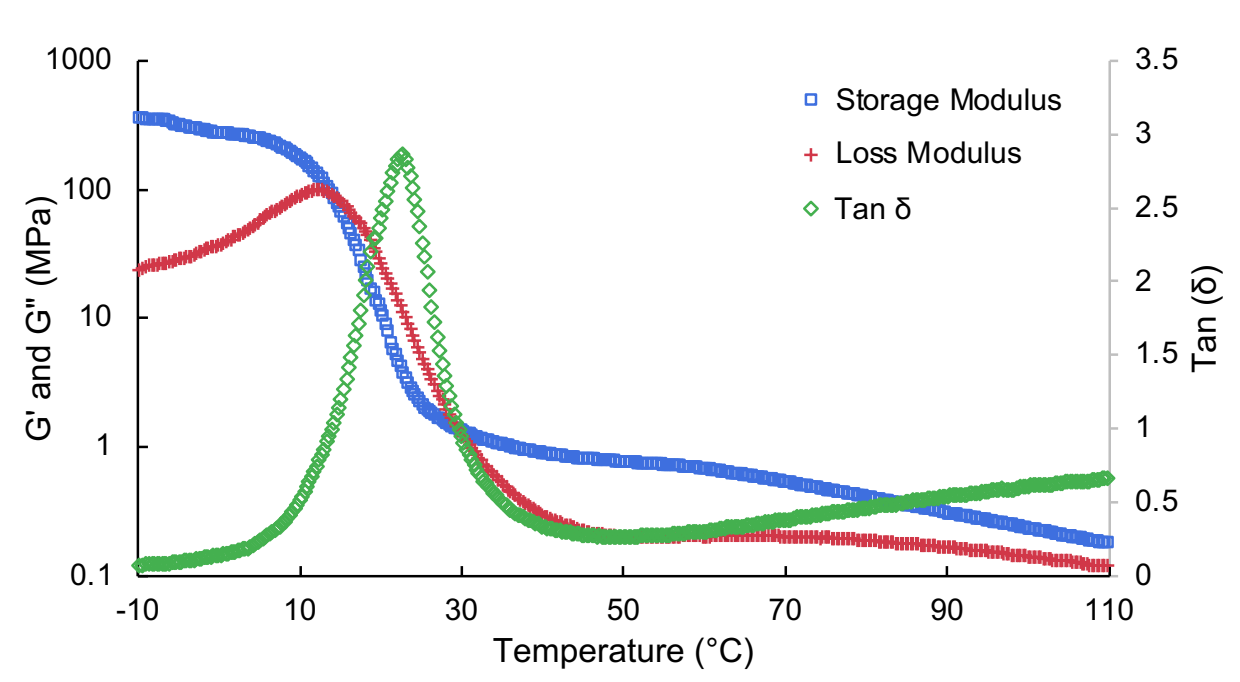


Figure S3.19: Temperature sweep of PαBP polymerized with 0.25% MBPE

0.25% HEMT 1000 3.5 Storage Modulus 3 + Loss Modulus 100 Tan δ 2.5 G' and G" (MPa) 10 2 (δ) 2 Tan (δ) 2 1 1 0.1 0.5 0.01 0 -10 10 30 50 70 90 110 Temperature (°C)

Figure S3.20: Temperature sweep of P α BP polymerized with 0.25% HEMT

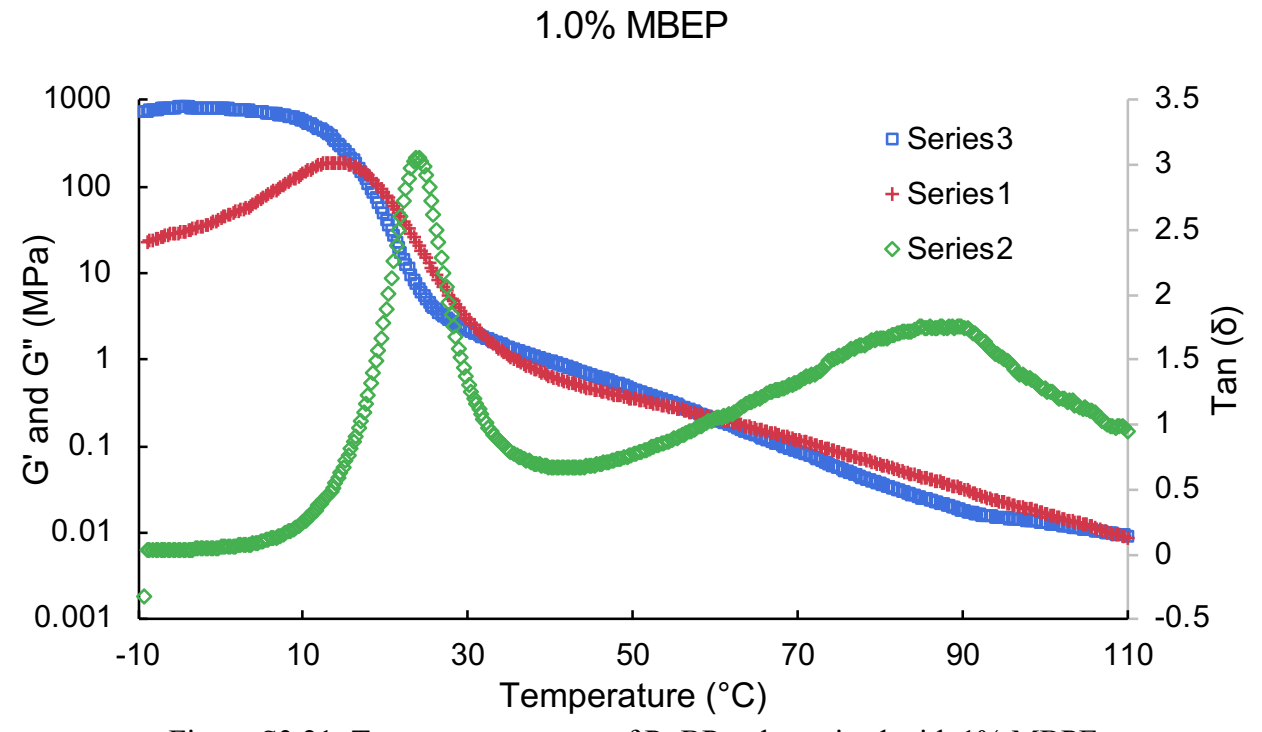


Figure S3.21: Temperature sweep of PαBP polymerized with 1% MBPE

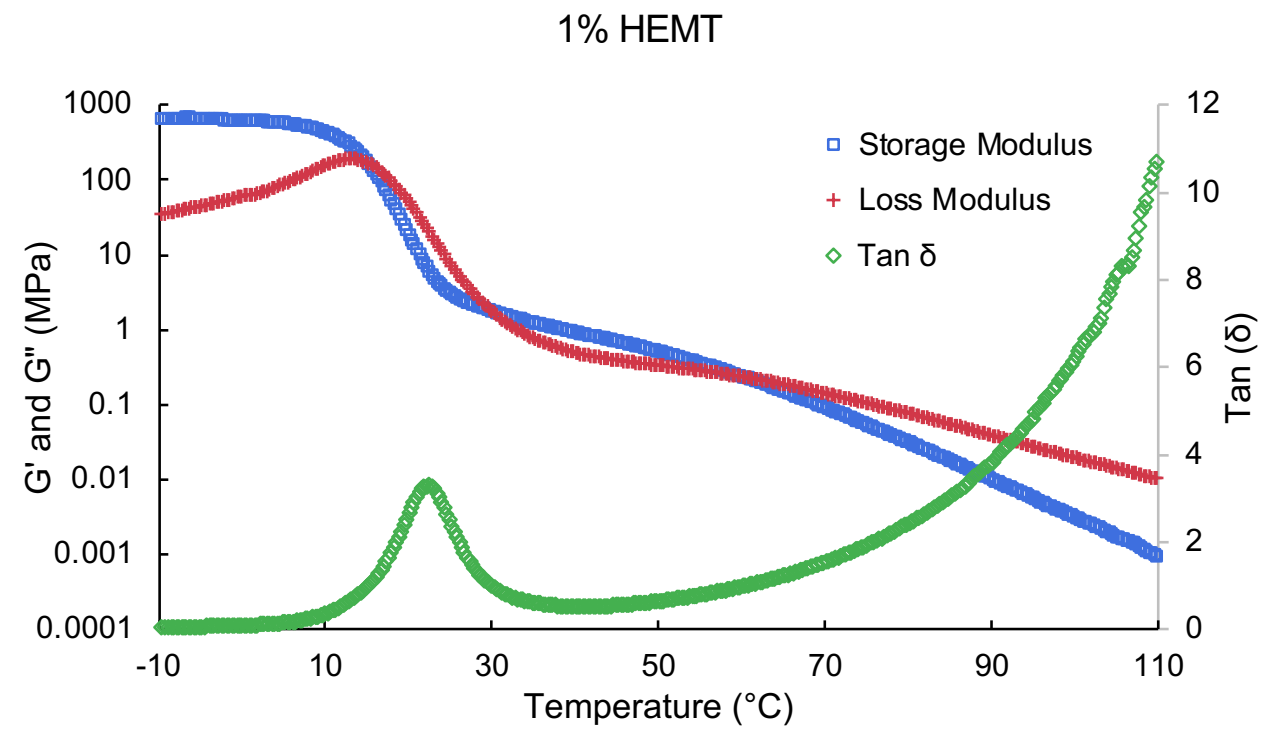


Figure S3.22: Temperature sweep of PαBP polymerized with 1% HEMT

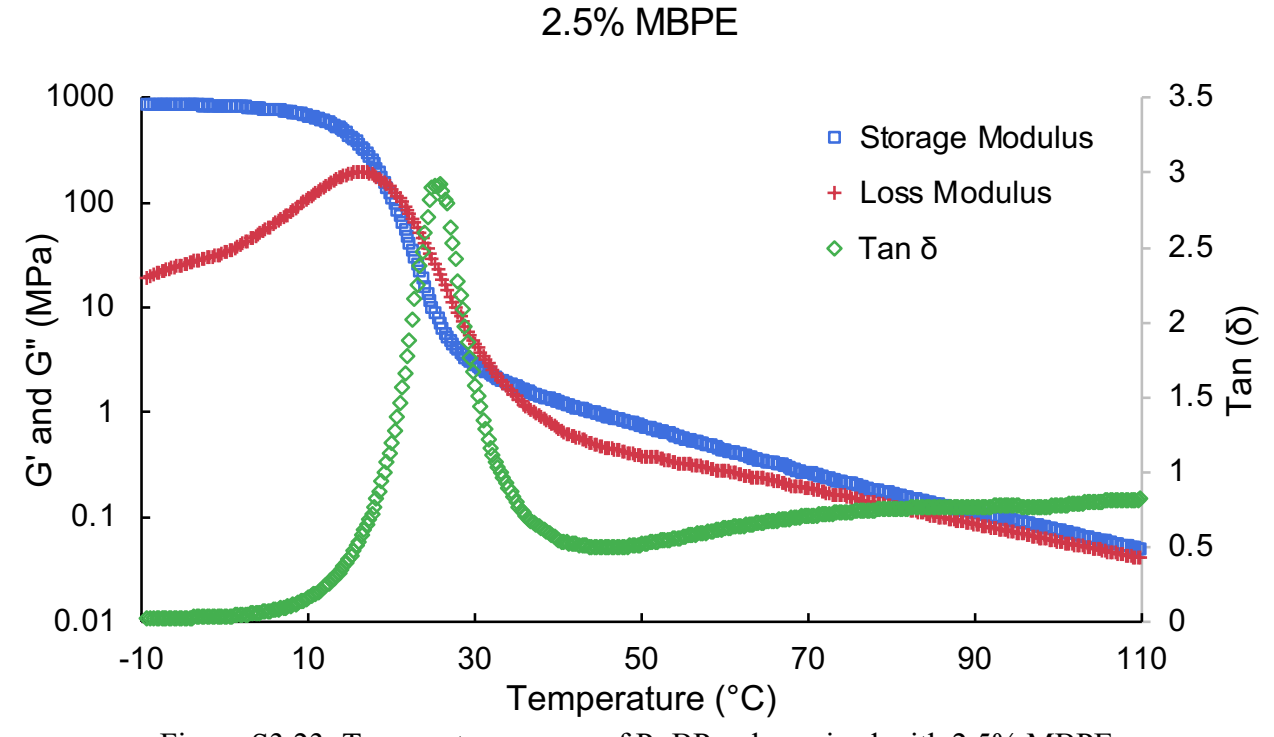


Figure S3.23: Temperature sweep of PαBP polymerized with 2.5% MBPE

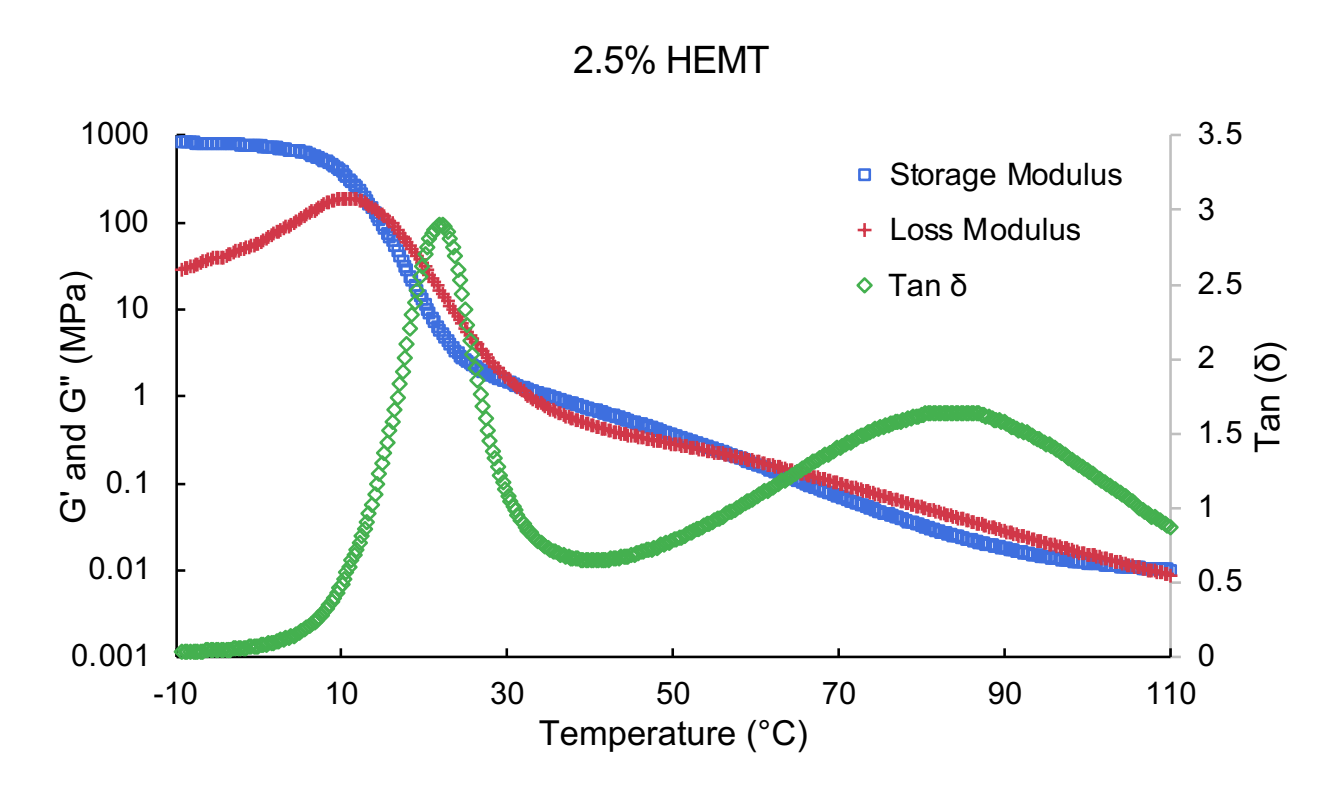


Figure S3.24: Temperature sweep of PαBP polymerized with 2.5% HEMT

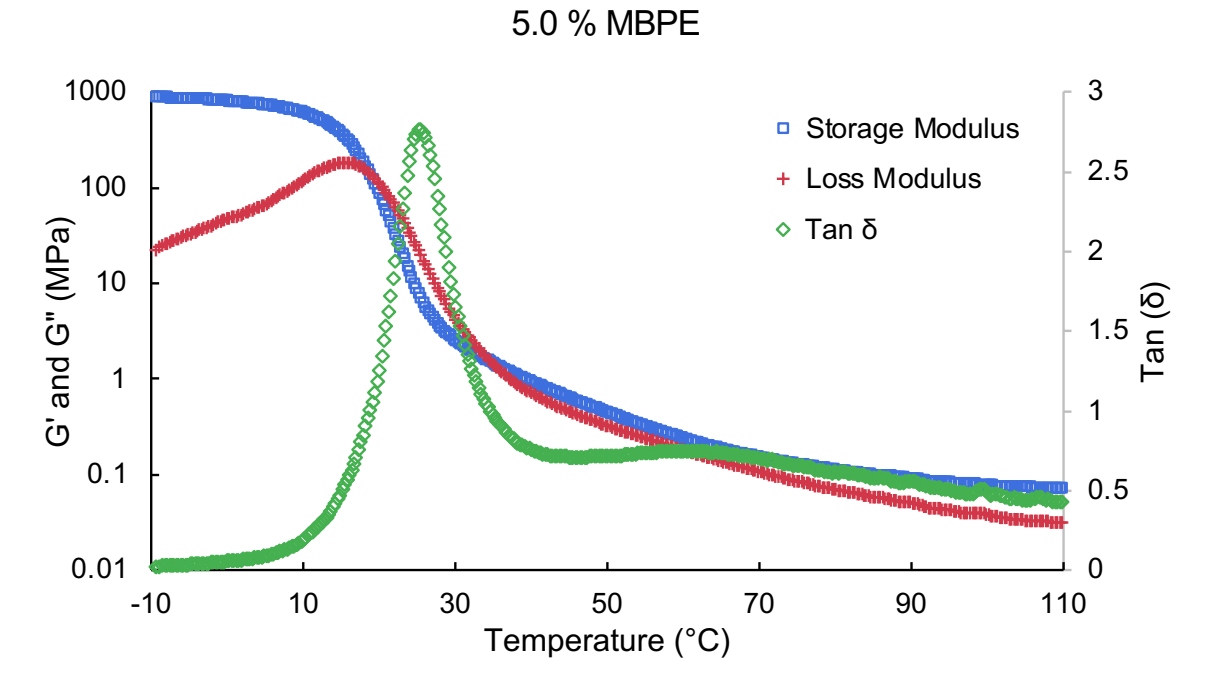


Figure S3.25: Temperature sweep of PαBP polymerized with 5% MBPE

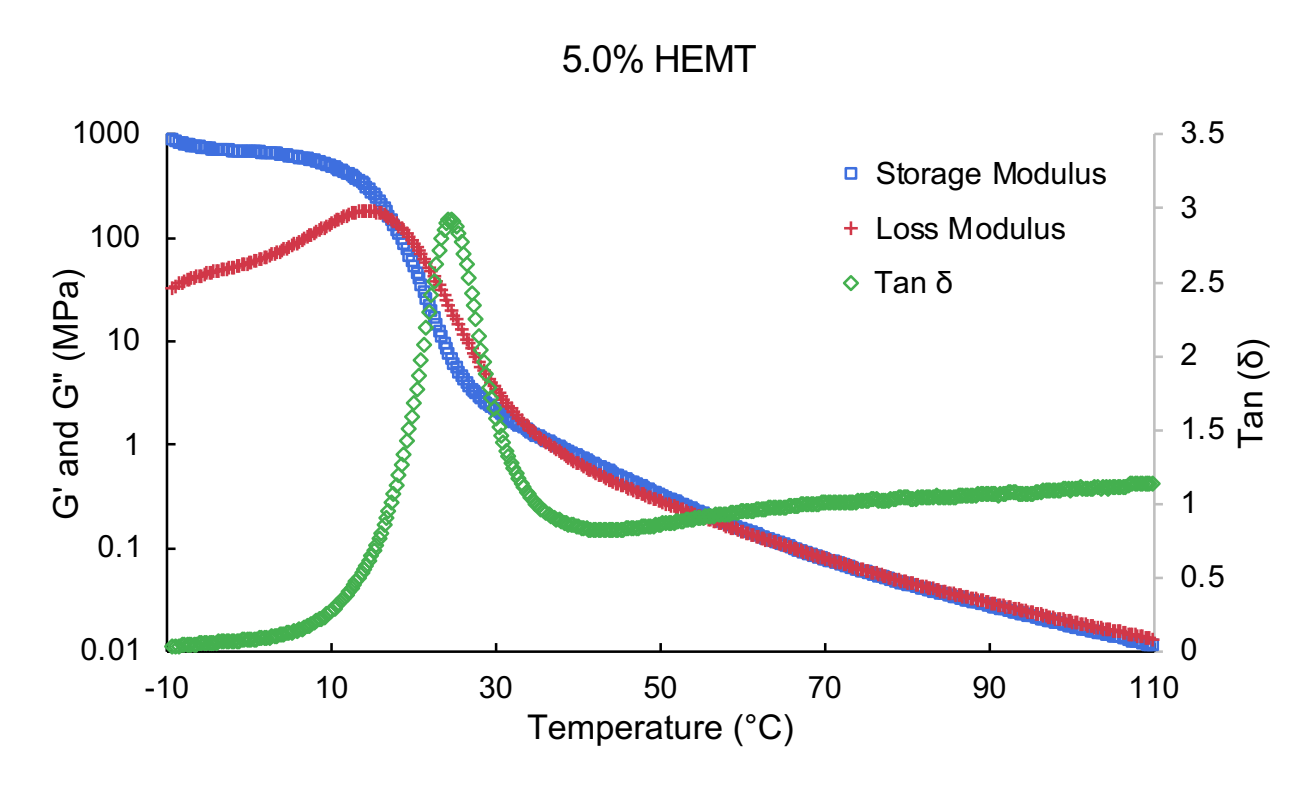


Figure S3.26: Temperature sweep of P α BP polymerized with 5% HEMT

APPENDIX C

SUPPLEMENTAL INFORMATION FOR CHAPTER 4

NMR Spectra of Monomers:

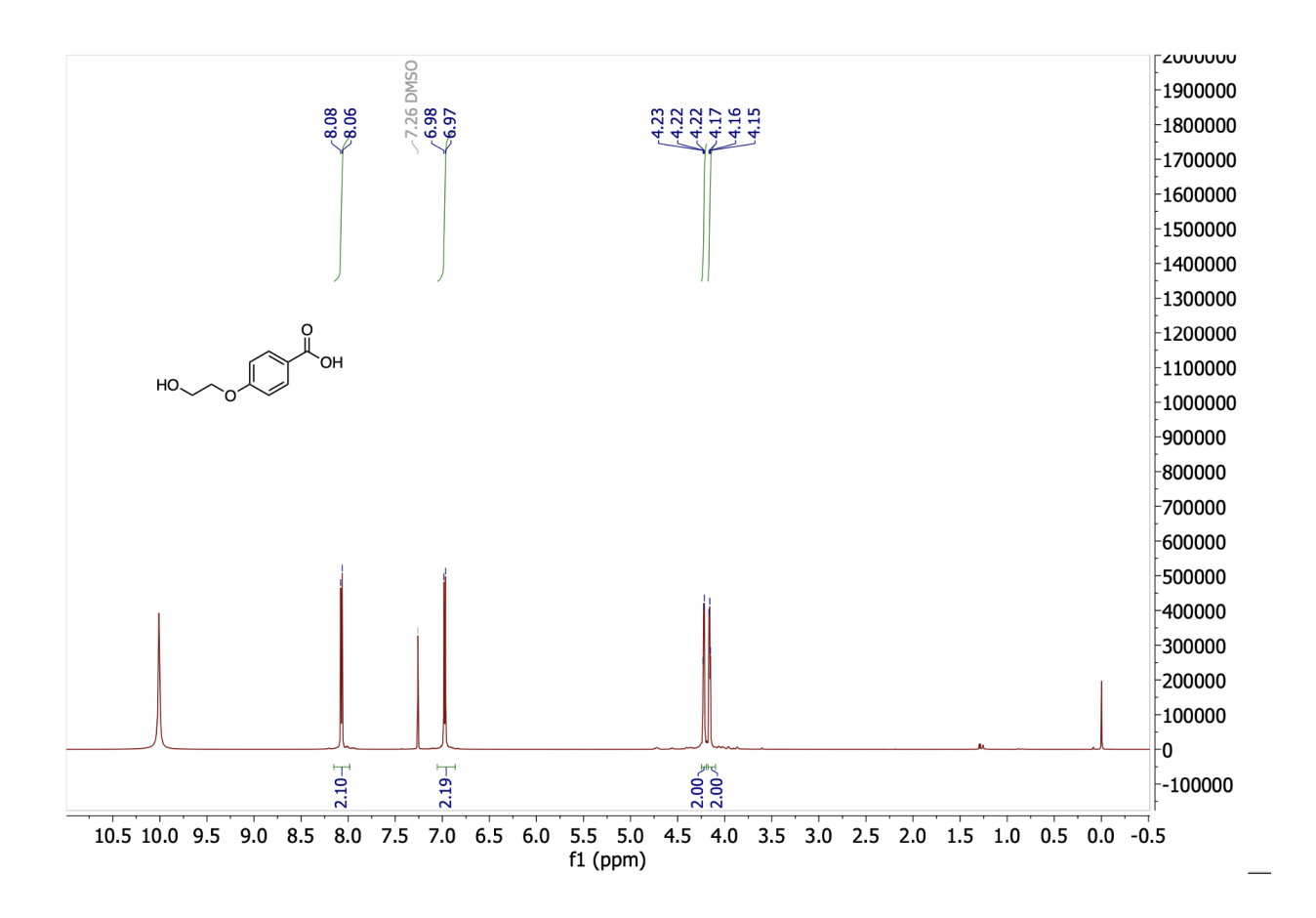


Figure S4.1: ¹H NMR Spectrum of ethylene benzoate in 6:4 CDCl₃: TFA-d

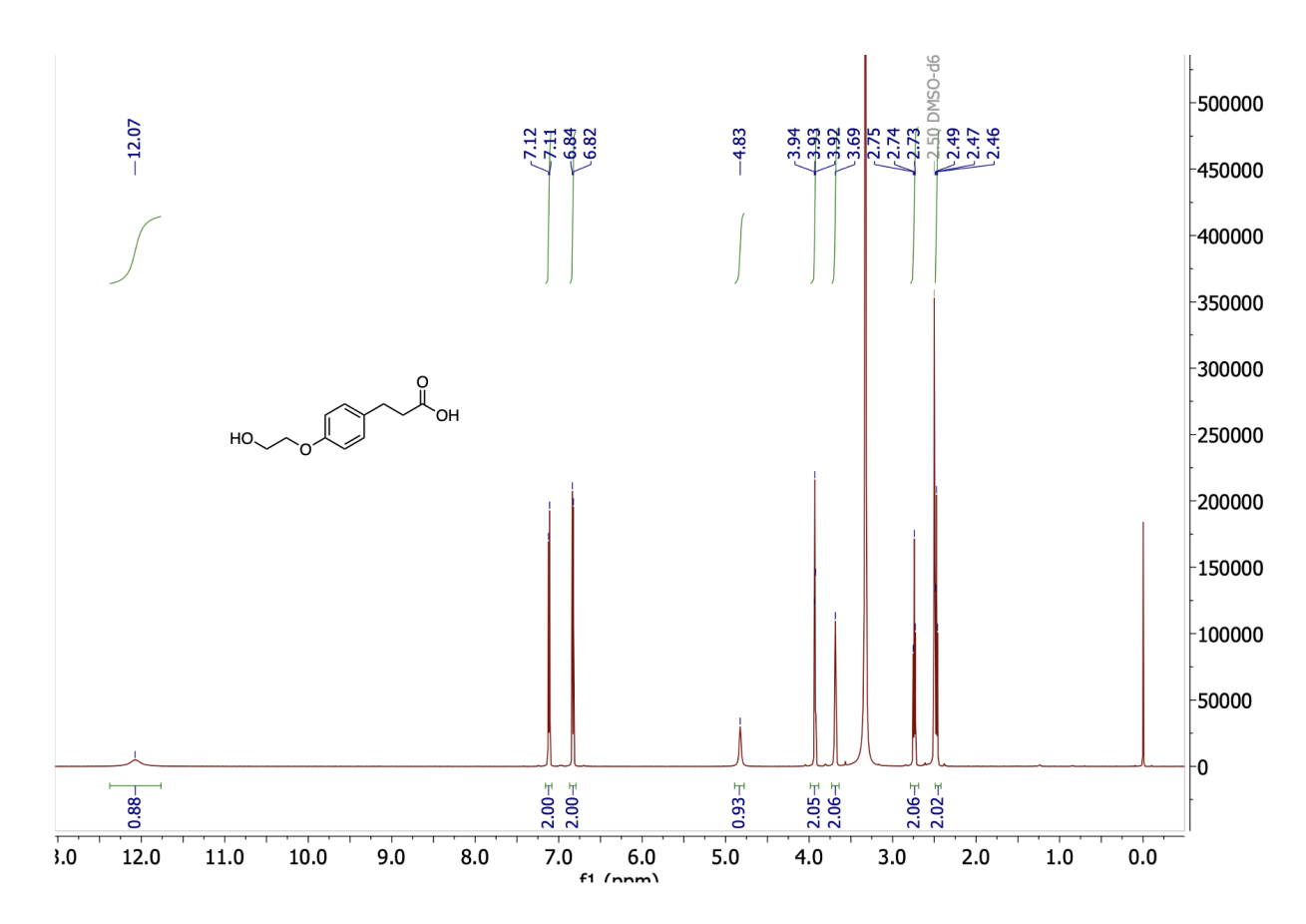


Figure S4.2: ¹H NMR Spectrum of ethylene phloreatate in CDCl₃

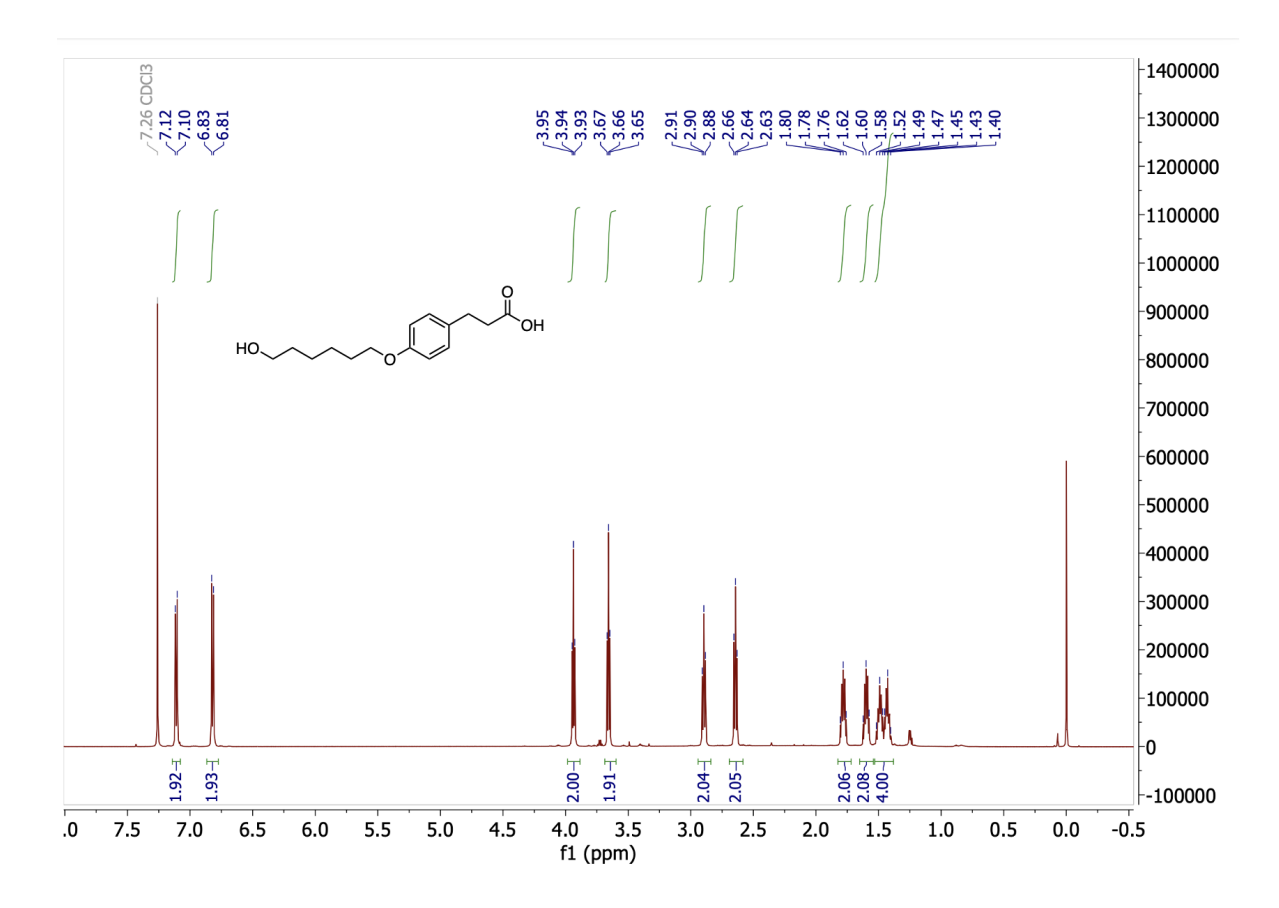


Figure S4.3: ¹H NMR Spectrum of hexamethylene phloretate in CDCl₃

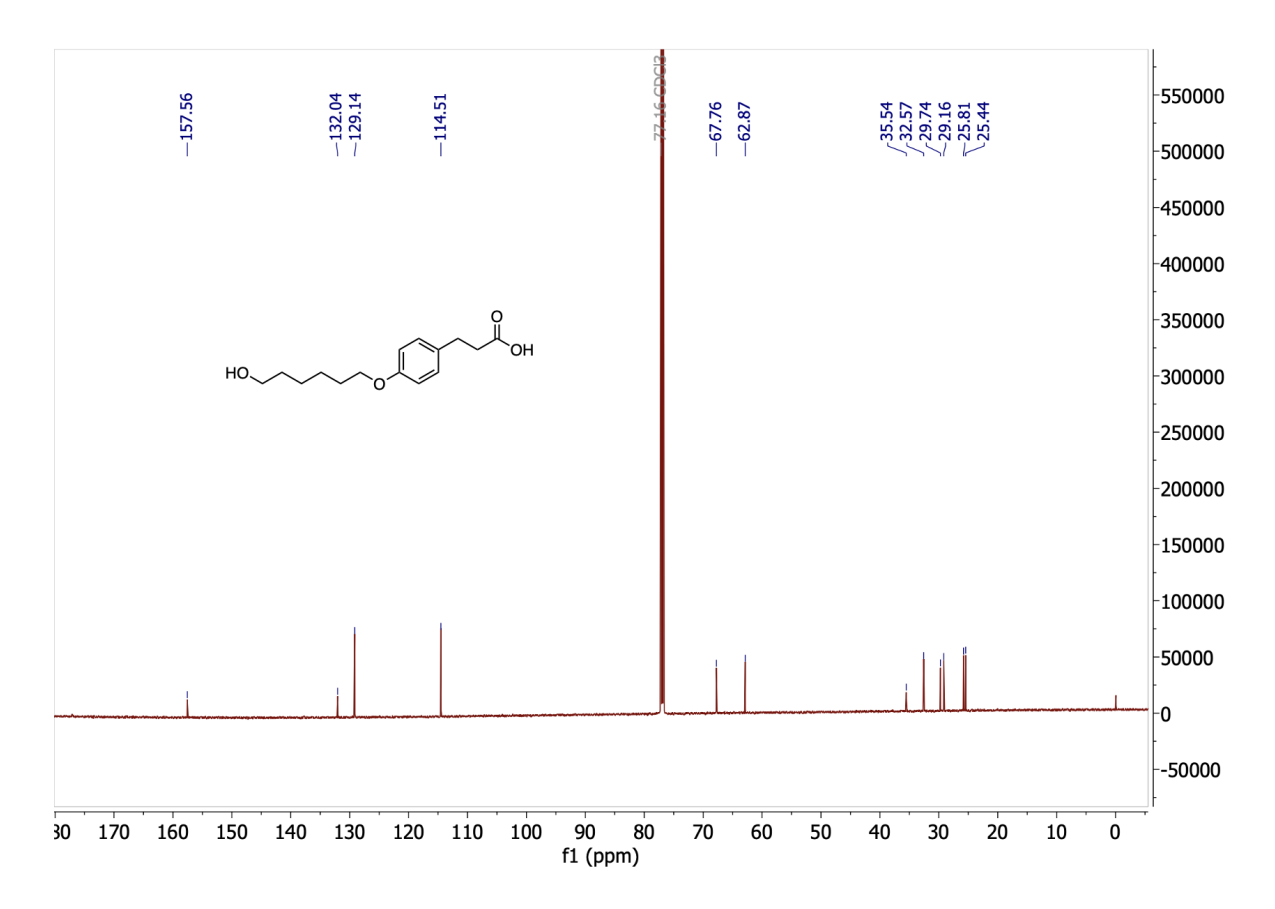


Figure S4.4: ¹³C NMR Spectrum of hexamethylene phloretate in CDCl₃